

**ORIGINAL**

# **New Approaches to the Measurement of Chlorophyll, Related Pigments and Productivity in the Sea**

**FINAL REPORT TO NASA  
Contract NAS7-969**

N93-13612

Unclass

G3/51 0121204

**C. R. Booth and D. A. Kiefer**

**September 15, 1989**

**Biospherical Instruments Inc  
4901 Morena Blvd., Suite 1003  
San Diego, CA 92117**

(NASA-CR-190879) NEW APPROACHES TO  
THE MEASUREMENT OF CHLOROPHYLL,  
RELATED PIGMENTS AND PRODUCTIVITY  
IN THE SEA Final Report, 1 Apr.  
1986 - 31 May 1989 (Biospherical  
Instruments) 200 p



# Report Documentation Page

1. Report No.	2. Government Accession No.	3. Recipient's Catalog No.	
4. Title and Subtitle  New Approaches to the Measurement of Chlorophyll, Related Pigments and Productivity in the Sea		5. Report Date September, 1989	6. Performing Organization Code
		8. Performing Organization Report No. Tech. Ref. 89-2	10. Work Unit No.
9. Performing Organization Name and Address  Biospherical Instruments Inc. 4901 Morena Blvd., Suite 1003 San Diego, CA 92117		11. Contract or Grant No. NAS7-969	13. Type of Report and Period Covered Final Report, 1 April 1986-31 May 1989
		12. Sponsoring Agency Name and Address  National Aeronautics and Space Administration Washington, DC 20546-0001	
15. Supplementary Notes  Kiefer is at University of Southern California			
16. Abstract  see executive summary			
17. Key Words (Suggested by Author(s))  Fluorescence, photoplankton, chlorophyll, primary production light		18. Distribution Statement  Star category 48(Oceanography)	
19. Security Classif. (of this report) unclassified	20. Security Classif. (of this page) none	21. No. of pages	22. Price

# MATERIAL INSPECTION AND RECEIVING REPORT

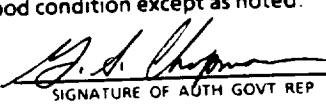
1. PROC. INSTRUMENT IDEN. (CONTRACT) <b>NAS7-969</b>	(ORDER) NO.	6. INVOICE	7. PAGE 1	OF 1
			8. ACCEPTANCE POINT	
SHIPMENT NO.	3. DATE SHIPPED <b>9/26/89</b>	4. B/L TCN	5. DISCOUNT TERMS <b>SBIR - 08.15-1315</b> <b>release date - 4/02/90</b> ✓	

PRIME CONTRACTOR <b>Biospherical Instruments, Inc.</b> 4901 Morena Blvd., Suite 1003 San Diego, CA 92117	CODE	10. ADMINISTERED BY <b>DCASMA San Diego</b> Building 4 AF Plant 19 4297 Pacific Highway San Diego, CA 92110-3289	CODE <b>S0514A</b>
---	------	--	-----------------------

SHIPPED FROM (If other than 9)	CODE	FOB:	12. PAYMENT WILL BE MADE BY	CODE
--------------------------------	------	------	-----------------------------	------

SHIPPED TO <b>NASA Resident Office JPL</b> 4800 Oak Grove Drive Pasadena, CA 91109	CODE	14. MARKED FOR	CODE
---	------	----------------	------

ITEM NO.	16. STOCK/PART NO. <small>(Indicate number of shipping containers - type of container - container number.)</small>	DESCRIPTION	17. QUANTITY SHIP/REC'D *	18. UNIT	19. UNIT PRICE	20. AMOUNT
01		Final Report - New Approaches to the Measurement of Chlorophyll, Related Pigments and Productivity in the Sea.	6 (1 Original, 5 Copies)		.00	.00

<b>PROCUREMENT QUALITY ASSURANCE</b> <b>A. ORIGIN</b> <input type="checkbox"/> PQA <input type="checkbox"/> ACCEPTANCE of listed items has been made by me or under my supervision and they conform to contract, except as noted herein or on supporting documents.		<b>B. DESTINATION</b> <input type="checkbox"/> PQA <input type="checkbox"/> ACCEPTANCE of listed items has been made by me or under my supervision and they conform to contract, except as noted herein or on supporting documents.		<b>22. RECEIVER'S USE</b> Quantities shown in column 17 were received in apparent good condition except as noted. <b>10/4/89</b> DATE RECEIVED  SIGNATURE OF AUTH GOVT REP	
DATE	SIGNATURE OF AUTH GOVT REP	DATE	SIGNATURE OF AUTH GOVT REP	TYPED NAME AND OFFICE * If quantity received by the Government is the same as quantity shipped, indicate by (✓) mark, if different, enter actual quantity received below quantity shipped and encircle.	
TYPED NAME AND OFFICE		TYPED NAME AND TITLE			

CONTRACTOR USE ONLY

## Executive Summary:

In the 1984 SBIR Call for Proposals, NASA solicited new methods to measure primary production and chlorophyll in the ocean. Biospherical Instruments Inc. responded to this call with a proposal first to study a variety of approaches to this problem. A second phase of research was then funded to pursue instrumentation to measure the sunlight stimulated naturally occurring fluorescence of chlorophyll in marine phytoplankton.

The monitoring of global productivity, global fisheries resources, application of above surface-to-underwater optical communications systems, submarine detection applications, correlation, and calibration of remote sensing systems are but some of the reasons for developing inexpensive sensors to measure chlorophyll and productivity. Normally, productivity measurements are manpower and cost intensive and, with the exception of a very few expensive multiship research experiments, provide no contemporaneous data. We feel that the patented, simple sensors that we have designed will provide a cost effective method for large scale, synoptic, optical measurements in the ocean.

This document is the final project report for a NASA sponsored SBIR Phase II effort to develop new methods for the measurements of primary production in the ocean. This project has been successfully completed, a U.S. patent was issued covering the methodology and sensors, and the first production run of instrumentation developed under this contract has sold out and been delivered.

PRECEDING PAGE BLANK NOT FILMED

## Table of Contents:

1. Executive Summary
2. Introduction
3. Background
4. Project Objectives
  - 4.1 Data Review
  - 4.2 Sensor Design, Calibration, and Signal Processing
    - 4.2.1 PNF-300 Vertical Profiling Natural Fluorometer
    - 4.2.2 INF-300 Integrating Natural Fluorometer
    - 4.2.3 Laboratory Fluorostat
    - 4.2.4 Calibration Activities
  - 4.3 Field Testing
    - 4.3.1 Scripps Mooring
    - 4.3.2 Calypso 86
    - 4.3.3 Calypso 86B
    - 4.3.4 BIOWATT II
    - 4.3.5 1987, 1988 Coastal Transition Zone Experiments
    - 4.3.6 Friday Harbor 1987
    - 4.3.7 Calypso 1987
    - 4.3.8 La Jolla 88
    - 4.3.9 SEEP-II
    - 4.3.10 Eureka 88
    - 4.3.11 Ameriez 3
    - 4.3.12 Akademik Akexsandr Nesmeyanov
    - 4.3.13 SCABB '89
    - 4.3.14 SEEP
    - 4.3.15 Key Largo
    - 4.3.16 Charleston Harbor
  - 4.4 Laboratory Research
  - 4.5 Modeling
5. Talks and Publications
6. Applications
7. Further Research
8. Summary
9. Acknowledgements
10. References
11. Appendix 11: PNF-300 Instruction Manual
12. Appendix 12: Pre-print: *"Natural fluorescence of chlorophyll a: Relationship to photosynthesis and chlorophyll concentration in the western South Pacific gyre"*
13. Appendix 13: Submitted Manuscript: *"Evidence for a Simple Relationship between Natural Fluorescence, Photosynthesis and Chlorophyll in the Sea"*

## 2. Introduction

The measurement of primary production in natural waters is of fundamental importance in ecological studies. Despite previous significant advances in the application of optical methods to biological oceanography (such as the remote sensing of sea surface color), direct measurements of primary production have remained expensive, time consuming, and subject to controversy. Primary production measurements of water samples inoculated with  $^{14}\text{C-HCO}_3$  provides ambiguous results, in part due to the poor simulation of ambient light and temperature fields. Thus, prior to the development of the *natural fluorescence* methods describe herein, our ability to gather such fundamental biological information contrasted with the extraordinarily rapid and extensive information gathered by oceanographic satellites.

The first phase of this three phase research project concentrated initially on reviewing three types of fluorometric techniques that were thought to offer the possibility of providing new and more rapid methods for the measurement of primary production and general taxonomic composition. In particular, three new types of fluorometric measurements were considered: 1) short-flash induced fluorescence, used to examine the kinetics of primary photochemistry; 2) multi-spectral fluorescence, used to characterize the taxonomic composition of the crop and photo-adapted state of the cells; and 3) the ambient solar-stimulated fluorescence (hereafter referred to as "Natural Fluorescence"), a natural by-product of light capture by the phytoplankton crop. Natural fluorescence was selected as the most promising method and the second phase ("Phase II") of this effort was proposed and funded by the NASA SBIR program. The third phase, the commercialization of the natural fluorometers, is proceeding well. The first production run of the new instrument has sold out and has been delivered to customers at leading oceanographic institutions.

Early in the Phase I research we realized that the natural fluorometer had the greatest scientific and commercial potential, and we proceeded to develop mathematical models to aid both in understanding natural fluorescence and in designing the instrument. A test platform was constructed and tested for two days at sea. The results of this test indicated that natural fluorescence was easily measured and suggested that the signal may provide accurate and rapid determination of the photosynthetic rate and chlorophyll concentration. For Phase II, we proposed to design and test new natural fluorometers as well as acquire as much information as possible about the relationship between natural fluorescence

and primary production. A new fluorometer (the PNF-300) was then tested in a number of cruises as detailed in section 4.3. Additionally, laboratory tests to verify the fluorescence models were conducted using a new type of laboratory growth system called a "Fluorostat" (see sections 4.4 and 12).

### **3. Background**

Natural fluorescence in the sea, which is the solar-stimulated emission of chlorophyll *a* in a narrow band centered at 683 nm, results from the absorption of light by the phytoplankton crop. Because red light is strongly absorbed by water, and because backscattering in the 683 nm region is low, upwelled solar radiation at the wavelengths of chlorophyll *a* emission disappears within the upper few meters of the water column. The remaining upwelling radiance in this spectral region comes almost entirely from the phytoplankton crop. A number of studies indicate that this fluorescence signal is sufficiently strong to be detected through the euphotic zone. Sugihara et al. (1984) considered Raman scattering as a possible alternate explanation of this signal and rejected it. Since it was first identified as originating from the crop of phytoplankton (Morel and Prieur, 1977; Neville and Gower, 1977), natural fluorescence has been widely investigated as a means for rapidly assessing the distribution and biomass of oceanic phytoplankton. Numerous mathematical descriptions have been presented of the relationship between natural fluorescence, the concentration of chlorophyll *a*, and the ambient light which excites the fluorescence (Gordon, 1979; Kattawar and Vastano, 1979; Kishino et al., 1984 a,b; Topliss and Platt, 1986).

### **4. Project Objectives and Performance**

The main technical objective of this project was to develop new types of instrumentation that permit the rapid measurement of chlorophyll and productivity in the ocean. The path to this objective involved several tasks. These tasks included the review of optical data collected during previous field experiments, the development of sensors and methods of calibration, field testing of these new sensors, laboratory measurements of natural fluorescence to collaborate the field measurements, and modeling activities. Added to these originally outlined tasks was the dissemination of information and the results of our natural fluorescence experiments to the scientific community through talks and publications. The following sections present a step by step discussion of these objectives and how they were met.

## **4.1 Data Review**

Phase II research started with a review of data collected between the close of the Phase I effort (June 1985) and the start of Phase II (April 1986). Originally it was anticipated that the first major piece of data would come from the long term (November 1985 to May 1986) bio-optical mooring that Biospherical Instruments installed in the Scripps Canyon in La Jolla during the performance of a NASA contract to develop Moored Spectroradiometers (Booth, et al. 1987). This project deployed 2 full suites of optical and physical sensors. One set was moored and one was used during profiles several times a week during sampling of biological parameters. Additionally, once a week, in-situ productivity and whole cell absorption spectra were obtained. Unfortunately, a sensor malfunction in one of the 36 channels of the vertical profiling system prevented meaningful natural fluorescence data from being recorded. The moored sensors were also equipped with natural fluorescence detectors and data from these were examined. Since the mooring was at a fixed depth (8 meters) and near-coastal waters and over a canyon, changes in the bio-optical environment at time scales shorter than the incubations complicated comparisons. For this reason, and to acquire data from lower and higher chlorophyll waters, a series of additional field experiments were planned and conducted. These experiments are listed in section 4.3. Several publications and talks resulted from these activities and they are listed in section 5 and in appendices 10 and 11.

As users of the PNF-300 sensor have been returning considerable amounts of data for review at Biospherical, it has become clear that the need for data analysis will continue beyond the extent of this contract. This is apparent considering the differences in results obtained using the MER based natural fluorescence sensors and the PNF-300. At this time we believe these differences are due to the physical sizes of the two sensor systems and the shadow that each casts where the natural fluorescence measurement is made. Geometrical models indicate that a 50% or more reduction in signal from the sensed volume of water may occur when using an MER-based system compared to the much smaller PNF-300. The MER spectroradiometer, with its approximately 14" diameter and a usual assortment of external sensors (salinity, temperature, pump, strobe fluorometer, transmissometer, and lowering frame) casts a large shadow compared to the region of water viewed by its downlooking radiance sensor. The 4" diameter PNF-300 with its wider (approximately two times the field of view) field of view is relatively unaffected by its own shadow when it is lowered by its own cable. While this shadow does not effect the PAR measurement, it does cause the plankton in the water suddenly to undergo a significant reduct in ambient light. This will cause the fluorescence

quantum efficiency of these plankton to appear low and the near surface light and fluorescence relationships to shift.

#### 4.2 Sensor and System Design, Calibration, and Software

Natural fluorescence ( $F_f(t,z)$ ) of chlorophyll *a* at a given depth (*z*) in the water column at time *t* is defined as the flux of light emitted by the chlorophyll in a suspension of phytoplankton of unit volume (units of  $E\ m^{-3}\ sec^{-1}$ ). The basic natural fluorescence sensor is quite simple, being composed of a photocell, optical filter, entrance optics, and amplifier. The bulk of the design effort is in the integration of these elements into a fully functional system that can be immersed in the ocean or used in the laboratory, and that will be useful over the full range of oceanographic concentrations of phytoplankton and levels of sunlight. Additionally, a wide variety of vehicles are used by the oceanographic community to sample the oceans. It is this diverse set of conditions that motivated the development of several forms of natural fluorescence sensors. Beyond all of these elements, the calibration, including the derivation of estimates of rates of photosynthesis and chlorophyll from the measured optical parameters, is of fundamental importance.

The original natural fluorescence sensors we constructed were channels in the upwelling radiance arrays of MER series spectroradiometers, and were designed to have a peak sensitivity at 683nm, the peak emission wavelength of chlorophyll *a* *in-vivo* (see figure 4.2.1). These sensors are also found in the MRP-200 sensors also manufactured by Biospherical Instruments and used in the Scripps Canyon Experiment to assess platform shading. These first natural fluorescence sensors is the "Lu683" interference filter based sensor with a nominal 10 nm spectral width when measured at 50% of the peak response (10nm FWHM).

As we began to obtain data from these sensors in oligotrophic waters, it became apparent that more sensitivity was needed to make meaningful measurements below the frequently deep chlorophyll maximum layer (e.g. 140 meters). For that reason, we decided to develop sensors that had a considerably wider bandwidth and collected most of the light emitted from fluorescence of chlorophyll. This is contrasted with the wider bandwidth (45 nm) sensor labeled "PNF" also in figure 4.2.1. Its performance allows natural fluorescence profiles to as deep as 175 meters in clear waters. Both of these sensors were used in the MER-1064 and MER-2020 instruments used in the Calypso 86 and 87 data sets, and the wider sensor is found in the PNF and INF series natural fluorometers. Descriptions of the dedicated natural fluorometers developed in this project are found in the following sections. A variant of this sensor is used in the laboratory fluorostat.

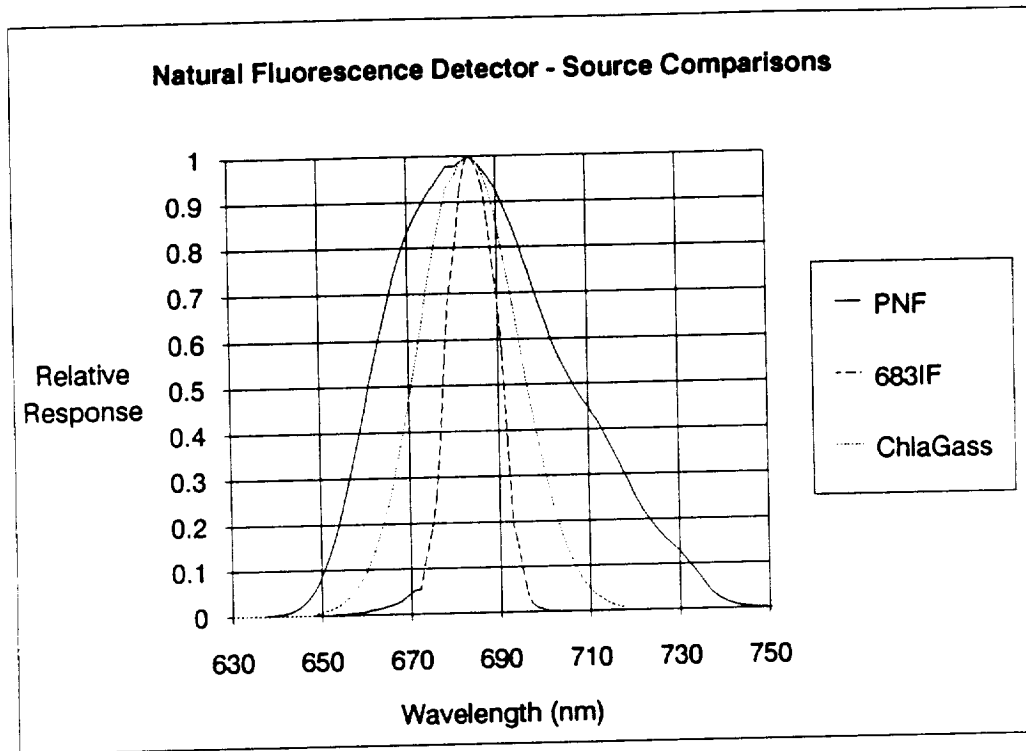


Figure 4.2.1 Spectral response of the Lu(683) MER standard radiance sensor and the PNF/INF natural fluorometer compared to the emission of chlorophyll.

The second difference in the various sensors in the field of view of the MER and PNF/INF series instruments. In the MER, the field of view is approximately 20° in water, but in the PNF/INF this is expanded to more than 30°. The implications of this change in view, combined with the much smaller size of the PNF/INF compared to the MER, render the PNF/INF relatively unaffected by the shadow from the instrument package itself. This contrasts with the sensed natural fluorescence in a typical MER deployment where significant shading exists, altering the perceived relationships of natural fluorescence and photosynthesis.

Natural Fluorescence sensors can be calibrated to report data in several units. Normally, radiance sensors are calibrated in radiometric units of microwatts\*cm<sup>-2</sup>\*nm<sup>-1</sup>. Units of measure more easily related to biological processes and to this particular project are E\*sec<sup>-1</sup>\*m<sup>-2</sup>\*str<sup>-1</sup>, expressing the radiance in terms of the total emission from a source like chlorophyll. This form is referred to here as L<sub>c</sub>. A third way of expressing natural fluorescence that permits direct comparison with carbon fixation rates, is E\*sec<sup>-1</sup>\*m<sup>-3</sup>, the per unit volume emission of photons from chlorophyll fluorescence. This last form is referred to here as F<sub>f</sub>.

The spectral responsivity of the natural fluorescence sensor is called  $R(w)$  and is in units of  $\text{volts} \cdot \text{E}^{-1} \cdot \text{sec} \cdot \text{m}^2 \cdot \text{str}$ ;  $w$ : wavelength in nm. The response of the sensor ( $V$ : volts) to a flux with the emission characteristics of chlorophyll,  $L_c(w)$ , in units of  $\text{E} \cdot \text{sec}^{-1} \cdot \text{m}^{-2} \cdot \text{nm}^{-1} \cdot \text{str}^{-1}$ , can be calculated in terms of a chlorophyll fluorescence signal as shown in equation 1.

$$L_u(\text{chl}) = \frac{V \cdot \int L_c(w) dw}{\int R(w) \cdot L_c(w) dw} \quad (1)$$

With the natural fluorometers, Biospherical Instruments supplies calibration constants enabling the data to be presented as  $L_u(\text{chl})$  from the following equation:

$$L_u(\text{chl}) = (V - \text{NatFlOffset}) / \text{NatFlScale} \quad (2)$$

$\text{NatFlOffset}$  is the sensor voltage when completely dark, and  $\text{NatFlScale}$  is the scale factor in units of  $\text{volts} / (\text{nE m}^{-2} \text{sec}^{-1} \text{str}^{-1})$ .

Calibration of the natural fluorescence sensors at Biospherical Instruments is performed by arranging the sensor being calibrated to view a source of known spectral radiance. This is normally an integrating sphere illuminated by an FEL type incandensent 1000 watt type Standard of Spectral Irradiance. Between the lamp and the sphere is positioned a interference filter with known transmission. Typically, this interference filter has the transmission characteristics shown in figure 4.2.1 (labelled "683IF"). The integrated quantum irradiance of the filter and lamp combination has been independently verified using a quantum detector, providing a double check using two completely independent methods of determining the quantum flux. The PNF-300 is arranged to view (in air) the exit port of the integrating sphere such that the field of view of the PNF-300 is completely filled. The voltage from the PNF-300 is then recorded.

The radiance of the rear surface of the integrating sphere is determined by the following equation

$$L_u(\text{cal}) = \frac{S_t \cdot A_{\text{ent}} \cdot t_f(w) \cdot E_l(w)}{A_{\text{exit}} \cdot \pi} \quad (3)$$

where  $S_t$  is the sphere throughput (a ratio),  $A_{ent}$  and  $A_{exit}$  are the entrance and exit port areas,  $E_l(w)$  is the standard lamp irradiance at the plane of the entrance port of the sphere, and  $t_f(w)$  is the filter transmission. Since the PNF-300 is to be used in water, it is necessary to correct for the change in field of view (FOV) of the detector when it is immersed. Following the analysis of Petzold and Austin (1988), the change in view of a radiance detector can be expressed as the ratio of the squares of the index of refraction of the media in which the device is to be used to the media in which it is calibrated. The scaling of the FOV is independent of the FOV itself. This has been confirmed by tests with in-water radiance sources and small FOV (MER) or large FOV (PNF-300) sensors.

Analysis of natural fluorescence data in  $L_u(chl)$  or radiance form is appropriate when the instrument is viewing a calibration source, or other sources such as planar corals or algal mats. In these cases, the measurement assumes that the source is a Lambertian emitter and the measurement represents the rate at which photons are emitted from that surface, per unit solid angle (steradian), and per unit surface area of the surface ( $m^2$ ). In such analysis, when working in water, it is necessary to account for the losses of the signal due to absorption by water using the Lambert-Beer relationship. In this case, following the discussion below, the absorption coefficient may be approximated by  $0.48 \text{ meters}^{-1}$ .

The natural fluorescence  $F_f(t,z)$  at time  $t$  and depth  $z$  for the volume of water that the sensor is viewing is calculated from the following relation:

$$F_f(t,z) = 4 * \pi * (k(PAR,t,z) + a(chl,t,z)) * L_u(chl,t,z) \quad (4)$$

where  $k(PAR,t,z)$  is the diffuse attenuation coefficient for scalar irradiance integrated over the spectral region of 400-700nm (Kiefer, et al, 1989).  $k(PAR,t,z)$  accounts for the attenuation of exciting irradiance as a function of depth below the sensor and is calculated from the vertical profile of PAR. The term  $4 \pi$  is a geometrical constant with the units of (1/steradians) used in transforming the radiance to a volume emission. The term  $a(chl,t,z)$  is the total absorption coefficient of the water plus constituents and this term accounts for the decay of the sensed signal as a function of distance from the sensor.  $a(chl)$  is a composite quantity composed of the sum of the absorption coefficients weighted by the spectral distribution of the emission of chlorophyll:

$$a(chl) = a_w(chl) + a_d(chl) + a_c(chl) + a_y(chl) + a_o(chl) \quad (5)$$

where  $a_w(\text{chl})$ ,  $a_d(\text{chl})$ ,  $a_c(\text{chl})$ , and  $a_y(\text{chl})$ , and  $a_o(\text{chl})$  are the absorption coefficients for pure water, detritus, chlorophyll, yellow substance, and other pigments, respectively. This weighting is calculated by

$$a(\text{chl}) = \frac{\text{Integral } (a_x(w) * L_c(w)) dw}{\text{Integral } L_c(w) dw} \quad (6)$$

where  $L_c(w)$  expresses the weighting factor describing the fluorescent emission of chlorophyll for each of the absorption components, and the various components of the absorption coefficient are represented by  $a_x(w)$ .

To evaluate the variability of the absorption coefficients in equation 4 we used particulate spectral absorption data  $a_p(w)$  (where  $a_p(w) = a_o(\text{chl}) + a_c(\text{chl}) + a_d(\text{chl})$ ) recorded for the Biowatt II data set and for data from an earlier cruise transect from Tahiti to New Zealand (Kiefer et al; 1989). The particulate absorptions,  $a_p(\text{chl})$ , is the sum of the detrital and plankton components, weighted as in (5) above. From these data we concluded that  $a_p(683)$  is not significantly different ( $r = .9999, n = 44$ ) from  $a_p(\text{chl})$ . Furthermore, comparison of the values of  $a_p(\text{chl})$  (mean = 0.0155, sigma = 0.00817) are much less than the values of  $a_w(683)$  (0.46, see Smith and Baker, 1981). A review of the literature (e.g. Kishino, et al; 1984) indicates that values of  $a_y(683)$  is much less than  $a_w(683)$ . For those reasons, in the natural fluorometer software we use the value of 0.5 for  $a(\text{chl})$ . This parameter is read from a calibration file and may be modified by the user, which may be necessary in highly turbid waters.

The signal from the natural fluorescence sensor  $L_u(\text{chl}, t, z)$  is a combination of signals from other sources in addition to the fluorescence of phytoplankton. These sources may include backscattered sunlight, raman scattering, and bioluminescence. Based on Sugihara (Sugihara, et al; 1984), we reject raman scattering, and judge only backscattered sunlight to be significant at these wavelengths, and only within the top few meters of the water column. To calculate the contribution to the  $L_u(\text{chl})$  signal due to backscattering, the following relationships are developed.

Austin (1974) has defined the parameter "Q" to describe the relationship between irradiance and radiance reflectance R:

$$R = \frac{E_u}{E_d} = \frac{L_u * Q}{E_d} \quad (7)$$

Using reflectance approximations developed by Morel and Prieur (1977),

$$R = \frac{1 - b_b}{3 (b_b + a)}, \quad (8)$$

and Smith's (1981) value for clearest natural waters,  $a(680) = .45$  and  $b_b = .0007$  (both meters<sup>-1</sup>), we can state the upwelling radiance  $L_u$  as a function of downwelling irradiance as the same wavelength:

$$L_u(w) = \frac{b_b(w) * E_d(w)}{3 * (b_b(w) + a(w)) * Q(w)} \quad (9)$$

If the light field were totally diffuse, then  $Q = \pi$  (steradians), and in the case where sidescattered downwelling irradiance makes an appreciable contribution, the value of  $Q$  will increase. The following restatement of (9) uses values of  $Q = \pi$  and the above cited absorption and backscatter coefficients:

$$.00016 = \frac{L_u}{E_d} \quad (10)$$

Examination of the behavior of equation 9 for realistically larger values of  $b_b(w)$ ,  $Q(w)$ , and  $a(w)$  will drive the factor in equation (10) downward toward the value of 0.0001 str<sup>-1</sup>. Figure 4.2.2 shows this ratio obtained in various profiles in the south Pacific there the surface chlorophyll a concentration ranged from .023 to .46 ug/l. Note that at all points the ratio is above 0.0001 and increasing with depth. We interpret this to mean that natural fluorescence is the dominant component of the upwelling radiance signal at 683 nm.

To evaluate the effect of this backscattered component as a function of depth, a reflectance value for seawater at 683 nm,  $R(683)$ , of 0.00016 as described above is used in calculating the upwelling radiance from reflected sunlight at depth  $z$ :

$$L_u(683,z)_b = E_d(683,0) * .00016 * e^{(-k(683)*z)} \quad (11)$$

where  $E_d(683,0)$  is the downwelling irradiance just below the surface. For depths greater than 2-5 meters,  $L_u(chl,z) \gg L_u(chl,z)_b$ , and thus the backscattered component can be neglected. In the natural fluorometer software, we consider  $L_u(chl,z)_b$  to be 0 for all depths. If experience shows that this is not a satisfactory assumption, then we suspect that a robust inference about the level of  $L_u(chl,z)_b$  could be drawn from measurements of  $E_o(PAR)$  and  $k(PAR)$  as measured with the PNF/INF-300.

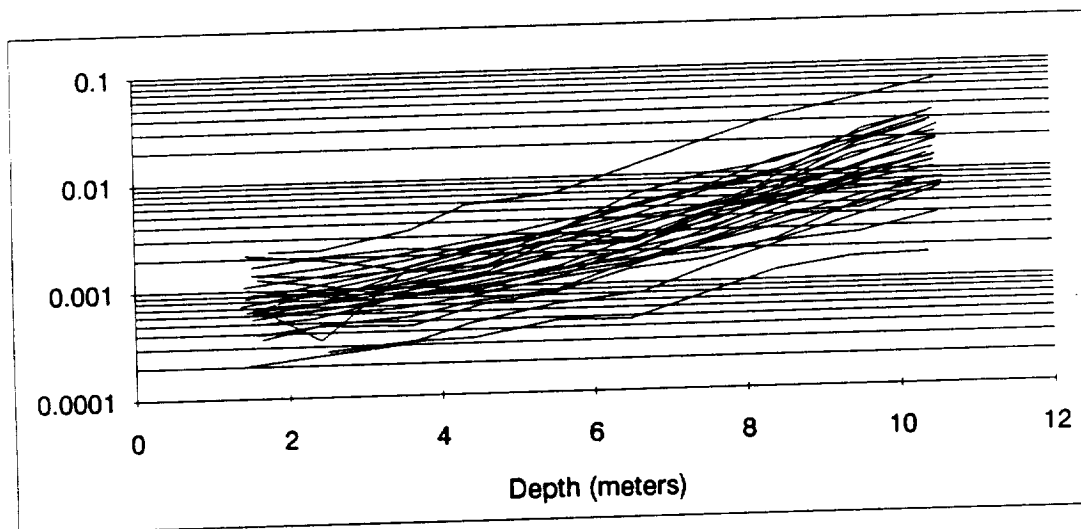


Figure 4.2.2. This is a plot of the ratio of  $L_u(683)/E_d(683)$  as a function of depth for various profiles the cruise Calypso86. Each line is one separate profile, 26 profiles in total. The data have been heavily smoothed to remove surface wave induced variation.

The relationship between natural fluorescence and photosynthesis will depend upon the probabilities that the light absorbed by a cell will be immediately transformed into either heat, fluorescence, or photochemical work. This simple relationship may be expressed phenomenologically:

$$F_f(t, z) = O_f(t, z) * F_a(t, z) \quad (12)$$

$$F_c(t, z) = O_c(t, z) * F_a(t, z) \quad (13)$$

$$F_c(t, z) = O_c(t, z) / O_f(t, z) * F_f(t, z) \quad (14)$$

where  $F_c(t, z)$ ,  $F_a(t, z)$ ,  $O_c(t, z)$ , and  $O_f(t, z)$  are, respectively, the rate of photosynthesis ( $\text{g-at C} \cdot \text{m}^{-3} \cdot \text{sec}^{-1}$ ), the rate of light absorption ( $\text{E} \cdot \text{m}^{-3} \cdot \text{sec}^{-1}$ ), the quantum yield of photosynthesis ( $\text{g-at C fixed/E absorbed}$ ), and the quantum yield of fluorescence ( $\text{E emitted/E absorbed}$ ). Since the instantaneous rate of light absorption,  $F_a$ , appears in both equations 7 and 8, its variability will cause proportional changes in both natural fluorescence and photosynthesis. This also makes natural fluorescence production estimates insensitive to the complications of accessory pigments.

In order to improve the predictive capability of natural fluorescence measurements, we have found a simple empirical formulation that relates the ratio of photosynthetic and fluorescence quantum yields to the irradiance of PAR:

$$F_c(t, z)/F_f(t, z) = O_c(t, z)/O_f(t, z) = (O_c/O_f)_{\max} * kcf / (kcf + E_o(\text{PAR}, t, z)) \quad (15)$$

$(O_c/O_f)_{\max}$ , an empirical constant, is the maximum value of the ratio of quantum yields, and  $kcf$ , another empirical constant, is the value of irradiance when the ratio is equal to half of its maximum value. An analysis of data from several cruises in which the MER series spectroradiometers were used gives "best fit" values for  $(O_c/O_f)_{\max}$  of 2.3 Carbon atoms/photon and  $133 \text{ mE m}^{-2} \text{ sec}^{-1}$  for  $kcf$ . Both of these parameter estimates are read from the calibration file of the PNF-300 or INF-300 and can be modified as necessary. The form of this equation that is used by the Natural Fluorometer software is

$$F_c(t, z) = (O_c/O_f)_{\max} * kcf * F_f(t, z) / (kcf + E_o(\text{PAR}, t, z)) \quad (16)$$

The correlation coefficient for the above mentioned data set for a multiplicative regression using equation 11 is 0.95, the slope is approximately 1, and the standard error of the estimate is 0.48. The difference between predicted and observed rates of photosynthesis indicate that 9 out of 10 predictions were within 65% of the measured rate. Due to shading that occurs with the MER series instruments, it will be necessary to modify the values for constants  $(O_c/O_f)_{\max}$  and  $kcf$  when calculating  $F_c(t, z)$  with equation 16 of 2.3 Carbon atoms/photon and  $133 \text{ mE m}^{-2} \text{ sec}^{-1}$  for  $kcf$ .  $(O_c/O_f)_{\max}$  will approach 1 due to shading and we suspect that  $kcf$  will also fall.

The natural fluorometer may also be used to predict the concentration of chlorophyll, although at reduced accuracy. As demonstrated by Gordon (1979),

Topliss (1985), and particularly Kishino and co-workers (1984a,b), the relationship between chlorophyll concentration and natural fluorescence is determined by the natural fluorescence coefficient, the quantum yield of natural fluorescence, and the mean chlorophyll *a* specific absorption coefficient for the phytoplankton crop:

$$\text{chl}(t, z) = Y_f(t, z) / ({}^\circ\text{ac}(\text{PAR}, t, z) * O_f(t, z)) \quad (17),$$

$$Y_f(t, z) = O_f(t, z) * \text{ac}(\text{PAR}) \quad (18)$$

Where  $Y_f(t, z)$  is the natural fluorescence coefficient, (following Gordon, 1979) with units of  $\text{m}^{-1}$ .  $Y_f(t, z)$  is simply calculated by dividing  $F_f(t, z)$  by  $E_o(\text{PAR}, t, z)$  yielding a method of calculating chlorophyll:

$$\text{chl}(t, z) = F_f(t, z) / (E_o(\text{PAR}, t, z) * O_f(t, z) * {}^\circ\text{ac}(\text{PAR}, t, z)) \quad (19).$$

The MER based data set referred to above allowed the prediction of  $\text{chl}(t, z)$  with a  $R^2 = 87.6\%$  ( $n = 77$ ) using a value of .453 for the product  $O_f(t, z) * {}^\circ\text{ac}(\text{PAR}, t, z)$ .

This data set included the effects of shading so  $O_f(t, z)$  was suppressed. It should be noted that there is no single value of  ${}^\circ\text{ac}(\text{PAR}, t, z)$  can be found since the spectral distribution that is integrated to compute PAR is constantly changing with depth and other factors. An expansion on this topic can be found in Collins, et. al., 1988 where it is shown that this parameters varies as a function of depth and the spectral distribution of irradiance (and thus chlorophyll concentration). Furthermore, the value  $O_f(t, z)$  is known to change with nutrients and light level.

The natural fluorometer software provides fully for the entry of the fluorescence efficiency  $O_f(t, z)$  or "QE(f)", and for the chlorophyll specific absorption coefficient  ${}^\circ\text{ac}(\text{PAR}, t, z)$  or "ac(PAR)". This is also true for the constants  $(O_c/O_f)_{\text{max}}$  kcf used in equation 16, making it easy for the customers to update their software as needed.

#### 4.2.1. PNF-300 Profiling Natural Fluorometer.

One of the main goals proposed in the original Phase I proposal was: "An overriding consideration in the examination of these components [of a new fluorometer] will be the cost and availability since the goal of this project is not to produce the most exotic oceanographic instrument but to produce one whose cost makes it easily accessible to the oceanographic community." The centerpiece instrument system developed under this contract is the PNF-300 Profiling Natural Fluorometer. This instrument system is a hand-lowered microprocessor-controlled sensor system offered in a turn-key configuration. This configuration includes the underwater sensor system with natural fluorescence, PAR, temperature, and depth sensors, a surface hemispherical scalar PAR irradiance sensor, battery power, cables, lowering frame and complete software. It has been deployed from an inflatable boat using a laptop computer and from large oceanographic ships. This instrument is now in full production and the first production run has been delivered to customers at major oceanographic institutions. It shows every sign of being a commercial success for Biospherical Instruments while providing both NASA and the oceanographic community in general with a powerful, yet inexpensive new research, survey and monitoring tool. The instruction manual for this instrument is found in Appendix 11 and the reader's attention is directed there for information on the instrument design, methods of use, and a full description of the software. Since this is not only a new instrument, but a new methodology, considerable effort was devoted to this instruction manual.

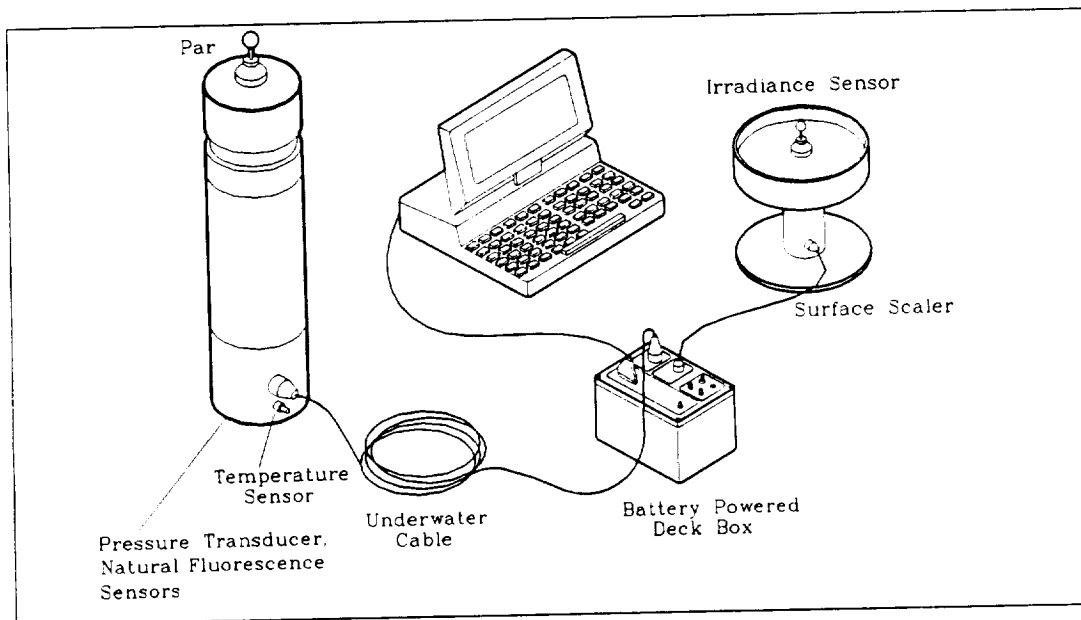


Figure 4.2.1. The PNF-300 Natural Fluorometer. The normally included lowering frame is not shown. The laptop computer is optional. Normal selling price is \$9450 complete except for computer.

The PAR sensors incorporated into the PNF-300 (and the INF-300) are improvements on the previous products of Biospherical Instruments (see Booth, 1974). They have been modified to improve both the spectral response conformity to PAR and to improve calibration stability.

Software for the PNF-300 instrument permits two modes of operation. The first mode, for vertical profiles, has full graphical display of all parameters during the cast, along with recording to disk or printer. The second mode of operation, which can be concurrently with the first mode, permits continuous integration of natural fluorescence and PAR, with optional recording of these integrals at user defined intervals. This permits the user to operate the instrument in several modes. First, between vertical profiles, the instrument can be continuously monitoring incident irradiance and both computing and displaying the daily irradiance integral, periodically recording the progress of this daily integration. If an *in situ* incubation is being conducted in close proximity of the ship, then the underwater PAR and natural fluorescence integrals are also recorded along with average temperature.

Software is also provided for the playback of vertical profiles, with calculation of the diffuse attenuation coefficient ("k") for PAR, calculated photosynthesis, and calculated chlorophyll concentration. These data are presented in both graphic and numerical form.

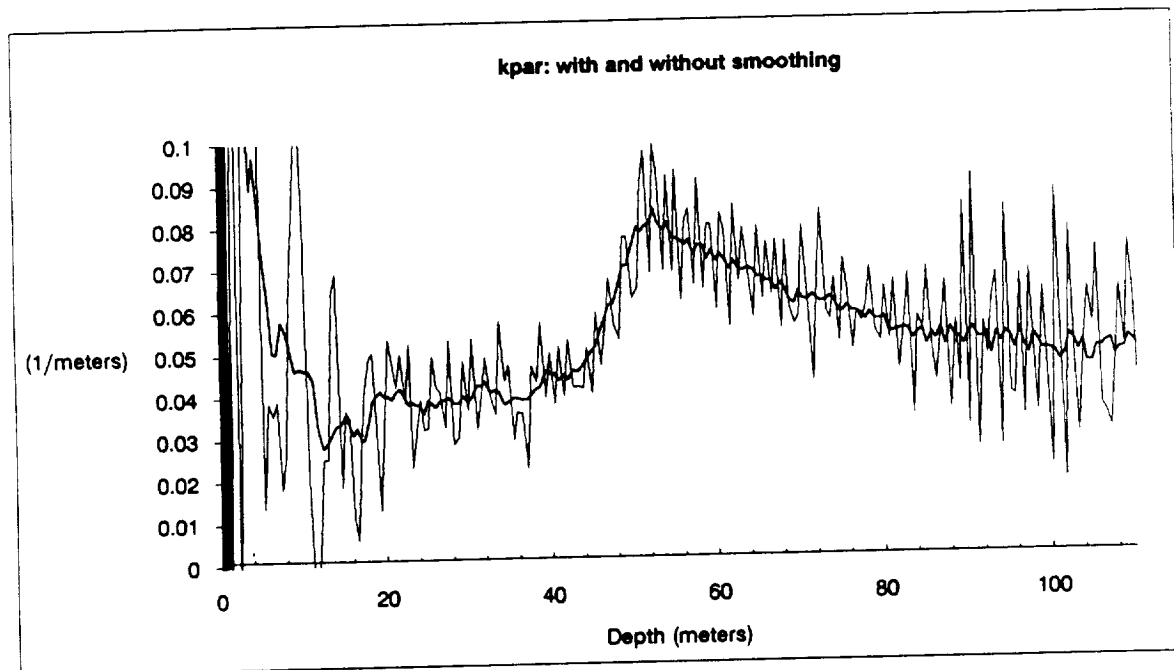


Figure 4.2.2.  $k(\text{PAR})$  as recorded by the PNF-300 and showing the results of applying smoothing to the calculation. This moving window linear smoothing is a user selectable feature of the PNF-300 software.

### 4.2.3. INF-300 Integrating Natural Fluorometer

The second new sensor that was developed under this contract is the INF-300 Integrating Natural Fluorometer. During the analysis of data in this contract, it became apparent that a version of the PNF-300 that could be attached to *in situ* incubation buoys at various depths would be superior to vertical profiling instruments like the PNF-300 when intercomparisons of productivity measurements

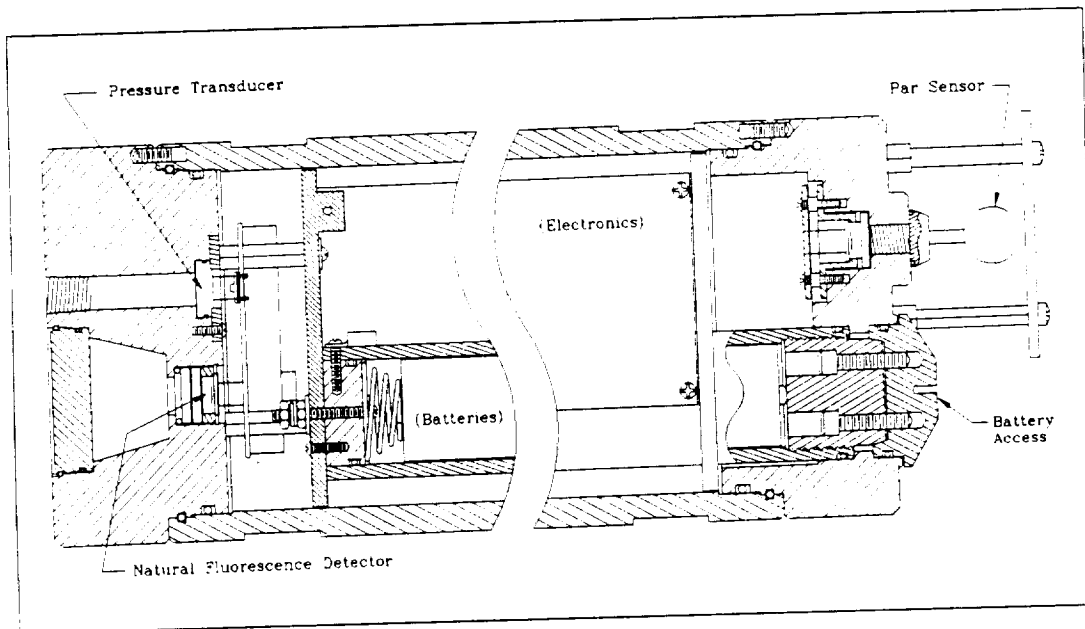


Figure 4.2.3. The INF-300 Integrating Natural Fluorometer shown in cutaway. Overall size is 5.25" diameter by 17.5".

were needed (while the MER-2020 could be used for this purpose, it is large and expensive, both to obtain and to use). Figure 4.2.3 shows the results from multiple profiles of natural-fluorescence throughout one day during the Calypso 87 cruise. These profiles were all made during one  $^{14}\text{C}$  incubation. We had only one MER-2020 available so the highest accuracy photosynthesis comparisons were made at only one depth and considerable assumptions were needed to fill in the gaps in vertical and temporal resolution at the other sampled depths.

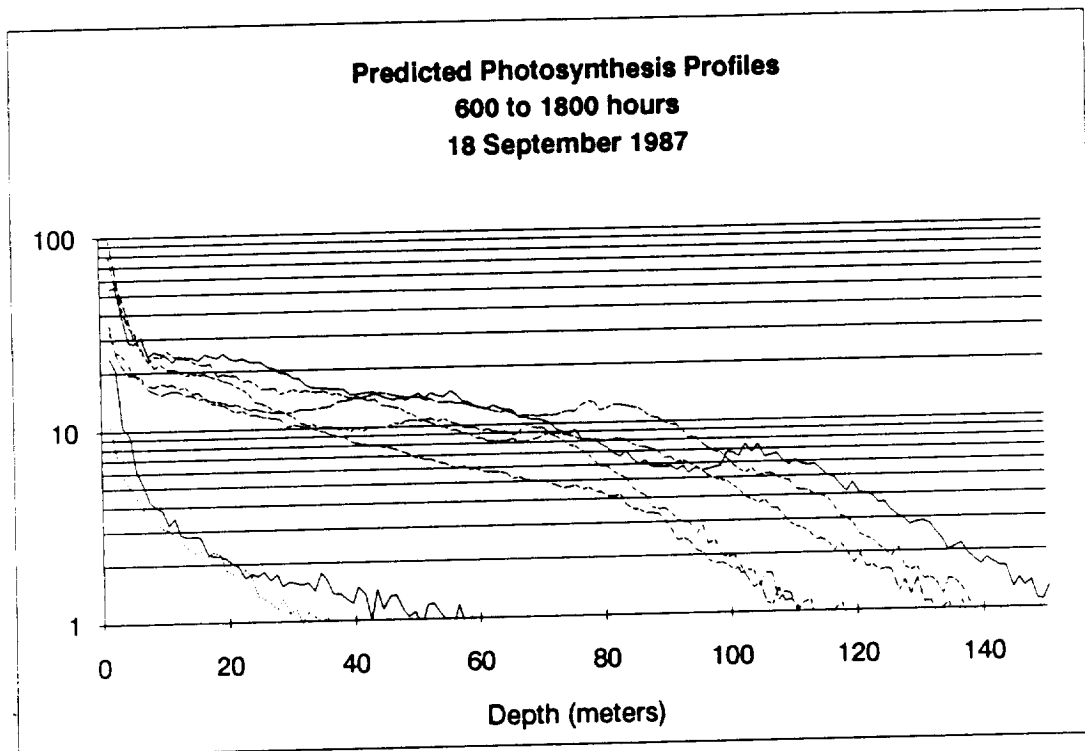


Figure 4.2.3 Repeated vertical profiles of natural fluorescence made during *in situ* incubations on Calypso 87 off Tahiti. Units are  $nE\ m^{-3}\ sec^{-1}$

This suggested that an internally recording version of the INF-300 might speed the acceptance of the natural fluorescence technique by greatly facilitating direct comparisons with  $^{14}C$  techniques. Additionally, potential customers first exposed to the PNF-300 frequently asked for methods of deploying an inexpensive system on short term moorings or drifters.

This instrument, although started late in the contract and still undergoing final development, already has booked orders. We foresee additional applications of this sensor, possible with relatively minor modifications, in deployments of drifters. This is an important oceanographic data gathering means that could be not addressed with the PNF-300. We anticipate that this sensor will also be a commercial success and we are devoting considerable company resources to insure its completion.

In the INF-300 development, we initially intended on designing natural fluorescence sensors that could be integrated with most types of oceanographic systems: CTDs, current meters, moored buoys, drifters, etc. We have found no standardization on sensor and power interfaces for such instruments. We also found that the wide dynamic range (approximately the range in chlorophyll concentration times the range in light levels found) requirements of our natural fluorescence

sensors would not easily be interfaced with the widely varying types of oceanographic systems and that a versatile solution would be to build an entirely self-contained and internally recording sensor that could "piggy-back" on other systems. This is an additional role anticipated for the INF-300.

#### 4.2.3. Laboratory Fluorostat

In order to obtain confirmation of the relationship of natural fluorescence to primary photosynthetic production, we needed to develop a method to study natural fluorescence under laboratory conditions. This meant that we needed a method of creating a miniature, "optically correct" ocean in the laboratory in such a manner that it could be maintained in continuous state for periods of weeks while careful monitoring of growth and natural fluorescence was conducted as nutrients and light was controlled.

The fluorostat is composed of a 2 liter water jacketed cylindrical glass reaction chamber with multiple optical ports. The chamber is illuminated from below with an intensity and spectrally controlled light source able to reach irradiance levels typical of near surface waters at midday. A nominally 2 cm diameter modulated tunable monochromatic light source irradiates a selected portion of the chamber that is also viewed by a photomultiplier based radiance telescope. This allows the measurements of natural fluorescence from both the growth light and the much dimmer monochromatic source.

The system is typically used to grow organisms (typically Dunaliella) under steady state conditions. Natural fluorescence changes are monitored with changing light and nutrient levels. A fuller description of this is found in section 4.4.

#### 4.2.4. Calibration Activities:

The final area of the engineering effort was to refine calibration techniques that allow higher accuracy and easier spectral radiance calibrations of the radiance sensors. One of the key advantages of the natural fluorescence technique is that the sensor can be calibrated using optical standards traceable to the National Institute of Standards and Technology (NIST). This allows consistent performance of the sensors and should provide a solid basis for years of intercomparability in monitoring long term trends in oceanic productivity.

Calibration of a natural fluorescence detector is more complicated than the calibration of a normal irradiance or radiance sensor. In the natural fluorescence

sensor, the desired calibration factor will specify how the sensor responds to a light source with a spectral distribution matching the *in vivo* emission spectra of chlorophyll *a*.

In the progress of this contract, several methods of calibration have been explored. The first calibrations that we tried were required positioning a Lambertian reflectance surface a known distance from a 1000 FEL type Standard of Spectral Irradiance and orienting the natural fluorescence detector to view this surface. The resulting radiance of the surface was then calculated from the irradiance of the standard lamp. The second approach used involves positing the entrance port of an integrating sphere at a specified distance from the standard lamp. The natural fluorescence radiance detector is oriented to view the interior of the sphere whose radiance can be calculated based on the sphere properties. It is this second approach that is normally used in calibration of the natural fluorescence detectors based on the 10 nm wide 683 nm interference filter. From a measurement of the spectral responsivity of the detector and its integral filters, a computation can be made of the detector's response to a source with the presumed spectral distribution of chlorophyll *a*.

The calibration method used for the PNF-300, which uses a significantly wider spectral bandpass for additional sensitivity, is based on using the integrating sphere with a calibrated interference filter. This method contrasts to the filterless technique as this technique is very dependent on a highly accurate determination of the spectral responsivity of the detector under calibration. In this method, the calibration source is made to resemble the source that will be measured in the field, that is, the distribution of fluorescence from chlorophyll.

### **4.3 Field Testing**

In the development of any new technique in research science, a considerable period of scientific scrutiny is inevitable before the technique is embraced. We have addressed this problem by devoting resources to putting prototype instruments into the hands of leading researchers in exchange for their feedback. This has led to participation in a number of cruises and experiments, considerably contributing to the success of this effort. With the exception of a cable failure, the hardware all functioned well, although considerable refinement in the operating software was suggested and subsequently incorporated and tested during the course of the experiments.

4.3.1. Scripps Mooring: Between November 1985 to May 1986 on a mooring

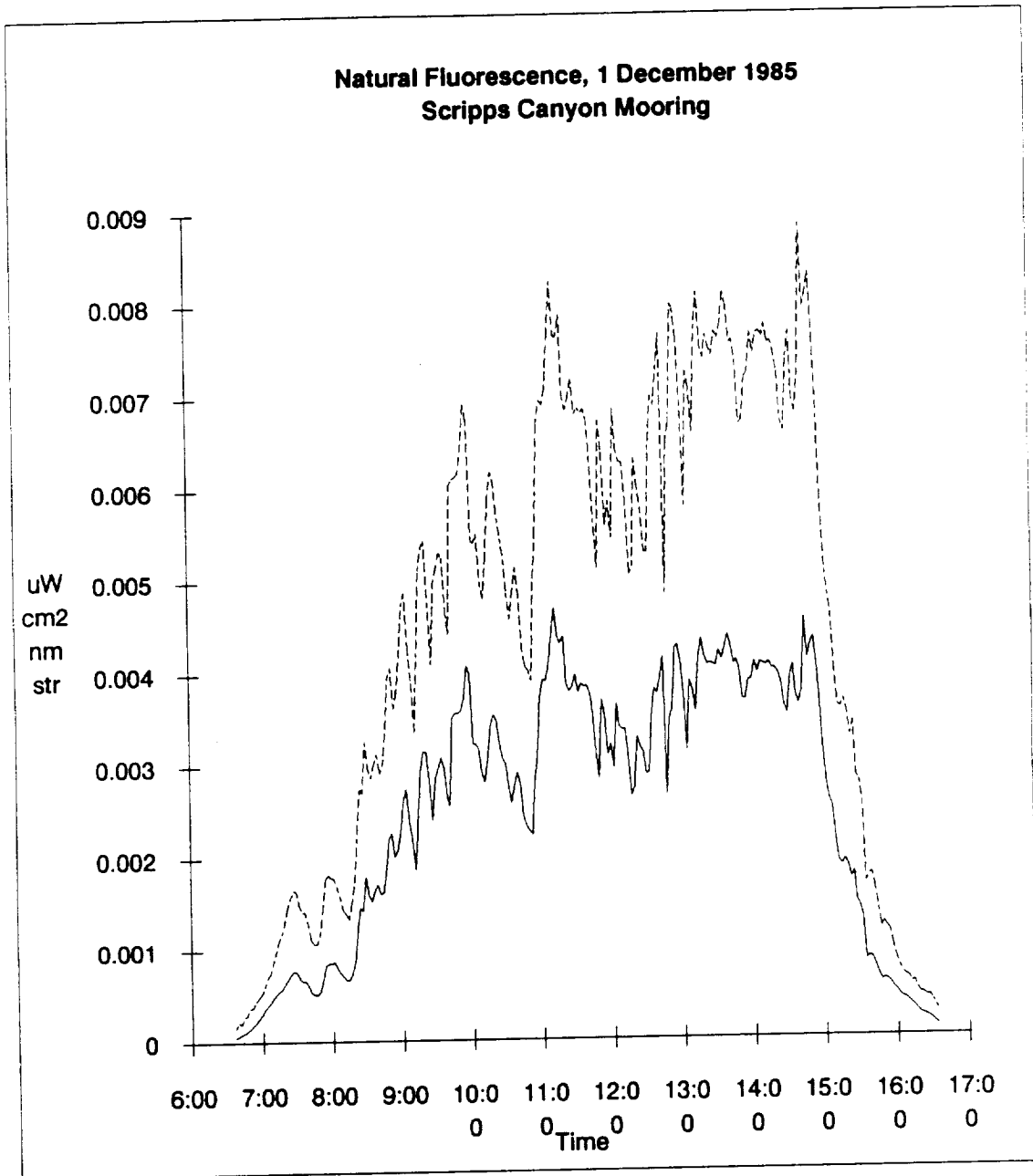


Figure 4.3.1. The course of natural fluorescence as recorded from the mooring 8 meters deep at the Scripps Canyon. The upper trace is the radiance sensor oriented to look slightly out of the shadow cast by the mooring platform. The lower trace is the radiance channel installed in the MER mounted in the center of the platform. Units of radiance at 683 nm.

located 1 km west of Scripps Institute of Oceanography in La Jolla, California, Biospherical Instruments installed a test platform to support the development of moored spectroradiometers (Booth, et al; 1987). In anticipation of receiving Phase

II support for this project, two predecessors of the natural fluorescence sensor were "bootlegged" onto the platform in the hope that a detailed study of natural fluorescence would be funded. A similar sensor was installed on a vertical profiling spectroradiometer deployed during periodic casts. This data has been of limited value for natural fluorescence studies because subsequent analysis has shown that the vertical profiling sensor was defective (non-linear). Consequently, only the natural fluorescence detectors on the mooring were of use, and only the *in situ* incubations occurring at the same depth are of use. Analysis of this data set is proceeding under a NASA contract to O. Holm-Hansen and B. Greg Mitchell at Scripps Institution of Oceanography with consulting by C. R. Booth.

4.3.2. **Calypso 86:** From November 29 to December 10, 1986, Booth, Kiefer, and S. Chamberlin joined R. C. Murphy of the Cousteau Society aboard the Calypso during a transect from Papiette, Tahiti to Auckland, New Zealand. The Cousteau Society made approximately 48 hours of shiptime available for our natural fluorescence studies and during that time several stations were occupied. Heavy seas prevented work during approximately one half of the cruise, but the instrumentation involved performed well. Instrumentation that was deployed included an MER-1064 Spectroradiometer modified with experimental natural fluorescence sensors. The first prototype natural fluorescence profiling system was also deployed in comparison with the MER bases sensors. During this cruise, an unsatisfactory attempt was made to use  $^{13}\text{C}$  based production measurements for comparison purposes. Details of this cruise are found in a preprint of a paper accepted by Limnology and Oceanography attached at the end of this report.

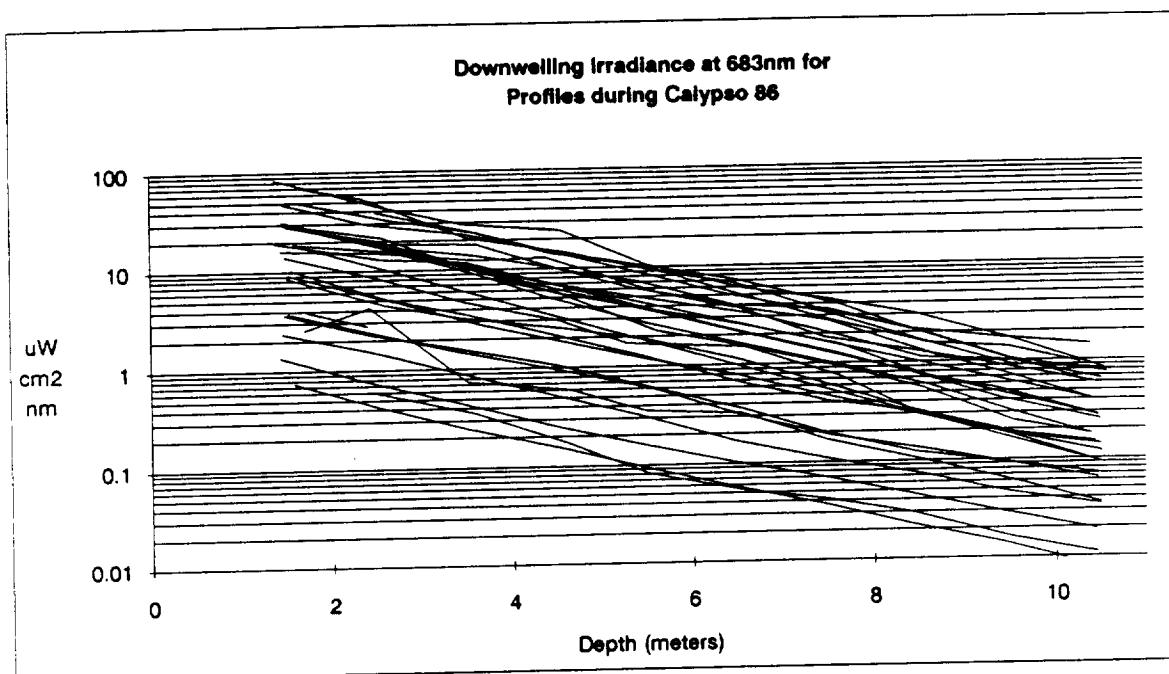


Figure 4.3.2 Downwelling irradiance (683nm) profiles during Calypso 86. Mean  $k(E_d(683))$  for these 26 profiles is  $0.482 \text{ meters}^{-1}$ . This contrasts with an average  $k(E_u(683))$  of  $0.143$  for the same casts.

**4.3.3. Calypso 86B:** After the successful tests of the first prototype natural fluorometer described above, this prototype was loaned to the Cousteau Society for use during their exploration of New Zealand and other waters of the south-western Pacific. Unfortunately, during a severe storm, the instrument was lost at sea. As a result of the experiences with the instrument on the first Calypso expedition, we decided not to duplicate the original prototype, but to redesign completely the packaging to take advantage of lower priced pressure transducers and to create a package more conducive to being lowered by hand with its own conducting cable.

**4.3.4. BIOWATT II:** The ONR funded BIOWATT II program provided the next opportunity for natural fluorescence studies when we were asked to provide 8 MER-2020 moored spectroradiometers for R. C. Smith of UCSB. We suggested including our natural fluorescence optical sensors in the upwelling radiance array of these instruments and Dr. Smith accepted, giving us access to the resulting data. To be more completely coupled into the BIOWATT II project, and to obtain the primary production data being collected by J. Marra of Lamont-Doherty, we also volunteered the use of the MER-1064 modified for natural fluorescence as used on Calypso 86. Thus, from BIOWATT II, we obtained the February 1987 to May 1987 moored time series, and extensive vertical profiled data from May and August of 1987. Natural fluorescence data during the entire 10 month mooring have been presented in talks by Smith, and also featured in an "Ocean Optics IX" presentation

by Booth and Smith titled "Moorable Spectroradiometers in the BIOWATT Experiment" that is appended here. A more detailed treatment of the BIOWATT data comparisons with in situ incubations is currently under preparation by Smith.

**4.3.5. 1987, 1988 Coastal Transition Zone Experiments:** Mark Abbott (OSU) and Booth jointly prepared and deployed (with C. Davis's help) a MER-2020 spectroradiometer with experimental natural fluorescence sensors, a strobe fluorometer, and beam transmissometer, during a 10 day period in June 1987 and for second, similar deployment in 1988. The instruments were mounted on a drifter and followed the evolution of a recently upwelled parcel of water off the central California coast. This configuration enabled us to compare directly strobe fluorometer and Natural Fluorescence sensors along with the transmissometer. Supporting data was taken by C. Davis (JPL) with a vertical profiling system. While these cruises provided for interesting comparisons with strobe fluorometers, *in situ* productivity data was not obtained. Results of these experiments have been submitted for publication by Abbott.

Figure 4.3.5 shows the 1987 drifter time record of PAR (computed from spectral irradiance) and calculated photosynthesis. It is interesting to note the decreasing rates of photosynthesis relative to irradiance during this series.

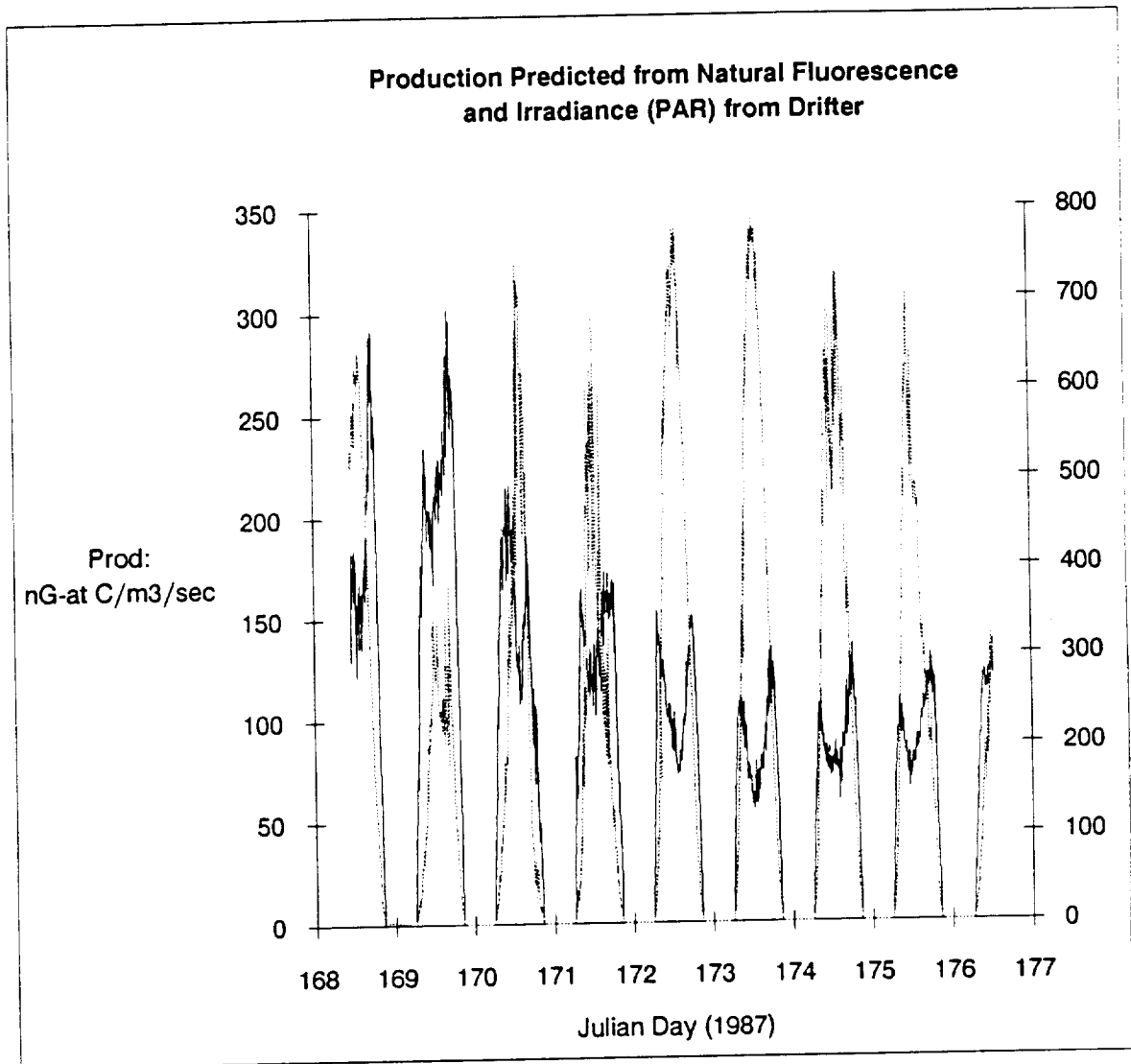


Figure 4.3.5. Predicted photosynthetic production time series from drifter during 1987 Coastal Transition Zone Experiment. Production (solid line) predicted from equation 16. PAR (dashed line and right axis, in  $\mu\text{E}/\text{m}^2/\text{sec}$ ).

4.3.6. Friday Harbor 1987. In July of 1987, Booth was invited to join scientists from JPL (D. Collins and C. Davis) at the end of the Marine Optics course run by the University of Washington. Two experiments were performed. First we installed a MER-2020 modified for natural fluorescence in a dockside mooring at a depth of 3 meters for a period of one week. We also deployed JPL's MER-1048 in a carefully controlled vertical profile from dockside in a manner that allowed centimeter resolution in a vertical profile. This vertical profile in almost perfectly calm water allowed a highly precise determination of the diffuse attenuation coefficient at 683nm, a parameter critical to the proper utilization of natural fluorescence data (Figure 4.3.6a). At the same deployment, R. Davis and M. J. Perry

(U. of W.) conducted several *in situ* dock-side incubations using  $^{14}\text{C}$  methods (Figure 4.3.6b). Results of these experiments were presented at the ASLO New Orleans meeting in 1988, and are included in the data set discussed in Appendix 13.

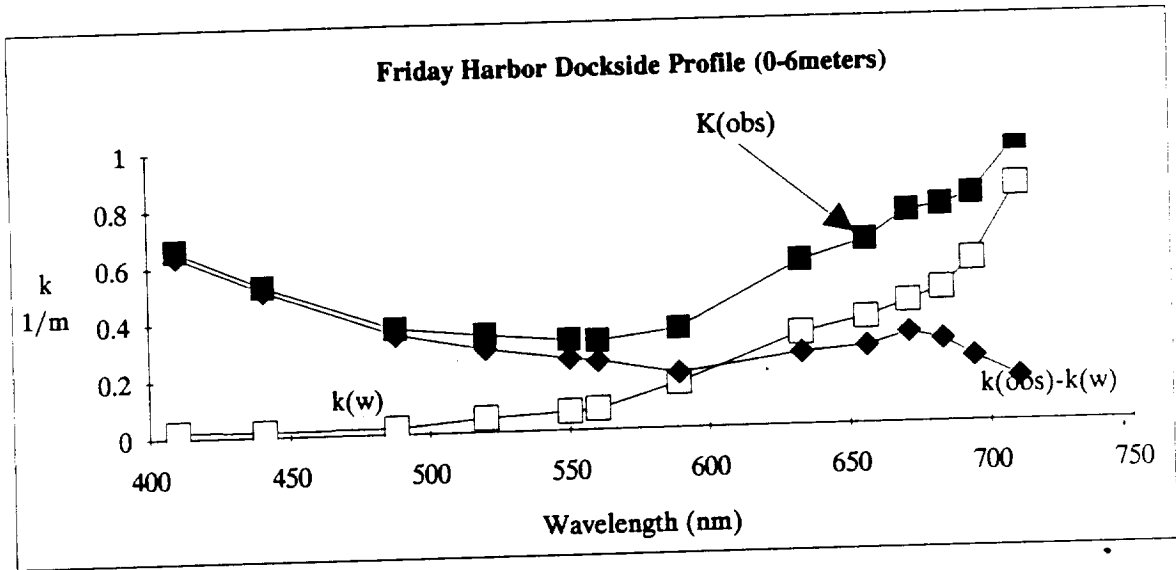


Figure 4.3.6a. Diffuse attenuation coefficients determined from a docksides vertical profile of downwelling irradiance at Friday Harbor. Solar zenith angle  $40^\circ$ ; beam transmission = 68% (.25m); chlorophyll concentration 4  $\mu\text{g/l}$ ;  $k(\text{PAR})$ , 0-6 meters,  $0.412\text{m}^{-1}$ .

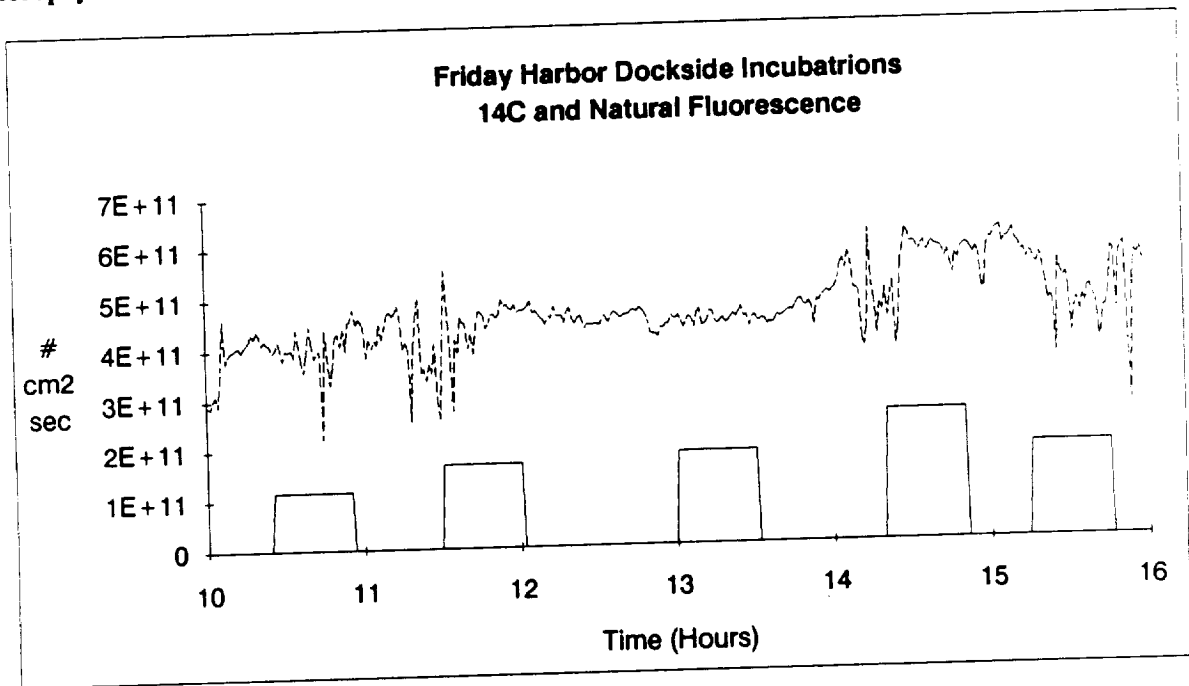


Figure 4.3.6b Docksides halfhour incubations compared with natural fluorescence measurements. Incubations were conducted at a depth of 5 meters. Units of both natural fluorescence (continous trace) are quanta/second/ $\text{cm}^3$  and production (boxes) in atoms carbon/second/ $\text{cm}^3$ . As shown in Appendix 13, near surface samples such as these exhibit fluorescence with higher efficiency than samples in lower light environments explaining the lower production measurements by  $^{14}\text{C}$  methods.

**4.3.7. Calypso 1987:** The Calypso was again offered for use in the testing of natural fluorescence studies between 18 September and 22 September, 1987. The location was the waters around Tahiti and Moorea and the conditions were ideal. During a period of 4 days at sea, we conducted both 4 sets of 12 hour *in situ* incubations and numerous 2 hour incubations. This cruise developed the most extensive set of comparisons between natural fluorescence and primary production as measured by the  $^{14}\text{C}$  technique. Preliminary results were also presented at the 1988 ASLO New Orleans meeting by S. Chamberlin (USC) and represent a chapter in Chamberlin's PhD thesis. This data composed the bulk of the material discussed in our 1989 submission to Deep Sea Research (see Appendix 13).

**4.3.8. La Jolla 88:** A short one day cruise off of La Jolla was conducted to test the operation of the newly redesigned Profiling Natural Fluorometer. No supporting data was acquired as this was intended mainly as a test of the integrity of the hardware and software, and to examine the feasibility of hand deployment. The tests were satisfactory and the instrument was prepared for testing.

**4.3.9. SEEP-II:** In March of 1988, P. Faulkowski (Brookhaven) tested at sea his new fluorescence double pulse instrument. We shipped the Profiling Natural Fluorometer to Faulkowski for deployment concurrently with his instrument. Unfortunately, heavy seas were encountered limiting the number of deployments. 13 separate verticals were performed. The instrument functioned perfectly. No *in situ* incubations were performed. We were unable to interpret double flash data in the same terms as the productivity estimates obtained with the PNF-300.

**4.3.10. Eureka 88:** On April 21, 1988, D. Kiefer and C. Booth were asked to consult with an environmental concern about the pollution paper mills cause to the ocean off Eureka, California. Financed by this environmental concern, intensive (56 profiles in 7 hours) tests of the Profiling Natural Fluorometer in a shallow, highly variable environment that extended from the surf zone seaward to approximately 1 km offshore were performed. This demonstration project was successful, and the results are currently in preparation for publication. The instrument functioned flawlessly.

**4.3.11. Ameriez 3:** In July and August 1988, S. Chamberlin (USC) deployed the PNF-300 24 times on 17 days on a cruise to Antarctica. This interdisciplinary cruise, led by N. Sullivan (USC), studied primary production in the near ice zone. The instrument functioned satisfactorily. Productivity data was unavailable for analysis during this contract, but is currently being performed by Chamberlin.

**4.3.12. Soviet-American-Vietnamese Expedition:** Phil Dustan (College of Charleston) borrowed a prototype PNF-300 for a 2.5 month cruise on the Russian oceanographic ship Akademik Akexsandr Nesmeyanov led by chief scientist Professor Titlyanov of Institute of Marine Biology, USSR Academy of Sciences. This cruise, from Singapore to the Seychelles and back, made stations across the Indian ocean and extended periods of research on coral communities in the Seychelles. While independent productivity estimates were not made, chlorophyll was measured. This cruise has also provided some of the deepest profiles of natural fluorescence. On this cruise, the only instrument malfunction of the prototype test series occurred when corals damaged the underwater cable and connector. It was able to be repaired at sea and data collection continued successfully.

**4.3.13. SCABB '89:** Cruise led by Jed Fuhrman (USC) on the New Horizon off California (31:50N, 124:06 W) where PNF-300 measurements were made by R. Renyolds. PNF-300 profiles were conducted to about 80 meters limited by available cable. Two days of  $^{14}\text{C}$  *in situ* measurements were made providing 10 comparable data points. Additional profiles with chlorophyll measurements were also made.

**4.3.14. SEEP-II.** J. Morrow took a PNF-300 prototype on a cruise off Norfolk, VA with P. Faulkowski between March 16 and March 24, 1989. During this cruise, 24 vertical profiles were performed. The instrument functioned perfectly. Data on  $^{14}\text{C}$  productivity and double flash fluorescence was not received until after the end of this contract and has not been analysed.

**4.3.15. Key Largo:** The second in a series of field measurements on corals with the PNF-300 was performed by P. Dustan. In this experiment, external "Gershun tube" field of view modifying devices were fitted on the PNF-300 to enable the measuring of a limited surface area of corals. These experiments used mid-water natural fluorescence sources to characterize the effects of these different field-of-views.

**4.3.16. Charleston Harbor.** P. Dustan's experiments in Charleston harbor with the PNF-300 is notable since it represents the only data from highly turbid estuarine waters.  $k(\text{PAR})$  measured in vertical profiles to 10-13 meters ranged between 1.0 and 1.6 meters<sup>-1</sup>. In these waters, chlorophyll and production estimates were obtained to a depth of about 5-7 meters, below the 0.02% PAR level. Here two profiles were taken along with extracted chlorophyll and the estimates appear to be within the expected range.

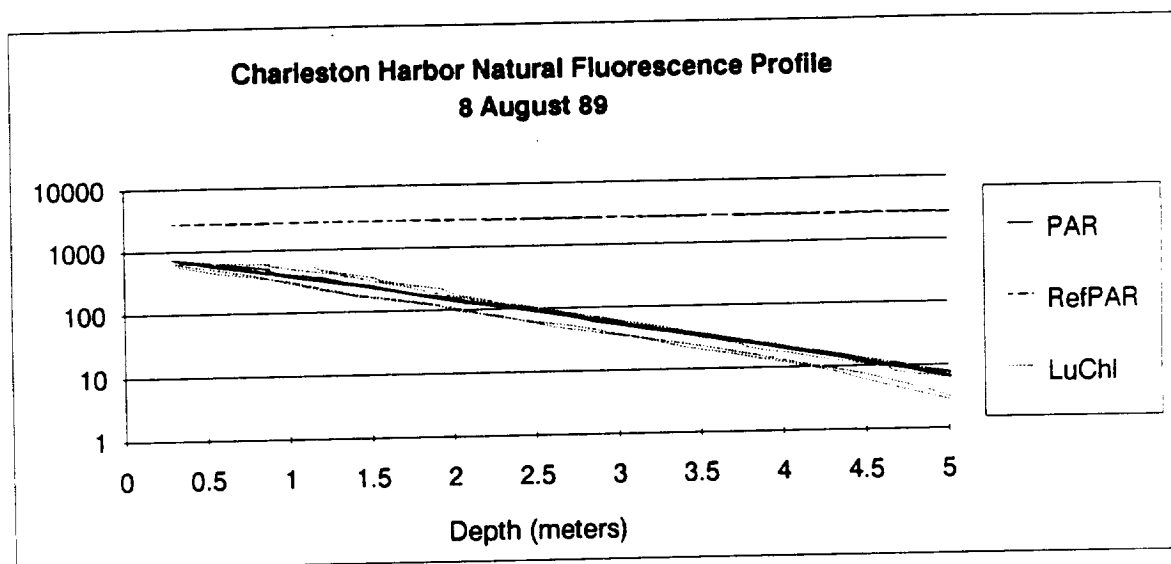


Figure 4.3.16. Profiles of natural fluorescence and PAR in Charleston Harbor.

4.3.17: During May, 1988, M. Lewis and P. Stegmann (Dalhousie University) deployed a PNF-300 prototype on a cruise to the Labrador Sea. This deployment was unique for two reasons. First, they devised buoyancy "wings" that, when combined with a special cable they also provided, allowed the instrument to drift away from the ship (and thus the ship's shadow), and then descend to depth and return. This cruise was also unique as it marked the highest chlorophyll waters encountered in the project (20  $\mu\text{g/l}$ ). Supporting chlorophyll and P vs I productivity data were not received until after the end of this project and thus were not included in the project data sets or analysis. From a cursory review of these data however, it appears that chlorophyll/fluorescence relationships here are significantly different than previously observed. Still remaining to be factored into the analysis are the effects of increased  $a(\text{chl},t,z)$  (see equation 4), and the changes in  $^{\circ}\text{ac}(\text{PAR},t,z)$  (see equation 19), both due to high chlorophyll.

#### 4.4 Laboratory Research

In order to examine the relationship between natural fluorescence and photosynthesis under conditions that are better defined than those in the field, we studied the growth and fluorescence of the marine chlorophyte *Dunaliella tertiolecta* in a specially constructed laboratory fluorometer ("Fluorostat"). This study was specifically designed to explore the relationship between natural fluorescence and photosynthesis under different light intensities and rates of nutrient supply. The Fluorostat allowed measurements of natural fluorescence and photosynthesis of cells in continuous or steady state growth. The growth rate of the

cultures was varied by changing either the light intensity or rate of nutrient supply. Specifically, we were interested in addressing the following questions: Does the ratio of photosynthetic rate to natural fluorescence vary with light intensity as indicated by our field study? Does this ratio vary with the availability of nitrogenous nutrients?

**Description of Fluorostat.** The Fluorostat is a chemostat fitted with specially designed optical components. The chemostat consists of a 2 liter, cylindrical glass reaction vessel with four optical ports positioned orthogonally. This vessel is thermally jacketed for temperature control. The conditions within the reaction vessel are largely controlled by a simple plumbing and mixing system. The rate of flow of nutrient medium into and out of the reaction vessel is controlled by a peristaltic pump. The reaction vessel is sampled by siphoning through a glass and silicon tubing line and is aerated through an additional line. The cell suspension is continuously stirred with a magnetic bar.

The optical components of the fluorometer consist of three parts. The reaction vessel is illuminated from below by a 500 watt tungsten "stage light". Light from the source is partially collimated by a Fresnel lens and then reflected at  $90^\circ$  by a dichroic filter that reflects only light of wavelengths less than 590 nm. Before passing through the base of the vessel, the growth illumination can be further attenuated by one or a combination of absorbing filters. These primary filters are blue transmitting (Schott BG 37), blue green transmitting (Schott BG 17), heat absorbing (Schott KG 3), and neutral density (50% transmission). The light entering the reaction vessel is greatly reduced at the shorter wavelengths because of the dichroic mirror and the primary filter. This spectral composition of the growth illumination is necessary in order to detect the natural fluorescence of chlorophyll *a*, and to simulate the spectral distribution of the oceanic light field. See figure 4.4.1 for examples of the spectral irradiances obtained.

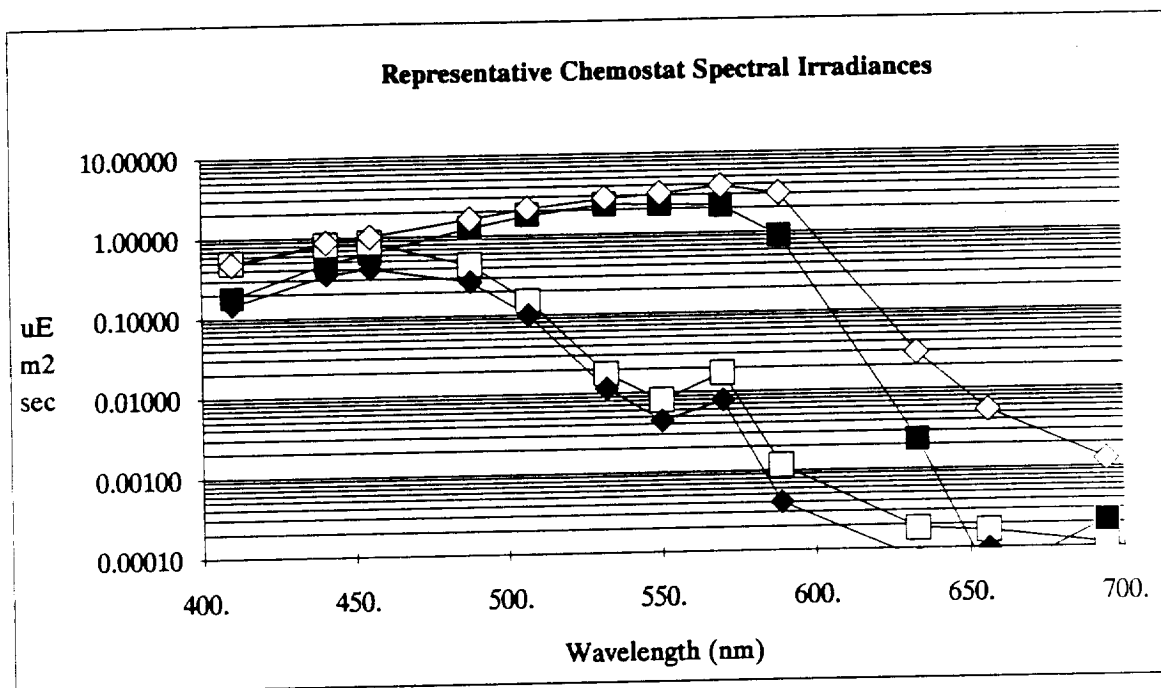


**Figure 4.4.1. Representative spectral irradiance distributions measured in the Fluorostat. Measured using an MER-1010 spectroradiometer positioned at the top of the Fluorostat.**

Fluorescence excitation spectra of the chlorophyll *a in situ* are obtained with a tungsten probe beam. The source of this beam is a 50W tungsten lamp, passed sequentially through a ISA H10 1200 groove/mm monochromator, a PTI OC-4000 mechanical chopper, a collimating lens, a short wavelength transmitting dichroic filter, and a beam splitter. This modulated monochromatic beam passes through the cell suspension, and is detected at a second optical port that views the directly opposed probe beam. The intensity of the probe is monitored continuously by a photodiode that receives a fraction of the incident beam from the beam splitter. The beam is modulated at 93 hertz over a pathlength of 19.3 cm. The detector port is fitted with a Hamamatsu R928 photomultiplier (PMT) mounted in a Gershun tube. The voltage to the PMT is controlled using a Pacific Instruments model 204 power supply. The Gershun tube includes a field stop that shields the photomultiplier from stray light and two secondary filters that transmit light only in the spectral region of chlorophyll *a* emission. One filter is an interference filter with a peak transmission at 683 nm and a band width of 20 nm, and the other filter is absorbing with a short wavelength cutoff at 640 nm. The output from the PMT consists of two components: a modulated signal proportional to the fluorescence excited by the probe beam and a continuous signal proportional to the fluorescence excited by the growth illumination. These two components are detected using an EG&G 5207 lock-in amplifier. Data acquisition and control of the chemostat is

achieved with an IBM-XT microcomputer interfaced to the lock-in via an IEEE-488 bus.

**Calibration.** We have derived an algorithm to transform the continuous voltage signal into natural fluorescence:

$$F_f = \frac{G_{dc} * V_{dc} * a(683)}{1 - \exp(a(683) * d)} \quad (21)$$

where  $G_{dc}$  is the quantum response of the culture fluorometer detector (in units of  $nE/m^2/sec/volt$ ).  $V_{dc}$  is the voltage from the photomultiplier amplifier induced by natural fluorescence.  $a(683)$  is the absorption coefficient of the cell suspension at the wavelength of peak emission by chlorophyll (in units of  $m^{-1}$ );  $a(683)$  is the sum of the absorption coefficient for water,  $a_w(683)$ , and the absorption coefficient of the cells in-suspension,  $a_c(683)$ .  $d$  is the diameter of the reaction vessel (in units of  $m$ ).

$G_{dc}$  was determined by measuring the spectral scalar irradiance and the continuous voltage signals from acetone solutions containing a known concentration of chlorophyll a, and introducing these values into the following equation:

$$G_{dc} = F_a(chl) * \frac{R(chl \text{ in vitro})}{R(chl \text{ in vivo})} * 1 - \exp(-a(683) * d) \quad (22)$$

$F_a(chl)$  is the quantum yield of chlorophyll a dissolved in 90% acetone (in units of  $E/E$ ).  $R(chl \text{ in vitro})/R(chl \text{ in vivo})$  is the ratio of the response of the fluorometer detector to the emission of extracted chlorophyll, which emits maximally at 676 nm, to the response of the detector to the emission of in vivo chlorophyll, which emits maximally at 683 nm (dimensionless).  $F_a(chl)$ , which is the rate of light absorption by a unit concentration of chlorophyll in solution (in units of  $\mu E/mg \text{ chl/sec}$ ), is calculated by integrating over the visible spectrum the product of the spectral scalar irradiance within the reaction vessel,  $E_o(w)$ , and the specific absorption coefficient of chlorophyll in extract,  $a_{chl}(w)$ .  $dV_{dc}/dchl$  is the change in the voltage signal with the change in the concentration of extracted chlorophyll in the reaction vessel (in units of  $volts * m^3 * mg^{-1} * chl$ ).

It is difficult to transform the voltage of the modulated signal into fluorescence units of  $nE \cdot m^{-3} \cdot sec^{-1}$  because the signal will likely depend upon the scattering properties of the cell suspension. On the other hand, in dilute suspensions relative fluorescence excitation spectra can be obtained by dividing the modulated voltage signal at a given wavelength,  $V_m(w)$ , by the relative radiance intensity of the incident modulated beam at that wavelength,  $I(w)$ .  $I(w)$  is determined by dividing the output of the external photodiode by the spectral quantum response of the diode. The spectral quantum response of the diode was measured with a QED-200 quantum detector.

Measurements:  $a_p(w)$ ,  $F_p$ ,  $C_c$ ,  $N_c$ ,  $u$ ,  $N_{uc}$ ,  $F_m(w)$ , chl.

Our study of the fluorescence and growth of Dunaliella tertiolecta included a number of measurements of the optical and chemical properties of the cell suspension at a specific steady state growth rate ( $u$ ). These measurements included in situ fluorescence excitation spectra of chlorophyll *a* ( $F_m(w)$ ), natural fluorescence ( $F_f$ ), spectral absorption coefficient of the cell suspension ( $a_c(w)$ ), the concentration of cells ( $N_{uc}$ ), cellular carbon ( $C$ ), nitrogen ( $N_c$ ), and chlorophyll. The fluorescence excitation spectrum provided information on the pigments responsible for chlorophyll *a* fluorescence. The absorption coefficient provided information about the rate of light absorption by the cell suspension. Specifically, the rate of light absorption by the suspension,  $F_a$ , is simply the integral of the product of the spectral scalar irradiance within the reaction vessel,  $E_o(w)$ , and the absorption coefficient:

$$a = \int a_c(w) * E_o(w) dw \quad (23)$$

The concentration of cells and chlorophyll provided information necessary to assess the establishment of steady state. When combined with the dilution rate,  $D$ , which is equal to the specific growth rate of the culture, the concentrations of cellular carbon and nitrogen provide information necessary to calculate net daily rates of carbon and nitrogen fixation,  $PC_{net}$  and  $PN_{net}$

$$PC_{net} = D * C \quad (24)$$

$$PN_{net} = D * N \quad (25)$$

The value of the ratio of carbon assimilation to natural fluorescence,  $PC_{net}/F_f$ , at different growth rates is of central importance to our study. The concentration of chlorophyll is of general interest.

Although analysis of the data obtained with the culture fluorometer is continuing, several important conclusions can already be drawn. First, the ratios of the rates of photosynthesis to natural fluorescence of Dunaliella in steady state growth are similar to the ratios measured in the field. As shown in section 4.4, the values for the ratio of gross photosynthetic rate to natural fluorescence in the field ranged between 0.3 and 5.0 gm-at C/E. The values of net photosynthetic rate to natural fluorescence for Dunaliella grown under a number of light intensities and rates of nutrient supply ranged between 0.2 and 5 gm-at C/E. This agreement not only helps to verify the calibration of the laboratory and field fluorometers, but also supports the assumption that studies of phytoplankton cultures will aid in the interpretation field measurements.

Second, for Dunaliella, rates of nutrient supply effect the ratio of photosynthesis to natural fluorescence. Figure 4.4.2 shows the ratio  $P_{net}/F_f$  for Dunaliella as a function of the specific growth rate of the culture. Because the scalar irradiance of photosynthetically available radiation within the reaction vessel, 365  $\mu\text{E}/\text{m}^2/\text{sec}$ , is sufficient for a maximal specific growth rate of 1.4  $\text{day}^{-1}$ , lower growth rates result from decreased rates of nutrient supply. The composition of the nutrient medium ensures that nitrate is the factor limiting both the concentration of cells in the reaction vessel and their growth rate. Such deprivation in the chemostat

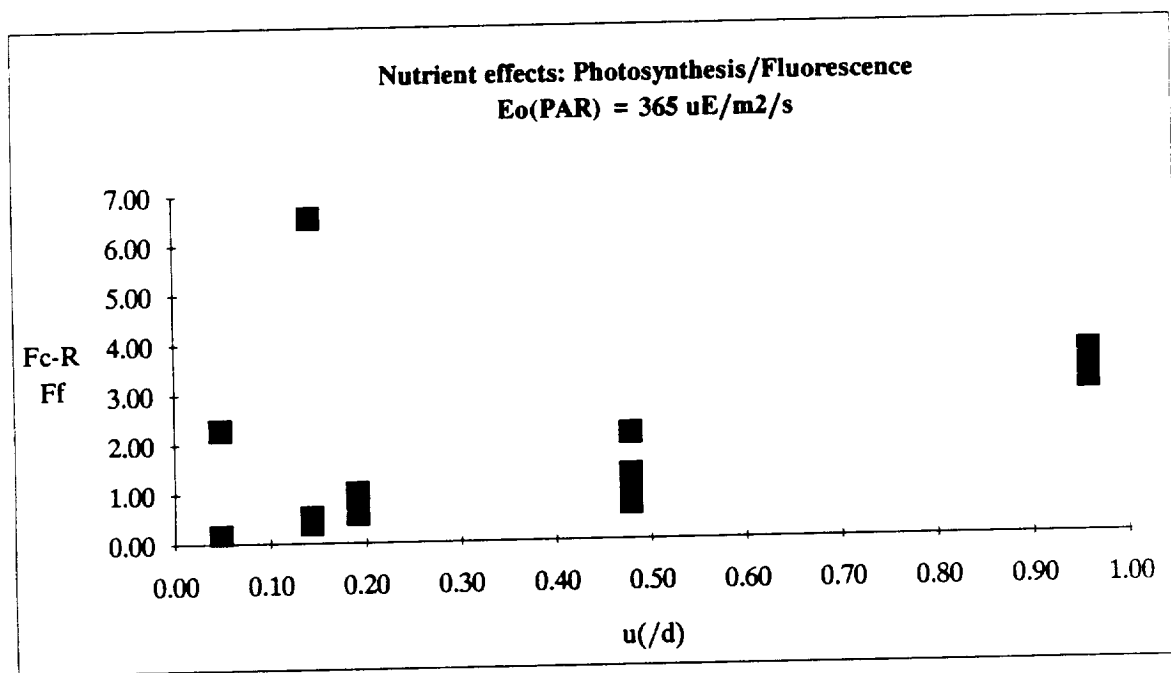


Figure 4.4.2. Photosynthesis/Natural Fluorescence ratio for different growth rates at 365 $\mu\text{E}/\text{m}^2/\text{s}$  irradiance level

yielded a range in growth rates from 0.05 to 1.4 d<sup>-1</sup> and a range in the ratio  $P_{net}/F_f$  from 0.2 to 5.

If the variability in the yields of photosynthesis and fluorescence caused by nutrient deficiency is a general feature of the natural phytoplankton crop, a potential problem for interpreting natural fluorescence exists. If the variability in nutrient limitation in the oceans is large, the accuracy of estimates of photosynthetic rate based upon measurements of natural fluorescence will be less. Specifically, photosynthetic rates in regions of nutrient deficiency will likely be overestimated and rates in regions of nutrient sufficiency will likely be underestimated. Of course, calibration of the natural fluorescence measurement by application of the <sup>14</sup>C measurement will aid in reducing any bias.

At present, we have no evidence that such variability occurs in the oceans. Our database on natural fluorescence and photosynthesis includes both oligotrophic and eutrophic waters. Thus, our assessment of the accuracy of estimating photosynthetic rate from measurements of natural fluorescence is conservative. Furthermore, we have not found significant differences in the ratio of photosynthesis to fluorescence between waters of differing nutrient concentrations. It is noteworthy that there is presently a considerable debate as to whether the growth rate of phytoplankton in the ocean is reduced significantly by nutrient limitation.

Third, in Dunaliella, light intensity also effects the ratio of photosynthesis to natural fluorescence. Figure 4.4.3 shows the ratio  $P_{net}/F_f$  for Dunaliella as a function of the specific growth rate of the culture. In these experiments, the growth rate of the cells was limited by the rate of supply on nitrate and thus equal to the dilution rate of the culture. The figures indicate that, at a given growth rate, the ratio  $P_{net}/F_f$  tends to decrease with increasing light intensity. This observation is consistent with our measurements of photosynthetic rate and natural fluorescence in the field, and in fact our formulation of the relationship between light intensity and the ratio of  $F_c/F_f$  for the field appears to apply as well to the culture.

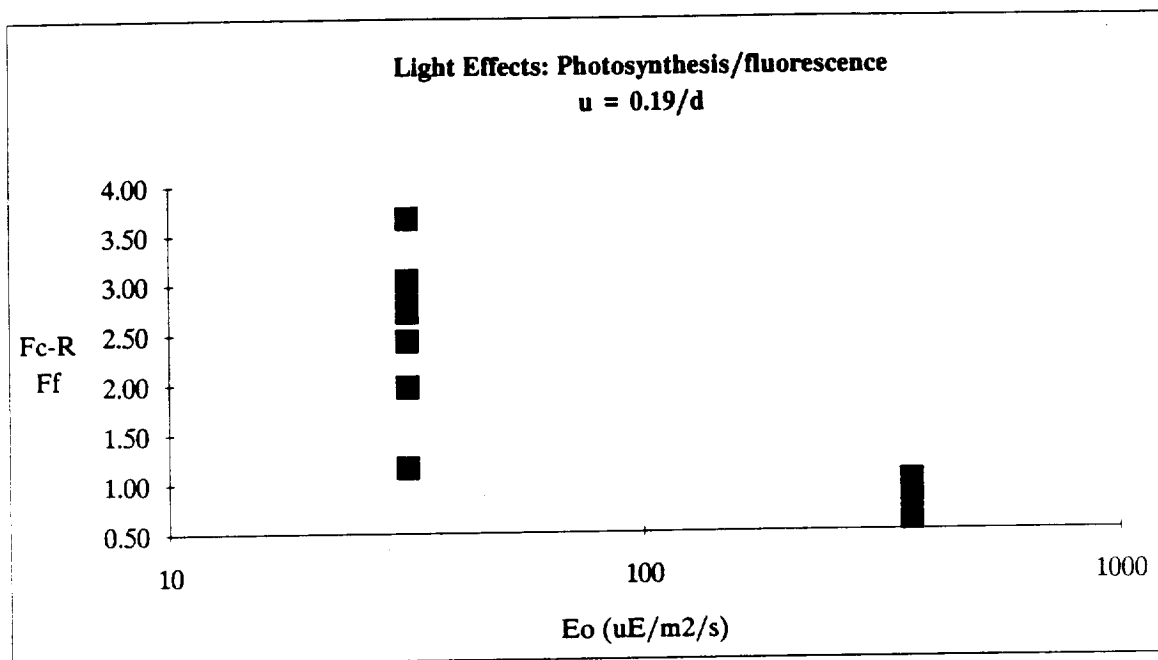


Figure 4.4.3. Light effects on photosynthesis/fluorescence ratio for *Dunaliella* when the specific growth rate of the culture is maintained by dilution at 0.19 doublings per day.

#### 4.5 Modeling

Models are used in this research effort for a variety of reasons. The most important model is of the relationship between phytoplankton growth and fluorescence. Other useful models include describing the attenuation and scattering of solar irradiance in the same spectral region as natural fluorescence. Models are also used to calibrate the sensor and compare the response of the sensor to a calibration source with the expected response to natural fluorescence in the ocean.

The relationship between phytoplankton growth and natural fluorescence is described in detail above (see equation 15) and in appendices 13 and 14. Basically, our models suggest that fluorescence is a natural byproduct of photosynthesis and that the balance between photosynthesis and fluorescence is well behaved and predictable. The principal departure from a linear balance in these two processes has been found to be related to the level of the ambient light. Empirical equations have been presented to address this imbalance, resulting in what we feel is acceptable prediction of primary photosynthetic production from natural fluorescence.

Empirical models were developed to handle the expected variability of natural fluorescence parameters using a data base of up and downwelling irradiance

and upwelling radiance within the upper 10 meters of the ocean. From these data, the diffuse attenuation coefficients for each profile was calculated over the intervals 1 to 5 and 6 to 10 meters depth. Particular attention was focused on  $E_d(683)$  within this depth range because of the potential of determining the attenuation coefficient at this wavelength with the minimum of interference from natural fluorescence itself. A summarization of these data is found in the following Table 1. It is interesting to note the relatively small variation in  $E_d(683)$  relative to the other parameters. This is important considering the assumption that variation in  $k(E_d(683))$  will reflect variation in  $a(683)$ , an important parameter in the natural fluorescence equations (see equation 4). Considering this importance, the ability of  $k(PAR)$  - a parameter measured by the PNF-300 - to predict  $k(E_d(683))$ , and thus indirectly  $a(683)$ , was also examined. Figure 4.5 shows the relationship of  $k(E_d(683))$  and  $k(PAR)$  within the upper 5 meters of the data set. Regression statistics on these data yielded an  $R^2$  of 84% ( $n=193$ ) and an equation of

$$k(E_d(683)) = 0.43 + (k(PAR) * 0.799$$

While this equation has not been incorporated into the PNF-300 software, this relationship may be valuable in the future, particularly in high chlorophyll waters (see section 4.3.17).

Table 4.5: Results of vertical profiles from cruises Calypso 86 and 87, Biowatt II (May 87), Scripps Canyon Mooring, JETZ87, and Friday Harbor (July 87). The JETZ and Friday Harbor data is courtesy of C. Davis (JPL).

Parameter	Mean	Coefficient of Variation
Number of samples	34416	
Number of profiles	203	
$k(E_d(683))$ : 1-5 meters	0.574	27.18%
$k(E_d(683))$ : 6-10 meters	0.527	1.73%
$k(E_u(683))$ : 1-5 meters	0.353	25.18%
$k(E_u(683))$ : 6-10 meters	0.130	37.31%
$k(L_u(683))$ : 1-5 meters	0.278	59.58%
$k(L_u(683))$ : 6-10 meters	0.187	207.03%
$k(E_d(488))$ : 1-5 meters	0.115	86.99%
$k(E_d(488))$ : 6-10 meters	0.111	108.71%
$k(PAR)$ : 1-5 meters	0.168	81.10%
$k(PAR)$ : 6-10 meters	0.132	79.76%

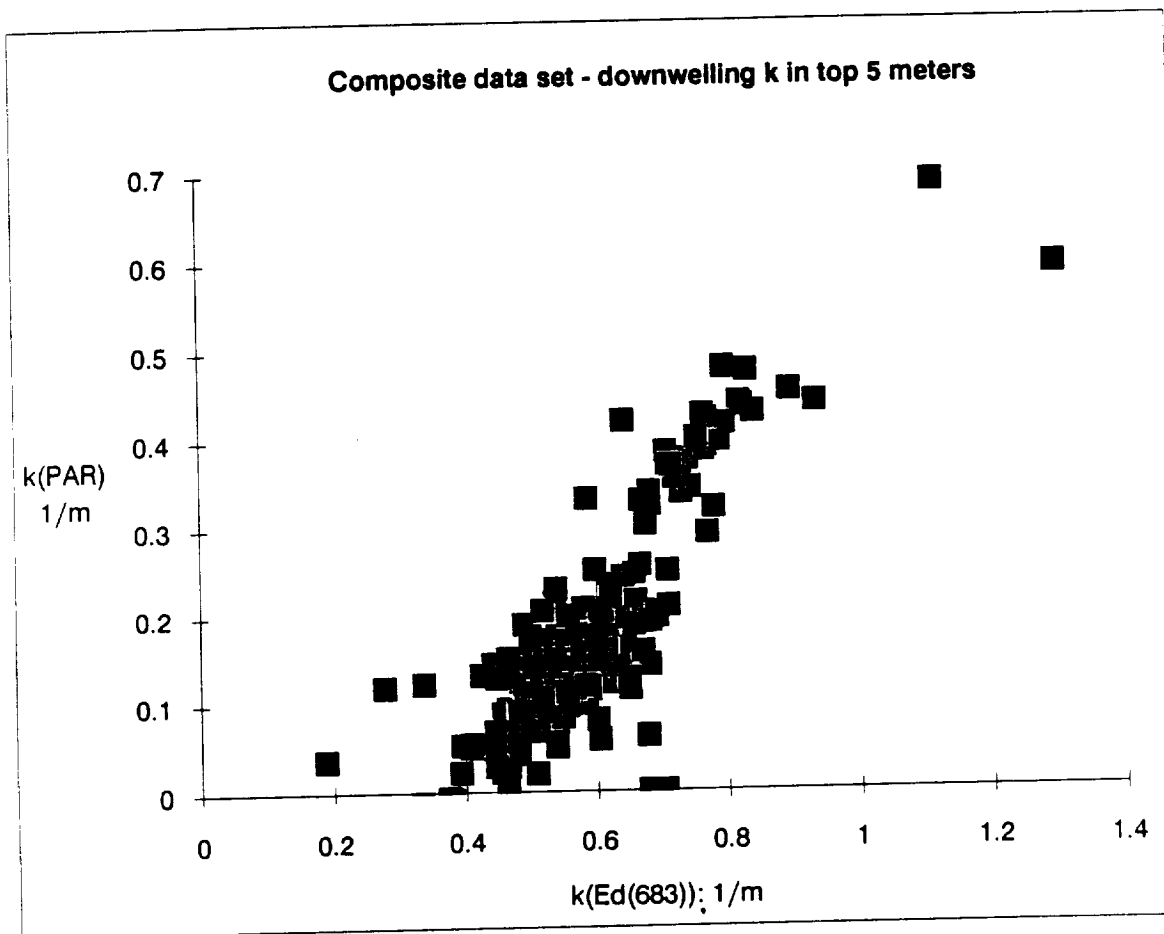


Figure 4.5. Using the same data set as described in Table 4.5, the relationship of  $k(\text{Ed}(683))$  with  $k(\text{PAR})$  in near the surface was examined.

## 5. Talks and Publications:

During the course of this project, a number of talks and publications resulted from field studies that were conducted to obtain measurements of natural fluorescence. The following two sections list publications that have either been submitted, accepted, or published. Other publications are currently being prepared. The first two papers, which focus entirely on natural fluorescence and the activities of this project, are included in the appendices.

### 5.1: Publications

5.1.1. "Natural fluorescence of chlorophyll a: Relationship to photosynthesis and chlorophyll concentration in the western South Pacific gyre". D. A. Kiefer, W. S.

Chamberlin, and C. R. Booth. *Limnology and Oceanography* - Status: in press- see Appendix 12.

5.1.2. "*Evidence for a Simple Relationship between Natural Fluorescence, Photosynthesis and Chlorophyll in the Sea*". W. S. Chamberlin, C. R. Booth, D. A. Kiefer, J. H. Morrow, and R. C. Murphy. Status: submitted to *Deep Sea Research*, July, 1989. - see Appendix 13.

5.1.3. "*Observations of phytoplankton and nutrients from a Lagrangian drifter off northern California*", M. R. Abbott, K. H. Brink, C. R. Booth, D. Blasco, L. A. Codispoti, P. N. Niiler, S. R. Ramp. Status: submitted to *Journal of Geophysical Research*, September 1989.

5.1.4. "*Moorable spectroradiometers in the BIOWATT experiment*." C. R. Booth and R. C. Smith. *Ocean Optics IX*. SPIE Vol. 925. pp 176-188. 1988.

5.1.5. "*Model of the photosynthetically available and usable irradiance in the sea*". D. J. Collins, C. R. Booth, C. O. Davis, D. A. Kiefer, and C. Stallings. *Ocean Optics IX*. SPIE Vol. 925. pp 87-101. 1988.

5.1.6. "*Method and apparatus for determining concentrations of chlorophyll and the rate of primary production in water*." C. R. Booth and D. A. Kiefer. United States Patent Number 4,804,849 issued 14 February 1989.

5.1.7 "*Light absorption, natural fluorescence, and photosynthesis in the open ocean*". Chamberlin, W. S. (1989). Ph.D. dissertation. University of Southern California, Los Angeles, California.

## 5.2: Talks:

5.2.1. "*Moored and Drifting Spectroradiometers for the Long Term Monitoring of Biological and Optical Variability*." C. R. Booth. Invited paper presented at the January 1988 Ocean Sciences Meeting in New Orleans.

5.2.2. "*Correlation between solar-induced fluorescence and primary production*". R. F. Davis and C. R. Booth. Presented at the January 1988 Ocean Sciences Meeting in New Orleans.

**5.2.3.** *"A field test of the relationship between natural fluorescence and primary production"*. W. S. Chamberlin, D. H. Robinson, and C. R. Booth. Presented at the January 1988 Ocean Sciences Meeting in New Orleans.

**5.2.4.** *"In-situ optics as observed from long term moorings"*. C. R. Booth. Invited talk presented at IAPSO XIX IUGG General Assembly, Vancouver, 20-23 August 1987.

**5.2.5.** *"In-situ oceanographic instrumentation supporting NASA remote sensing of ocean color"*. C. R. Booth. Presented at the 1987 Council for Optical Radiation Measurement (CORM) Annual Symposium at the National Bureau of Standards, Gaithersburg, Maryland, May 28-29, 1987.

## **6. Applications:**

The monitoring of global productivity, global fisheries resources, application of above surface-to-underwater optical communications systems, submarine detection applications, correlation and calibration of remote sensing systems are but some of the reasons for developing inexpensive sensors for the measurement of chlorophyll and productivity. Normally, productivity measurements are manpower and cost intensive and, with the exception of a very few expensive multiship research experiments, provide no contemporaneous data. We feel that the simple sensors we have developed provide a cost effective method for large scale, synoptic, optical measurements in the ocean.

Initially this project focused on the determination of gross photosynthetic production in open ocean waters. After demonstrating that the technique was well founded and could be applied successfully in these environments, additional applications were pursued. Measuring productivity on coral reefs has long been a difficult problem, but preliminary results obtained in this project indicate that the natural fluorescence method may provide a rapid method of accessing coral reef vitality. Preliminary measurements in a reservoir in Los Angeles have indicated that the natural fluorescence technique may be used as the basis for an early-warning system for detecting algal blooms in potable water supplies. We are also pursuing other environmental monitoring applications that may be addressed with natural fluorescence methods.

## 7. Technology Spinoffs:

A unique application for natural fluorescence technology has been introduced in the City of Los Angeles, California. In 1989, after demonstrating the PNF-300 to researchers at the Los Angeles Department of Water and Power, Kiefer and J. H. Morrow at the University of Southern California were contracted to develop a system for monitoring phytoplankton growth rates in a metropolitan reservoir using PNF-300 based remote-sensing instrumentation. The goal of this pilot study is to determine if early detection of a phytoplankton bloom can help reduce the amount of plankticide required to treat a reservoir.

A hybrid instrument package has been developed, called the REOS or Remote Electro-Optical Sensor. The heart of the system is a PNF-300 natural fluorometer to measure phytoplankton growth rates and auxiliary membrane sensors for dissolved oxygen, pH, conductivity, and oxidation/reduction potential. An oceanographic data cable connects the sensor package with a data acquisition system station ashore. Data from each sensor is logged continuously by a host computer also located on the site. Using a modem connected to a telephone line, DWP may contact the reservoir host computer directly and have complete access to this system, remotely and in real time.

Coupled with a heuristic model of phytoplankton dynamics for the reservoir, DWP anticipates that the REOS natural fluorescence monitor may be an important management tool for the early detection of plankton blooms in metropolitan reservoirs. At meetings of the Americal Water Works Association, this system was shown to a large number of scientists and administrators from around the world who expressed a high level of interest. The REOS system may turn out to be an important spinoff of this NASA developed technology.

An additional spinoff of this technology is currently under development at Biospherical Instruments. In our TABOSS project, we are building a towed fiber optic based vehicle that measures upwelling radiance and downwelling irradiance with high spectral resolution. This will enable us to not only measure natural fluorescence around 683 nm, but will provide high resolution measures of other naturally fluorescing pigments, perhaps phycoerytherin or chlorophyll *c*.

Natural fluorescence measurements in coral was not originally anticipated in this project, but provocative results have been obtained because of P. Dustan's efforts. Preliminary results indicate that natural fluorescence may prove to be an important tool in large scale surveys of coral reefs.

## 8. Further Research Indicated

While this project succeeded in meeting most of the goals outlined in the proposal and succeeded in producing a commercially successful instrument, more work needs to be done to answer all of the questions that have arisen during this project. Further laboratory studies are currently underway at USC by Kiefer that will expand upon the results presented here. The laboratory effort has yielded results showing that natural fluorescence can be measured in the laboratory, and that the results obtained in the field fall within the range of those obtained in the laboratory. The laboratory studies concentrated on one species grown over a range of nutrient and light conditions. In the future, additional species will also be examined as part of a Ph.D. effort by R. Reynolds at USC.

All of the field data that has been used in published studies of natural fluorescence in this project have come from MER based sensors. As indicated above, preliminary results being obtained from the PNF-300 sensors deployed in the prototype testing and in subsequent sales yield different regression coefficients in comparisons with other types of production measurements. At this time, we believe that this may be partially due to the shadow cast by the MER based sensors and that modifications to the equations will compensate for these effects. Only through further analysis of these data and the cooperation of users will this be verified. The utility of the natural fluorometers in the prediction of chlorophyll concentration may be overshadowed by the ability of these instruments to predict physiological state given an independent estimate of chlorophyll.

All of the efforts in this project have been directed at the detection of fluorescence from chlorophyll *a*. Other photosynthetic pigments, notably phycoerythrin, may also exhibit fluorescence measurable with modified natural fluorometers. With the sensors used in this project we have not been able to measure phycoerythrin fluorescence in the ocean, but with sensors that we have under development and using a combination of fiber optics and high resolution spectroradiometry we may be successful.

A wide variety of instrument systems are used by oceanographers to collect data. These systems include drifters, moorings, profilers, and others. The development of the PNF-300 and INF-300 natural fluorometers only address part of the needs of the community. Other forms of natural fluorometers will be needed in the future and these technologies will need to be developed. Areas of work include towed sensors (currently being addressed by Biospherical Instruments with our

TABOSS package) and telemetering sensors for drifters where recovery may be impossible.

In addition to obtaining estimates of primary production, the natural fluorescence method is able to predict chlorophyll concentration from the natural fluorescence and light measurements. Prediction of chlorophyll concentration from natural fluorescence, as shown in Appendix 12, is based on estimates of the specific absorption coefficient for plankton. In these studies, we have used a single value for this coefficient although we know that this is not the best approach. As Morel (1978), and later Collins (1988) point out, this value changes with depth since it is based on the spectrum of PAR which changes with depth. Incorporation of models such as Collins has proposed should improve the ability of natural fluorescence sensors to predict chlorophyll.

Laboratory studies indicate a significant nutrient effect exists with fluorescence efficiencies. The best method to incorporate this relationship to improve the predictive ability of natural fluorometers has not been developed. A combination of both additional laboratory measurements and field measurements of natural fluorescence combined with nutrient information is needed.

## **9. Conclusions**

The measurement of primary production is one of the most important activities of oceanographers at sea, yet it is also one of the most time consuming and inaccurate of measurements. If primary production can be measured accurately, rapidly, and economically, as this study suggests, it is likely that our understanding of spatial and temporal variability in this parameter will expand rapidly with extensive application of this new technique. Our initial studies indicate that the measurement of natural fluorescence will at least partially fulfill this promise. If the utility of our natural fluorometers is validated by the scientific community, we expect that they will become a standard piece of oceanographic equipment, perhaps as commonly used as a CTD. Such expectations are not unreasonable given the importance of the information, the low cost of the proposed instrument, and the simplicity of its design and deployment. Furthermore, several other areas of application are promising -- pollution impact, reef vitality, water reservoir eutrophication are some of the areas presently being explored.

## 10. Acknowledgements:

This project would not have been possible without the encouragement of Don Collins at JPL. Don provided valuable discussion, comments and assistance along the way.

At USC, W. S. (Sean) Chamberlin, Dale Robinson, Sung Yang, and John Morrow were invaluable assistants.

Special thanks goes to Captain and Madam Jacques-Yves Cousteau and members of the Cousteau Society who graciously sponsored the field activities of the Calypso86 and Calypso87 cruises. We would like to point out that in addition to providing the services of the Calypso at no charge. The Cousteau Society also paid for all transportation expenses for both equipment and personnel, and some of the needed supplies. Also, in respect for Captain Cousteau's wish to keep Calypso a radioactive-free ship, the Cousteau society chartered a second vessel solely for the use and transport of  $^{14}\text{C}$  used in the Calypso87 expedition.

Special thanks also to Dr. Phil Dustan (College of Charleston) who endured several months on a Russian oceanographic vessel to bring back the first measurements of natural fluorescence from both the Indian Ocean and from coral reefs. Considerable valuable feedback in refinement of the PNF-300 was obtained from his experiences.

At Biospherical Instruments, major segments of the electronic design were done by Curtis Carlson. Mechanical design was organized by Brad Roth and Keith Cheskey. Software was written by Michael Weber. George Grider was responsible for the design and execution of the PNF-300 instruction manual.

## 10. References:

- Booth, C. R., B. G. Mitchell, and O. Holm-Hansen (1987). Development of Moored Oceanographic Spectroradiometer" Biospherical Instruments Technical Reference 87-1.
- Booth, C. R. (1974). The design and evaluation of a measurement system for photosynthetically active quantum scalar irradiance. *Limnology and Oceanography* 21: 326-336.
- Collins, D. J., C. R. Booth, C. O. Davis, D. A. Kiefer, and C. Stallings. "A Model of the Photosynthetically Available and Usable Irradiance in the Sea." SPIE Vol. 925 Ocean Optics IX, pp 87-100 (1988).
- Gordon, H. (1979). Diffuse reflectance of the ocean: the theory of its augmentation by chlorophyll a fluorescence at 685 nm. *Applied Optics*, 18, 1161-1166.
- Kattawar, G. W. and J. C. Vastano (1982). Exact 1-D solution to the problem of chlorophyll fluorescence from the ocean. *Applied Optics*, 21, 2489-2492.
- Kiefer, D. A., W. S. Chamberlin, and C. R. Booth (1989). Natural fluorescence of chlorophyll a: Relationship to photosynthesis and chlorophyll concentration in the western South Pacific gyre. *Limnology and Oceanography*, in press.
- Kishino, M., S. Sugihara, and N. Okami (1984a). Influence of fluorescence of chlorophyll a on underwater upward irradiance spectrum. *La mer*, 22, 224-232.
- Kishino, M., S. Sugihara, and N. Okami (1984b). Estimation of quantum yield of chlorophyll a fluorescence from the upward irradiance spectrum in the sea. *La mer*, 22, 233-240.
- Morel, A. (1978). Available, usable and stored radiant energy in relation to marine photosynthesis. *Deep-Sea Research*, 25, 673-688.
- Morel, A. and L. Prieur (1977). Analysis of variations in ocean color. *Limnology and Oceanography*, 22, 709-722.
- Neville, R. A. and J. F. R. Gower (1977). Passive remote sensing of phytoplankton via chlorophyll a fluorescence. *Journal of Geophysical Research*, 82, 3487-3493.

**Final Report NAS7-969: Natural Fluorescence**

Petzold, T. J. and R. W. Austin. "Characterization of MER 1032", Visibility Laboratory Technical Memorandum EN-001-88t, 1988.

Smith, R. C., and K. S. Baker (1981). Optical properties of the clearest natural waters. *Applied Optics*, 20: 177-184.

Sugihara, S., M. Kishino, and N. Okami (1984). Contribution of Raman scattering to upward irradiance in the sea. *Journal of the Oceanographical Society of Japan*, 40: 397-404.

Topliss, B. J. (1985). Optical measurements in the Sargasso Sea: solar stimulated chlorophyll fluorescence. *Oceanologica Acta*, 8, 263-270.

Topliss, B. J. and T. Platt (1986). Passive fluorescence and photosynthesis in the ocean: implications for remote sensing. *Deep-Sea Research*, 33, 849-864.

**Final Report NAS7-969: Natural Fluorescence**

**Appendix 11**

**PNF-300 Instruction Manual**

---

# The PNF-300 Profiling Natural Fluorometer

## User's Manual

**Biospherical Instruments, Inc.**

4901 Morena Blvd., San Diego, CA 92117 (619) 270-1315

FAX: 619/270-1513/TELEX: 7400446 ROCK UC

---

# Limited Warranty

BIOSPHERICAL INSTRUMENTS INC. warrants this Profiling Natural Fluorometer PNF-300 (the Product) to be in good working order for a period of one (1) year parts, and for a period of ninety (90) days labor from the date of purchase. Should this Product fail to be in good working order at any time during the above stated warranty period, Biospherical Instruments Inc. will, at its option, repair or replace this Product at no additional charge except as set forth below. Repair parts and replacement Products will be furnished on an exchange basis and will be either reconditioned or new. All replacement parts and Products become the property of Biospherical Instruments Inc. This limited warranty does not include service to repair damage to the Product resulting from accident, disaster, misuse, abuse, or non-Biospherical Instruments Inc. modification of the Product.

Limited Warranty service may be obtained by delivering the Product during the warranty period to Biospherical Instruments Inc. at its San Diego, California service center, showing proof of purchase. If this Product is delivered by mail, you agree to insure the Product or assume risk of loss or damage in transit; to prepay shipping charges to the San Diego, California service center; to use the original shipping container or equivalent; and to pay for return shipping charges.

ALL EXPRESS AND IMPLIED WARRANTIES FOR THIS PRODUCT INCLUDING THE WARRANTIES OF MERCHANTABILITY AND FITNESS FOR A PARTICULAR PURPOSE, ARE LIMITED IN DURATION TO THE ABOVE WARRANTY PERIOD, AND NO WARRANTIES, WHETHER EXPRESS OR IMPLIED, WILL APPLY AFTER THIS PERIOD. SOME STATES DO NOT ALLOW LIMITATIONS ON HOW LONG AN IMPLIED WARRANTY LASTS, SO THE ABOVE LIMITATIONS MAY NOT APPLY TO YOU.

IF THIS PRODUCT IS NOT IN GOOD WORKING ORDER AS WARRANTED ABOVE, YOUR SOLE REMEDY SHALL BE REPAIR OR REPLACEMENT AS PROVIDED ABOVE. IN NO EVENT WILL BIOSPHERICAL INSTRUMENTS INC. BE LIABLE TO YOU FOR ANY DAMAGES, INCLUDING ANY LOST PROFITS, LOST SAVINGS OR OTHER INCIDENTAL OR CONSEQUENTIAL DAMAGES ARISING OUT OF THE USE OF OR INABILITY TO USE SUCH PRODUCT, EVEN IF BIOSPHERICAL INSTRUMENTS INC. HAS BEEN ADVISED OF THE POSSIBILITY OF SUCH DAMAGES, OR FOR ANY CLAIM BY ANY OTHER PARTY.

SOME STATES DO NOT ALLOW THE EXCLUSION OR LIMITATION OF INCIDENTAL OR CONSEQUENTIAL DAMAGES FOR CONSUMER PRODUCTS, SO THE ABOVE LIMITATIONS OR EXCLUSIONS MAY NOT APPLY TO YOU.

THIS WARRANTY GIVES YOU SPECIFIC LEGAL RIGHTS, AND YOU MAY ALSO HAVE OTHER RIGHTS WHICH MAY VARY FROM STATE TO STATE.

# Notice

Photosynthetic rate measurements based on the natural fluorescence techniques represents the leading edge of ocean sciences technology. As in any new methodology, refinements will occur as this becomes more widely used and discussed. We urge you to keep in touch with Biospherical's technical staff in reporting any anomalies you encounter. As we have not tested this technology under all conditions, we suggest you obtain confirming independent estimates where possible.

The information contained in this document is subject to change without notice.

BIOSPHERICAL INSTRUMENTS MAKES NO WARRANTY OF ANY KIND WITH REGARD TO THIS MATERIAL, INCLUDING, BUT NOT LIMITED TO, THE IMPLIED WARRANTIES OF MERCHANTABILITY AND FITNESS FOR A PARTICULAR PURPOSE. Biospherical Instruments shall not be liable for errors contained herein or for incidental consequential damages in connection with the furnishing, performance, or use of this material.

This document contains proprietary information which is protected by copyright. All rights are reserved. No part of this document may be photocopied, reproduced, or translated into another language without the prior written consent of Biospherical Instruments, Inc.

Copyright 1989 by BIOSPHERICAL INSTRUMENTS, INC.

IBM is a registered trademark of International Business Machines Corp.  
IBM PC is a product of International Business Machines Corp.

## Printing History

First Edition -- August 1989

# Precautions

**PROTECT THE UNDERWATER CABLE AND CONNECTOR.** Properly clamp the cable onto the lowering frame. Avoid any sharp bend in the cable. Make sure the cable is tightly clamped. A loose clamp will result in the cable slipping and possibly kinking under the small radius bend. *On more than one occasion, cables have been damaged by failure to tighten the cable.* The underwater connector is the most vulnerable part of the system. Do not step on it, or strike it while plugged into the instrument.

**PROTECT THE COMPUTER AND DISCS.** The PNF-300 system is designed to be used in a marine environment. However, most laptop computers are not. Keep the computer protected as much as possible. Also, do not leave the floppy disks lying out in the open; sunlight and moisture will ruin them. Keep disks sealed in a plastic bag, or something watertight, when they are not being used.

Always keep at least two extra copies of the program disk around. Discs have been known to fail or get lost at some of the worst times.

**PROTECT THE INTEGRATED CIRCUITS.** A person walking across a carpet on a dry day can generate a static charge of over 10,000 volts. The resulting discharge can destroy an integrated circuit. Use standard anti-static equipment any time the instrument is opened up and the components removed.

**AVOID THE SHADOW.** The underwater instrument package should be positioned for lowering on the side of the ship toward the sun. If the instrument is lowered into the shadow created by the ship, this shadow will contaminate measurements for depths up to 100 meters. When positioning the ship and the sensor, the wind direction is also a factor since the wind or wind-driven currents can push the ship over the sensor when it is being lowered, thereby causing shadowing. The surface PAR sensor should be mounted so that it will not be shaded by the upper parts of the ship, and so that it is not seeing reflections from the ship's superstructure.

**MAINTAIN PROPER CALIBRATION.** Calibration of the instrument is determined by data contained in the calibration certificate issued with the instrument, and updated on subsequent recalibrations. It is your responsibility to enter these values on your working floppy discs and keep them updated. *The calibration files supplied with the original software are for example only and must be updated before instrument use.*

**CARRY SPARE CABLE AND BATTERIES.** For extended operations, it is prudent to carry a spare underwater cable, and spare rechargeable batteries for the deckbox and the laptop computer.

# Contents

	Page
LIST OF FIGURES.....	ix
WELCOME.....	xi
1. GETTING STARTED.....	1-1
Setup and Checkout.....	1-2
Selecting a Computer.....	1-5
2. USING THE INSTRUMENT.....	2-1
Vertical Profiles and Integrated Logging.....	2-2
Seven Simple Steps to Proper Instrument Use.....	2-2
Some Do's and Don'ts.....	2-5
3. USING THE SOFTWARE.....	3-1
How Does the Software Work?.....	3-1
How to Use the GO300 Acquisition & Display Program.....	3-2
How to Use the PROGRAPH Profile Graphing Program .....	3-11
How to Use the LOGGRAPH Log Graphing Program .....	3-17
4. THEORY OF OPERATIONS.....	4-1
Theoretical Background.....	4-1
What is Natural Fluorescence?.....	4-2
Stimulated Fluorescence--An Early Method.....	4-2
Direct Measurements of Photosynthesis.....	4-3
Limitations.....	4-3
Advantages.....	4-4
Who Are the Users?.....	4-4

5. MAINTENANCE AND REPAIR.....	5-1
Maintenance.....	5-2
Repair .....	5-3
Incorrect Data.....	5-3
Cable--What to Do If It Breaks.....	5-3
O-Ring Leaks.....	5-3
Should Flooding Occur.....	5-4
List of Suppliers.....	5-4

## APPENDICES

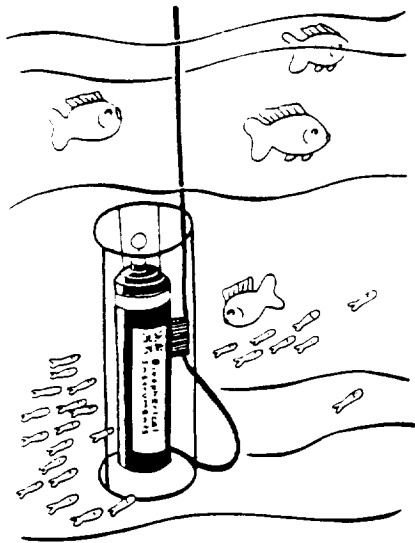
A. TECHNICAL DESCRIPTION.....	A-1
B. INSTRUMENT CALIBRATION AND DEFAULT SETTINGS.....	B-1
C. SOFTWARE INSTALLATION.....	C-1
D. RESEARCH PAPER "Natural Fluorescence in the Sea".....	D-1
E. INTERPRETING THE DATA: Seven Sample Profiles.....	E-1

# Illustrations

Figures	Page
1-1 Performing the Bench Test.....	1-1
1-2 PNF-300 System Components.....	1-2
1-3 Clamping the Underwater Cable .....	1-3
2-1 Using the Instrument.....	2-1
2-2 Avoiding the Ship's Underwater Shadow.....	2-3
2-3 Lowering the Unit Vertically.....	2-4
2-4 Washing off the Instrument.....	2-5
2-5 Storing Discs in a Ziplock Bag.....	2-6
2-6 Avoid the Ship's Shadow.....	2-7
3-1 Using the Software.....	3-1
3-2 The GO-300 Opening Screen.....	3-3
3-3 The Functional Display Menu.....	3-4
3-4 List of GO-300 Program Functions.....	3-5
3-5 Profile Parameters Menu.....	3-7
3-6 List of GO300 Profile Parameters.....	3-8
3-7 Sample GO300 Profile.....	3-10
3-8 PROGRAPH Opening Screen.....	3-12
3-9 PROGRAPH Default Setting Screen.....	3-13
3-10 Profile Graph Screen.....	3-15
3-11 CSV Conversion Screen.....	3-17
3-12 Log Graph Selection Screen.....	3-18
3-13 Graph of Selected Log Variable.....	3-19
3-14 Typical .CSV Spreadsheet of PNF-300 Data File.....	3-20

Figures	Page
4-1 Regression Diagram.....	4-1
5-1 Troubleshooting the PNF-300.....	5-1

# Welcome



Congratulations. With the Profiling Natural Fluorometer PNF-300, you now own the latest technology in photosynthesis measuring devices. The lightweight design permits lowering the instrument to as deep as 200 meters in a few minutes' time, and from platforms as small as outboard-powered inflatables. The unique portability is made possible by the low power usage of the natural fluorometer, a revolutionary tool that measures biofluorescence directly.

By measuring the natural fluorescence directly, you'll be using the most accurate method of recording photosynthetic productivity known. The natural light method has other advantages. All measurements are made during daylight hours, freeing up evenings for planning tomorrow's work based on today's results. Learning to use the menu-driven software that collects the data and plots profiles in real time takes no more than a few minutes. We hope you will enjoy your PNF-300 Profiling Natural Fluorometer.

## Features

- Instantaneous Measurement of Production in the water column
- Profiles of Primary Production, Temperature, and PAR
- Records both Time Series and Depth Profiles
- Fully computerized, display/operation with Laptop PC
- Cost Effective
- Complete Systems available

## On the Special Nature of Light and Its Measurement.

Before you begin using your PNF-300, you should spend a moment considering an important difference between this instrument and most other oceanographic instruments.

Most instruments measure *scalar* values (i.e. temperature, salinity, water clarity), and these values typically vary over a limited range, perhaps an order of magnitude (i.e. factor of ten). Current meters tend to be treated with a bit more respect because of the *vector* nature of their measurements (i.e. currents have speed and

direction). Still, the range of measured current speeds rarely exceed 3 orders of magnitude (i.e. 0.1 to 100 cm/sec).

Newcomers to the world of natural fluorescence may find it tricky, at first, to measure what amounts to a vector quantity (upwelling radiance), especially one with such a large dynamic range. The PNF-300 measures vertically-traveling light (upwelling radiance--as well as the scalar downwelling irradiance), and therefore must be kept pointing straight down. In this sense, the PNF-300 is more like that of a current meter than the CTD (conductivity, temperature, and depth) measuring device. Proper orientation is crucial.

More important still, the background noise of light in the ocean varies nearly as much as the signal itself. This noise consists primarily of unwanted shadows that darken the sensors, including both underwater sensors and the surface sensor. If these shadows are not avoided, it becomes difficult to discern the true signal.

## How the User's Manual Can Help...

This manual contains many useful tips for the proper use of the instrument and the proper interpretation of the data. Beginning with **Chapter 1 "Getting Started"** you'll become familiar with the hooking up the components and bringing the instrument on line. The next two chapters tell you how to operate the instrument in the field (**Chapter 2 "Using the Instrument"**) and later to analyze the data (**Chapter 3 "Using the Software"**).

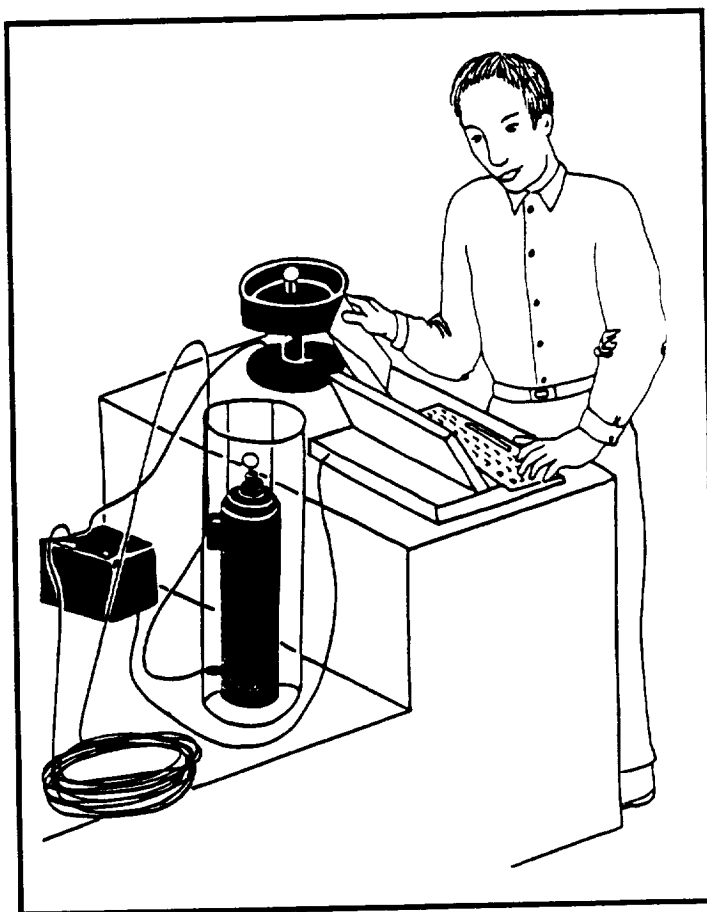
Before getting your feet wet, you would be wise to at least glance through some of the more theoretical sections of the manual. **Chapter 4 "Theory of Operations"** is a brief overview for the layman of the history of and theory behind measuring bioluminescence in the sea. (The quantitative theory and the validating field data recorded by the PNF-300 are found in **Appendix D.**) Sample PNF-300 data recorded over a variety of environmental conditions (i.e. turbulent seas, clouds, etc.) can be of great help for interpreting the analyzed data. These sample records are contained in **Appendix E.** The usual technical data on the instrument are also contained in the Appendices (**Appendix A, B and C**).

The PNF-300 User's Manual is designed for easy access, both as a learning tool and as a reference. Using the manual as a guide, and with a little practice, you will be making real-time productivity measurements with accuracy and ease.

# 1. Getting Started

This chapter covers the initial installation and checkout of the Profiling Natural Fluorometer. The bench test should be run upon receipt of the instrument and again on the day before deployment. The purpose of the test is to familiarize the user with the equipment, to check for proper battery voltage, and to detect any possible problems while they can still be repaired. Note: Prior to unpacking the instrument, read the list of precautions contained in the preface. Lack of attention to these simple precautions may damage or totally ruin your instrument, or at least create doubt as to the validity of the data.

**Figure 1-1. Performing a Bench Test.** The test should be carried out as soon as you receive the instrument, and within 24 hours prior to using it in the field. This allows time to recharge the battery, if needed.



---

## Setup and Checkout

After the instrument has been unpacked, and before taking it to the field, a cursory bench test should be performed. To obtain a better understanding of the instrument, the technical product description (Appendix A) should be reviewed. The five-step test requires only a few minutes' time. If any difficulties arise, check Chapter 5 "Maintenance and Repair."

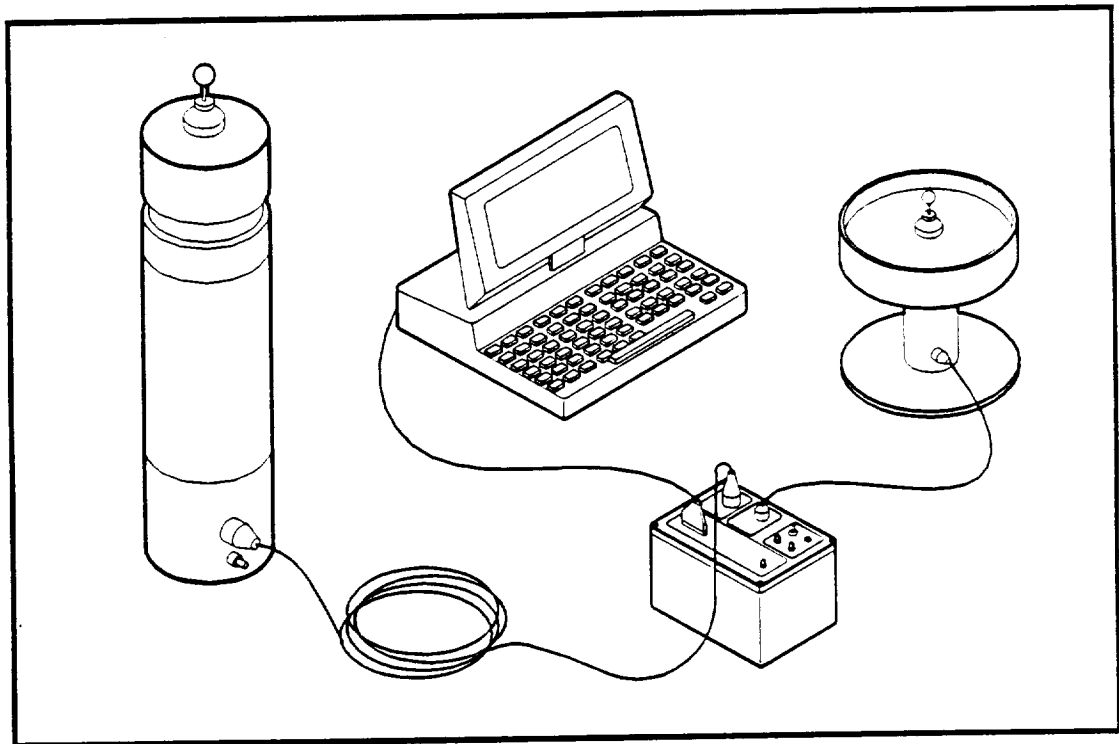


**Figure 1-2.** PNF-300 System Components. The system comes complete with underwater and surface sensors, deckbox (with charger), cable, lowering frame (not shown), and menu-driven software. Laptop computer is optional.

To test the system, perform the following steps:

**Step 1.** Install the system.

**Step 2.** Power up the deck box and the computer.

**Step 3.** Start the program.

**Step 4.** Check the sensors and the battery.

**Step 5.** Set the calibration constants and configuration parameters.

## Step 1. Install the system.

### PLUGGING IN THE CABLE.

To plug the cable into the underwater instrument, align the two small bumps on the connector sheath with the largest of the four connector pins. Bubbles sometimes form in the connector sheath of the underwater connector, and can cause leakage and a bad connection. To bleed the bubble, squeeze the sheath as you push the underwater connectors together. The connector should fully mate.

The first step requires loading the software into the recording IBM-PC compatible computer (see Step 4, and Appendix C "Software Installation"). Connect the components as shown in Figure 1-2. *The underwater instrument should be installed inside the lowering frame* (not shown in Figure 1-2). The normal operational mode for the instrument requires use of all the components. As the main processor is contained in the underwater unit, many of the steps below can be conducted *without* the surface sensor. Make sure that the underwater cable connectors are correctly seated (see note). Prior to actual use, make sure that the cable clamp on the lowering frame is *tightly* gripping the underwater cable, and the cable is properly curved (Figure 1-3). Failure to properly clamp the cable can result in an excessively sharp bend, causing the cable to break.

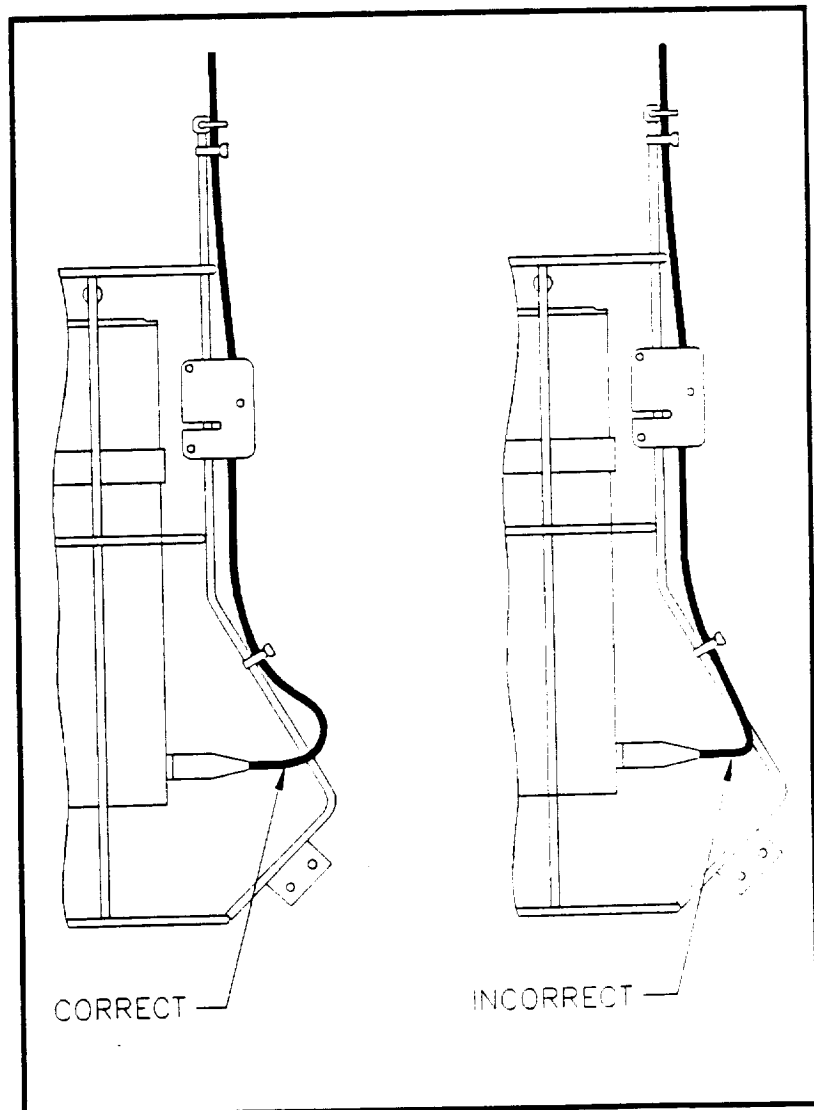


**Figure 1-3.** The correct way to clamp the underwater cable onto the lowering frame. *Failure to tighten the cable clamp can cause the conductors to sever and the instrument to fail.*

## **Step 2. Power up the deckbox and the computer.**

When received from the factory, the deck box battery should be completely charged. With the deck box connected to the underwater unit, turn on the deckbox. The power light on the deckbox should come on and the data light should produce a steady blink. The blinking light indicates the proper connection of the underwater unit, but not necessarily that of the surface light sensor.

## **Step 3. Start the program.**

With the computer connected to the deck box, call up the Data Acquisition program. From the DOS prompt on the computer, type GO300, then press ENTER. If the underwater unit has been properly connected, the GO300 Opening Screen will appear (see Figure 3-2, Chapter 3). If not, the check-cable message described in Step 4 will appear--recheck underwater cable connection. Press ENTER again to call up the Functional Display Menu (Figure 3-2). This Functional Display menu contains a data display window showing the real-time data measurements.

## **Step 4. Check the sensors and battery.**

Once you have installed the system, it is important to verify that you are collecting real data. The fastest way to do this is to expose the sensors to light, note the readings, and then completely darken the sensors and note these dark readings. The values should match the light/dark range of values found in Appendix C. The battery voltage should fall within a range of 8 to 13 volts.

## **Step 5. Set the calibration constants and configuration parameters.**

Setting the parameters can be done without connecting either the underwater or surface sensor. This step is necessary at least for setting up the proper graphic card (see note "Selecting the Proper Screen" next page) and proper printer. Also, the default calibration values must be set prior to operating the instrument in the field. *The current contents of the CALIBR8.G30 file are incorrect, and must be updated with the latest values contained in the current calibration worksheet.* To set the current calibration constants, refer to the steps in Appendix B.

**SELECTING THE PROPER SCREEN.** The current software supports four different types of graphic cards. The CPU displays information on the monitor through an integrated board known as a graphics card. The PNF-300 supported cards are: (1) Type 2 CGA Color card common to most laptops and desktops, (2) Type 9 EGA card found in the newer desktops, (3) Type 12 VGA cards found in the top-of-the-line desktops, and (4) Type 11 MCGA cards found in the new PS2 family of microcomputers. Still under development is the Hercules Graphic card support for monochrome monitors.

Should the underwater unit be disconnected (or improperly connected), OR should the deckbox not be turned on (or the battery be insufficiently charged), the following screen will appear: Device timeout, check RS232 cables and instrument power. Or Press <ESC> to change configuration. If it is your intention to have the sensor connected for sensor testing, check the connection of the RS232 cable, the underwater cable, and the instrument power. If, however, you want merely to set the configuration parameters or calibration constants, press ESC.

Upon pressing the ESC key, the program will advance to Step 3, Set the Profile Parameters of the GO300 Acquisition and Display Program (Chapter 3 "Using the Software"). As shown in Figure 3-5 (Chapter 3), the parameters include logging interval, maximum plotting depth, plotting temperature, Com Port, data drive and archive time, printer definition, screen type, and calibration constants. A complete description of each of these parameters are contained in Chapter 3. The parameters are selected by pressing one of the number keys 2 through 9. Selecting the desired parameter calls up a screen which prompts the user to enter the desired parametric value.

This completes the bench test and software configuration of the PNF-300. You are now ready to deploy the instrument.

---

## Selecting a Computer

The instrument operates best with an IBM PC-compatible laptop computer for making field measurements. Portability is a key feature of the PNF-300 system, and having the computer close by is essential to using the real time data graphing feature. A host computer in the laboratory with a large storage capacity and high speed processing is useful for further data processing and storage. For further details on configuring the host computer file directories, and on some further considerations about configuring your laptop computer, see Appendix C.

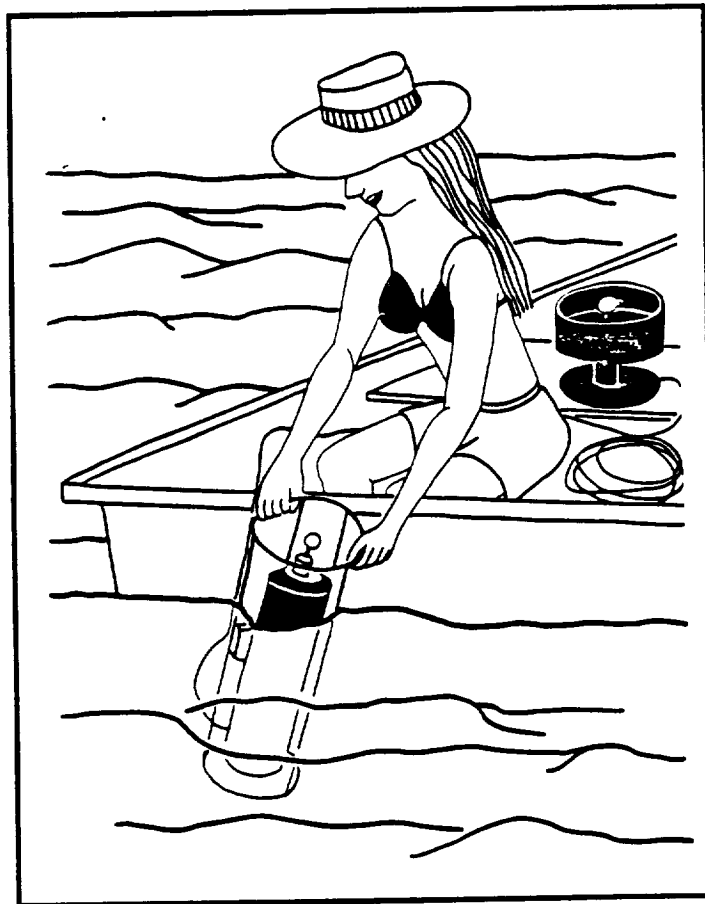
---

## 2. Using the Instrument

Before actually deploying the instrument, give it a cursory bench test according to the procedures contained in Chapter 1 "Getting Started."

Once you have gained a brief experience with the instrument, you are ready to record actual data. Be sure to go over the software section, at least the initial portion covering the GO300 Acquisition and Display program. Included in this chapter are seven simple steps to proper instrument use, complete with a few do's and don'ts to keep in mind.

**Figure 2-1.** Using the instrument.  
The operator is being careful not to accidentally allow her shadow or any other shadow to fall across the surface light sensor.



## Vertical Profiles and Integrated Logging

There are two basic modes of data recording in the PNF-300 software: **vertical profiles** and **integrated logging**. Vertical profiles are recorded when you lower the instrument into the water column and retrieve it. This allows the display and analysis of data as a vertical profile of the water column with depth. Integrated logging, on the other hand, records all parameters as time-averaged data, usually from a single point, and allows you to analyze your results as a function of time. An example of this might be where you wanted to record the time history of natural fluorescence, temperature, and underwater and surface PAR while the instrument is suspended at a fixed depth during an incubation. Another example might be where you were conducting shipboard incubations in the sun and you wanted to record the light history on the surface PAR sensor during the incubation. Another example might have you alternating between these activities during the day, generating one day long log file and several vertical profiles.

The bulk of instructions below are concerned with measuring vertical profiles. Instructions on using the integrated logging software are contained in Chapter 3

## Seven Simple Steps to Proper Instrument Use

The steps to proper instrument deployment can be grouped into three phases: pre-deployment, deploying the instrument, and post deployment.

### PREDEPLOYMENT

**Step 1. Prepare the instrument.** Connect the system, uncap the light sensors, and clean the natural fluorescence window. *Use care in wiping the window, using tissue so as not to scratch the glass.* Position the surface sensor. Make sure the *surface sensor* will not be shaded by the upper parts of the ship, or any passing personnel. Nor should it see reflections from the ship's superstructure.

**Step 2. Check the ship's drift.** The ship should be at all stop, and the screws not be turning. Check with the bridge watch to make sure the instrument will deploy away from ship's shadow. The ship's drift is crucial to this avoidance. The optimum combination of wind and sun angle to help avoid immersion in the shadow has the wind coming from the direction of the sun. (A lowered weight on the end of a line makes a fine makeshift drogue used to measure drift just prior to deployment.)

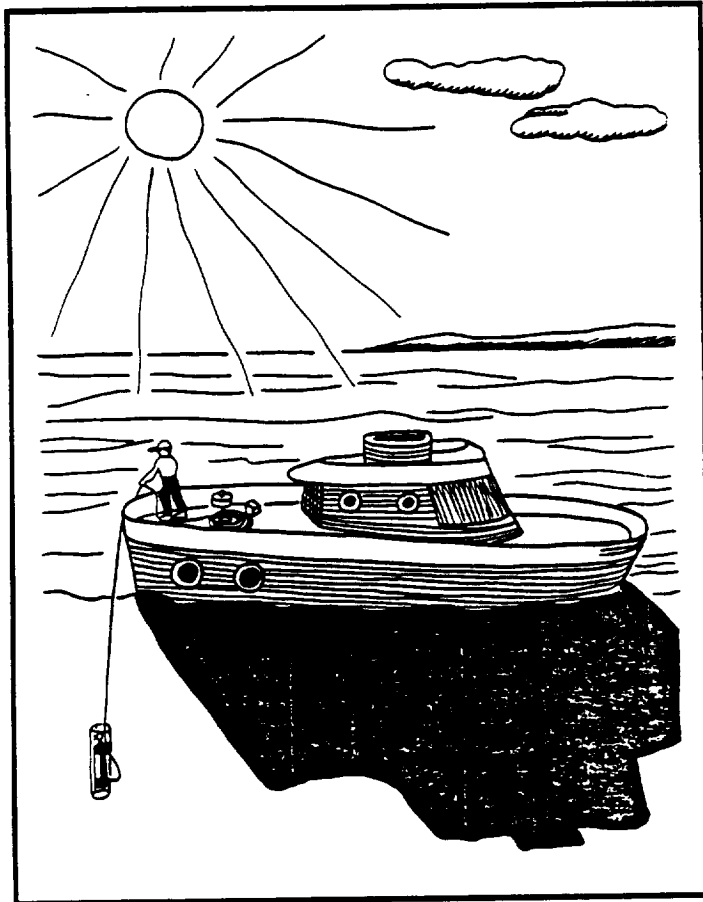


**Figure 2-2.** Avoiding the Ship's Underwater Shadow. Such shadows can not always be avoided, but the user should be aware of their deleterious effects on the data.

**Step 3. Wet the cable.** Wet down the cable for ease of paying out the line. This will wash off some of the salt crystals, and will save your hands. Gloves are also helpful.

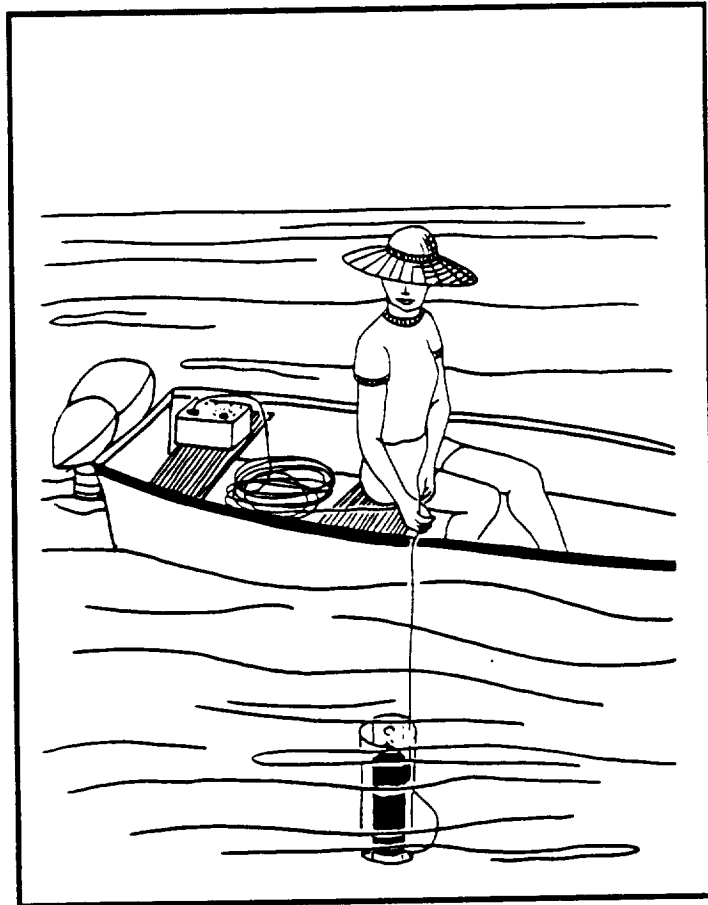
## DEPLOYING THE INSTRUMENT

**Step 4. Immerse the instrument.** Enter the GO300 program on the laptop computer, then go into the Functional Display menu. (See Step 3 in "Getting Started.") If the instrument has been sitting in the sun on deck and is thus hot, and you are lowering it into cold water, letting the instrument cool down before starting the profile will allow the pressure transducer to reach a stable zero or surface reading. Press **F5**. This starts the recording function. The instrument is now ready to deploy.

**Step 5. Deploy the instrument.** Pay out the line, keeping sufficient tension in the line to keep the instrument pointing straight down Lower the instrument at a steady rate of approximately 1/2 meter

per second. Monitor the data light on the deck box making sure that it continues blinking. When the full cable length has been payed out, or the instrument has reached the intended depth, retrieve the instrument, taking care not to tangle the cable. Depending upon your preferences, you may not wish to record data on the upcast. If not, press **F6** before retrieving the instrument. Alternately, you may wish to stop the cast with the instrument at the bottom of the cast, and restart recording, making the upcast a separate profile. Otherwise, data from the up and downcasts will be processed and averaged together.

**Figure 2-3.** Lowering the Unit Vertically. Consideration should be given to the fact that the instrument actually measures the vertical (upwelling and downwelling) light.



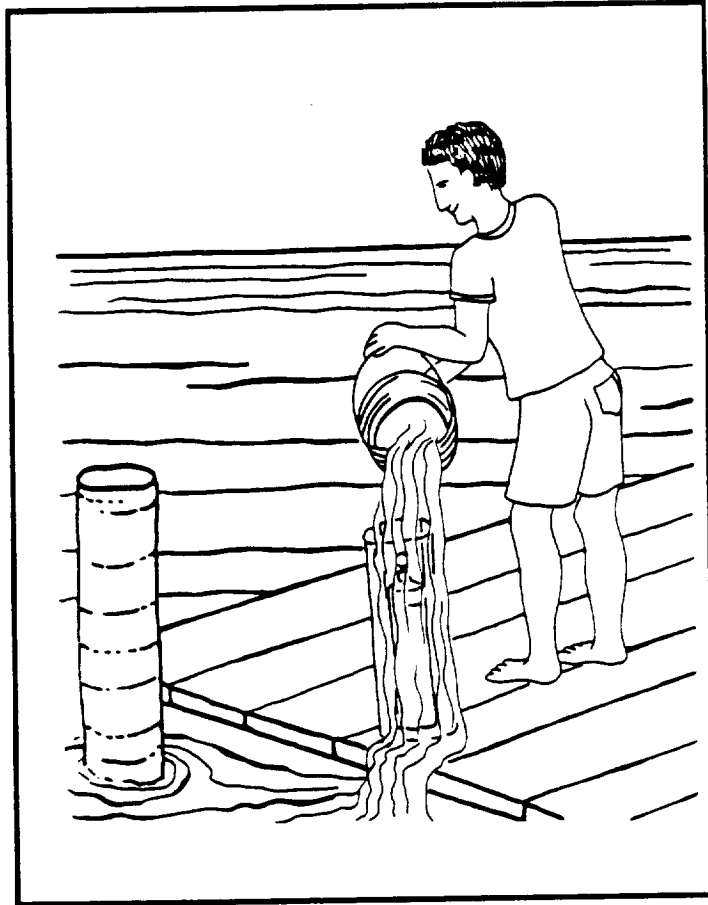
## POST DEPLOYMENT

**Step 6. Stop Recording and Verify Data Record.** After the sensor has been brought out on the deck, verify that the Functional Display menu says the sensor is on deck by noting the deck reading. To stop the recording, press **F6**. The data file is now safely stored.

**Step 7. Rinse off the instrument.** Rinse the instrument with fresh water (use a bucket if no hose is handy), disconnect, and store. Salt water can ruin the connectors and corrode metal surfaces. Return

to the laboratory with the laptop computer for data transfer and analysis.

**Figure 2-4.** Giving the instrument a fresh water bath. This is one of the most important steps to good maintenance you can perform. Be sure to wash off the underwater cable as well. Salt buildup on the cable often rubs off onto the instrument.



This concludes the chapter on instrument use. Some tips on what to do and what *not* to do can be helpful.

## Some Do's and Don'ts

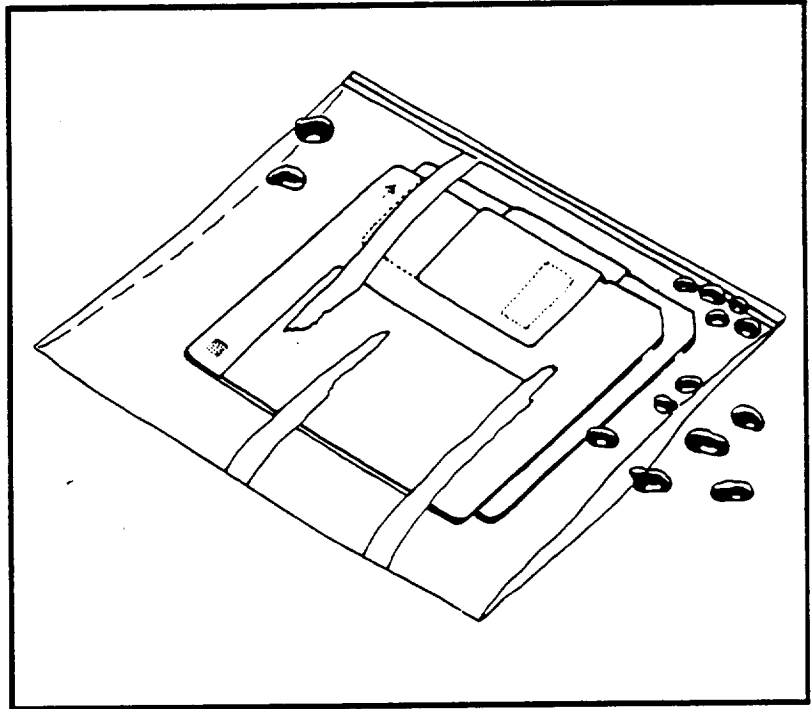
Extensive use of the PNF-300 over a variety of logistic and weather conditions has proven the durability and reliability of both the instrument and the software. Here are a few tips that will help your PNF-300 deliver accurate and reliable data.

### DO'S

1. Store any floppy disks that are kept in air conditioned spaces in a Ziplock bag. Allow the package to warm outside before taking the disks out of the bag and into the moist air. This prevents condensation which could harm the disk.

2. Use "RAM disk" or "virtual disk" on the laptop computer. This eliminates the need to write data to floppy disk, a process which can slow the recording of data.
3. Use a supplementary 12V battery (the boat battery may be okay--consult your computer manual first) for the laptop computer. This practice ensures against loss of power during long surveys.

**Figure 2-5.** Storing the Disks in a Ziplock Bag. This protects the disks from salt and moisture.

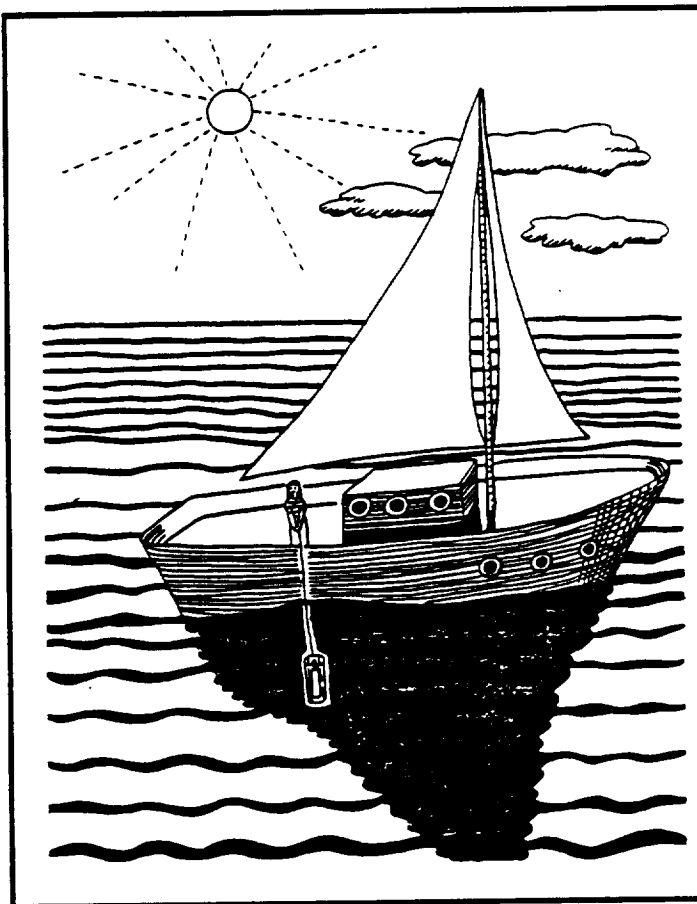


4. Place the surface light sensor close to the instrument lowering point. Especially on larger vessels, this practice reduces the risk of uneven cloud shadowing of the surface unit and the underwater unit.
5. Allow ample room for error and fatigue, as ocean work is extremely taxing, even in the best weather.
6. Make sure that the surface PAR sensor remains clear of shadows from the ship's structure or passersby. This also includes the instrument operator (see Figure 2-2).
7. Maintain the practice of using a log book. Environmental conditions of wind, clouds, sea surface, and general station accounting is often crucial for proper data analysis.

## DON'TS

1. **Don't** permit the instrument to enter the ship's shadow.

**Figure 2-7.** Avoid the shadow. By now the reader is undoubtedly familiar with this cardinal rule.



2. **Don't** use the cable as mooring line, even for tying up a lightweight inflatable boat. **Don't** allow the line to kink. Avoid walking on the cable.
3. **Don't** lower the unit in a jerky motion. This will cause an erratic calculation of the attenuation coefficient. For an example of a profile measured incorrectly in this fashion, see Appendix E "Interpreting the Data."
4. **Don't** overload the sensor. Under some circumstances one of the sensor channels in the instrument may go into overload. This will frequently happen when the natural fluorescence sensor is exposed

to bright light such as that reflected off the deck of the ship or over a shallow, light-reflective bottom. In this case, readings in all of the sensor channels will be disturbed. Such an overload is not likely to occur with the probe in deeper waters, and in any event is not harmful to the instrument.

## **In Conclusion...**

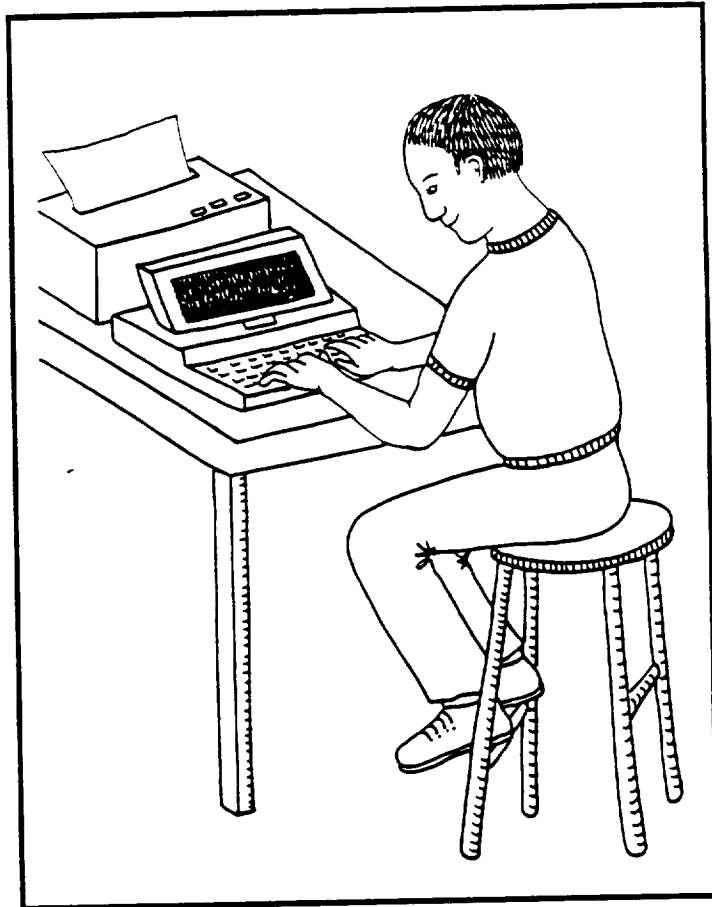
These simple steps and precautionary measures should be enough to help you obtain a proper measurement and recording of the applicable data. To make use of the full power of the system, several menu-driven programs have been developed for plotting and further analysis. A step-by-step procedure for using the software is contained in the next chapter.

---

## 3. Using the Software

Once you've learned the basics of deploying the instrument, you'll need to become familiar with its more powerful recording and analytical features.

**Figure 3-1.** Using the Software. Having a host computer is useful for post-survey data analysis and storage.



### How Does the Software Work?

The PNF-300 software allows you to record the data, to produce graphs, and make other analyses. The three easy-to-use programs consist of a single on-site recording program and two programs for post-survey analysis. The on-site recording program also contains real time plotting capability.

All three programs can be loaded and operated on a laptop computer, although a larger host computer is recommended for the two post-acquisition programs for improved speed. The PNF-300 programs are:

Program	Command
Acquisition and Display	GO300
Profile Graphing	PROGRAPH
Log Graphing	LOGGRAPH

---

## How to Use the GO300 Acquisition and Display Program

The Acquisition and Display program GO300 is used to record the measured data. It also can be used to graph the data during real time recording. The program stores the binary files (both profiles and time series) received through the deck box, and converts the data to digital and graphic output. The program is menu driven, and contains a number of easy-to-use features.

To use the GO300 program, carry out the following menu-driven steps.

- Step 1.** Open the GO300 Screen
- Step 2.** Select a Program Function
- Step 3.** Set the Profile Parameters
- Step 4.** Display the Profile

**WHAT IS A FILE?** A word that once meant a cardboard folder stored in a drawer has forever been altered by the computer revolution. Today, a "file" generally refers to a set of data or information stored inside a computer's memory. A PNF-300 file contains all the data recorded during a single "cast," or lowering of the instrument. Files usually are named according to the date and time they were recorded. Original data files are recorded in volts, without calibration constants applied. CSV files have calibration constants applied.

## Step 1: Open the GO300 Screen

To call up the opening screen, and to change the downcast file name, type GO300 from the DOS prompt, then press ENTER. The opening screen will look like this (Figure 3-2):

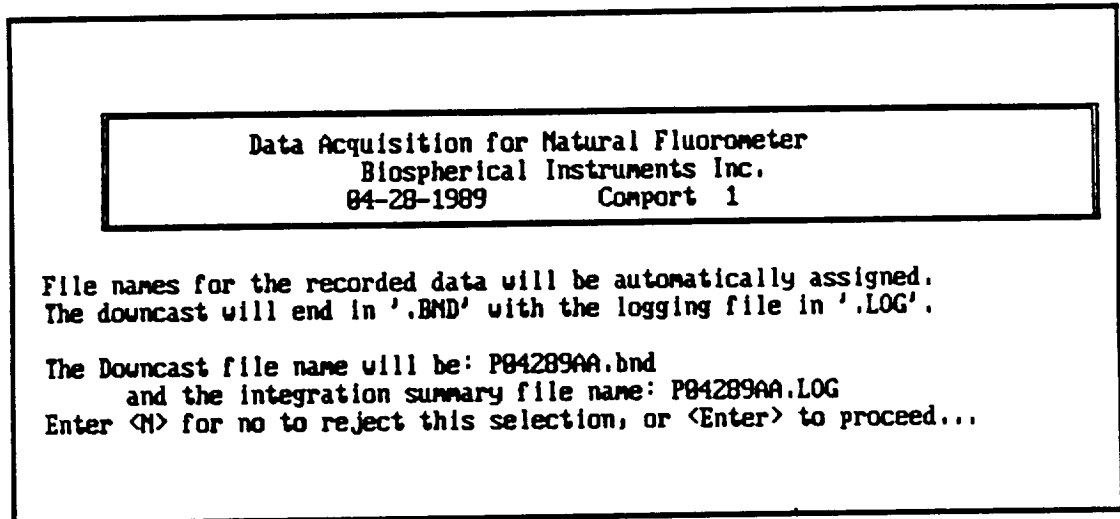


Figure 3-2. The GO300 Opening Screen

The downcast file name appears in the center of the opening screen. The file name format is:

**EXAMPLE OF A FILE NAME.** The file name on the opening menu above is P04289AA.LOG. This denotes the first set of data AA recorded on April 28, 1989. The file extension .LOG signifies a time series taken at a single depth and position. Selecting the letter N allows a change of the file name. Press ENTER to recall the Functional Display menu. The initial P denotes the product.

PMDDY@@.EXT, where:

MM is the digital month

DD is the digital day of the month

Y is the last digit of the year

@@ is the autoincrementing serial letter, from AA, AB, etc. through ZZ (676 files per day).

EXT is the file extension, where:

.BND denotes profile files (BiNary Downcast)

.LOG denotes log files

To change the file name, select the letter N. Then type in the desired file name.

## Step 2: Select a Program Function

The Functional Display menu displays most, but not all, of the ten user-selected functions for the Data Acquisition and Display program. It also contains a data display screen that shows the latest recorded values of all recorded parameters.

The Functional Display menu is automatically displayed after the opening screen. The Functional Display menu looks like this (Figure 3-3):

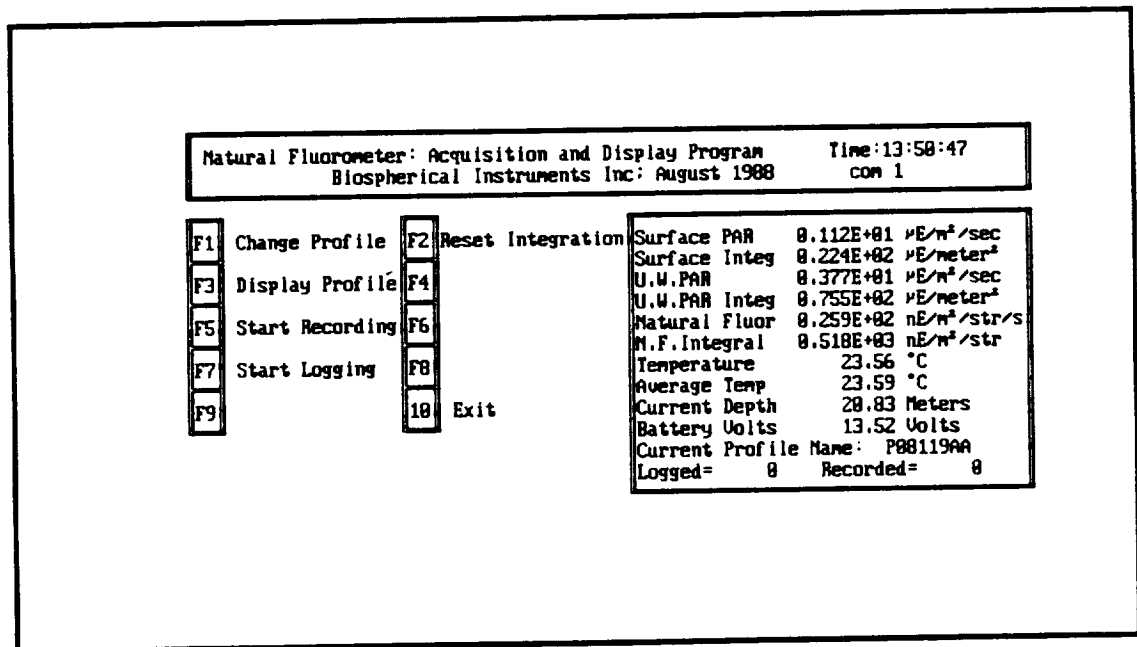


Figure 3-3. Functional Display Menu

Note that a data display screen showing the latest data measurements appears on the function menu. The measurements are as follows: Surface irradiance (Surface PAR), underwater irradiance (U.W. PAR), Natural Fluorescence (Natural Fluor), integrated light values (of the above three measurements), instantaneous and average water temperature (Temperature and Average Temp), Current Depth (meters), Battery Volts, File name, file size (following the name--in bytes), number of Recorded (profile) points, and number of Logged (time series) points.

The integrated light values (Surface Integ, U.W. PAR Integ, and N.F.Integ) are continuously computed from the three light values by summing them from time zero to the present. The Average Temperature likewise is computed from the entire series of values recorded from time zero. Pressing the F2 Reset Integration key will zero the integrated values.

## What Are the Program Functions?

The program functions permit the operator to start and stop instrument recording, to graph and print the recorded profiles, and to control other important parameters. These functions are operated from the Functional Display menu or from the Graphing Display Profile function (F3). The complete listing and description of program functions are:

Key & Name	Description
F1--Change Profile	Sets profile parameters.
F2--Reset Integration	Resets integration value to zero.
F3--Graphing Display Prof.	Plots data profile on screen.
F4--Exit Profile	Returns to Functional Display menu.
F5--Start Recording	Starts the profile data recording.
F6--Stop Recording	Stops the profile data recording.
F7--Start Logging	Starts the log (time series) recording.
F8--Stop Logging	Stops the log (time series) recording.
F9--Print	Print data profile.
F10--Exit	Exit the program.

Figure 3-4. List of GO300 Program Functions

## How Do The Functions Work?

A complete description of the ten program functions follows:

**F1 Change Profile.** This function allows the user to set a number of profile graphing parameters (i.e. temperature range, ComPort, Printer, etc.) used in the real-time graphing function. Instructions on

how to set these parameters are given in "Step 3: Calling up the Change Profile Menu" below.

**F2 Reset Integration.** The software automatically sums the three light values (surface PAR, underwater PAR, and natural fluorescence) and averages the temperature values from time zero to present. By selecting the Reset Integration function, the user resets the integrated or temperature average value to zero.

**F3 Graphing Display Profile.** This function graphs the data profile and displays the graph on the screen. The selection of the function does not interrupt the data recording. Instructions on how to view the graph and how to print it are given in "Step 4: Calling up the Display Profile Menu" below.

**F4 Exit Profile.** This function is not displayed on the Function Display menu, but rather appears (along with the F9 Print function) on the profile graph. Selection of the F4 Exit Profile returns the screen to the Function Display menu.

**F5 Start (profile) Recording.** This function begins recording the displayed profile data onto the computer's disk.

**F6 Stop (profile) Recording.** This function does not initially appear on the menu, but does come up once the F5 Start Recording key is selected, at which time the Start Recording function disappears. This can be used to exit the Graphing Display Profile function F3, returning to the Functional Display menu. The graph may be later recovered using the PROGRAPH program..

**F7 Start Logging.** This function begins recording the displayed logging data onto the computer's disk.

**F8 Stop Logging.** This function does not initially appear on the menu, but does come up once the F7 Start Logging key is selected, at which time the Start Logging function disappears. This can be used to exit the Graphing Display Profile function F3, returning to the Functional Display menu. The graph may be later recovered using the PROGRAPH program.

**F9 Start Print.** This function is not displayed on the menu, but rather appears (along with the F4 Exit Profile function) on the profile graph. Make sure you have a proper printer (HP LaserJet-compatible or Epson-compatible--no daisy wheels or Diablos) and that it is properly configured (see Appendix C).

**F10 Exit.** This function exits from the Function Display menu back to the opening menu and simultaneously halts all data recording. The user is asked to verify with the prompt: Confirm that you want to quit by entering Y.

Once you have looked the various functions, you will next need to become familiar with the various profile parameters called up with the F1 Change Profile function.

### Step 3: Set the Profile Parameters

The Profile Parameter menu displays a number of recording and graphing parameters, and is called by the F1 key from the Functional Display menu. The Change Profile menu is shown below.

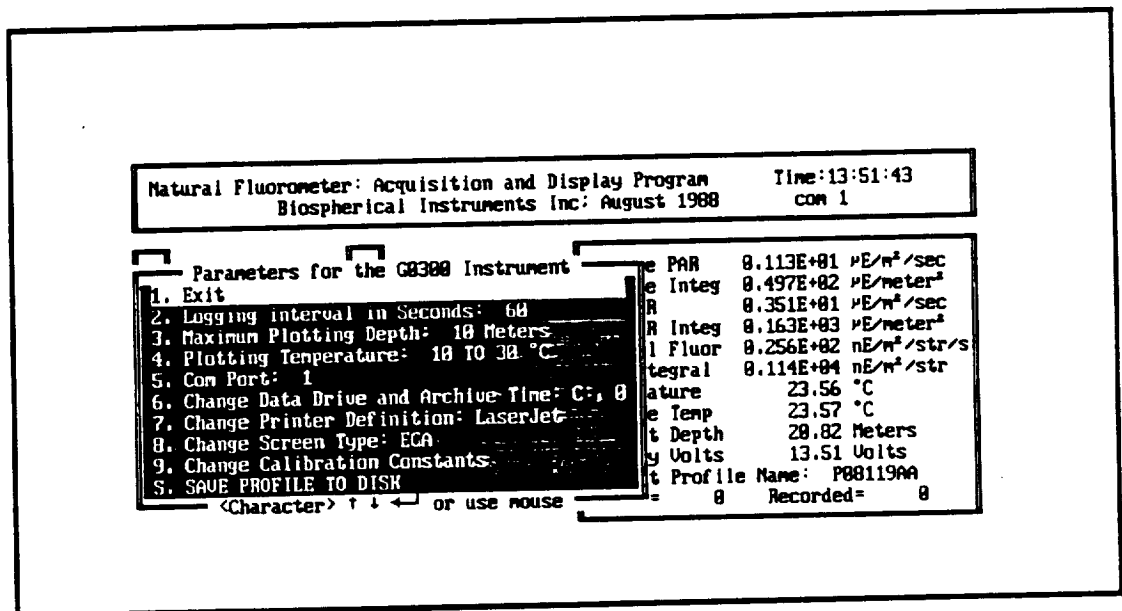


Figure 3-5. Profile Parameter Menu

As shown above, the Profile Parameter menu contains a number of parameters governing the recording and graphing functions. These can be altered. Parameters are selected using the *number keys only*, not the F-number keys.

## What Are the Profile Parameters?

When plotting a real-time profile, the computer needs to know the proper plotting limits before making the plot. Also, for easier comparison of plots, you may wish to have all the plots scaled the same. The following functions allow easy editing of these parameters.

Key	Profile Function (incl. default values)
1	Exit
2	Change Logging (default, 60 sec.)
3	Change the maximum plotting depth (default, 200 m)
4	Change the plotting temperature range (default, 5 to 30)
5	Change the communication port (default, Com. 1)
6	Change data drive and archive time (default, drive B; 15 min.)
7	Set printer
8	Set screen
9	Set calibration
S	Save selected parameters.

Figure 3-6. List of GO300 Profile Parameters

## How Do The Profile Parameters Work?

Several of the profile parameters appearing on the Change Profile Menu are elaborated on. These can be altered by pressing the indicated key.

- 2 Logging Interval (seconds). Used for the logging mode (F7) only. The default interval is 60 seconds. This parameter is used to control the time resolution of the log file. Increasing the sampling period decreases the resolution but extends the lifetime of your battery powered computer if you are *not* using

the RAM disk. When selecting the logging interval it is important to consider how much data will be recorded over your observation time. For example, if you set the logging interval to 3 seconds, a profile taking 51 minutes will create a logging file 37 Kbytes long. When you turn this into a CSV file, it will be 121 Kbytes long. If you were to let it run for a full 24 hours, then it would be 2.6 MB in size. If you were recording to a floppy disk, the disk would become full and the logging would be stopped. Remember that approximately 36 bytes are recorded each time a cycle is logged. A rate of one sample per 60 seconds is relatively safe creating files at a rate of 53 Kbytes per day.

- 3 **Maximum Plotting Depth.** Used for scaling the ordinate of the profile graph viewed during real-time recording. (See F3 Display Profile function.)
- 4 **Plotting Temperature Range.** Used for scaling the temperature profile graph viewed during real time recording. (See F3 Display Profile function.)
- 5 **Com Port.** Allows the user to switch the ComPorts on host computer.
- 6 **Data Drive and Archive Time (Minutes).** On lap top computers where data are stored to RAM, as a safety practice the user is recommended to archive the data to a floppy diskette. The Archive Time sets the archive interval in minutes. It is recommended the archive time be set to 15 to 30 minutes. (For complete details on the advantages of writing data to RamDisc, hard drives, or floppies, see Appendix C.)
- 7 **Printer.** This allows the user to select between an Epson dot matrix printer and an HP LaserJet laser printer.
- 8 **Display screen.** This allows the user to select between various graphics cards for EGA, CGA, VGA, and MCGA screens. (See note "Selecting the Proper Screen," Chapter 1, Step 4.)
- 9 **Change Calibration constants.** See Appendix B.
- S **Save Profile to Disk.** The function allows all parameter changes to be saved for future sessions.

## Step 4: Display the Profile

The real-time graphing function (F3) allows the user to view and print the profile as the data are recorded. An example of a real time profile graph is shown below (Figure 3-7).

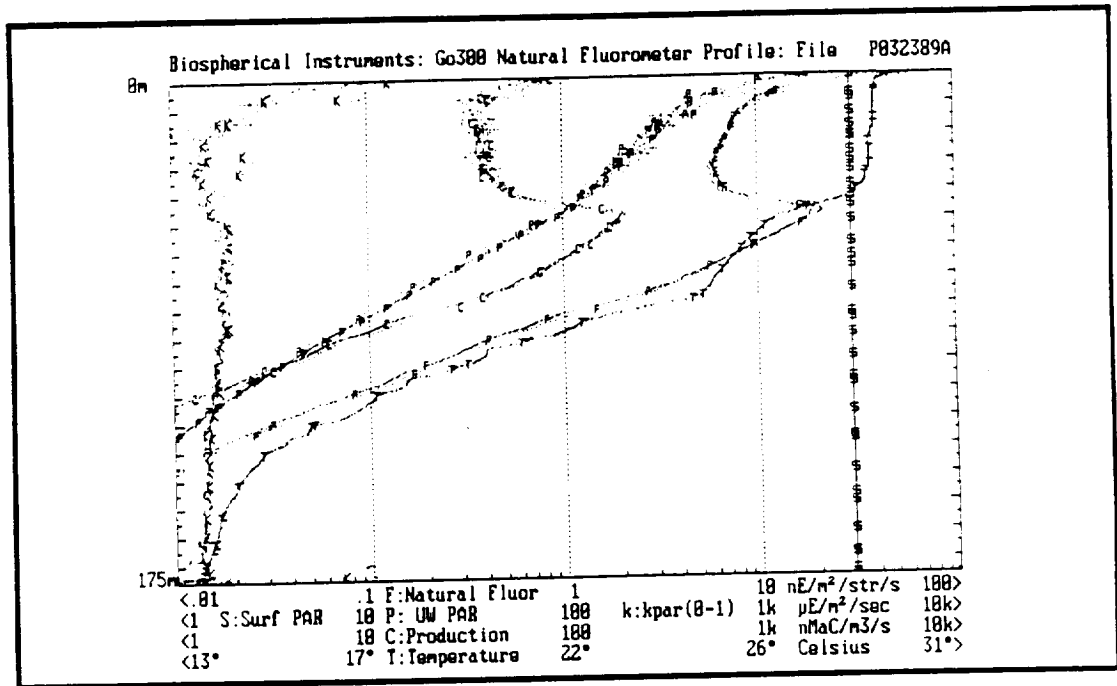


Figure 3-7. Sample GO300 profile .

## What are the Graphing Functions?

As seen in the upper right hand corner of the graph (Figure 4-4), the graphing function contains two additional active functions: the F4 Exit function and the F9 Print function.

**F4--Exit.** The exit function ends the display and returns the screen to the Functional Display menu.

**F9--Print.** The print function prints any type screen (CGA, EGA, VGA, or MCGA) to an Epson compatible or an HP LaserJet compatible printer. This must be correctly set up prior to printing. See Step 3 above.

## What other functions work from the graph?

The following functions can also be used in the Display Profile mode.

**F5--Start Recording**

**F6--Stop Recording**

**F7--Start Logging**

**F8--Stop Logging**

**F10--Exit**

The F6 Stop Recording and F8 Stop Logging functions both cause loss of the graph and return to the Functional Display menu. Once the data have been recorded and the instrument stored, you are now ready to begin using any of the plotting and data analysis programs.

---

## How to Use the PROGRAPH Profile Graphing Program

The PROGRAPH Profile Graphing program (1) graphs the data, (2) modifies various recording and graphing parameters, and (3) prepares the data in a comma-separated-value (CSV) format. The first two functions are covered as steps 1-4 below. The CSV-conversion is covered as Step 5.

The graphing feature allows either autoscaling of the graph coordinates or manual adjustment of the limits. The graph can be printed to a variety of Epson compatible or HP LaserJet compatible printers. An important feature of PROGRAPH is that it allows calculation of production from natural fluorescence, and the calculation of kPAR. It also allows the averaging of data collected over specified depth intervals.

To use the PROGRAMPH Profile Graphing program, carry out the following menu driven steps. In order of their appearance, the steps are:

**Step 1.** Open the PROGRAMPH screen.

**Step 2.** Change the default parameters.

**Step 3.** Plot the graph.

**Step 4.** Print the profile graph.

**Step 5.** Create a comma-separated-value (CSV) file.

## Step 1: Open the PROGRAMPH Screen

To call up the opening (Select-a-File)screen, and to graph and possibly print a .BND file, type **PROGRAMPH** from the DOS prompt, then press **ENTER**. The opening PROGRAMPH screen looks like this(Figure 3-8):

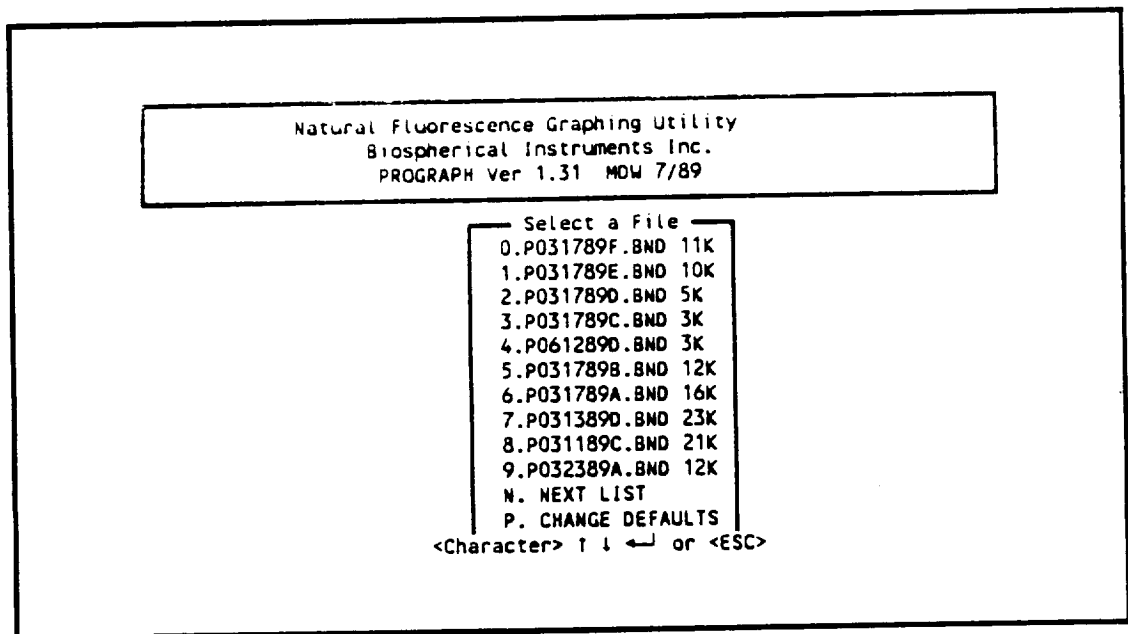


Figure 3-8. The PROGRAMPH Opening Screen

The opening screen displays all applicable .BND files sorted with the most recent files on top.

## Step 2. Change the Default Parameters

This step permits the user to select one or more of the measured values to be included on the plot. It also allows enabling of the surface light correction and the attenuation coefficient kPAR, parameters which help correct for the passage of cloud shadows and the effects of surface mixing respectively (see Appendix E "Interpreting the Data").

To call up the Default Setting menu, type **P** from the opening (Select-a-File) screen. The PROGRAMH Default Setting menu looks like this (Figure 3-9):

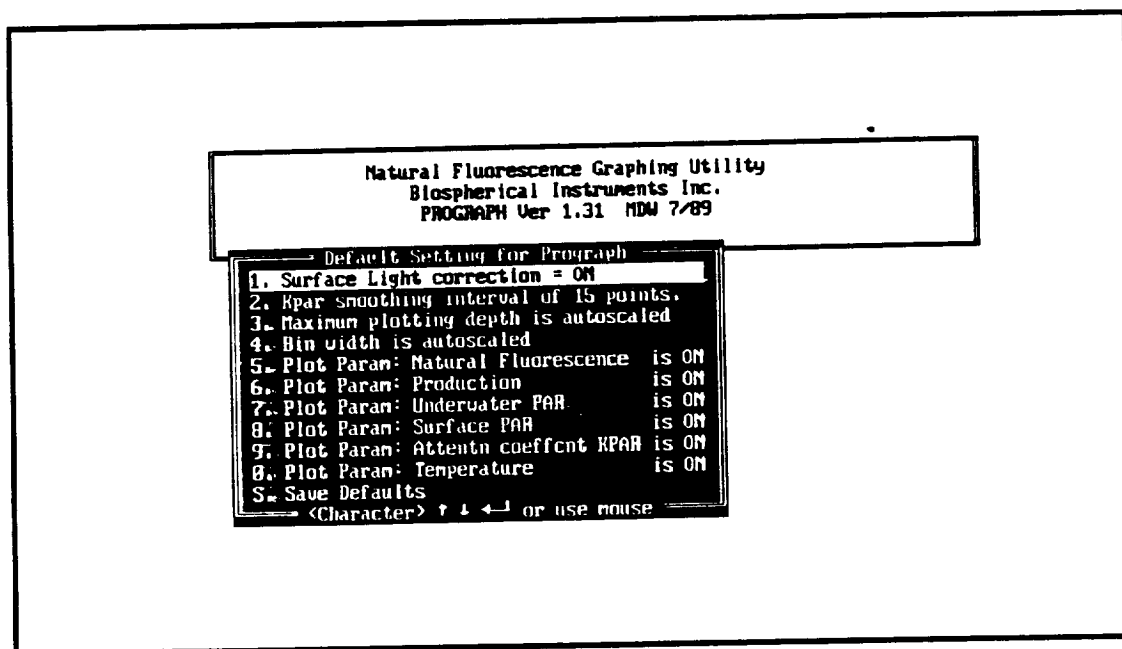


Figure 3-9. The PROGRAMH Default Setting Screen

To change any of the profile default settings, press the applicable number, then press **ENTER**. Once the new default values and settings are set, press **S**. To return to the opening (Select-a-File) menu, press the **ESC** key. The following is an elaboration on default options numbers 1,2, and 3.

**Default 1.** The surface light correction allows you to specify if you wish the software to calculate the ratio of the underwater PAR to the surface PAR and use this ratio in the calculation of the diffuse

attenuation coefficient for PAR ( $k(\text{PAR})$ ). Set this value to ON to enable this correction (the value will toggle from ON to OFF by highlighting the entry using the cursor keys and pressing ENTER).

**Default 2. The  $k(\text{PAR})$  smoothing interval** allows you to set the interval in observation points over which  $k(\text{PAR})$  is calculated. In the calculation of  $k(\text{PAR})$  at a specific depth, underwater PAR values collected over a range of observations before and after the desired observation are considered. This range of data are specified as the "smoothing interval." The selected values are then natural log transformed and a straight line is fit through the PAR (or PAR ratio) observations versus depth. The slope of this line is equivalent to the attenuation coefficient. We have found this method to be superior to other smoothing methods we have tried, but it does require that the measurements have been made over a sufficiently large depth range, usually at least 3 meters. If not, the results will be erratic. We recommend a value here of 15 points. If conditions were very rough during the profile, then try doubling this value. Generally, values less than 10 points will give very noisy values of  $k(\text{PAR})$ . Values greater than 50 will lose most of the detail of  $k(\text{PAR})$  in a vertical profile, and will slow down the data reading process.

**Default 3. Maximum plotting depth** allows you to choose either autoscaling for the maximum depth, or to enter its value manually. You may prefer to enter it manually if you want all of your plots to be scaled the same. To change from the ON condition to manual scaling, highlight the entry and press ENTER. A secondary menu will appear.

**Default 4. Bin width** controls the depth interval size for the table that follows the PROGRAPH graph (see Figure 3-10). The setting allows you to choose either autoscaling for ten intervals (bin size rounded up to the nearest integer), or to set your own bin size (number of meters). Selecting 0 selects the autoscale. The bin width in Figure 3-10, for example, has been set at 10 (meters).

Default options 5,6,7,8,9, and 0 will permit you to toggle On and Off the plotting of various variables. For example, if you are using a low-resolution CGA graphics display, you may wish to set some of the parameters Off to improve the quality of the display.

### Step 3. Plot the graph.

To select a file for plotting or conversion to comma-separated-value .CSV file, type in the serial number. Or press Next list, Previous list. Or use the arrow key, then press ENTER. After file selection has been made, the program will first read the binary data applying the calibration constants, then will calculate the attenuation coefficients. When the calculations are complete, the screen will display a menu

that reads PLOT/CONVERT TO CSV. Step 5 describes converting to the .CSV file. To plot the file, press P (or use the arrow to select PLOT, then press ENTER). The graph will look like this (Figure disk):

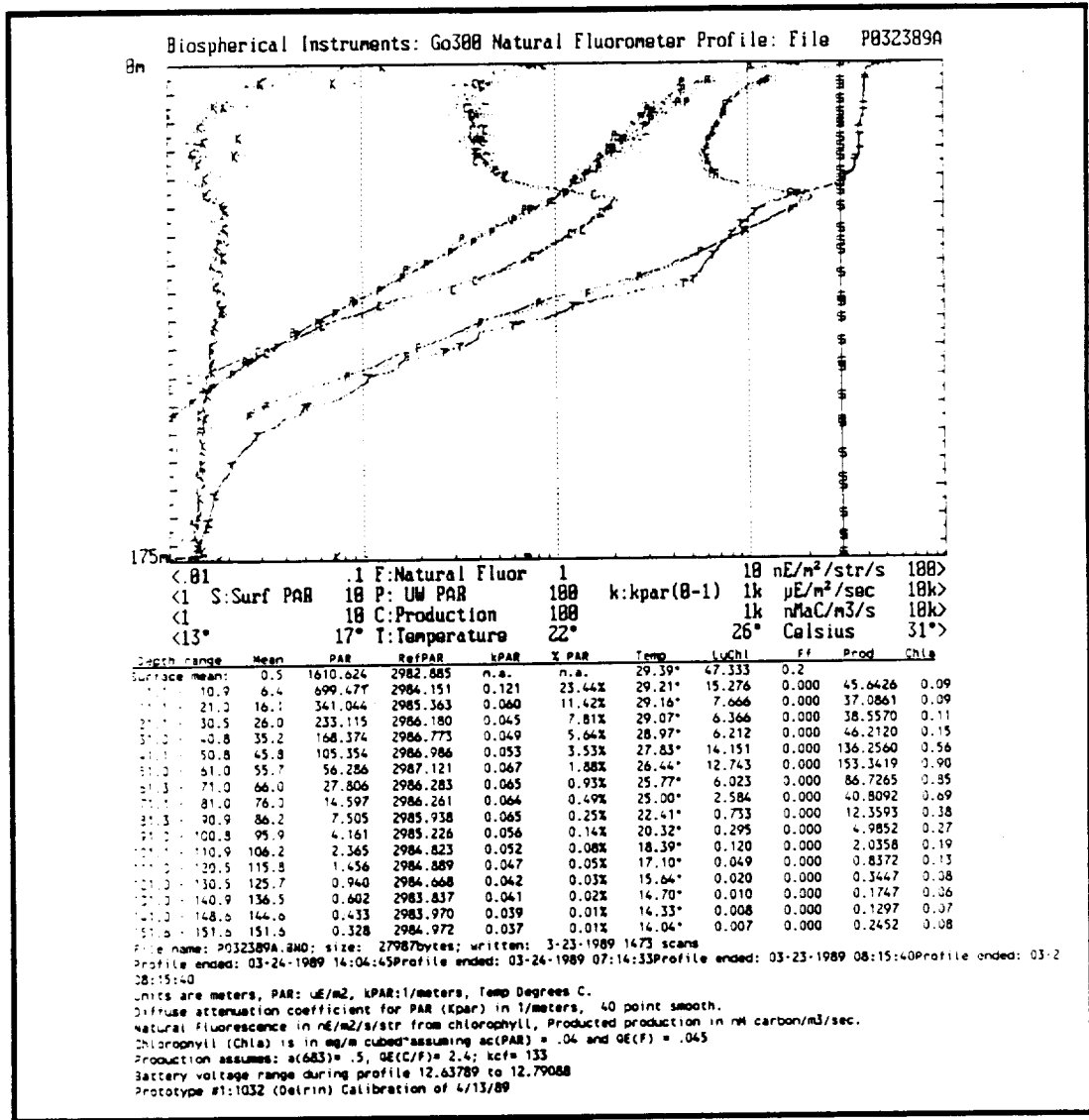


Figure 3-10. Profile Graph Screen.

The profile graph screen displays the graph of the selected file. The screen prompts the operator to press the F9 key for a printout.

Figure 3-10 shows the output of the ProGraph program as seen on a LaserJet printer and with a VGA type graphics device. (If you have a CGA display, the display will be considerably less detailed.) In addition to the plot, a table of summarized data are displayed below. In this table, the first two columns of data list the depth over which data were collected and averaged to create the rest of the parameters in that line. The third column contains the mean depth

for the row. The remaining columns contain the underwater PAR, the reference or surface PAR, the attenuation coefficient for PAR, the percentage of underwater PAR relative to the surface PAR, the average temperature, and four natural fluorescence parameters: Lu(Chl) is the natural fluorescence signal expressed as a radiance,  $F_f$  is the same parameter converted to a volume emission, and Prod has this parameter converted to a production rate. The last column is a rough measure of the chlorophyll concentration. For more information on these parameters and how they are calculated, see Appendix D. At the bottom of the plot is a listing of data about the profile and a list of the assumptions governing the calculation of production and chlorophyll. The final line displays the header from the calibration file.

#### Step 4. Print the Profile Graph

To print the graph display in Figure 3-10, press **F9**. Make sure you have set up the proper printer (Step 3, GO300 program). The graph is plotted, along with a summary table of measured values at depth intervals of 10 meters. These 10-meter intervals are automatically selected now, but should be changed according to the user's requirements via the PROGRAPH Default Setting screen. Pressing any other key invokes a prompt on the bottom of the screen that asks if another profile file is to be graphed. Answer Yes or No. An **N** returns the program to the DOS prompt. A **Y** recalls the opening menu. Repeat Steps 1 and 3. If new values are to be plotted or new parameters invoked, repeat Step 2.

#### Step 5. Create a Comma-Separated-Value (CSV) File

The CSV format is useful for analysis by means of a spreadsheet program (user-supplied). The program converts the binary .BND files into the workable comma separated value files (.CSV) from the calibration figures supplied with the unit. To properly view the .BND file, the user must possess a spreadsheet program. (A distorted view of the .BND file will at least verify the file's existence using the MDOS TYPE command.)

To convert a binary .BND file into a comma-separated-value .CSV file, select a file as detailed in Step 3. At the menu PLOT/CONVERT TO CSV, press **C**. Or with the arrow key, select the CONVERT TO CSV option, then press **ENTER**.

After the selection has been made, the CSV conversion utility will display a conversion screen with the percent of the file left to convert shown in the lower right hand corner. The screen looks like this (Figure 3-11):

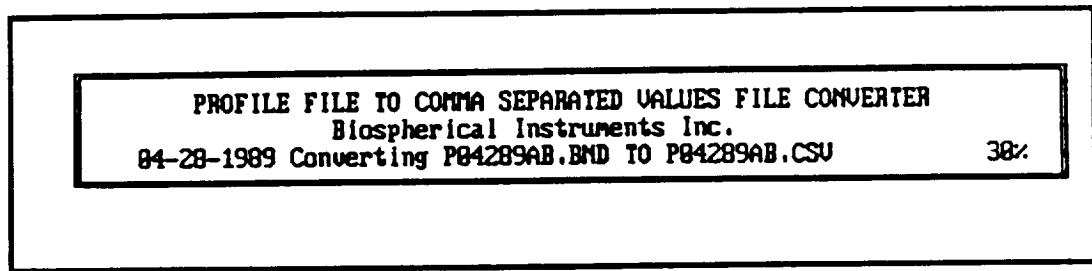


Figure 3-11. The CSV Conversion Screen

Upon completion of the conversion, the program will ask if another profile file is to be converted. Answer Yes or No. A Y will recall the opening menu. An N will return the program to the DOS prompt.

---

## How to Use the LOGGRAPH Log Graphing Program

The Log Graphing program LOGGRAPH converts any selected .LOG file into graphic form. It allows the operator to graph each of the eight variables as a function of time; a hard copy of the plot can be printed. And it permits converting the .LOG file into a comma-separated-value (CSV) file.

To use the LOGGRAPH program, carry out the following menu driven steps. In order of their appearance, the steps are:

- Step 1. Open the LOGGRAPH screen
- Step 2. Select a .LOG file
- Step 3. Select the logged variable
- Step 4. Print the graph
- Step 5. Convert to a .CSV file

### Step 1. Open the LOGGRAPH Screen

To call up the opening screen, and to graph and possibly print a .LOG file, type LOGGRAPH from the DOS prompt, then press ENTER. As with the PROGRAPH opening screen (Figure 3-8), a LOGGRAPH opening screen will display all applicable .LOG files

sorted in chronological order with the most recent file on top. To the right of each file appears the file size in bytes.

## Step 2: Select .LOG File

To select a file for graphing, type the file serial number (0 through 9), **N**ext list, **P**revious List, or use the arrow keys to highlight the file desired, then press **ENTER**. Once the selection has been made, a menu will appear allowing the user to choose between **PLOT** and **CONVERT TO CSV**. Step 5 describes how to convert to a .CSV file. To plot the selected file, type **P**, or select the (upper) **PLOT** line on the menu and press **ENTER**.

Once the desired .LOG file has been selected and the Plot function has been selected, the program will ask for the type of graph to be viewed. The eight-logged variables plus an exit key will be viewed on the graph selection screen as shown here (Figure 3-12).

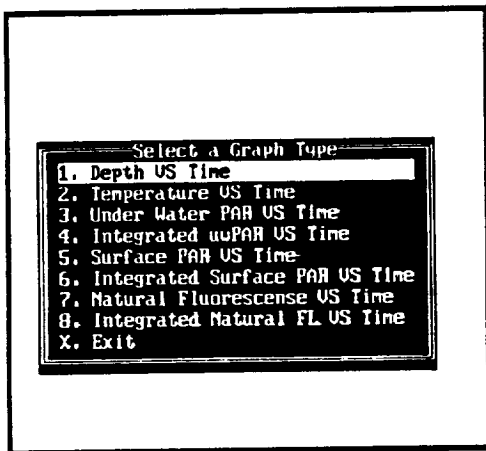


Figure 3-12. Log Graph Selection Screen

## Step 3. Select the Logged Variable

To select a variable for plotting, type one of the numbers (1-8) as shown above, then press **ENTER**. A prompt alerts the operator to press the **F9** key for a printout.

The graph coordinates will appear, followed by the time series plot. For most files, the conversion should take no more than

a few seconds. The plot of integrated surface light (PAR) versus time is shown below (Figure 3-13).

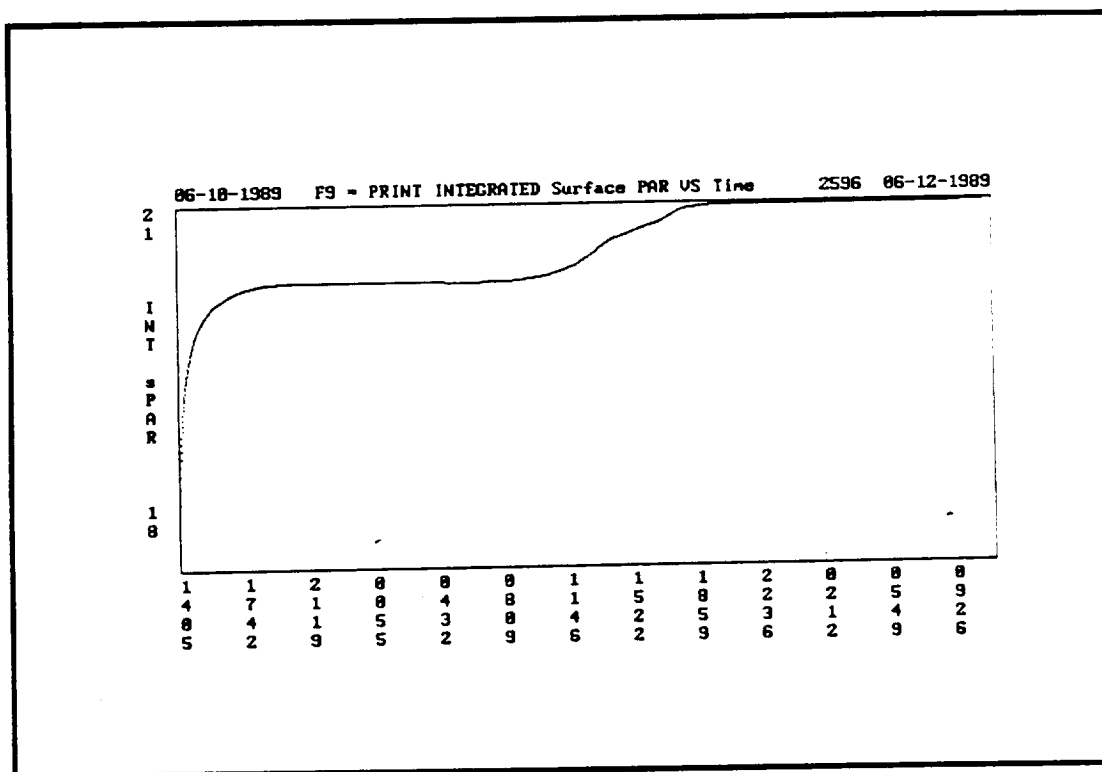


**Figure 3-13.** Graph of Selected Log Variable. Here the integrated surface PAR is plotted against time. The horizontal axis is given in 24-hour time.

#### Step 4. Print the Graph

To print the graph display above, press **F9**. Pressing any other key invokes a prompt on the bottom of the screen that asks if another profile file is to be graphed. Answer **Yes** or **No**. An **N** returns the program to the DOS prompt. A **Y** recalls the opening menu.

#### Step 5. Convert to .CSV file.

This function is useful for tabulating the time series data, and converts data into CSV form using the calibration values. From the Log Graph Selection Screen (Figure 3-14) the user selects the file or files to be converted. Once the selection has been made, a menu will

appear allowing the user to chose between PLOT and CONVERT TO CSV. To select the conversion program, press C or select the (lower) CONVERT TO CSV line on the menu and press ENTER.

The following is a .CSV file after it was loaded into a spreadsheet (EXCEL):

A	B	C	D	E	F	G	H	I	J
DATE	TIME	DEPTH	TEMP	SURF PA	INT SF PA	UW PAR	INT UW P	NAT FL	INT NAT F
3/24/89	13:57:23	0.184489	29.90104	1.66E+17	3.99E+18	4.94E+16	1.46E+18	0.708006	16.33296
3/24/89	13:57:26	0.329668	30.33994	1.66E+17	4.48E+18	4.45E+16	1.62E+18	0.744627	18.48384
3/24/89	13:57:29	0.136096	30.33994	1.66E+17	4.98E+18	5.04E+16	1.78E+18	0.712889	20.70551
3/24/89	13:57:32	0.086527	30.26014	1.66E+17	5.48E+18	3.8E+16	2.01E+18	0.620116	22.57806
3/24/89	13:57:35	3.243547	29.42223	1.66E+17	5.98E+18	2.74E+16	2.1E+18	0.296158	23.77261
3/24/89	13:57:37	6.830248	29.24267	1.66E+17	6.48E+18	1.64E+16	2.16E+18	0.158531	24.34326
3/24/89	13:57:41	10.62466	29.16287	1.66E+17	6.97E+18	1.36E+16	2.2E+18	0.119623	24.73173
3/24/89	13:57:43	13.9276	29.14292	1.66E+17	7.47E+18	9.27E+15	2.24E+18	0.103602	25.0584
3/24/89	13:57:46	17.63469	29.20277	1.66E+17	7.97E+18	8.34E+15	2.26E+18	0.080105	25.3213
3/24/89	13:57:49	21.37319	29.08307	1.66E+17	8.47E+18	6.69E+15	2.28E+18	0.064541	25.52866
3/24/89	13:57:52	25.1158	28.98332	1.66E+17	8.97E+18	5.7E+15	2.3E+18	0.056912	25.70641
3/24/89	13:57:55	28.70631	28.86362	1.66E+17	9.47E+18	4.76E+15	2.32E+18	0.050809	25.86555
3/24/89	13:57:58	32.45695	28.82372	1.66E+17	9.97E+18	3.97E+15	2.33E+18	0.044859	26.00547
3/24/89	13:58:01	36.05516	28.80377	1.66E+17	1.05E+19	3.24E+15	2.34E+18	0.040129	26.13043
3/24/89	13:58:04	39.65714	28.64417	1.66E+17	1.1E+19	2.74E+15	2.35E+18	0.038298	26.24548
3/24/89	13:58:07	43.89035	28.54441	1.66E+17	1.15E+19	2.18E+15	2.36E+18	0.036467	26.35869
3/24/89	13:58:10	47.65757	28.58431	1.66E+17	1.2E+19	1.79E+15	2.36E+18	0.032539	26.46004
3/24/89	13:58:13	51.42888	28.56436	1.66E+17	1.25E+19	1.41E+15	2.37E+18	0.033016	26.55864

Figure 3-14. A typical PNF-300 data file tabulated by a spreadsheet (from the .CSV file).

As shown above, the CSV file parameters are written in the following order: date, time (HH:MM:SS), average depth (meters), average temperature (degrees), average surface PAR, integrated surface PAR, average underwater PAR, integrated underwater PAR, average Lu(Chl), and integrated Lu(Chl). The parameters  $F_p$  and calculated production are not calculated since knowledge of  $k(\text{PAR})$  is necessary. To calculate  $F_p$  and production, either run PROGRAPH on a vertical profile taken in the same water, preferably at the same time as the integrated readings, to calculate  $k(\text{PAR})$ . See Appendix D for the appropriate equations.

---

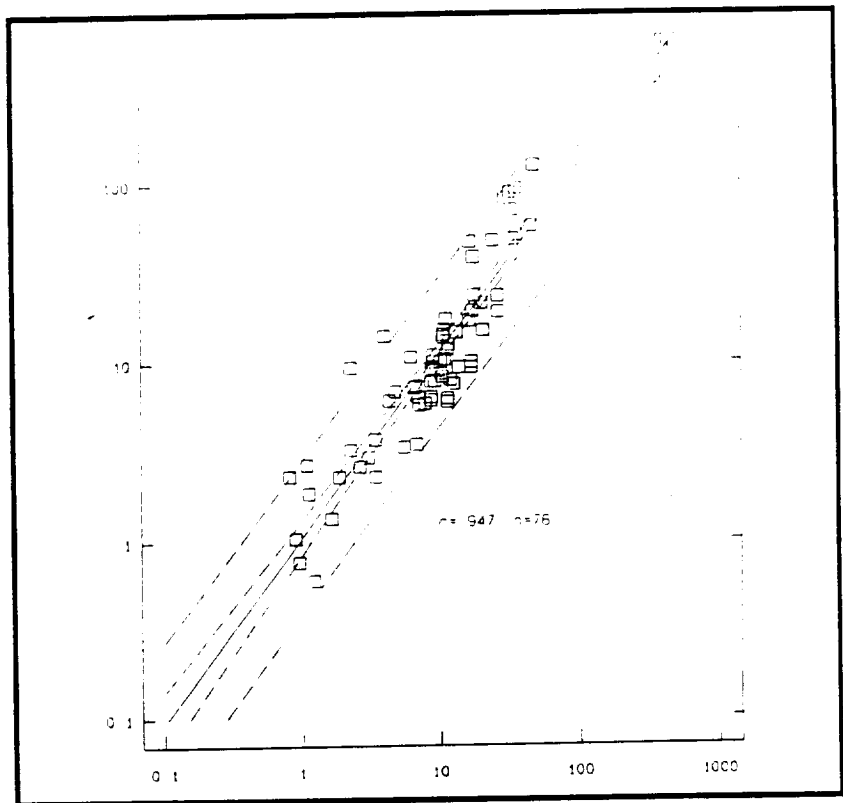
## **In Conclusion...**

With a little practice on the GO300 Acquisition and Display Program, you should have no difficulty using the Profiling Natural Fluorometer's complete software package. Once the data are safely stored on disk, you can immediately begin using one or more of the post-deployment programs, namely PROGRAMPH or LOGGRAPH. These simplified utilities can be learned and mastered while plotting data graphs and producing spreadsheets. Good luck!

## 4 Theory of Operations

This chapter gives the user a brief overview of how the instrument measures photosynthesis. The section also contains uses of the instrument, as well as who are the users. For a description of the theory of natural fluorescence and the evidence that validates its use for measuring primary production, along with an extensive bibliography, see the research paper "Natural Fluorescence and Photosynthesis," Appendix D.

**Figure 4-1.** Regression diagram for production measured using carbon 14 method (vertical) versus natural fluorescence (horizontal).



### A Layman's Primer

Not long after the Secchi disk was invented by Angelo Secchi, the first optical oceanographer, scientists began looking for relationships between light and plant growth in the sea. Recently, the attenuation of light was measured and its spectral qualities mapped. With knowledge of the standing stock of phytoplankton,

biologists have been modeling primary production--the rate at which inorganic carbon is incorporated into cellular material.

As light measuring instruments became more sensitive, a small, anomalous signal in the red end of the spectrum became apparent. Suspecting scattered sunlight or an artifact, investigators soon latched on to the true source--chlorophyll, the key ingredient to photosynthesis.

Today, many years after the first light measurements were made, scientists now recognize that photosynthesizing plants not only are dependent on incoming radiation, but they emit a light of their own.

## What Is Natural Fluorescence?

Natural fluorescence is the solar stimulated fluorescence of chlorophyll *a* in the phytoplankton crop. Measurements of natural fluorescence is a new optical method of assessing both gross photosynthetic rate and chlorophyll *a* concentration within the water column, and is a cost effective, rapid, non-invasive technique. Since the system is purely optical and radiometrically calibrated, measurements are highly reproducible.

Beginning with the post-war oceanographic revolution, oceanographers were making optical electronic measurements related to a variety of biological and defense concerns. The light viewed in the ocean is complex and varies considerably with the changing environment (i.e. water clarity and depth, and incidental sunlight). Despite their crudeness, the optical measurements of that day could broaden considerably the painfully slow techniques of light-and-dark-bottle uptake of oxygen and later radioactive carbon <sup>14</sup>C. In 1977, investigators tied the faint but distinct signal centered at 683 nm to a standing stock of phytoplankton. Scientists were on to the basic secret of natural fluorescence, but one more step remained.

## Stimulated Fluorescence--An Early Method

The fluorescence given off by chlorophyll *a* was exploited by oceanographers as early as the 1960's. The first optical techniques used underwater strobes to induce a more distinct fluorescent response from the organism. Such power-intensive methodology was developed not for measuring phytoplankton productivity, but chlorophyl concentration. The difference being similar to measuring the size of a person's bank account rather than their annual earnings.

Production, like earnings, gives a more dynamic picture.

Concentration measurements using stimulated fluorescence remains a standard technique today. Production estimates may be made, but these are based on these concentration measurements, with traditional equations of production versus standing crop size used for the conversion. This technique is similar to estimating a company's earnings based on its holdings, using standard interest rates as a conversion factor. Obviously this method has its shortcomings, as it is generally known that some companies are able to accomplish more with a given amount of money than others. What has been needed is a method to measure production rates directly.

In the past decade, several investigators have recognized that unstimulated (natural) fluorescence could be used to estimate standing crop sizes. Not until the mid 1980s was the idea seriously considered that a plant's natural fluorescence could be related directly to its photosynthetic output.

## Direct Measurements of Photosynthesis

Developed under contract to NASA, the technique of measuring photosynthesis by way of natural fluorescence has been used in numerous environments. Results acquired by a variety of users, including the Cousteau Society, the Jet Propulsion Laboratory, University of Southern California, and the Lamont-Doherty Geophysical Observation. The results of 76 such measurements (taken in the central South Pacific, the western Sargasso Sea, and two sheltered bays covered a 1500 fold range in production between 2 and 150 meters depth) and indicated that photosynthesis is highly correlated ( $r > 0.9$ ) with natural fluorescence (see Figure 4-1). The theoretical framework for examining natural fluorescence and photosynthesis is contained in Appendix D.

## Limitations

Several complications exist in interpreting natural fluorescence in the sea. These include (1) signal contamination by detrital chlorophyll such as phaeopigments, (2) the anomalously high photosynthesis-to-fluorescence ratio of Synechococcus, (3) the inhibiting effects on the production-to-fluorescence ratio caused by a severe nutrient depletion, (4) restriction of measurements to that of gross photosynthesis rates (losses of fixed carbon by respiration are unrelated to the fluorescence signal), and (5) reflection from shallow bottoms or use within the upper few meters where scattering is high.

C2

## Advantages

Despite these limitations, it was felt that the measurement of natural fluorescence would significantly improve ocean productivity studies. The advantages of such a low-powered, lightweight, in-situ system are:

- The measurements provides detailed spatial and temporal information on photosynthesis that can not be achieved by incubation of water samples that have been inoculated with carbon 14.
- Profiles of natural fluorescence can aid in choosing sampling depths and light intensities for incubation, extrapolating or interpolating information obtained by the traditional carbon 14 method.

Based on the demonstrated worth of the technique, a fully-computerized turnkey system was developed.

## What Are the Uses?

The PNF-300 also is useful for mapping or monitoring the distribution of chlorophyll concentration and photosynthetic rate. Specific applications include examining the environmental impacts of coastal installations, including oil terminals, offshore platforms, coastal power plants, and recreational harbors. Potential impacts on the bioproductivity can also be documented in the fresh water regimes surrounding river front and lake shore operations.

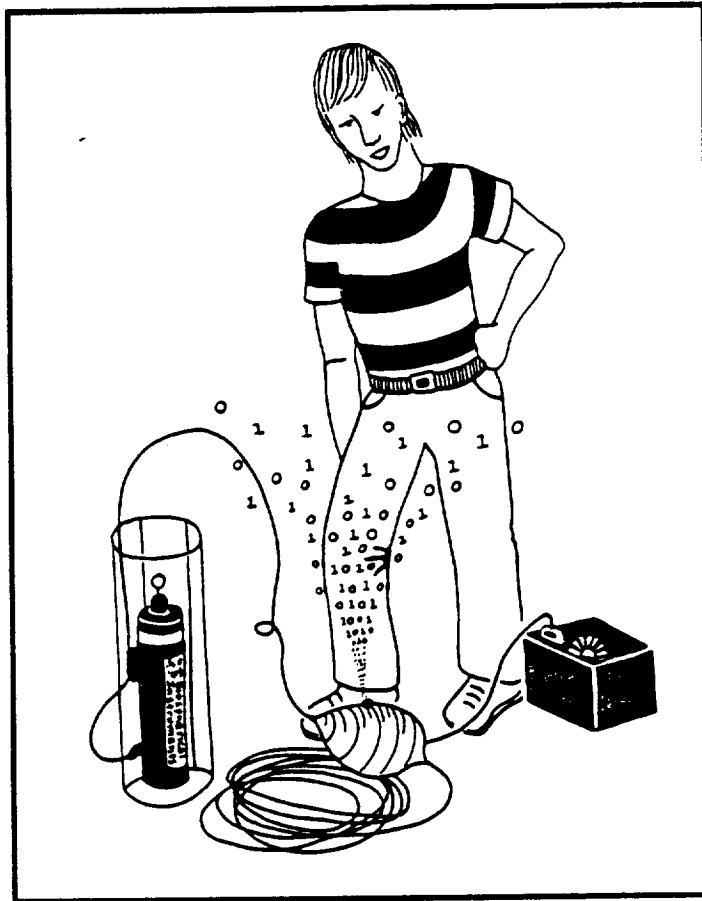
## Who Are The Users?

Owing to the wide range of disciplines inherent in this work, the PNF-300 in general and PNF-300 Instruction Manual specifically is aimed at users with a minimum of oceanographic knowledge and only modest computer literacy. An understanding of basic photosynthesis at the undergraduate level is needed to properly use the instrument under the normal variety of field conditions. Some familiarity with the DOS operating system is needed to operate the recording device: an IBM PC or PC-compatible computer (user-supplied). Using the step-by-step format of the manual, you should be able to obtain useful, real-time photosynthesis measurements on your first day out.

## 5. Maintenance and Repair

Maintenance of the PNF-300 is simple and straightforward, consisting primarily of proper cleaning, storage and use of the instrument. Maintenance items are covered below. Repairs to the instrument require spare parts, and are therefore unlikely to be done successfully outside the factory. Because the most likely component to fail is the underwater cable or the cable connectors, it is strongly recommended that the user on an extended survey carry a spare PNF-300 underwater cable. On an extended operation, it is also recommended you carry a spare battery. Instrument calibration, another factory procedure, is covered in Appendix B.

**Figure 5-1.** Troubleshooting the PNF-300. The most common failures are caused by damaged cables or connectors.



---

## Maintenance

Most maintenance of the PNF-300 should be carried out daily, or whenever the instrument is used. These steps consist of (a) washing the underwater unit, (b) cleaning the Teflon balls and windows, and (c) storing the sensors and cables out of the sun.

**a) Rinse the PNF-300 system.** Wash the instrument with fresh water after every use. 1) **DO NOT** allow your PNF-300 to dry with salt water on it. Salt left on anodized aluminum for long periods of time **WILL** corrode the aluminum. We have seen anodized aluminum instruments shipped back to us which had been stowed for months with drops of salt water left on them. *These unmaintained instruments had 1/4-inch deep holes eaten into the aluminum.*

**b) Clean the PAR Sensors (Teflon Ball).** Clean both balls on the underwater and deck units. The Teflon ball may become dirty during normal use. Do not attempt to rotate or remove the Teflon sphere. Tampering with the Teflon ball could will the calibration. The ball may be cleaned gently with warm water, soap or a solvent such as acetone or alcohol using a soft tissue or towel. Do not use acids, abrasive cleaners or brushes, as these will mar the surface of the sphere and void the instrument's calibration. Should the sphere become damaged or heavily soiled, return the instrument to the factory for service and recalibration.

**c) Clean the natural fluorescence window.** The clear window at the bottom of the instrument is made of Plexiglass, and is therefore relatively easy to scratch if you are careless. It has been recessed slightly in order to help offer some protection to the Plexiglass surface. Solvents should not be used to clean Plexiglass. Warm water and dishwasher detergent should be used with a very soft lint-free cloth. If you have numerous fine scratches in the Plexiglass window, they can be removed with a Plexiglass polishing compound.

**d) Store the cables and sensors in a safe place *and* out of the sun.** The underwater cable used with the PNF-300 is designed for the normal longitudinal tensions of a marine environment, but not for sustaining sideways forces. The Impulse connector plug at the underwater end of the cable is made of soft rubber, and gives very little structural protection to the electrical contacts contained within it. Sideways forces on this connector when it is mated can break the connections inside the plug. Be sure to disconnect the cable from the PNF-300 underwater unit whenever you remove the unit from its lowering frame. Sunlight causes premature aging in plastics (such as the cable jackets) and overheating of the instrument electronics. Storing the instrument in direct sunlight may cause the electronics to age more quickly, possibly causing your PNF-300 to fail or go out of calibration prematurely. Also, scratches and nicks in the Teflon ball

or the bottom windows of the underwater sensor will affect the calibration of your unit.

---

## Repair

Problems with the instrument fall under two major categories: the transmission of unusable data, or no transmission at all.

In the first category, one or more channels incorrectly report the analog voltage, the channels do not sense the correct level, or the transmitted data can not be programmed.

### Incorrect Data

If the surface light reading is incorrect, carefully check the cables and connectors of both the surface light sensor and the underwater sensor.

If the cables and connectors are operating properly, the problem is likely caused by failure of one of the integrated circuits (input or output). *Failure can be caused by excess voltage on the analog channels, even if the overload lasts only a microsecond.* A person walking across a carpet on a dry day can generate a static charge of over 10,000 volts. The resulting discharge can destroy an integrated circuit.

If the analog voltage is incorrectly reported, the most likely component at fault is the analog input multiplexer, U11 (see Appendix A). If the digital input/output channels are incorrect or impossible to control, the digital buffer (U12) may be at fault. If replacement of these units does not correct the problem, the factory should be consulted for further instructions.

### Cable--What to Do If It Breaks

A break in the cable is generally not field repairable. Marine cables are pressure sealed along their entire length and also contain a Kevlar strip for strength, which must remain intact. For this reason it is best to carry a spare on extended surveys. In the event that data are received intermittently or not at all, check the cable for cuts or kinks. This is the first thing to check for. As an alternative, contact the underwater connector manufacturers for a field repair kit (see below list of suppliers).

## O-Ring Leaks

The electronics in the underwater unit must be kept dry. The unit is sealed using O-rings at all joints. These O-rings must be treated carefully and installed correctly, otherwise the unit can be permanently ruined. Make sure whenever you reassemble an instrument with O-rings that the O-ring groove and mating surface are absolutely clean and free of particles, marks, or scratches. The O-ring should be carefully cleaned, inspected for nicks or flaws, and coated with O-ring grease (Dow Corning 111). Scratches in the mating surface that are so small as to be invisible to most people can cause the unit to flood.

## Should Flooding Occur...

Should the unit become flooded, the best way to dry the components is to immerse them in alcohol (methyl, denatured, or high proof ethyl alcohol). First rinse the unit with fresh water to get rid of as much of the salt as possible. Then rinse with alcohol. This may save the components that have not yet undergone corrosion. The instrument should be recalibrated.

## Should the Battery Become Discharged...

The instrument will shut off whenever the battery voltage gets below 8 or 9 volts. Should this occur, plug the battery charger into the deck box and allow it to charge for up to 12 hours.

## List of Suppliers

To obtain spare connectors or batteries, or both, contact any of these suppliers:

### Underwater Connectors

**Impulse Enterprises**, 8274 Ronson Road, San Diego, CA 92024

**Bratner & Assoc. (SeaCon)**, 1240 Vernon Way, El Cajon, CA 92020

### Deck Box Batteries

**Panasonic**, Battery Sales Div., P.O. Box 1511, Secaucus, NJ 07094,  
Telephone: (201) 348-5266

---

# Appendix A. Technical Description

The Profiling Natural Fluorometer (PNF-300) is an instrument for the measurement of upwelling radiance (with a wavelength response centered at the chlorophyll *a* fluorescence peak) and associated properties. This instrument is intended to be lowered from a ship with the instrument supported by its own cable and the outputs from the sensors displayed on an IBM PC or compatible computer.

In addition to the upwelling radiance sensor, sensors are provided for the measurement of photosynthetically active radiation (PAR) both at the underwater sensor and at a separate deck mounted sensor, pressure (yielding package depth), temperature, and battery voltage. The entire system operates under battery power, assuming that the required PC is also battery powered.

The personal computer interfaces to the deck box using the RS-232 or serial port found on most personal computers. Data is transmitted from a microprocessor based data acquisition system located in the underwater instrument package. These data are binary in nature and transmitted at 9600 baud. A computer program is provided for the host personal computer that acquires these data, and displays them on the screen while recording the binary data stream on disk. If available, the computer should be equipped with a hard disk since the time required to retrieve data, display it in engineering units, and record it to disk will cause the program to lag behind if you are writing to a floppy disk. If the PNF-300 must be used with a floppy disk, then beware that, by the end of a profile lasting 10 minutes, the display can be several minutes behind in recording and displaying the data. This is because we use a communications buffer so that every scan is captured, even if the computer is unable to keep up with the transmissions due to slow disk access times. It is imperative, in this case, not to stop the computer until the depth display shows that the instrument is on the surface or part of the profile will be lost.

---

## Technical Overview

The system Controller for the PNF is a CMOS version of the Z8 microcontroller. The A/D conversion circuitry consists of an eight channel analog multiplexer followed by a programmable gain amplifier which feeds a twelve bit A/D converter (with polarity, 13 effective bits). The details of this board are described in the following section.

In addition to digitizing the signals from the underwater sensors, the Z8 system controller and data acquisition system also measures the battery voltage and the surface light. It should be pointed out that, contrary to normal procedure, the voltage output from the surface irradiance sensor is sent down the underwater cable to the Z8 controller where it is digitized. This design was constructed to simplify the electronics, but it decreases slightly the range over which surface irradiance can be reliably digitized. However, the surface sensor gives accurate readings until somewhat past sunset.

## Data Acquisition

The PNF-300 data acquisition subsystem consists of a Z8 microprocessor connected to a 12 bit plus sign integrating analog to digital converter. The input to the analog to digital converter is selected by an eight input multiplexer. The output of the multiplexer is fed to a programmable gain amplifier (PGA) which, under microprocessor control, automatically selects the gain with the highest resolution possible for the signals amplitude.

In a normal operation cycle, the microprocessor selects the first channel with the multiplexer, the gain is set to "1" and a conversion is done. If the measured voltage is less than .5885 Volts the gain of the PGA is increased to 16 and another conversion is completed. If the input voltage is less than .0367 Volts the gain of the PGA is further increased to 256 and another conversion is done. The data is stored in a buffer and the next channel is sampled in a like manner. Conversion time is a function of the input voltage and a low input voltage will require three conversions while a high voltage will require only one.

After the required number of channels have been sampled and the data are stored in the buffer, the buffer is transferred to the output buffer. The output buffer will be sent, preceded by the ASCII character "S". The "S" character is a Hex 53.

## Data Block Format

The data string begins with an ASCII character "S" followed by two bytes per channel. Assuming eight analog channels, then the data string will be 17 bytes long, and will take about 17 milliseconds to be transmitted at a baud rate of 9600 baud.

## Analog Format

Each analog channel is digitized into two data bytes (16 data bits). The upper 13 bits are coded as "two's complement" binary data. Two's complement data quantify all the data bits if the number is negative. The most significant bit is the sign bit; if '0', the number, is positive, if '1', the number, is negative. The next 12 bits are the data bits or the magnitude.

## Two's Complement Format

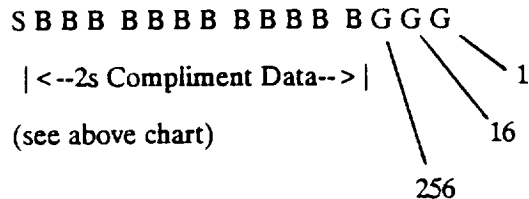
S B <-----> B

0 1111 1111 1111	=	4095
0 0000 0000 0100	=	4
0 0000 0000 0000	=	0
1 1111 1111 1111	=	-1
1 1111 1111 1011	=	-5
1 0000 0000 0000	=	-4095

Where S is the sign bit, and B are the data bits.

The final three bits are the gain bits. Bit 0 On indicates a gain of 1. Bit 1 On indicates a gain of 16. Bit 2 On indicates a gain of 256. Only one gain bit should be on at a time. All three gain bits On indicate an over-range condition.

## Gain Bit Format



The instrument is calibrated to read + or - 10.000 volts full scale. The smallest resolution element (SRE), data gain of one, is 2.442 millivolts (0.002442 volts). This SRE value is found by dividing the full scale (10.0) volts by the maximum reading (4095). Examples of calculated readings are given below.

## Calculations of Smallest Resolution Element

First Byte	Second Byte	Voltage	Formula
0000	0000 0100	= 0 volts	$0 * \text{SRE} / 256$
0000	0000 1100	= .00000954 volts	$1 * \text{SRE} / 256$
0100	0000 0001	= 5.0012 volts	$2048 * \text{SRE} / 1$
1011	1111 1001	= -5.0012 volts	$-2048 * \text{SRE} / 1$
0111	1111 1001	= 10.0000 volts	$4095 * \text{SRE} / 1$

---

## Schematics

The following schematics describe the PNF-300 instrument:

**Deckbox Schematic.** The PNF-300 Deckbox includes the power supply, battery charging and RS232 interface circuitry for the entire PNF-300 system (except the laptop computer).

**Z8 Microprocessor Schematic.** Located in the underwater instrument, the Z8 microprocessor is the main controller and data acquisition circuitry for the PNF-300 instrument. The voltages for the five sensors are connected to U7, pins 4,5,6,7,12, for connection to channels 1-5 respectively. The optional RS-232 circuitry is installed.

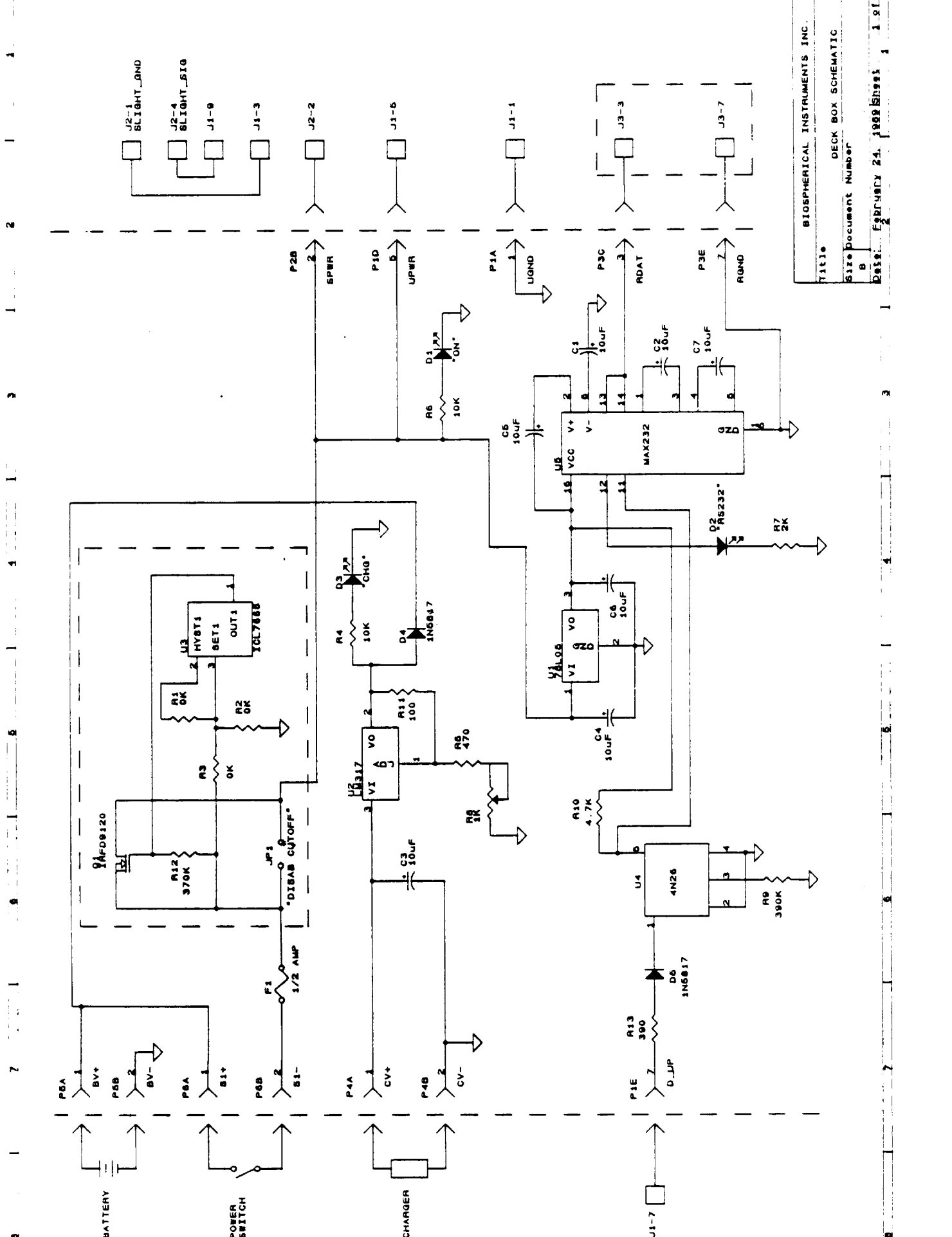
**Z8 Power Board Schematic.** Also located in the underwater instrument, this contains the power conditioning and interface for the underwater electronics.

**Lower Sensor Board Schematic.** Located in the underwater instrument, this is the analog sensor board that measures natural fluorescence (upwelling radiance), pressure, and temperature.

**Upper Sensor Board Schematic (PAR--photosynthetically available light)** . Shows the analog sensor board that measures surface PAR (downwelling irradiance.)

**Underwater Unit Interconnections Schematic.** Shows the various modules within the underwater unit are connected.

**Instrument Cable Wiring Schematic.** Depicts the wiring and pin matching for the cables to the underwater and surface sensors.



Title	BIOSPHERICAL INSTRUMENTS INC.
Size	DECK BOX SCHEMATIC
Document Number	B
REV	00
Date	FEBRUARY 24, 1989 Sheet 1 of 1

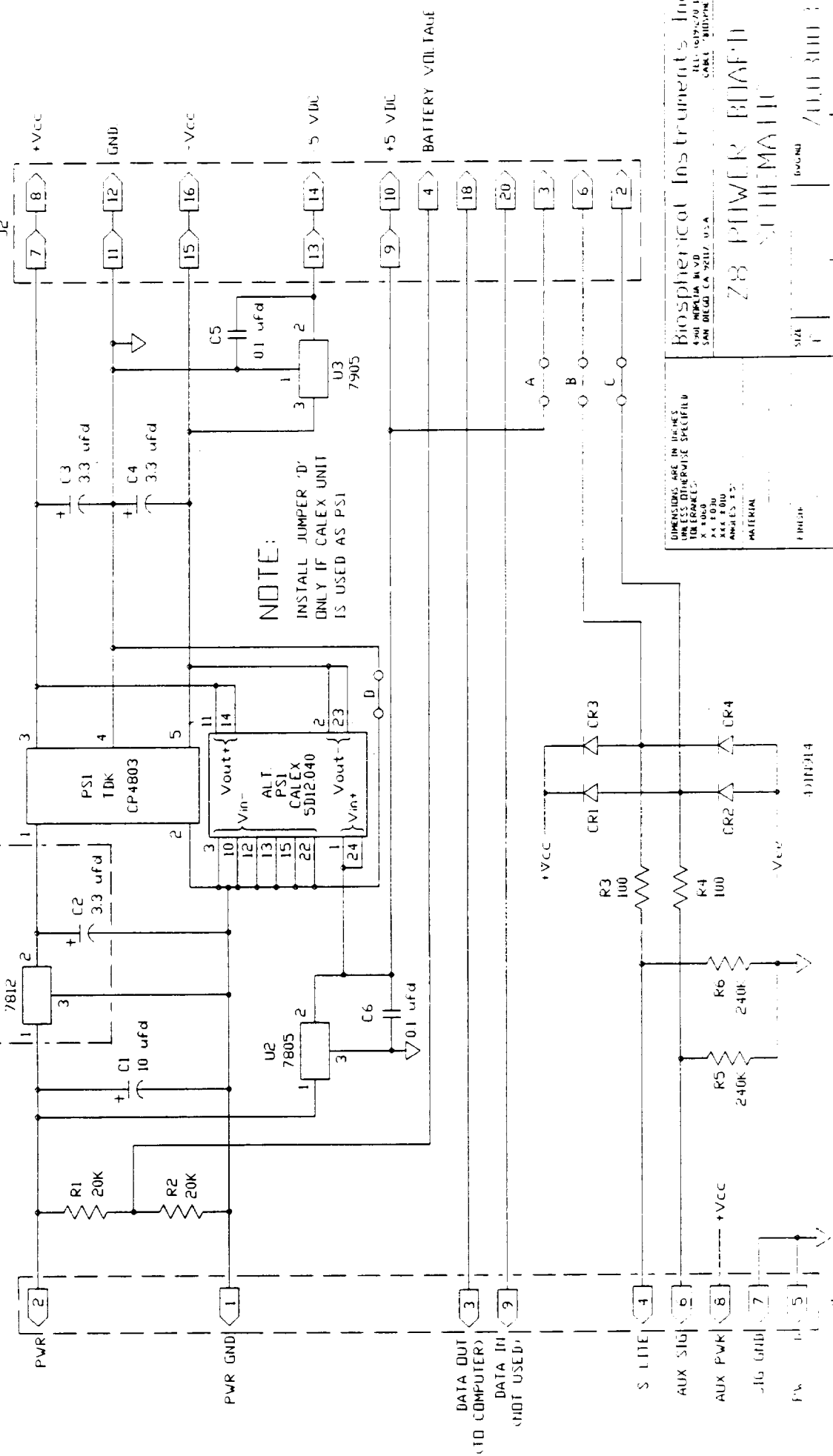


**NOTES**

- 1-ALL SYMBOLS PER ANSI Y13.2
- 2-ALL RESISTANCE VALUES IN OHMS

**NOTE:**  
 U1 AND C2 INSTALLED  
 ONLY IF TDK UNIT  
 IS USED AS PSI

**NOTE:**  
 INSTALL JUMPER 'D'  
 ONLY IF CALEX UNIT  
 IS USED AS PSI



UNLESS OTHERWISE SPECIFIED  
 DIMENSIONS ARE IN INCHES  
 TOLERANCES:  
 X 0.005  
 X 0.010  
 X 0.020  
 X 0.050  
 X 0.100  
 MATERIAL  
 FINISH

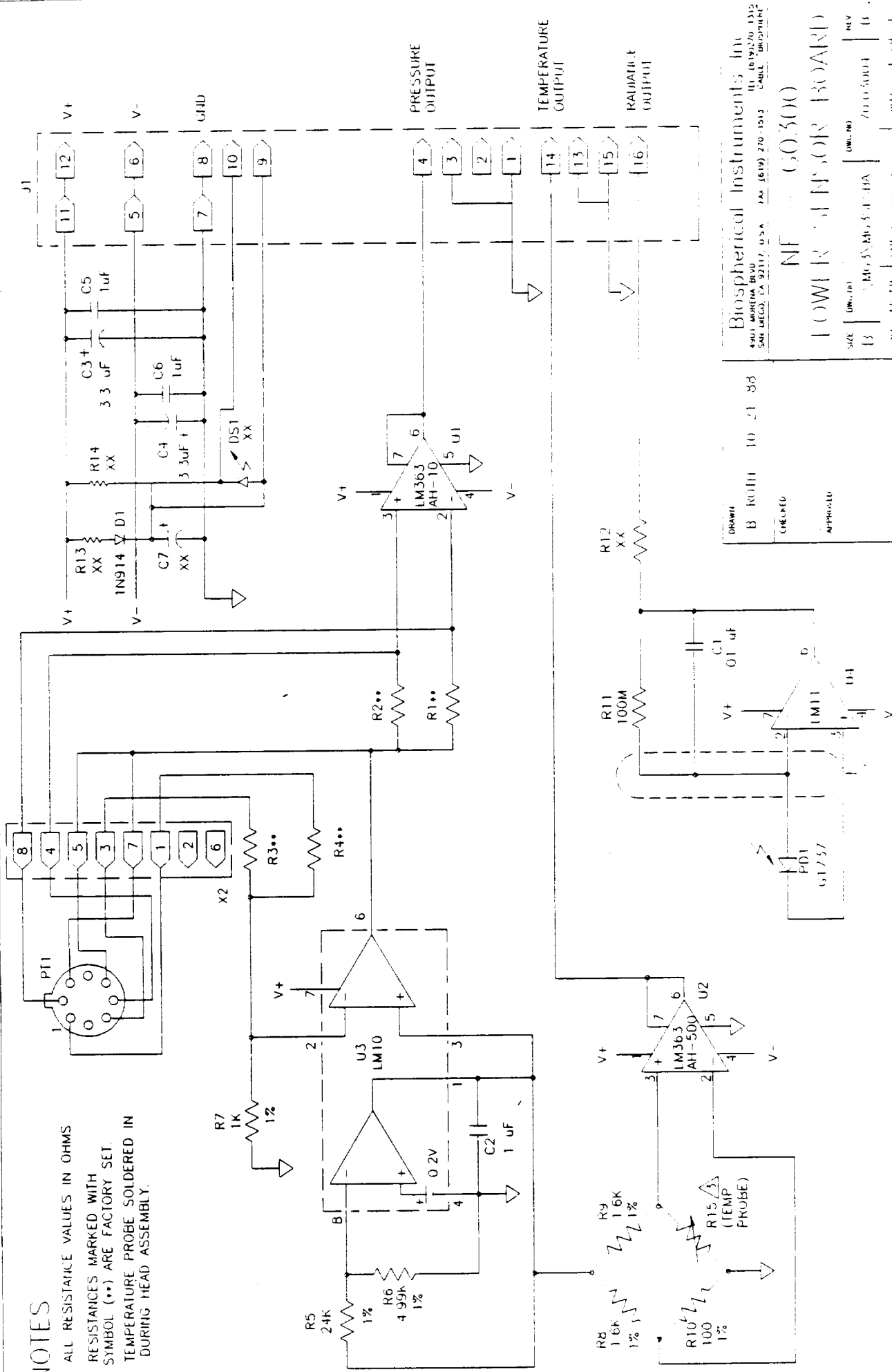
**Biospherical Instruments, Inc.**  
 4300 MIRAMAR BLVD  
 SAN DIEGO, CA 92117, U.S.A.  
 TEL: (619) 570-0145  
 CABLE: BIODPHEI

**Z8 POWER BOARD**  
 SERIAL MATRIAL

SIZE: P  
 QUANTITY: 1000  
 DATE: 11/18/80  
 DRAWING: 100-1

### NOTES

1. ALL RESISTANCE VALUES IN OHMS
2. RESISTANCES MARKED WITH SYMBOL (\*\*) ARE FACTORY SET.
3. TEMPERATURE PROBE SOLDERED IN DURING HEAD ASSEMBLY.

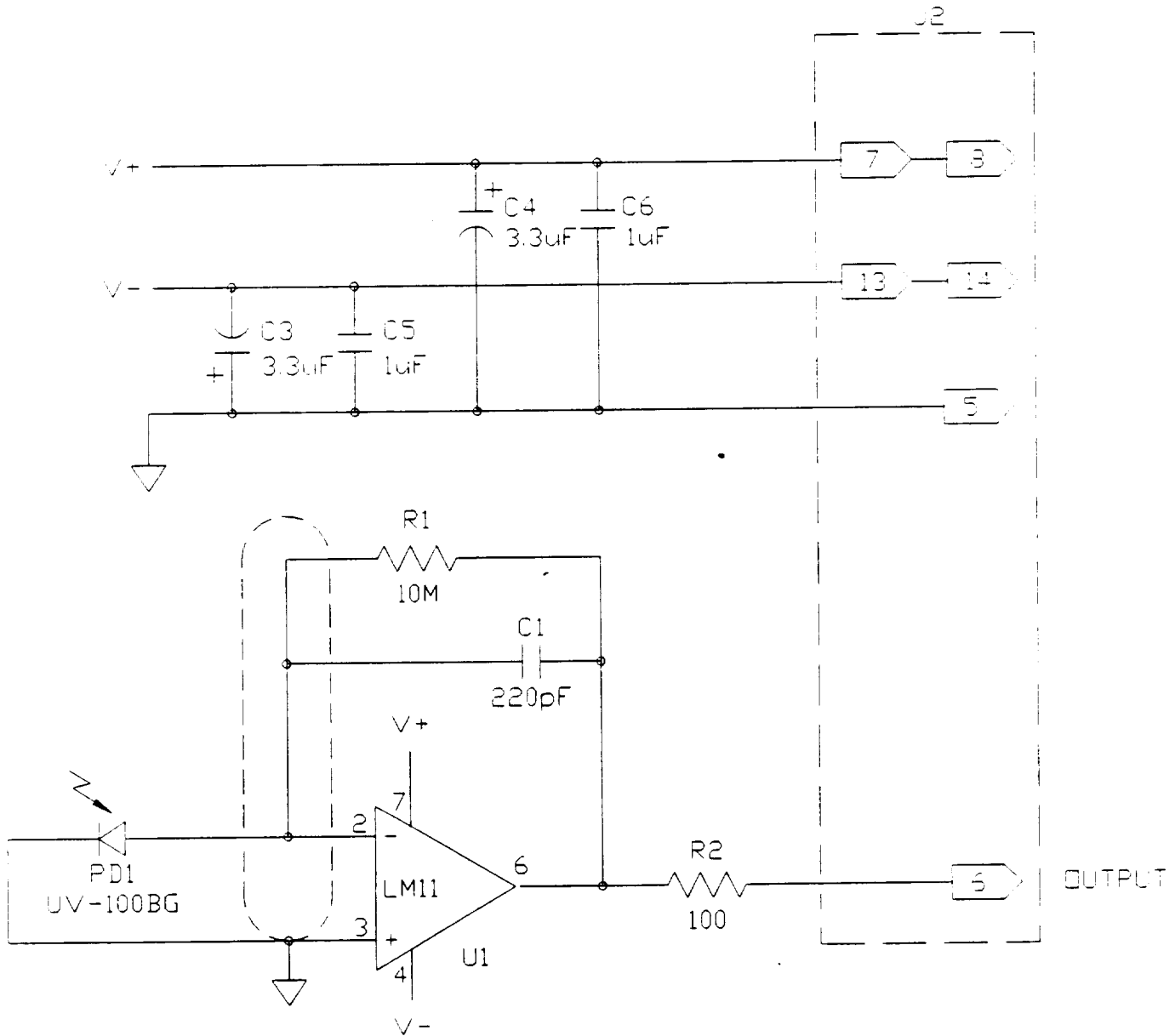


DRAWN: B KUH  
 CHECKED: [ ]  
 APPROVED: [ ]  
 DATE: 10 21 88  
 NF-60300  
 LOWER SENSOR BOARD  
 Biospherical Instruments Inc.  
 4901 WORTHING BLVD  
 SAN DIEGO, CA 92117, U.S.A. FAX (619) 270-1513  
 TEL (619) 270-1512  
 CABLE: BIOCARTINC  
 SIZE: B  
 REV: B

# NOTES

1-ALL SYMBOLS PER ANSI Y13.2

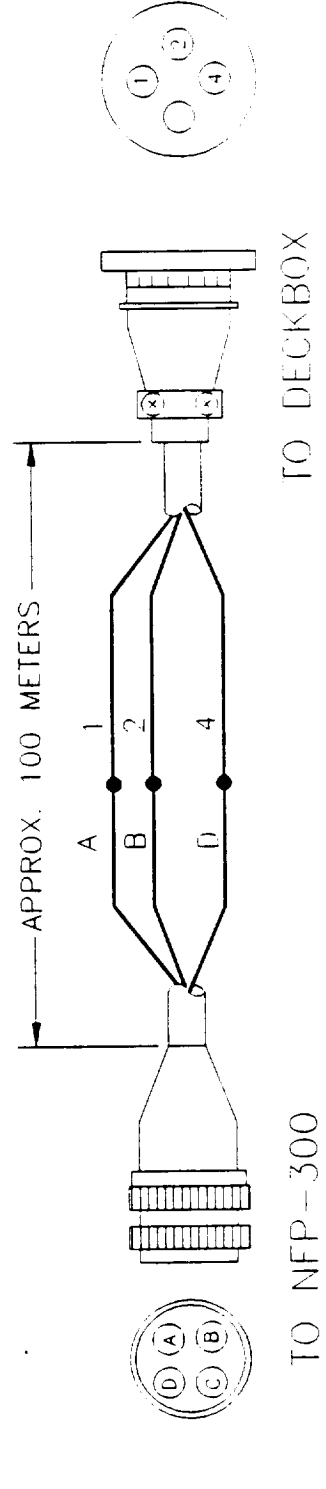
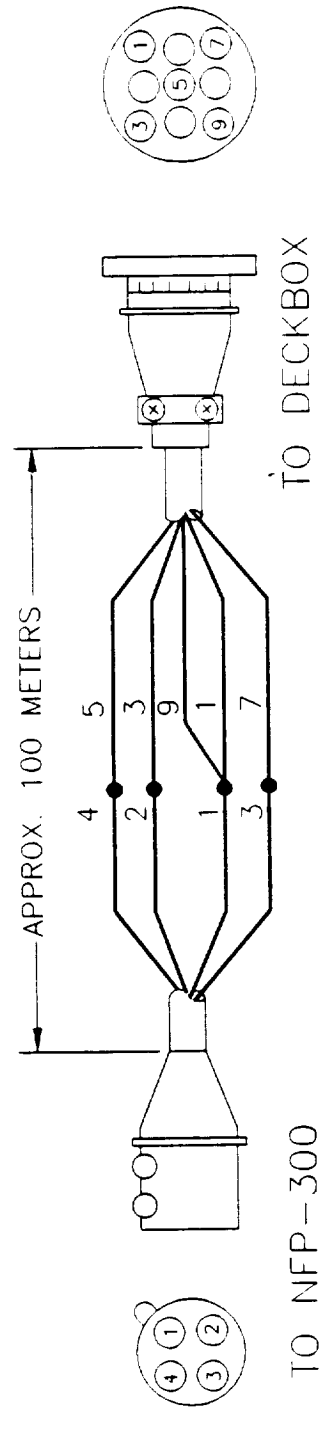
2-ALL RESISTANCE VALUES IN OHMS



DIMENSIONS ARE IN INCHES UNLESS OTHERWISE SPECIFIED TOLERANCES: X ±.060 XX ±.030 XXX ±.010 ANGLES ±.5°		Biospherical Instruments Inc. 4901 MORENA BLVD. SAN DIEGO, CA 92117, U.S.A.		TEL 619-270-1315 CABLE 'BISOPHEFE'	
MATERIAL: _____		<h2>UPPER SENSOR BOARD SCHEMATIC</h2>			
FINISH: _____		SIZE A	DWG. NO. UPSENSCH.DWG	7010300E	
DO NOT SCALE DRAWING		SCALE NONE	DATE	AD	SHEET 1 OF 1



REV	DESCRIPTION	DATE	BY
A			



Biospherical Instruments Inc.  
 4901 MORENO BLVD  
 SAN DIEGO, CA 92117, U.S.A.    TEL: (619) 270-1315  
 FAX: (619) 270-1513    CABLE "BIOSPHERE"

CABLE SCHEMATICS  
 P/N: 500

FILE NAME: NFPM-6202015A    DWG. NO: 62.02015    REV: A

MATERIAL:	N/A	FINISH:	N/A
DRAWN:	KC	DATE:	8-4-89
CHECKED:		APPROVED:	
APPROVED:		TOLERANCES:	UNLESS OTHERWISE SPECIFIED
		XX 1 010	0.5 /
		XXX 1 005	FRACTION

---

# Appendix B. Instrument Calibration

This section contains brief instructions on calibrating the instrument, a procedure that is generally not recommended, but may be required on distant surveys where returning the instrument to the factory is impractical. It also contains the format for the CALIBR8.G30 calibration constant file. The components described below are found in the schematic drawings, Appendix A.

## Calibrating the Analog/Digital Converter

Calibrating the A/D converter may be necessary *only if readings on all the variables are suspect*. Because this procedure also entails subsequent recalibration of all the sensors, an A/D converter calibration should be done only when sensor calibrations can be carried out as well. (See "In Conclusion").

The instrument must be disassembled to calibrate the A/D converter. Also, a pair of calibration constants must be *temporarily* altered. Before doing so, however, make sure to write down the existing values (which may, under unusual circumstances, differ from the latest factory calibration values recorded on the current calibration worksheet). Carry out the following 14 steps.

1. In the calibration file, change the scale for the depth channel to 1, and its offset to 0. (See the above section "Setting the New Calibration Constants" for modifying the calibration file CALIBR8.G30.)
2. Leave all electrical connectors hooked up. You should be able to open the unit by removing the screws from the sides of the lower head and pulling the head off while twisting slightly. Don't rotate the lower head more than about half a turn.
3. Remove the U7 chip from the Z8 CPU board and carefully bend pin 4 up slightly. Replace the chip so that pin 4 is left out of its pin socket.
4. Connect the disassembled underwater unit to the deckbox and laptop computer as usual. Don't bother connecting the surface sensor.
5. Cover the PAR and Natural Fluorescence sensors of the underwater unit using a dark cloth.
6. Connect a high resolution volt meter to pin 4 of chip U7.
7. Connect a 9.9 voltage source to chip U7 pin 4 and the voltmeter.
8. Turn on the instrument and the laptop computer. Verify that the system is running properly.
9. Adjust the R3 rheostat until the depth channel output on your laptop screen exactly matches the input voltage reading on your meter.

10. After adjusting R3, repeat steps 7 and 8 using a very low voltage (i.e. 1 mv). The input and the output should match to within 1 to 2 mv. This checks the zero setting, or offset. Failure for the low voltages to match can not be corrected using the R3 rheostat (the offset errors are removed using the offset calibration values in software.)
11. Once the high end has been set and the low end has been checked, turn off the deckbox. Carefully remove chip U7 from the Z8 board again and bend pin 4 back to the normal position.
12. Reinsert chip U7 so that all pins are inserted in their proper sockets. Verify that the unit is operating.
13. Clean and inspect the O-rings carefully before reassembling the underwater unit.
14. All sensors should be recalibrated, and the calibration file reset to the new calibration values.

## Translation Coefficients

All PNF-300 sensor readings are reported as voltage values. The software in the laptop computer translates these values into the appropriate units. In calibrating the instrument, the proper coefficients for the translating equations are empirically derived. These coefficients, or calibration values, are then used to translate sensor voltages into meaningful values.

Three types of translating equations convert voltages to desired measurements, depending on the type of sensors: optical, pressure, and temperature. Consult your calibration certificate (inside cover) for an explanation of these constants.

1. **Optical Sensor Equation.** Both the PAR and natural fluorescence optical sensors are translated from voltage output to optical units through a linear first order algebraic equation ("Scale" and "Offset").
2. **Pressure Transducer Equation.** The equation to translate the pressure transducer output voltage into a depth reading is a second order polynomial equation.
3. **Temperature Sensor Equation.** The temperature transducer voltage output is translated into degrees C using a first order linear algebraic equation.

## Calibration File

The calibration file for the PNF-300 is named CALIBR8.G30, and contains the following (Prototype #1 calibrated March 9, 1989). *These values are outdated, and are to be used for formatting purposes only.*

```

"Depth",-5.0778,60.41634,0.6970741
"Under PAR",-0.0042494,0.000143
"Battery", 2.5
"Temperature",8.2683,10.597498
"Natural Fluor",-0.01568,0.000229,0.5,2.4,133,0,0
"Surface PAR",-0.000735,-0.00837
"CHLA",0.4528,1

```

Figure B-1. Format for CALIBR8.G30 Calibration File (example values shown).

where the values are listed in the order of the coefficients in the translating equations. See description of equations above.

### Setting the New Calibration Constants

To change any of these values, type GO300 at the DOS prompt, press ESC if no instrument is attached. If an instrument is attached, press the F1 key, then press 9. The following screen will appear (Figure B-2):

```

Natural Fluorometer: Acquisition and Display Program      Time:13:52:12
Biospherical Instruments Inc: August 1988                con 1

Parameters for the G8300 Instrument      e PAR  8.118E+01  $\mu E/m^2/sec$ 
Calibration for the G8300 Instrument       $m^2/sec$ 
1. Exit                                      $m^2/sec$ 
2. Depth (C0^2+Bu*A): A=-8.645 B= 82.583 C= 1.3312     $m^2/str/s$ 
3. Underwater PAR (u-0)/S: S=-.0018887 O= .000267     $m^2/str$ 
4. Battery (u*S): S= 2.5
5. Temperature (u*S)+O: S= 8.486 O=-.6738
6. Nat Fl (u-0)/S: S=-.01581 O= 0.3683 = .5 QE(cf)= 2.4 kcf= 133
7. Surface PAR (u-0)/S: S=-.0009473 O= .00122
8. Chlorophyll AC(PAR)= .04 QE(F)= .045
9. SAVE PROFILE TO DISK
<Character> ↑ ↓ ← → or use mouse

```

Figure B-2. Instrument Calibration Menu

where S value is the scale and O is the offset (for the linear equations). Choose the variable(s) that need(s) to be changed using the arrow keys or selecting a number 2-8. Enter the new value, then press S to save value(s) to disc.

## **In Conclusion...**

The above procedure is sufficient for calibrating the A/D converter only. Calibration of the various sensors, at present, must be carried out by the factory. In an emergency, telephone the factory for information on doing this yourself.

---

# Appendix C. Software Installation

Appendix C describes how to load the PNF-300 software into your laptop computer, and describes the format for the profile configuration file. Also contained is a discussion of various considerations for configuring the laptop computer's memory.

Software for the PNF-300 consists of five files: three executable files and two support files (Figure C-1).

<u>File Name</u>	<u>Contents</u>
GO300.EXE	Main data acquisition program.
PROGRAPH.EXE	Profile data graphing program.
LOGGRAPH.EXE	Log data graphing program.
CALIBR8.G30	Calibration constants--display, convert and graph data.
DEFAULTS.G30	User-defined preferences for the GO300 program.

**Figure C-1.** List of Program Files. These files are to be loaded into a subdirectory (i.e. PNF300).

## Installing the Software

To install the software in the laptop computer, create a subdirectory (i.e. PNF300) in either the RAM disk or hard disk of the laptop computer. From the applicable prompt (B:> or C:>) type MD PNF300, then press ENTER. Insert the distribution disk into the disk drive. Use the COPY command to transfer the files from the disk to the subdirectory in the RAM disk or hard drive. For example, if the directory were placed in the C drive, type COPY A:\*. \* C:\PNF300. The files will be copied from the distribution disk into your PNF300 file directory. NOTE: The calibration values contained in the CALIBR8.G30 file on the distribution disk are *incorrect*, and are provided for formatting information only. You must enter the updated calibration values contained on the calibration worksheet prior to interpreting the output data (See Appendix B).

## Setting up the Data Directories

Data directories should be set up, preferably one directory for each survey or experiment. These directories should be sub-directories under the PNF300 directory. Suitable directory names might contain a geographic name and, as a suffix, the date (i.e. TAHITI.623, BAHAMA.D25). Data directories are set up using the DOS MD command. A copy of each one of the two support files CALIBR8.G30 and DEFAULTS.G30 should be included in each data directory. To facilitate calling up

the programs from within the data directories, you should add a line to your AUTOEXEC.BAT file (located in the root directory). For a C drive, for example, set up the path PATH = C:\;C:\DOS;C:\UTIL;C:\PNF300; (refer to your DOS manual concerning the PATH statement.)

## Installing the Printer and Monitor

A discussion of the factors to consider for selecting a printer and monitor screen are contained in Chapter 1 "Getting Started." Instructions on selecting the proper configuration is contained in Chapter 3 "Using the Software."

## Format of Configuration File

The format for the default file DEFAULTS.G30 is (Figure C-2):

<u>Parameter</u>	<u>Comments</u>
"Graphic Device", 9	Values: 2--CGA; 3--HERC; 9--EGA; 12--VGA
"Com Port", 1	Communication port number
"Log.Interval", 60	In seconds
"Max Depth", 200	In meters (see "Unit.of.Measure")
"Temp Range", 0, 30	In Celsius (see "Temp.Scale")
B:, 15, "", 1	B--Archive Drive (for computer's RamDiscs). 15--Archive period in minutes (0 deactivates). "--Epson printer. "100" is for HP LaserJet. 1--Printer port LPT1.
Surface Light Corr, 1	1 = On; 0 = Off
Spread, 15	# of pts. for k(PAR) calculation
MaxDepth, 0	0 = Autoranging
Plot Vars(#--Vars), 3,1,3,6	Types of variables plotted

**Figure C-2.** Sample Default file DEFAULTSG30. These values can be set using Step 3 of the GO300 program (see Chapter 3 "Using the Software").

The format for the calibration file CALIBR8.G30 is shown in Appendix B.

## Notes on Using Battery Powered Laptop Computers, Hard Drives, and RamDisc

Three methods are used for recording onto computers: 1) recording to floppy disk, 2) recording to "RamDisc," or memory, and 3) recording to a hard disk. None of these is perfect, but this following discussion may suggest which is best for your application.

### Recording Onto Floppy Disk

This method is the safest but slowest method. Normally a computer saves up data in an internal buffer before actuating the drive mechanism and writing the data. On some laptops that we have seen, the process of starting up the floppy drive and writing data can take several seconds. This may happen every 10-30 seconds, meaning that significant computer time is spent on the chore, possibly causing the instrument's data transmission to overrun the ability of the computer to digest the data. The GO300 program has made provisions for a considerable buffer to lessen the possibility of data loss. This buffer may lead to some disconcerting behavior during normal operation, particularly when using a floppy disk. You may complete a profile to 100 meters, for example, lift the instrument aboard the ship, and look at the display and see a report that the instrument is still at 20 meters! If you keep watching, the depth will decrease gradually until it finally agrees that it is on the deck of the ship. The delay reflects the backlog of data being processed from the instrument. If your computer exhibits this symptom, it is important not to stop the profile before your computer catches up with the data stream, or this backlogged data will be discarded!

### Recording Onto RAM Disk

You may wish to set aside part of your computer's memory to appear as a disk drive, often referred to as RamDisc, or RamDrive. An example of how to do this is described in the MS-DOS 3.3 manual under the topic "Ramdrive.sys". Another example of such a device driver is "VDISK". Consult your computer's manual for information on how to set up such a drive.

The advantage of such a drive is that it is very fast, and your computer should have no problem keeping up with the data acquisition. A second advantage is that the laptop computer will last longer between recharging the battery since it does not have to turn on the power hungry floppy drive as often. The drawback is that if you turn off the computer or the battery dies, the data are lost (in most laptops). This is not a problem if you are using only the logging mode of the GO300 software since it has the ability to periodically transfer the RamDisc-recorded data to the floppy, but this may be a problem in recording vertical profile data. If you do record to RamDrive, be sure to transfer the data to floppy before turning off the computer. Also, remember to keep the computer's battery fully charged. It is our preference to use a laptop computer setup with a RamDisc, even with these risks. A further caution--try using your RamDisc in the lab and see how the computer behaves when it gets full. We have encountered a type of RamDisc device that sometimes caused the system to

re-boot, losing all data in RAM when it got full, which is most disconcerting after logging a half-hour vertical profile!

## Recording Onto Hard Disk

This option is perhaps the best when operating on a larger oceanographic vessel. Most hard disks require considerable power, making it impractical to directly record on them under battery power. If your laptop computer has a hard disk and you are operating under battery power, perhaps in a small bobbing inflatable boat, the best procedure may be to use RamDisc and transfer the data at the end of a profile to either the hard disk or to a floppy. We have no more problems with hard disks operated on oceanographic ships than we have had in the lab, but under both conditions we have had failures. The best procedure when using a hard disk is to conduct frequent backups no matter what you are doing.

**Appendix 12**

Submitted copy of "Natural Fluorescence of chlorophyll a: Relationship to photosynthesis and chlorophyll concentration in the western South Pacific gyre", D. A. Kiefer, W. S. Chamberlin, and C. R. Booth. Published in *Limnology and Oceanography*, **34** (5), 1989, 868-881.

155

Natural fluorescence of chlorophyll a: Relationship to  
photosynthesis and chlorophyll concentration in the western South  
Pacific gyre

by

D. A. Kiefer, W. S. Chamberlin, and C. R. Booth<sup>1</sup>

Department of Biological Sciences, University of Southern California,  
Los Angeles 90089-0371

<sup>1</sup>Biospherical Instruments Inc., San Diego 92117

Running head: Natural fluorescence and photosynthesis



## Abstract

A new optical instrument, designed specifically for the measurement of the natural or solar-induced fluorescence of chlorophyll a, was deployed in the tropical and temperate waters of the western South Pacific gyre. During the 12 days of transit from Papeete, Tahiti, to Auckland, New Zealand, measurements were made of the vertical distribution of temperature, salinity, upwelling radiance and downwelling irradiance at selected wavelengths, the beam attenuation coefficient at 683 nm, the scalar irradiance of photosynthetically available radiation, and the nadir radiance at 683 nm, which is the wavelength of peak emission by chlorophyll a. In addition, water samples were collected at regular depth intervals and analyzed for the concentration of chlorophyll a, and for the spectral absorption coefficient of cells and associated detrital particles.

In order to examine the relationship between natural fluorescence and the size and photosynthetic rate of the phytoplankton crop, several simple equations were derived and applied to the analysis of the data. One relates the nadir radiance at 683 nm to the total fluorescence emitted by the phytoplankton crop within the field of view, another relates natural fluorescence to the concentration of chlorophyll a, and a third relates natural fluorescence to the gross rate of photosynthesis of the crop. We found that even in the extremely oligotrophic waters of the central south Pacific gyre, natural fluorescence was easily measured throughout the euphotic zone at depths below 6 m. As found in previous studies, the value of natural fluorescence varied spatially and temporally with ambient scalar irradiance of PAR and the

concentration of chlorophyll a. The quantum yield of fluorescence, which varied five fold, averaged about 0.035 photons emitted to photons absorbed, and generally decreased with increasing levels of exciting irradiance. Most importantly, we found natural fluorescence to covary closely with calculated rates of photosynthesis. A linear regression of calculated photosynthetic rate on fluorescence yielded a correlation coefficient of 0.84 and a slope of 2.0 atoms of carbon fixed per photon emitted as fluorescence.

Table of Symbols:

Symbol	Explanation	Units
F <sub>f</sub>	natural fluorescence	Ein m <sup>-3</sup> s <sup>-1</sup>
F <sub>c</sub>	photosynthesis	g-at carbon m <sup>-3</sup> s <sup>-1</sup>
F <sub>a</sub>	light absorption	Ein m <sup>-3</sup> s <sup>-1</sup>
E <sub>0</sub>	scalar irradiance	Ein m <sup>-2</sup> s <sup>-1</sup>
Lu(683)	upwelled radiance at 683 nm	Ein m <sup>-2</sup> str <sup>-1</sup> s <sup>-1</sup> nm <sup>-1</sup>
a <sub>c</sub>	absorption coefficient for phytoplankton	m <sup>-1</sup>
°a <sub>c</sub>	chlorophyll-specific cellular absorption	m <sup>2</sup> (mg chl) <sup>-1</sup>
a <sub>p</sub>	chlorophyll-specific particle absorption	m <sup>2</sup> (mg chl) <sup>-1</sup>
a <sub>w</sub>	absorption coefficient for water	m <sup>-1</sup>
k	diffuse attenuation coefficient	m <sup>-1</sup>
Φ <sub>f</sub>	quantum yield of natural fluorescence	Ein emitted/Ein absorbed
Φ <sub>c</sub>	quantum yield of photosynthesis	g-at C fixed/Ein absorbed
Ψ <sub>f</sub>	natural fluorescence coefficient	m <sup>-1</sup>
μ	mean cosine of light field	dimensionless
K <sub>φ</sub>	half-saturation constant for φ <sub>c</sub>	Ein m <sup>-2</sup> s <sup>-1</sup>
λ <sub>ex</sub>	excitation wavelength	nm
λ <sub>em</sub>	emission wavelength	nm

Natural fluorescence of chlorophyll a: Relationship to photosynthesis and chlorophyll concentration in the western South Pacific gyre

Recent analyses of the spectrum of upwelling irradiance in the ocean have shown the contribution by the fluorescence of chlorophyll a. This signal from the crop of phytoplankton was first identified by Morel and Prieur (1977) from subsurface measurements of spectral diffuse reflectance and Neville and Gower (1977) from measurements of nadir radiance above the sea surface. Shortly thereafter, Gordon (1979) and Kattawar and Vastano (1982) presented a mathematical description of the relationship between this natural or solar induced fluorescence, the concentration of chlorophyll a, and the ambient light intensity which excites the fluorescence. More recently, Kishino et al. (1984 a,b), Topliss (1985), Topliss and Platt (1986), Dirks and Spitzer (1987), and Preisendorfer and Mobley (1988) have further investigated factors affecting natural fluorescence in the field.

The natural fluorescence of chlorophyll may be important to the study of the distribution and growth of phytoplankton in the sea since it is one of the few measurements that can be made without perturbation of the crop. The measurement is rapid and yields information that is of high spatial and temporal resolution. Moreover, the signal can be monitored by remote sensors such as those placed on aircraft (Gower and Borstad 1981) or moorings and drifters (Dickey 1988). In the work described below, we attempted to answer several questions about the natural fluorescence of chlorophyll a: What optical measurements provide the most sensitive

and reliable measurement of natural fluorescence, and what accessory information is necessary to interpret the signal? Is the fluorescence signal detectable throughout the euphotic zone, particularly in highly oligotrophic waters where the crop is smallest and penetration of solar radiation deepest? How does the signal vary with the concentration of chlorophyll a, and is there a simple yet accurate formulation describing the relationship between natural fluorescence, chlorophyll a, and ambient light? Does the signal provide information about the photosynthetic rate of the crop, and what mathematical formulation is necessary to obtain such information?

We have addressed these questions by designing and building a new submersible radiometer specifically for the measurement of natural fluorescence. During an oceanographic research cruise in latter November and early December of 1986, the instrument was routinely deployed from the exploration and research vessel Calypso during its direct voyage from Papeete, Tahiti, to Auckland, New Zealand. Our analysis of the optical and biological data obtained from vertical profiles indicates that natural fluorescence can be measured throughout the euphotic zone and provides valuable biological information about the size and photosynthetic rate of the phytoplankton crop.

We thank Dr. Richard Murphy, Madame Cousteau, Captain Falco, Bertrand Sion, and the other crew of Calypso for their professional and enthusiastic help during the cruise. We also thank John Morrow for providing logistics and programming support, and two anonymous reviewers whose comments were helpful.

### Field Measurements

As mentioned earlier, the track is a southwestward transect of the South Central Pacific gyre between Papeete and Auckland during 28 November to 10 December, 1986. Sampling of the water column at each station consisted of both continuous monitoring of physical and optical properties during vertical profiling of the upper 100 to 150 m of the water column (Table 1) and collection of water samples. The instrument package lowered from the ship included a MER-1048 Reflectance Spectroradiometer (Biospherical Instruments, Inc.) configured as a Bio-Optical Profiling System (Smith et al. 1984). Optical and physical properties measured included downwelling and upwelling irradiance, upwelling radiance ( $L_u$ ), scalar irradiance of PAR ( $E_o(\text{PAR})$ ), pressure (depth), conductivity, temperature, and beam transmission at a wavelength of 660 nm. Data from the MER-1048 and its associated sensors were recorded on a shipboard personal computer. Approximately 5 sets of readings from all sensors were digitized and averaged for each 1-m depth increment. The system was lowered at a rate of  $1 \text{ m s}^{-1}$ , and the ship was normally positioned to minimize its shadow cast.

A typical sampling procedure consisted of an initial round trip profile to 130-140 m, followed by a second cast which included the deployment of 6 10-liter Niskin bottles (General Oceanics, Inc.). Data were also recorded on this second cast, and the 6 bottles were tripped using a messenger.

In order to make measurements of natural fluorescence with a hand lowered instrument, we designed and constructed a prototype

"natural fluorometer". This instrument combined the Lu(683,z) sensor with a Eo(PAR,z) sensor in a single underwater package. A second Eo(PAR) sensor on board enabled us to simultaneously monitor incident light, a crucial parameter when predicting daily production from measurements of natural fluorescence during cloudy periods. Additional sensors included a pressure transducer for depth measurements and a temperature sensor.

The prototype, designed by Biospherical Instruments, Inc., digitized the underwater signals at the sensors using a data acquisition system with a dynamic range of  $10^6$ . Digitized data were transmitted to the surface where deck electronics also digitized data from a surface irradiance sensor (QSR-240, Biospherical Instruments, Inc.). These digital data were combined and transmitted to a computer for display, storage and analysis. Data from both the MER-based profiling system and from the prototype natural fluorometer were compared at several stations.

During the upcast, six depth intervals were routinely analyzed for their concentrations of chlorophyll *a* and phaeophytin, and for the spectral absorption coefficients of suspended microscopic particles. Chlorophyll *a* and phaeopigments were measured fluorometrically (Holm-Hansen et al. 1965). The spectral absorption coefficient of suspended microparticles, which includes phytoplankton and detritus, was calculated from measurements with a spectrophotometer (Bausch and Lomb 2000) according to Mitchell and Kiefer (1988). Attempts were made to measure photosynthetic rates using  $^{13}\text{C}$  as a tracer (Slawyk et al. 1977). Unfortunately, in our hands, the method did not prove reliable.

### Mathematical formulation

Previous theoretical or mathematical descriptions of the contributions to the submarine light field by the naturally occurring fluorescence of chlorophyll a have been based upon downwelling and upwelling irradiance (Gordon 1979; Kishino et al. 1984a; and Topliss 1985). We chose instead to measure scalar irradiance for wavelengths in the visible region of the spectrum and upwelling radiance in the more restricted region of chlorophyll a emission. Scalar irradiance is the preferred measure of light available for photosynthesis and fluorescence of phytoplankton since the cells within the crop are best described as spherical collectors in a light field of unknown radiance distribution. The measurement of upwelling radiance is also advantageous since the intensity of the path radiance contributed by sunlight is smallest, and thus the ratio of fluorescence to scattered light is largest at all depths.

We will now show that by invoking several reasonable assumptions, one can obtain a relatively simple yet accurate mathematical description of the submarine fluorescence field in terms of these two optical parameters. Analysis of the natural fluorescence field consists of three problems: distinguishing between the contributions by solar path radiance and fluorescence emission to the measured vertical radiance, determining the effects of the attenuation with depth of the exciting irradiance within the field of radiance detection, and determining the effects of the attenuation of the fluorescence emitted by cells within the field of radiance detection. The derivation not only proves that none of these three

problems is significant, but also aids our understanding of the relationship between the natural fluorescence signal, ambient light intensity, and the local concentration of phytoplankton.

### Definition of Natural Fluorescence

Consider a small volume of seawater containing cellular chlorophyll whose fluorescence emission at wavelength,  $\lambda_{em}$ , is excited by light at wavelength,  $\lambda_{ex}$ . The rate of light absorption by the cells within the volume is simply the product of the incident scalar irradiance and the absorption coefficients of the suspended cells:

$$F_a(\lambda_{ex}) = a_c(\lambda_{ex}) E_o(\lambda_{ex}) \quad (1a)$$

Integration of this equation over the spectrum of visible light (400 to 700 nm) yields the rate of absorption of photosynthetically available radiation. In practice calculation of  $F_a$  is difficult because of uncertainties in the value and spectral distribution of  $a_c(\lambda_{ex})$  and spectral distribution of  $E_o(\lambda_{ex})$ . By necessity estimates of the rate of light absorption by the crop are commonly made by the approximation:

$$F_a = a_c(\text{PAR}) E_o(\text{PAR}) \quad (1b)$$

Fluorescence emitted by the cells at wavelength,  $\lambda_{em}$ , and excited by wavelength,  $\lambda_{ex}$ , is simply the product of the flux of absorbed light and the quantum efficiency of fluorescence:

$$F_f(\lambda_{ex}, \lambda_{em}) = \Phi_f(\lambda_{ex}, \lambda_{em}) F_a(\lambda_{ex}) \quad (2a)$$

The emission spectrum of chlorophyll a in phytoplankton is Gaussian in shape, has a width of half maximal emission of about 25 nm and centers at 683 nm (Collins et al. 1985). The value of the total quantum yield of fluorescence in the far red is 27 times that of the fluorescence in a 1-nm wide band centered at 683 nm, i.e. the total fluorescence emitted in the far red is 27 times the fluorescence emitted at 683 nm (following Gordon 1979). If we assume that the quantum yield of fluorescence is generally independent of the wavelength of excitation, and that the fluorescence excitation spectrum is similar in shape to the absorption spectrum (e.g. Forster and Livingston 1952; Neori et al. 1986; Mitchell and Kiefer 1988), one can represent total natural fluorescence emitted as the product of the total quantum yield and the total rate of light absorption by cells within the unit volume:

$$F_f = \Phi_f F_a = \Phi_f ac(\text{PAR}) E_o(\text{PAR}) \quad (2b)$$

We define  $F_f$  as natural fluorescence.

### Natural Fluorescence, Nadir radiance, and Scalar Irradiance

Eq. 2b provides the basis for deriving a simple relationship of the relationship within the water column between the upwelled radiance of fluoresced light measured at depth  $z$  and the exciting scalar irradiance at that depth. We will restrict our measurements to

depths where the contribution to  $L_u(\lambda_{em})$  by solar path radiance is insignificant and the dominant contribution comes from fluorescence. We have found that this restriction is not severe, and depending on the stability of the sea surface, this condition will exist at depths from 3-5 m (Booth, unpublished data). To quantify the relationship between the vertical radiance of fluoresced light and the exciting scalar irradiance, we invoke three assumptions concerning the radiance distribution and the homogeneity of the water column immediately below the natural fluorometer.

First, we assume that the water column below depth  $z$  is homogeneous within the distance or pathlength from which the fluorescence signal is detected. Under such conditions the vertical distribution of exciting scalar irradiance can be simply described in terms of the law of Lambert-Beers:

$$E_o(\lambda_{ex}, z+dz) = E_o(\lambda_{ex}, z) \exp(-dz k(\lambda_{ex}, z)) \quad (3)$$

where  $k(\lambda_{ex}, z)$  is the attenuation coefficient for scalar irradiance at depth  $z$ , and is measured directly by the natural fluorometer.

Second, we assume, as have all previous workers, that fluorescence from cells is isotropic. Under such a condition the relationship between total fluoresced light from the unit volume of cell suspension and the emitted radiance is simple, and Eq. 2 can be expressed:

$$L_u(\lambda_{ex}, \lambda_{em}) = F_f(\lambda_{ex}, \lambda_{em}) / (4 \pi) \quad (4)$$

Third, within this depth interval of homogeneous water we assume that the radiance distribution of the fluoresced light is diffuse. Under such a condition the attenuation of light emitted from a small volume of seawater at a distance below the detector is simply described in terms of the Lambert-Beers law and the absorption coefficient of seawater. Thus, the vertical radiance detected at depth  $z$  that is contributed by the cells at a distance  $dz$  from the radiance detector is:

$$Lu(\lambda_{ex}, \lambda_{em}, dz) = Ff(\lambda_{ex}, \lambda_{em}, dz) \exp(-dz a(\lambda_{em}, z)) / (4 \pi) \quad (5)$$

$a(\lambda_{em})$  is equal to the sum of the absorption coefficients for water and all suspended and dissolved materials. Since the value of the absorption coefficient for water is large at wavelengths of chlorophyll a fluorescence, e.g.  $a_w(683) = 0.48 \text{ m}^{-1}$ , and attenuation is exponential, the depth interval of fluorescence detection is short even in the clearest of waters.

After substituting the right hand side of Eq. 3 into Eq. 5 and integrating over the depth interval from the depth  $z$  to infinity, one obtains after rearrangement the following formulation of the fluorescence emitted from a unit volume of sea water at depth  $z$ :

$$Ff(\lambda_{ex}, \lambda_{em}, z) = 4 \pi Lu(\lambda_{ex}, \lambda_{em}, z) (k(\lambda_{ex}, z) + a(\lambda_{em}, z)) \quad (6)$$

Thus, if one knows the value  $a(\lambda_{em}, z)$ , one can measure the vertical distribution of natural fluorescence from profiles of  $Lu(\lambda_{ex}, \lambda_{em}, z)$  and  $E_o(\lambda_{ex}, z)$ ;  $k(\lambda_{ex}, z)$  is obtained by solving Eq. 3. In waters of low to

moderate turbidity, the sum  $k(\lambda_{ex}) + a(\lambda_{em})$  is approximately constant.

Eq. 6 is presented in terms of monochromatic light of excitation, and emission. One can obtain the total light emitted from a unit volume at depth by doubly integrating the right hand side of this equation over the spectra for fluorescence excitation and fluorescence emission. An alternative and less rigorous approach is to invoke assumptions similar to those found in Eqs. 1b and 2b. Thus, the absorption coefficient at 683 nm provides an approximate value of  $F_f$ , and  $k(\text{PAR})$  provides an approximate value for the attenuation of total exciting radiation:

$$\int_{400}^{700} (a(\lambda_{em}) Lu(\lambda_{em}) d\lambda_{em}) / \int_{400}^{700} (Lu(\lambda_{em}) d\lambda_{em}) = a(683) \quad (7a)$$

$$\int_{400}^{700} (k(\lambda_{ex}) Lu(\lambda_{ex}) d\lambda_{ex}) / \int_{400}^{700} (Lu(\lambda_{ex}) d\lambda_{ex}) = k(\text{PAR}) \quad (7b)$$

Thus, natural fluorescence is estimated from the measurement of nadir radiance at 683 nm by:

$$F_f(z) = 4 \pi 27 Lu(683,z) (k(\text{PAR},z) + a(683,z)) \quad (8)$$

Note that  $Lu(683,z)$  is in units of  $\text{Ein m}^{-2} \text{str}^{-1} \text{s}^{-1} \text{nm}^{-1}$ .

Like Gordon (1979), we find it useful to identify the product  $\Phi_f ac(\text{PAR})$  found in Eq. 2b as the natural fluorescence coefficient. This coefficient, which has units of  $\text{m}^{-1}$ , will not only be used to calculate

chlorophyll *a* concentration, but also can be applied to a calculation of daily rates of photosynthesis. It is simply calculated by dividing  $F_f(z)$  by  $E_0(z)$ :

$$\Psi_f(z) = 4 \pi \int_0^{\infty} L_u(683, z) (k(\text{PAR}, z) + a(683, z)) / E_0(\text{PAR}, z) \quad (9)$$

### Linearity and Pathlength: a 2-Component Model

To describe the range of conditions under which field measurements of Lu683 and PAR can yield for  $F_f$ , we will describe the effects of attenuating and absorbing components on natural fluorescence. Our 2-component description of attenuation and fluorescence in the sea is based upon evidence accumulated over the last 20 yrs. that in most coastal and all oceanic waters the major source of optical variability is the crop of phytoplankton and the associated detrital particles (e.g. Morel and Prieur 1977; Smith and Baker 1978). Accordingly, we represent the attenuation coefficient for PAR and the absorption coefficient at 683 in terms of a constant and a variable component:

$$k(\text{PAR}) = (a_w(\text{PAR}) + a_p(\text{PAR}) \text{ chl}) / \mu \quad (10)$$

$$a(683) = a_w(683) + a_p(683) \text{ chl} \quad (11)$$

The value in white light for  $a_w(\text{PAR})$  of 0.04. In clear waters  $a_w(683)$  is approximately equal to  $k(683)$  (Smith and Baker 1981), and its value is about 0.46. From our measurements of chlorophyll and the coefficients of spectral absorption by particles and diffuse

attenuance, we have determined the average values for  $^{\circ}ap(\text{PAR})$  and  $^{\circ}ap(683)$  to be 0.03 and 0.01, respectively. These values include the average contribution by phytoplankton and detritus. In this model, the mean cosine of the light field is given a value of 0.8 (Jerlov 1976).

Eqs. 10 and 11 were substituted into eq. 8, which was then solved as a function of the concentration of chlorophyll  $a$  (Fig. 1). The relationship between the nadir radiance of fluoresced light and the concentration of chlorophyll  $a$  is approximately linear for concentrations less than about  $2 \text{ mg m}^{-3}$ . Although the comparison is rough, this prediction of a curvilinear relationship between the nadir radiance and concentration of chlorophyll  $a$  is supported by measurements of Kishino et al. (1984b) in the northwestern Pacific. Their regression of upwelling irradiance in the red versus chlorophyll  $a$  concentration indicates that as concentrations of chlorophyll increase, the rate of increase of the fluorescence signal diminishes (cf. our Fig. 1, Eqs. 9, 10). At concentrations below  $2 \text{ mg m}^{-3}$ ,  $k(\text{PAR}) + a(683)$  changes little, and its value is about  $0.52 \text{ m}^{-1}$ . This generalization is not true at higher concentrations, so that in eutrophic waters, one must obtain values for the sum of  $a(683)$  and  $k(\text{PAR})$  by either direct measurements or by estimation. Since the natural fluorometer measures  $E_o(\text{PAR})$ , values for  $k(\text{PAR})$  can be directly measured.

It is noteworthy that the minimum value of  $aw(683) + kw(\text{PAR})$  (for water alone) is approximately  $0.52 \text{ m}^{-1}$ . This defines the maximum pathlength for the vertical radiance measurement of natural fluorescence; over 95 % of the signal comes from within 6

meters of the fluorometer. If vertical gradients in chlorophyll concentration are sufficiently large within this pathlength, the natural fluorometer will tend to smooth structure.

## RESULTS

### Vertical Distribution of Lu(683) and Eo(PAR)

During transit from Papeete to Auckland the instrument package was lowered over 30 times in waters that ranged from highly oligotrophic to moderately eutrophic. The concentration of chlorophyll *a* at the surface in the central waters of the southern gyre was as low as 0.023 mg m<sup>-3</sup> and as high as 0.47 mg m<sup>-3</sup> at the western boundary. Conversely, surface water temperatures, which ranged from 23.5°C to 17.7°C, were highest in the central gyre and lowest off the coast of New Zealand. The depth of the mixed layer showed no latitudinal gradients, and varied from 26-60 m.

We have chosen 2 stations, one oligotrophic and the other mesotrophic, as examples of the range in optical patterns that were observed (Fig. 2a,b). Cast 1201-M1 was in the oligotrophic waters of the central gyre at 23°53'S, 161°37'W, and cast 1209-M5 was in the mesotrophic waters of the western boundary of the gyre at 36°15'S, 171°9'E. In shallow waters Lu(683) consists of two components, the fluorescence of chlorophyll *a* and backscattered sunlight. One notes at both stations that in the upper 6 m of the water column the value of Lu(683) drops sharply with depth and then decreases more slowly and regularly with depth. The rapid decrease near the surface is primarily caused by the attenuation of scattered sunlight at 683 nm.

Below 6 m the strong absorption of red light by water has effectively removed most path radiance from the sun, and the signal is dominated by the fluorescence of chlorophyll *a*. Below this depth the attenuation of Lu(683) with depth roughly parallels the attenuation of Eo(PAR), a feature to be expected since Eo(PAR) is a measure of the intensity of fluorescence excitation.

A comparison of the vertical distributions for the two stations reveals differences that are to be expected of oligotrophic and mesotrophic waters. Lu(683) and Eo(PAR) decrease much more gradually with depth at the oligotrophic station than at the mesotrophic station. At 1201-M1, natural fluorescence is still measureable at 130 m, which is near the bottom of the euphotic zone. At 1209-M5, Lu(683) is measureable only to a depth of 60 m. Note that for comparable intensities of PAR, the value of Lu(683) is about 5 times higher at the mesotrophic station, and thus roughly proportional to the increased concentration of chlorophyll *a*.

The distinct difference in the vertical distributions between the reflectances for 488 vs. 683 nm is a manifestation of the differences in the radiance distribution (Fig. 3a,b). At both stations the values for reflectances at 488 nm are about 0.01 and are relatively constant with depth. Since there is no fluorescence source at depth at 488 nm, the value of reflectance at this wavelength is determined largely by inherent optical properties. Likewise, at both stations, the values for reflectances at 683 nm increase almost a thousand fold in the upper 20 m. Below this depth the value for reflectance remains relatively constant, having a value of about 0.2. This pattern of distribution is explained by changes in the radiance distribution

affected by the marine fluorescent light field. Below 20 m, the source of both nadir radiance and downwelling irradiance is natural fluorescence. Since emission by phytoplankton is isotropic, the radiance distribution of this light in relatively clear waters will be diffuse. The average value of 0.4 for radiance reflectance is close to the value of 0.318 expected for a completely diffuse light field (Preisendorfer 1976). In waters shallower than 20 m, the rapid increase in radiance reflectance with depth is primarily due to changes in the relative contributions by scattered solar radiation and fluorescence to the downwelling irradiance.

The vertical distribution of chlorophyll at the two stations (Fig. 4) is characterized by a subsurface chlorophyll maximum, 85 m at the oligotrophic station, and 60 m at the mesotrophic station. Above the chlorophyll maximum increases in chlorophyll concentration with depth are most likely caused by changes in the cellular chlorophyll concentration. In this interval the concentration of particles as measured with the transmissometer changed little with depth. Below the chlorophyll maximum, decreases in chlorophyll with depth are paralleled by decreases in particle concentration. Clearly, the vertical distribution of the ratio  $Lu(683)/E_o(PAR)$  is similar to that of chlorophyll a. A similar ratio of fluorescence signal to ambient light was found by Kishino et al. (1984a) and Topliss (1985) to be an indicator of chlorophyll a concentration.

#### Diurnal Distribution of Lu(683)

During two days of the cruise, Calypso remained on station from sunrise to sunset, yielding information on the diurnal

distribution of natural fluorescence (Fig. 5). It is obvious, in these waters where the concentration of chlorophyll at a given depth did not change significantly during the sampling period, that changes in  $Lu(683)$  with time are largely determined by changes in the intensity of exciting light,  $E_o(PAR)$ . The flatter shape for  $Lu(683)$  at 10 m relative to the shape at 50 m suggests that the quantum yield for fluorescence may be lower at higher light intensities. It is worth noting that measurements of photosynthesis with oxygen electrodes on cultures (Marra et al. 1985) and closed natural systems indicate similar diurnal patterns between light intensity and photosynthetic rate.

## DISCUSSION

### Fluorescence and the Crop

The concentration of chlorophyll a has been commonly calculated from measurement of stimulated *in situ* fluorescence since the introduction of the method by Lorenzen in 1966. As demonstrated by Gordon (1979), Topliss (1985), and particularly Kishino and co-workers (1984a,b), the natural fluorescence of chlorophyll also provides an index of chlorophyll a concentration. The relationship between chlorophyll concentration and natural fluorescence is determined by the natural fluorescence coefficient, (Eq. 9), the quantum yield of natural fluorescence (Eq. 2), and the mean chlorophyll a specific absorption coefficient for the phytoplankton crop:

$$\text{chl} = \Psi_f / (\Phi_f \sigma_{ac}(\text{PAR})) \quad (12)$$

As discussed in Falkowski and Kiefer (1985), the accuracy with which the concentration of chlorophyll a can be estimated from measurements of the fluorescence coefficient will depend upon the constancy of  $\Phi_f$  and  $\sigma_{ac}(\text{PAR})$  in the field. For example, the value of  $\sigma_{ac}(\text{PAR})$  may vary with the pigment composition of the crop as well as the size distribution of the cells and their intracellular concentration of pigments (Morel and Bricaud 1981). Additionally,  $\Phi_f$  may vary with a number of other factors including the ambient light intensity and nutrient concentration and the species composition of the crop.

The measurements of chlorophyll concentration and fluorescence coefficient during Calypso '86 suggest that over the broad geographical region which we sampled variations in these two parameters within the water column were not large. The relationship between  $\Psi_f$  and chlorophyll a appears linear for these waters of low to moderate concentration of chlorophyll (Fig. 6). Linear regression analysis of 82 pairs of data yielded a slope of 2100  $\text{mg m}^{-2}$ , and a value for  $r^2$  of 0.90. According to Eq. 12, the reciprocal of the slope is a mean value of the product of the quantum yield for fluorescence and the chlorophyll a specific absorption coefficient of the phytoplankton crop. In fact, this value for the slope compared well with independent measurements of absorption and fluorescence in the laboratory. For example, the reciprocal value of the slope in Fig. 6, 0.00047, is close to the value of 0.00042 for the

product of  $\rho_{ac}$ , 0.012 (Mitchell and Kiefer 1988) and  $\Phi_f$ ,  $0.035 \pm 0.005$ .

We examined more closely the quantum yield of natural fluorescence, introducing measured values of chlorophyll a and  $\Psi_f$ , and a constant value of  $0.012 \text{ m}^2 (\text{mg chl})^{-1}$  for  $\rho_{ac}$  into equations 1b and 2, and solving for values of  $\Phi_f$  for all discrete water samples. We found that the values were variable, ranging between 0.02 and 0.09, and averaging 0.04. A similar analysis by Kishino et al (1984b) yielded comparable values. The plot (Fig. 7) of  $\Phi_f$  versus  $E_o(\text{PAR})$  suggests that there is a dependence of quantum yield upon light intensity. At higher irradiances the average value of  $\Phi_f$  appears to decrease. Quantum yields of photosynthesis for cultures and natural crops also have been shown to decrease with increasing light intensity (Tyler 1975; Mitchell and Kiefer 1988).

### Fluorescence and Photosynthesis

The relationship between natural fluorescence and the instantaneous rate of photosynthesis can be crudely examined by applying the phenomenological Eq. 2 to both natural fluorescence and photosynthesis:

$$F_f = \Phi_f F_a \quad (2)$$

$$F_c = \Phi_c F_a \quad (13)$$

$$F_c = F_f (\Phi_c / \Phi_f) \quad (14)$$

Since the instantaneous rate of light absorption appears as a variable in Eqs. 2 and 13, its variability in the sea will cause proportional changes in  $F_f$  and  $F_c$ . Thus, variations in the rates of photosynthesis caused by changes in the size and the pigment composition of the crop, and the intensity and spectral composition of the light field, will be paralleled by variations in natural fluorescence.

This link between natural fluorescence and photosynthesis is expressed concisely by Eq. 14: the ability to predict rates of photosynthesis from measurements of natural fluorescence will depend solely upon the the ratio of quantum yields for fluorescence and photosynthesis (carbon atoms/photons). If the ratio is constant or predictable, good estimates of production can be expected. Unfortunately, not much is known about the quantum yields of fluorescence and photosynthesis for phytoplankton under natural growth conditions. With the exception of the work on flash-induced fluorescence by Falkowski and co-workers (1986), almost all recent measurements of the fluorescence of chlorophyll in phytoplankton have been made with fluorometers that provide a constant excitation intensity and a spectral composition of the light different from ambient.

On the other hand, enough is known about the quantum yields of fluorescence and photosynthesis to indicate that both yields are likely to vary in the ocean. Increase in light intensity has been shown in the field to cause decreases in the quantum yields of both photosynthesis (e.g. Tyler 1975) and fluorescence (e.g. Kiefer 1973a). In addition, studies of marine diatom cultures indicate that nutrient

deficiencies increase the quantum yield of fluorescence (Kiefer 1973b) and decrease the quantum yield of photosynthesis (Cleveland and Perry 1987).

Here we do not wish to speculate on the behavior of  $\Phi_f$  and  $\Phi_c$  for natural populations, but merely mention that fluorescence, photosynthesis, and heat production are the three main transformations of absorbed light, and, as such, have been viewed as competing processes; increases in one transformation leads to decreases in others (e.g. Topliss and Platt 1986). Since fluorescence and photosynthesis are only two of the three possible pathways of de-excitation of photosystem II, however, a simple inverse relationship between variations in the two quantum yields is by no means assured.

As mentioned previously, we attempted unsuccessfully to compare direct measurements of daily rates of photosynthesis using  $^{13}\text{C}$  with estimates based upon vertical profiles of instantaneous rates of natural fluorescence. As an alternative to direct comparison, we have compared instantaneous natural fluorescence at a given depth with calculations of instantaneous rates of photosynthesis based upon the concentration of chlorophyll  $a$  and the scalar irradiance (Fig. 8).

The calculated rate was obtained by introducing values of chlorophyll  $a$  and scalar irradiance into the formulation of Kiefer and Mitchell (1983):

$$F_c = \alpha_{ac}(\text{PAR}) \Phi_{\max} K_{\Phi} \text{chl } E_o(\text{PAR}) / (K_{\Phi} + E_o(\text{PAR})) \quad (15)$$

where  $\sigma_{ac}(\text{PAR})$ ,  $\Phi_{\text{max}}$ , and  $K_{\Phi}$  are constants having values of  $0.012 \text{ m}^2 (\text{mg chl})^{-1}$ ,  $0.1 \text{ mol carbon Ein}^{-1}$ , and  $2,400 \mu\text{Ein m}^{-2} \text{ h}^{-1}$ . This formulation, derived from a culture of a small marine diatom, correlates well with measured rates of photosynthesis and has been successfully applied to estimates of daily photosynthesis in the field (Bidigare et al. 1987; Marra and Heinemann 1987; Chamberlin 1989). It is also consistent with the empirically derived field model of Ryther and Yentsch (1957).

An important feature of this formulation is the assertion that under steady state conditions of growth, the quantum yield of photosynthesis is independent of temperature and nutrient availability and depends solely on light intensity; the quantum yield decreases with increasing irradiance. Unfortunately, since the formulation does not include a description of photoinhibition, predictions of rates of photosynthesis at high light intensities near the sea surface are likely to be too large. In addition, we note that Cleveland and Perry (1987) have found that the quantum yield of photosynthesis and the chlorophyll specific absorption coefficient vary as a function of the cellular nitrogen quota in batch cultures of *Chaetoceros gracilis*. Thus, under conditions of severe nutrient limitation in the field, the values of the two coefficients used in the above formulation may differ. Also, as much as five-fold variability in the chlorophyll specific absorption coefficient has been observed for laboratory cultures (Bricaud et al., 1988), although Chamberlin (1989), using the spectral decomposition technique of Morrow (1988), observed only two-fold variations in the chlorophyll specific absorption coefficients of phytoplankton in the Sargasso Sea and the

western South Pacific Ocean. The mean value of  $0.013 \text{ m}^2 \text{ m}^{-1}$  reported by Chamberlin (1989) is nearly identical to the value used in the above formulation, and the assumption of constancy is probably not restrictive. As mentioned above, variations in the chlorophyll specific absorption coefficient affect both fluorescence and photosynthesis, and variations in this coefficient will be tracked by variations in fluorescence and photosynthesis. Thus, it may be expected that a comparison of natural fluorescence productivity to model estimates will yield an underestimate of the precision of the natural fluorescence method since variations in  $^{\circ}\text{ac}$  (PAR) will be reflected in the natural fluorescence measurements and not in model estimates.

Nonetheless, the regression of natural fluorescence on calculated production appears linear, passes through the origin, and has a correlation coefficient of 0.84 ( $n=82$ ,  $y=0.007 + 2.0x$ ). The slope of the regression, which should equal the average value of  $\Phi_c/\Phi_f$ , is 2.0, which is quite reasonable. Multiplying this factor by the average fluorescence quantum yield of 0.035, calculated earlier, provides an average quantum yield for photosynthesis of  $0.07 \pm 0.02$ . The 82 data points upon which this regression is based come from all depths below 5 m. The samples contained between 0.02 and  $0.75 \text{ mg m}^{-3}$  of chlorophyll and were collected at irradiances that ranged over one hundred-fold. This comparison, which includes a large geographic sample, suggests to us that with further testing natural fluorescence may prove to be a reliable measure of photosynthesis.

We propose that daily rates of photosynthesis,  $F_c(z, \text{daily})$  can be estimated from measurements of instantaneous rates of natural

fluorescence at depth by taking the product of the fluorescence coefficient,  $\Psi_f$ , the integrated daily flux of scalar irradiance,  $E_o(\text{PAR},z,\text{daily})$ , and the ratio of the quantum yields,  $\Phi_c/\Phi_f$ :

$$F_c(z,\text{daily}) = (\Phi_c(z)/\Phi_f(z)) \Psi_f(z) E_o(\text{PAR},z,\text{daily}) \quad (16)$$

In a subsequent paper, we will compare rates of photosynthesis predicted by measurements of natural fluorescence with photosynthetic rates measured using the cellular incorporation of  $^{14}\text{C}$ - bicarbonate. These results, which comprise data from several investigators in eutrophic to oligotrophic environments, demonstrate the feasibility of estimating primary production from measurements of natural fluorescence.

#### Application

If natural fluorescence proves to provide a reliable estimate of either chlorophyll a concentration or photosynthesis, its measurement may provide a new means of examining the natural crop of phytoplankton. The natural fluorometer is compact, it requires little electrical power, and the measurement is sufficiently rapid that the instrument can acquire detailed temporal and spatial information. On the other hand, measurements are limited to daylight hours. The estimation of gross daily photosynthetic rate by measurement of natural fluorescence is particularly attractive since it has several advantages over measurements in incubated water samples. First, unlike many determinations with incubated water samples, natural fluorescence is measured *in situ* without significant perturbation to the sample. Samples incubated under simulated *in*

*situ* conditions are likely to experience changes in temperature and in light intensity and spectral composition, and temperature. Second, the effects of natural motion of the crop may introduce a large error in the estimate of photosynthetic rate from incubated samples. For example, both vertical and horizontal motion of water may complicate the interpretation of photosynthetic rates measured in incubated samples. The complications include variability caused by a patchy distribution of the crop as well as variability in light as water parcels are transported to different depths. A similar problem arises when one attempts to measure the photosynthetic rate of a species, such as dinoflagellates, that migrate vertically during the course of an incubation. Third, contamination of a water sample during sampling and incubation, of course, is not a concern when measuring natural fluorescence. Fourth, the limited number of measurements of photosynthetic rates that can be made with incubated samples can reduce the precision of the calculation of total production within the water column, particularly where the vertical distribution of the crop is highly variable.

Because of the simplicity and rapidity of the measurement, the natural fluorometer may prove useful to oceanographic surveys. The natural fluorometer can be deployed with a CTD, providing data on the vertical distributions of the concentration of chlorophyll and of the rate of photosynthesis over a large area. Such an application is particularly useful if one wishes to map regions where the current field is complex and the distribution of phytoplankton variable. Production in and around oceanographic fronts can likely be more accurately described in terms of natural fluorescence than incubation

techniques. In addition, the instrument may prove helpful when conditions at sea are severe, making traditional measurements of primary production difficult. Because of its size and low requirements for power, the natural fluorometer can also be deployed on moorings. The measurements of scalar PAR and natural fluorescence can, in theory, provide instantaneous information at specific depths over seasonal and annual periods.

## References

- Bidigare, R.R., R.C. Smith, K.S. Baker, and J. Marra. 1987. Oceanic primary production estimates from measurements of spectral irradiance and pigment concentration. *Global Biogeochemical Cycles* 1: 171-186.
- Bricaud, A., Bedhomme, A-L., and A. Morel. 1988. Optical properties of diverse phytoplanktonic species: experimental results and theoretical interpretation. *J. Plank. Res.* 10: 851-873.
- Chamberlin, W.S. 1989. Light absorption, natural fluorescence and photosynthesis in the open ocean. Ph.D. dissertation. Univ. Southern California, Los Angeles, CA.
- Cleveland, J.S., and M.J. Perry. 1987. Quantum yield, relative specific absorption and fluorescence in nitrogen-limited Chaetoceros gracilis. *Marine Biology* 94: 489-497.
- Collins, D.J., D.A. Kiefer, J.B. SooHoo, and I.S. McDermid. 1985. The role of reabsorption in the spectral distribution of phytoplankton fluorescence emission. *Deep-Sea Research* 32: 983-1003.

- Dirks, R.W.J. and D. Spitzer. 1987. On the radiative transfer in the sea, including fluorescence and stratification effects. *Limnol. Oceanogr.* 32: 942-953.
- Falkowski, P. and D.A. Kiefer. 1985. Chlorophyll *a* fluorescence in phytoplankton: relationship to photosynthesis and biomass. *J. Plank. Res.* 7: 715-731.
- Falkowski, P.G., K. Wyman, A.C. Ley, and D.C. Mauzerall. 1986. Relationship of steady-state photosynthesis to fluorescence in eucaryotic algae. *Biochimica et Biophysica Acta* 849: 183-192.
- Forster, L.S. and R. Livingston. 1952. The absolute quantum yields of the fluorescence of chlorophyll solutions. *J. Chem. Phys.* 20: 1315-1320.
- Gordon, H. 1979. Diffuse reflectance of the ocean: the theory of its augmentation by chlorophyll *a* fluorescence at 685 nm. *Appl. Opt.* 18: 1161-1166.
- Gower, J.F.R. and G. Borstad. 1981. Use of the in vivo fluorescence line at 685 nm for remote sensing surveys of surface chlorophyll *a*. In: Oceanography from Space, J.F.R. Gower, ed., Plenum Press, New York and London. pp. 329-338.

- Holm-Hansen, O., C.J. Lorenzen, R.W. Holmes, and J.D.H. Strickland. 1965. Fluorometric determination of chlorophyll. *J. Cons. Int. Explor. Mer* 30: 3-15.
- Jerlov, N.G. 1976. *Marine Optics*. 2nd ed., Elsevier Scientific Publ. Co., 259 pp.
- Kattawar, G.W. and J.C. Vastano. 1982. Exact 1-D solution to the problem of chlorophyll fluorescence from the ocean. *Applied Optics* 21: 2489-2492.
- Kiefer, D.A. 1973a. Fluorescence properties of natural phytoplankton populations. *Marine Biology* 22: 263-269.
- Kiefer, D.A. 1973b. Chlorophyll *a* fluorescence in marine centric diatoms: responses of chloroplasts to light and nutrients. *Marine Biology* 23: 39-45.
- Kiefer, D.A. and B.G. Mitchell. 1983. A simple, steady state description of phytoplankton growth based on absorption cross section and quantum efficiency. *Limnol. Oceanogr.* 28:770-776.
- Kishino, M., S. Sugihara, and N. Okami. 1984a. Influence of fluorescence of chlorophyll *a* on underwater upward irradiance spectrum. *La mer* 22: 224-232.

- Kishino, M., S. Sugihara, and N. Okami. 1984b. Estimation of quantum yield of chlorophyll *a* fluorescence from the upward irradiance spectrum in the sea. *La mer* 22: 233-240.
- Lorenzen, C.J. 1966. A method for the continuous measurement of in vivo chlorophyll concentration. *Deep-Sea Res.* 13: 223-227.
- Marra, J., K. Heinemann, and G. Landriau, Jr. 1985. Observed and predicted measurements of photosynthesis in a phytoplankton culture exposed to natural irradiance. *Mar. Eco. Prog. Ser.* 24: 43-50.
- Marra, J., and K.R. Heinemann. 1987. Primary production in the North Pacific Central Gyre: new measurements based upon <sup>14</sup>C. *Deep-Sea Research* 34: 1821-1829.
- Mitchell, B.G. and D.A. Kiefer. 1988. Variability in pigment specific particulate fluorescence and absorption spectra in the north eastern Pacific Ocean. *Deep-Sea Res.* 35: 665-689.
- Morel, A., and A. Bricaud. 1981. Theoretical results concerning light absorption in a discrete medium, and application to specific absorption of phytoplankton. *Deep-Sea Res.* 28: 1375-1393.

- Morel, A. 1978. Available, usable and stored radiant energy in relation to marine photosynthesis. *Deep-Sea Res.* 25: 673-688.
- Morel, A. and L. Prieur. 1977. Analysis of variations in ocean color. *Limnol. Oceanogr.* 22: 709-722.
- Morrow, J.H. 1988. Light absorption and photoadaptation in naturally occurring marine phytoplankton communities. Ph.D. dissertation. Univ. So. Calif., Los Angeles.
- Neori, A., M. Vernet, O. Holm-Hansen, and F.T. Haxo. 1986. Relationship between action spectra for chlorophyll *a* fluorescence and photosynthetic O<sub>2</sub> evolution in algae. *J. Plank. Res.* 8: 537-548.
- Neville, R.A. and J.F.R. Gower. 1977. Passive remote sensing of phytoplankton via chlorophyll *a* fluorescence. *J. Geophys. Res.* 82: 3487-3493.
- Preisendorfer, R.W. 1976. *Hydrologic Optics*. U.S. Department of Commerce, NOAA, ERL.
- Preisendorfer, R.W., and C.D. Mobley. 1988. Theory of fluorescent irradiance fields in natural waters. *J. Geophysical Res.* 93: 10,831-10,855.

- Ryther, J.H. and C.S. Yentsch. 1957. The estimation of phytoplankton production in the ocean from chlorophyll and light data. *Limnol. Oceanogr.* 2: 281-286.
- Slawyk, G., Y. Collos and J-C. Auclair. 1977. The use of  $^{13}\text{C}$  and  $^{15}\text{N}$  isotopes for the simultaneous measurement of carbon and nitrogen turnover rates in marine phytoplankton. *Limnol. Oceanogr.* 22: 925-932.
- Smith R.C. and K.S. Baker. 1978. Optical classification of natural waters. *Limnol. Oceanogr.* 23: 260-267.
- Smith, R.C. and K.S. Baker. 1981. Optical properties of the clearest natural waters (200-800 nm). *Applied Optics* 20: 177-193.
- Smith, R.C., C.R. Booth, and J. Starr. 1984. An oceanographic bio-optical profiling system. *Appl. Optics.* 23: 2791-2797.
- Topliss, B.J. 1985. Optical measurements in the Sargasso Sea: solar stimulated chlorophyll fluorescence. *Oceanol. Acta* 8: 263-270.
- Topliss, B.J. and T. Platt. 1986. Passive fluorescence and photosynthesis in the ocean: implications for remote sensing. *Deep-Sea Res.* 33: 849-864.

Tyler, J.E. 1975. The in situ quantum efficiency of natural  
phytoplankton populations. *Limnol. Oceanogr.* 20: 976-  
980.

## Figure Legends:

Fig. 1. Plot of values for the ratio of natural fluorescence,  $F_f$ , to nadir radiance at 683 nm,  $Lu_{683}$ , calculated as a function of the concentration of chlorophyll  $a$ . The figure also shows values for the absorption coefficient at 683 nm and the diffuse attenuation coefficient for photosynthetically available radiation. Values were calculated from Eqs. 8, 10, and 11.

Fig. 2. A.  $Lu_{683}$ , PAR, and temperature versus depth for an oligotrophic station in the central gyre of the South Pacific Ocean ( $23^{\circ}53'S, 161^{\circ}37'W$ ). B.  $Lu_{683}$ , PAR, and temperature versus depth for a mesotrophic station near New Zealand ( $36^{\circ}16'S, 176^{\circ}26'E$ ).

Fig. 3. A. Reflectance ratio at 683 and 488 nm for the oligotrophic station. B. Reflectance ratio at 683 and 488 nm at the mesotrophic station. Note the contribution by natural fluorescence at both stations.

Fig. 4. A.  $Lu_{683}/PAR$  and chlorophyll concentration versus depth for the station 1201-M1. B.  $Lu_{683}/PAR$  and chlorophyll concentration for station 1209-M5.

Fig. 5. Diurnal distribution of  $Lu_{683}$  and PAR at 10 and 50 m for the mesotrophic station, 1209-M5. Avg. chl(10m)=0.344, St. dev.=0.038 (n=4); Avg. chl(50m)=0.51, St. dev.=0.067 (n=4)

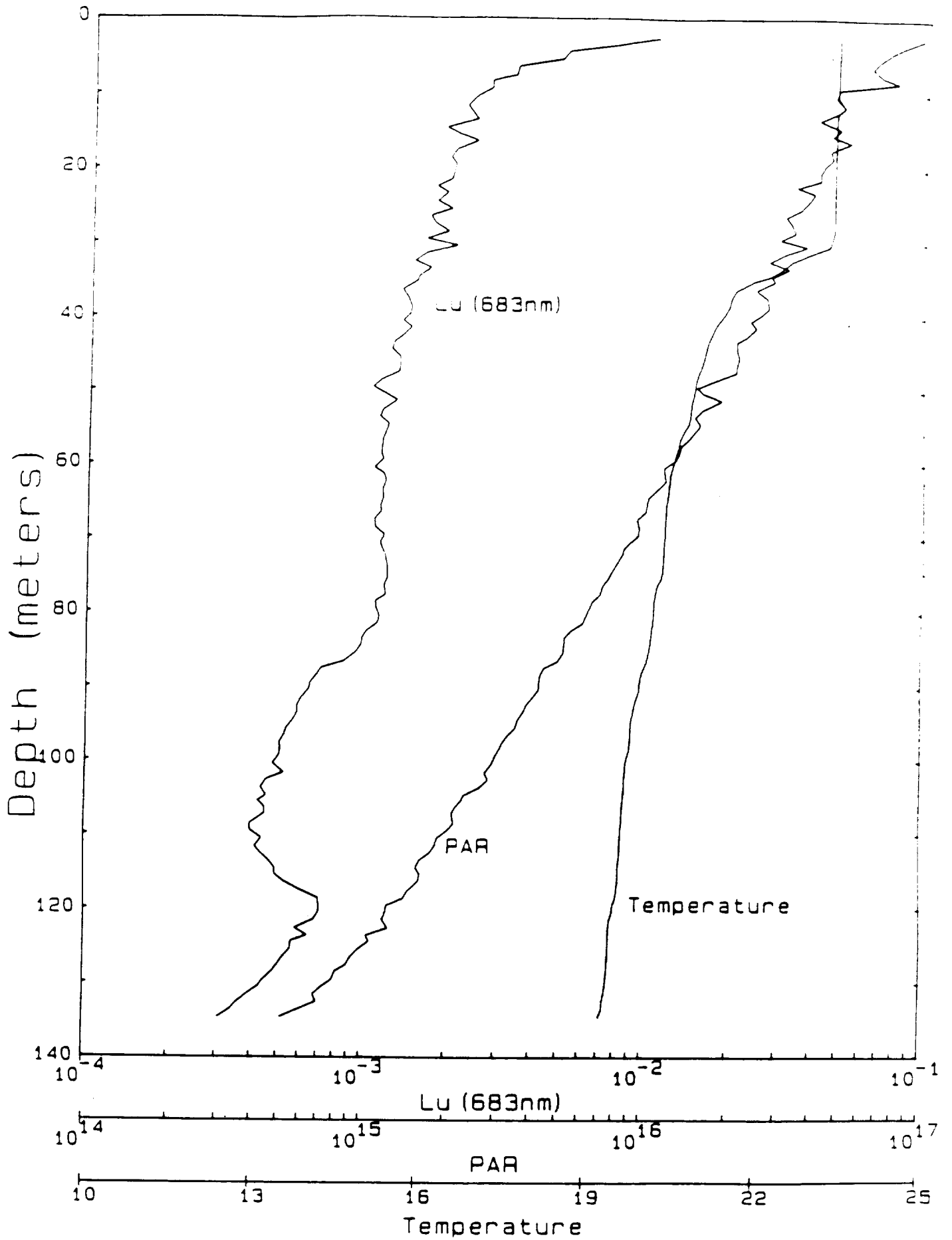
Fig. 6. Quantum yield of natural fluorescence ( $\Phi_f$ ) as a function of the scalar irradiance of PAR for all stations. The values were calculated by introducing values for  $E_o(\text{PAR})$  and  $F_f$  into Eq. 2b.

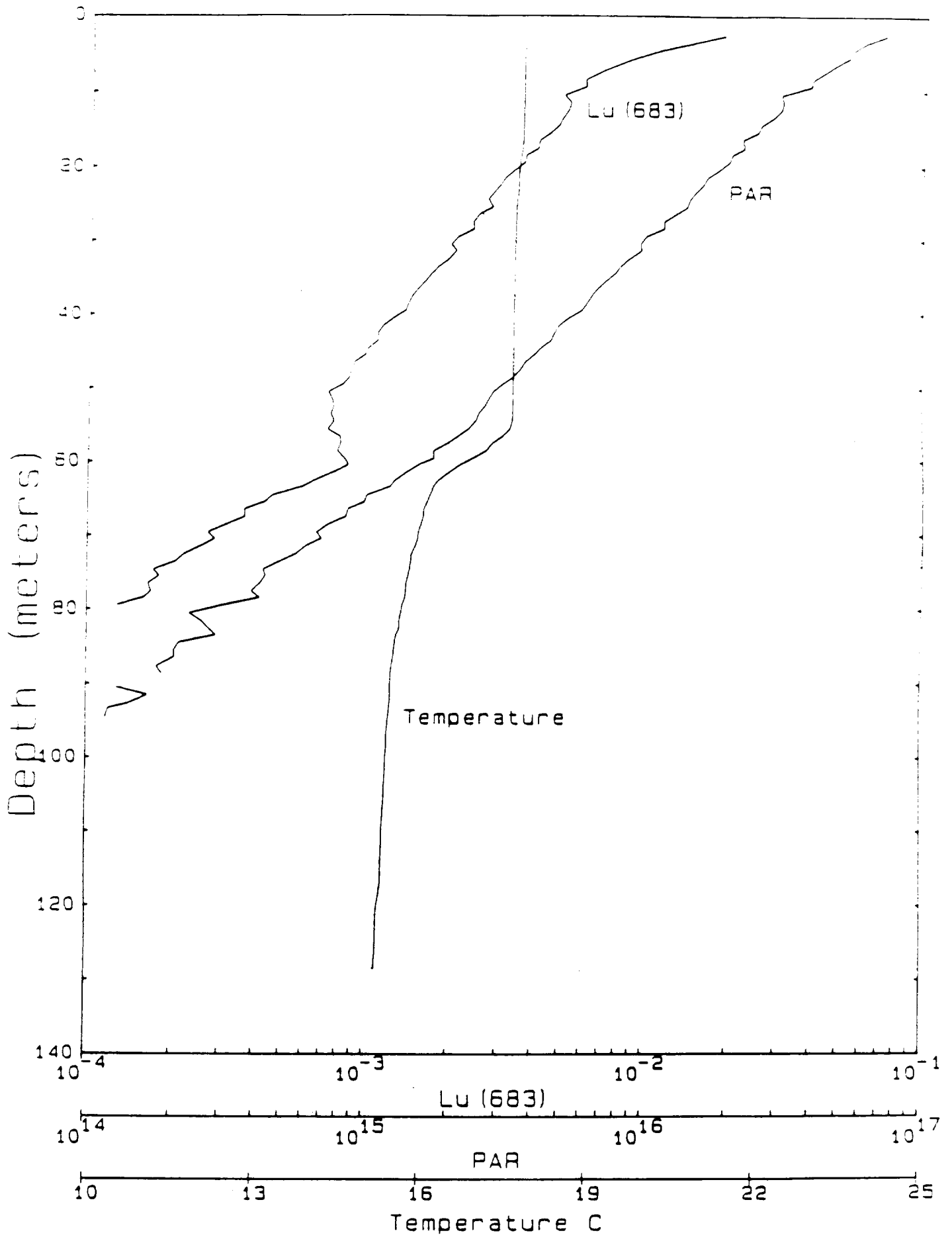
Fig. 7. Plot of the natural fluorescence coefficient ( $\Psi_f$ ) versus chlorophyll a for all stations ( $n=82$ ;  $y=0.02 + 2100x$ ;  $r^2= 0.90$ ).

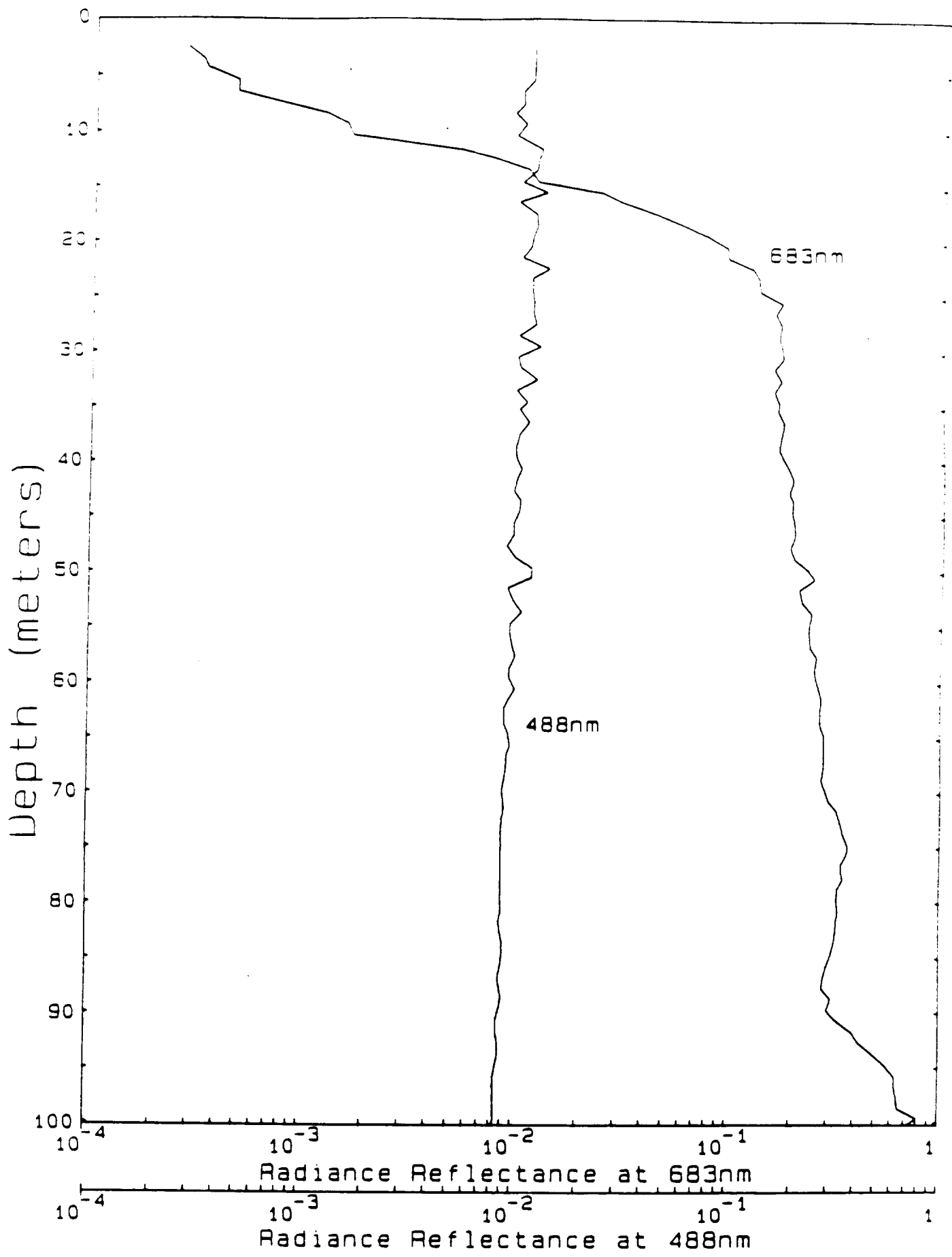
Fig. 8. Plot of natural fluorescence,  $F_f$ , versus calculated production ( $n=82$ ;  $y=0.007 + 2.0x$ ;  $r^2= 0.84$ ). Productivity was calculated by introducing measured values of  $E_o(\text{PAR})$  and chlorophyll a into the Kiefer-Mitchell model of phytoplankton growth.

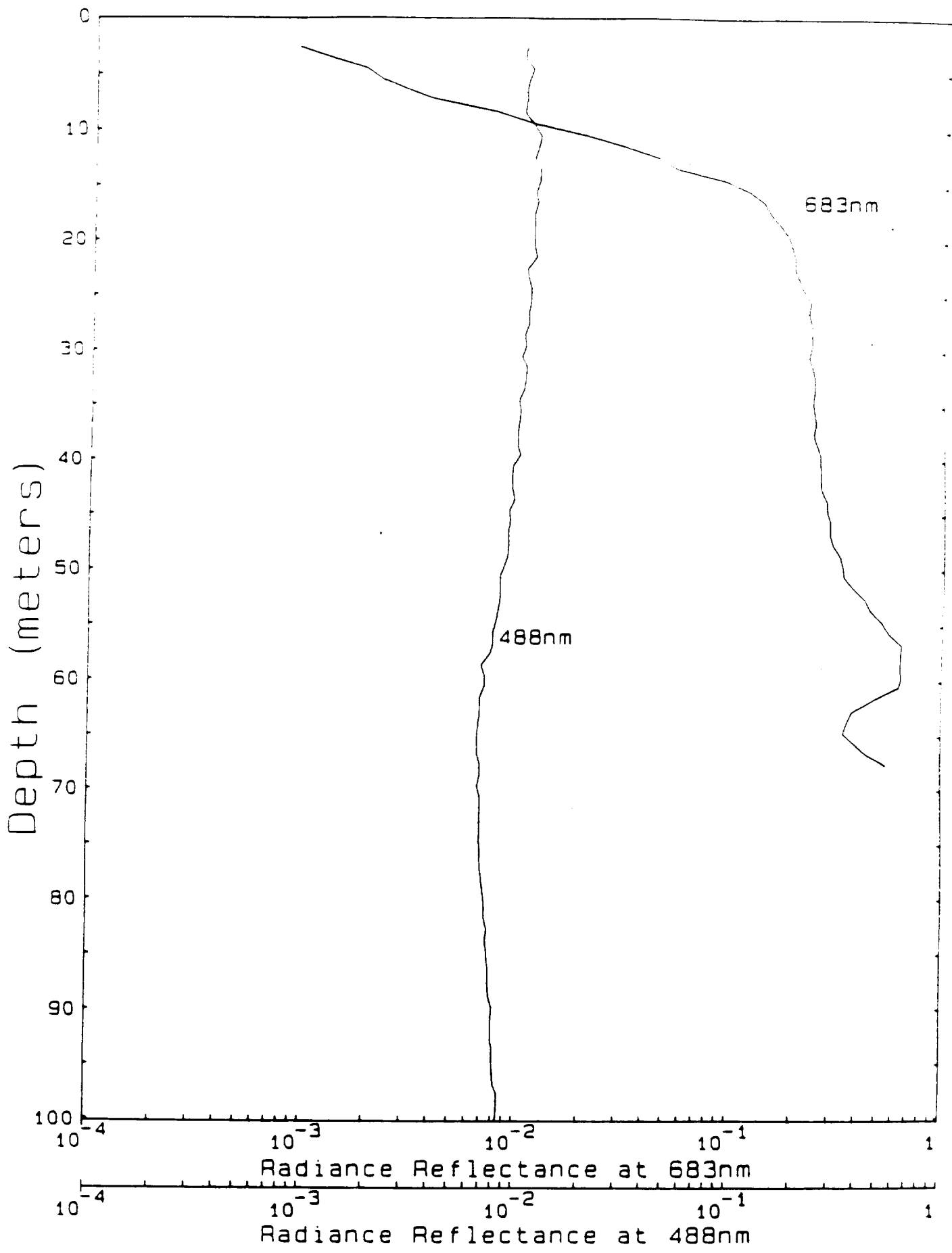
Table 1: Calypso '86 Station Summary

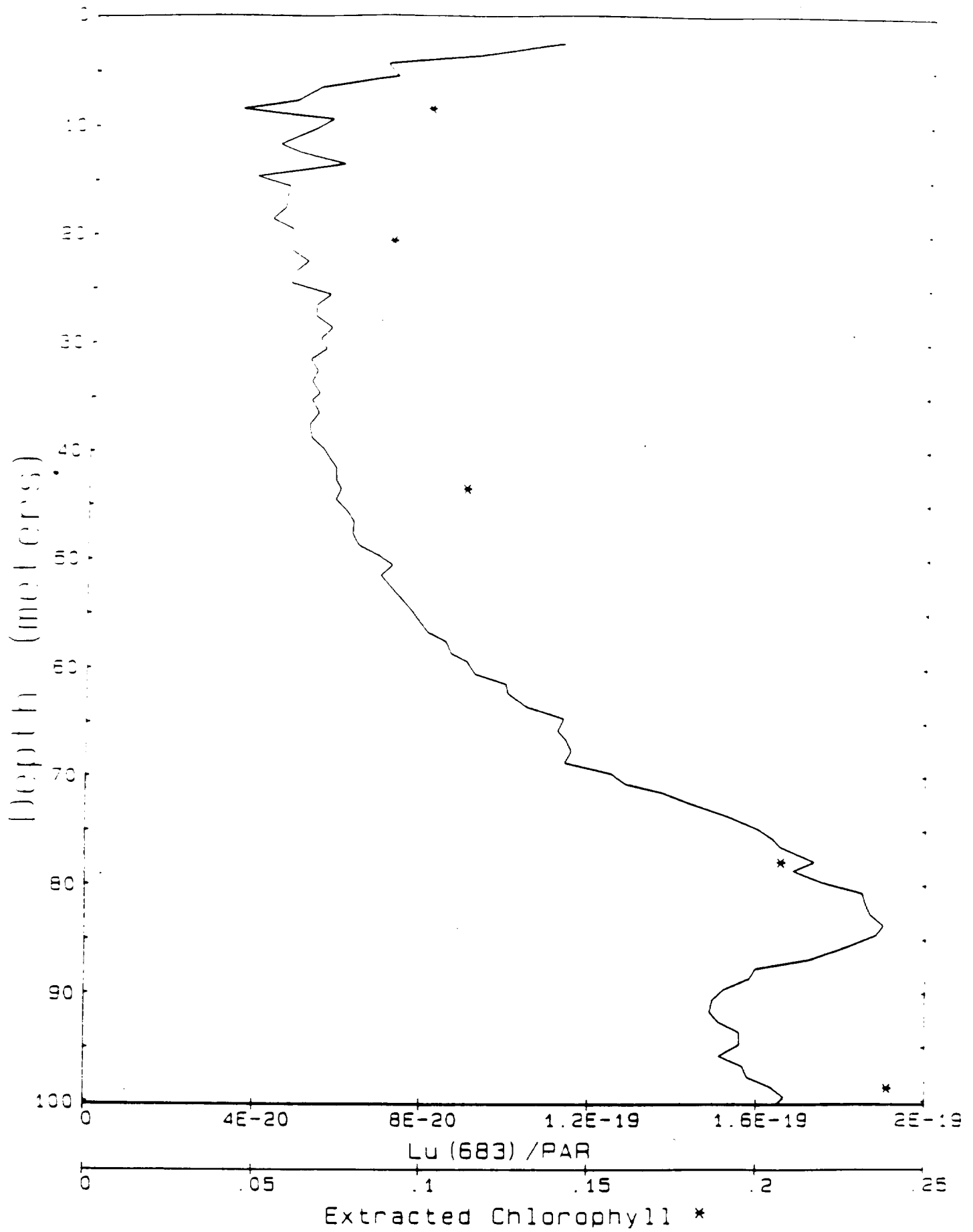
Station no.	Date	Time (GMT)	Position	Surface temp. °C	Mixed layer (m)	Integrated chl (mg m <sup>-2</sup> )
1130-M1	30 Nov.	2113	21:44.52S, 157:55.19W	21.19	46	8.53
1201-M1	01 Dec.	2013	23:52.55S, 161:37.37W	23.38	37	13.60
1201-M2	01 Dec.	0022	24:25.68S, 161:58.08W	23.49	30	8.42
1202-M3	02 Dec.	1914	25:37.46S, 164:37.46W	22.38	50	7.27
1202-M4	02 Dec.	0051	25:32.75S, 164:30.28W	22.42	30	8.81
1204-M1	04 Dec.	1911	28:38.74S, 170:31.71W	21.19	26	29.95
1204-M2	04 Dec.	0005	29:08.32S, 171:08.64W	20.85	45	32.09
1205-M1	05 Dec.	1935	31:15.40S, 173:45.87W	18.30	30	26.80
1207-M1	07 Dec.	0111	35:01.79S, 178:47.98 E	17.31	52	48.87
1209-M1	09 Dec.	1735	36:15.89S, 176:26.09 E	17.77	50	41.99
1209-M5	09 Dec.	2015	36:15.89S, 176:26.09 E	17.80	55	35.77
1209-M10	09 Dec.	0009	36:21.73S, 176:16.13 E	17.89	60	39.39
1209-M12	09 Dec.	0329	36:21.73S, 176:16.13 E	17.92	57	32.37
1209-M14	09 Dec.	0550	36:22.66S, 176:15.24 E	17.97	50	33.05

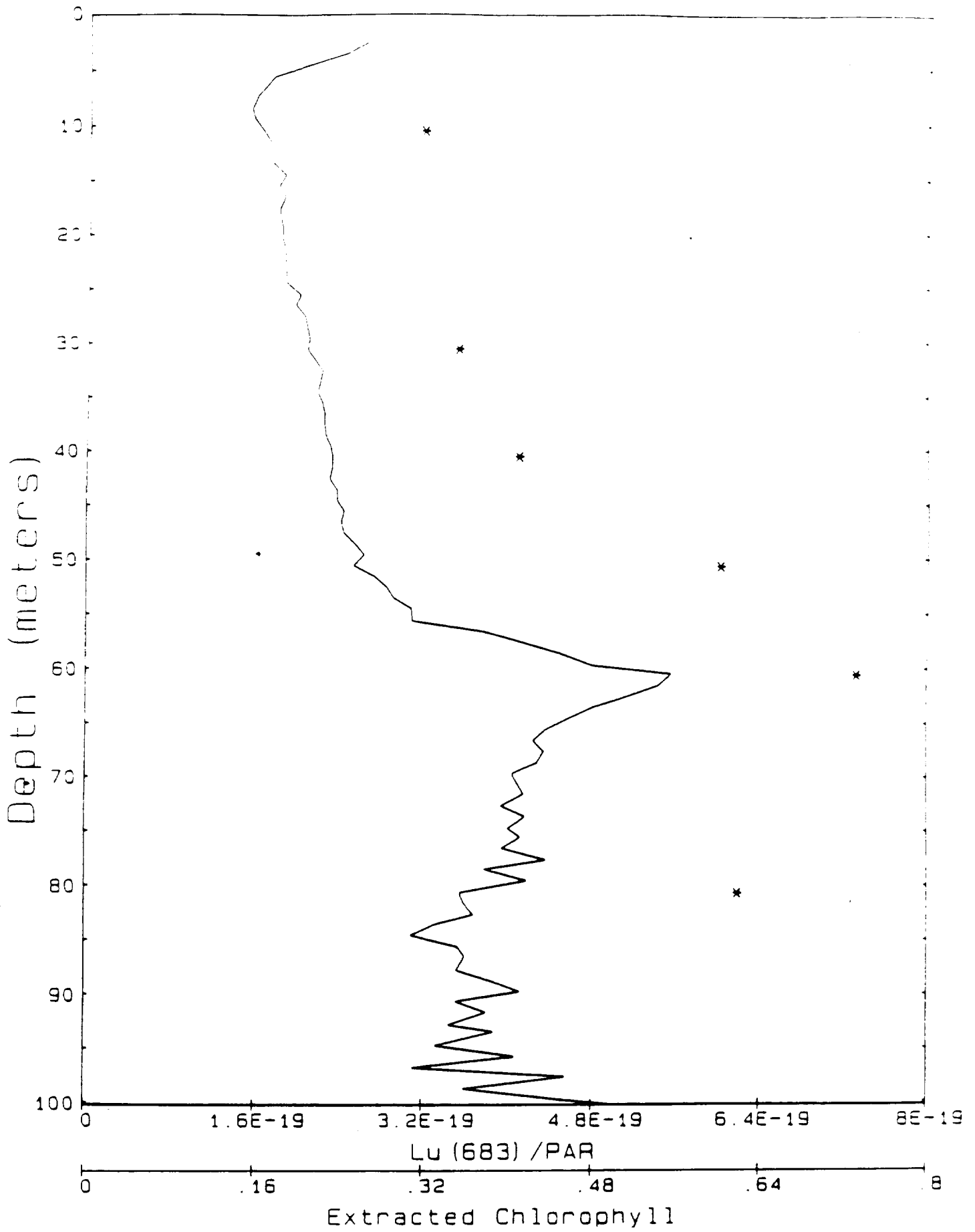


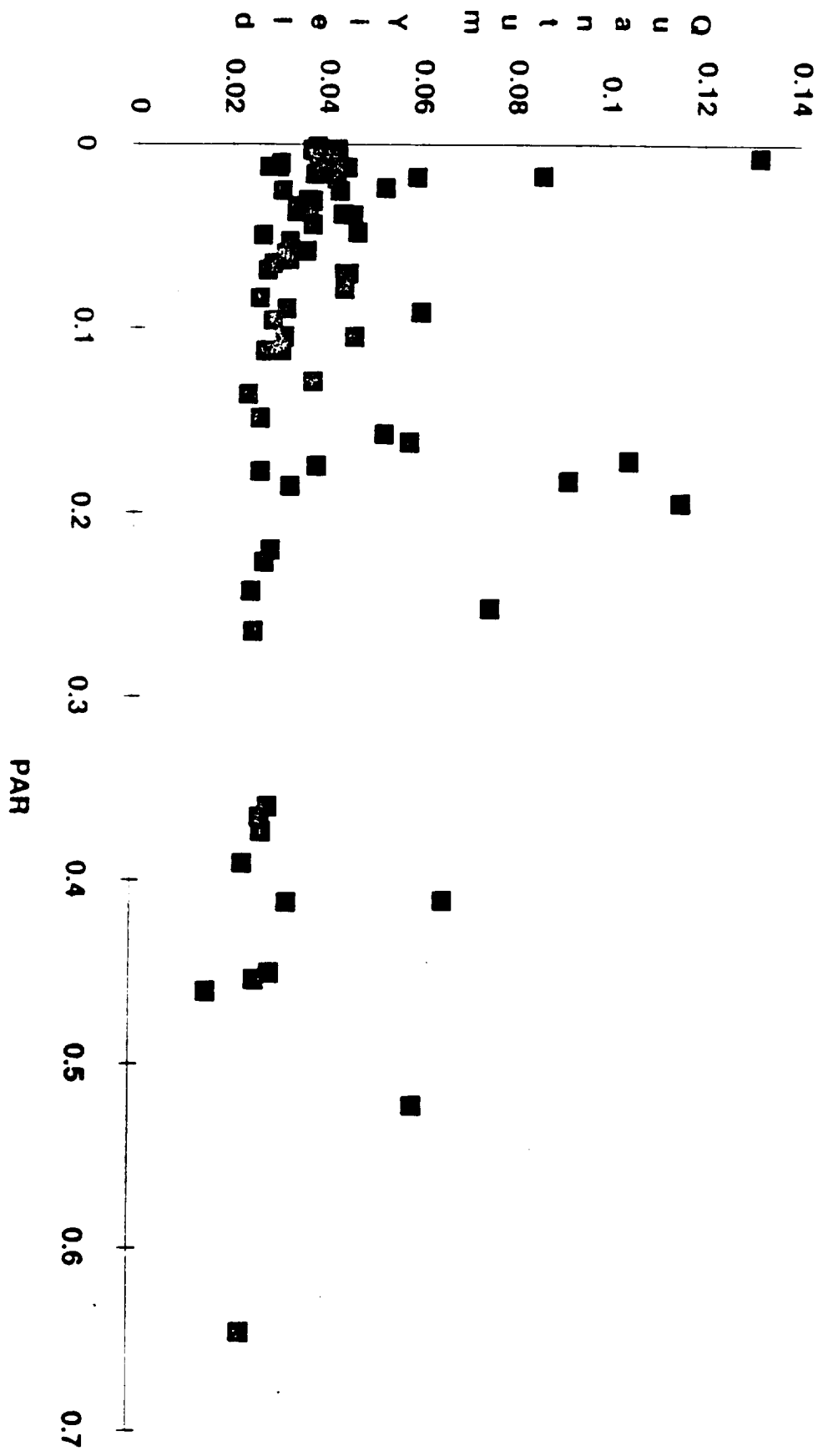


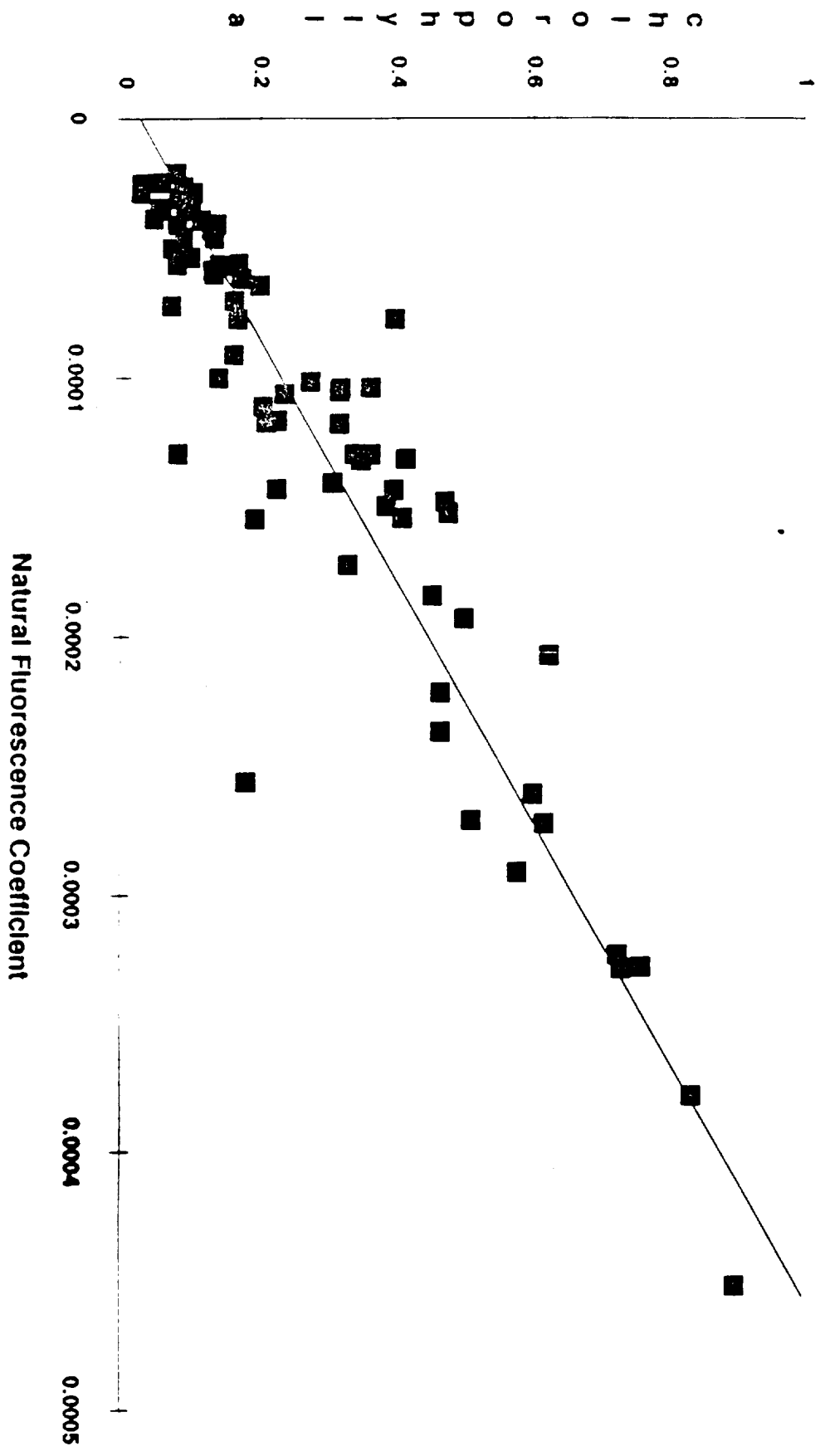


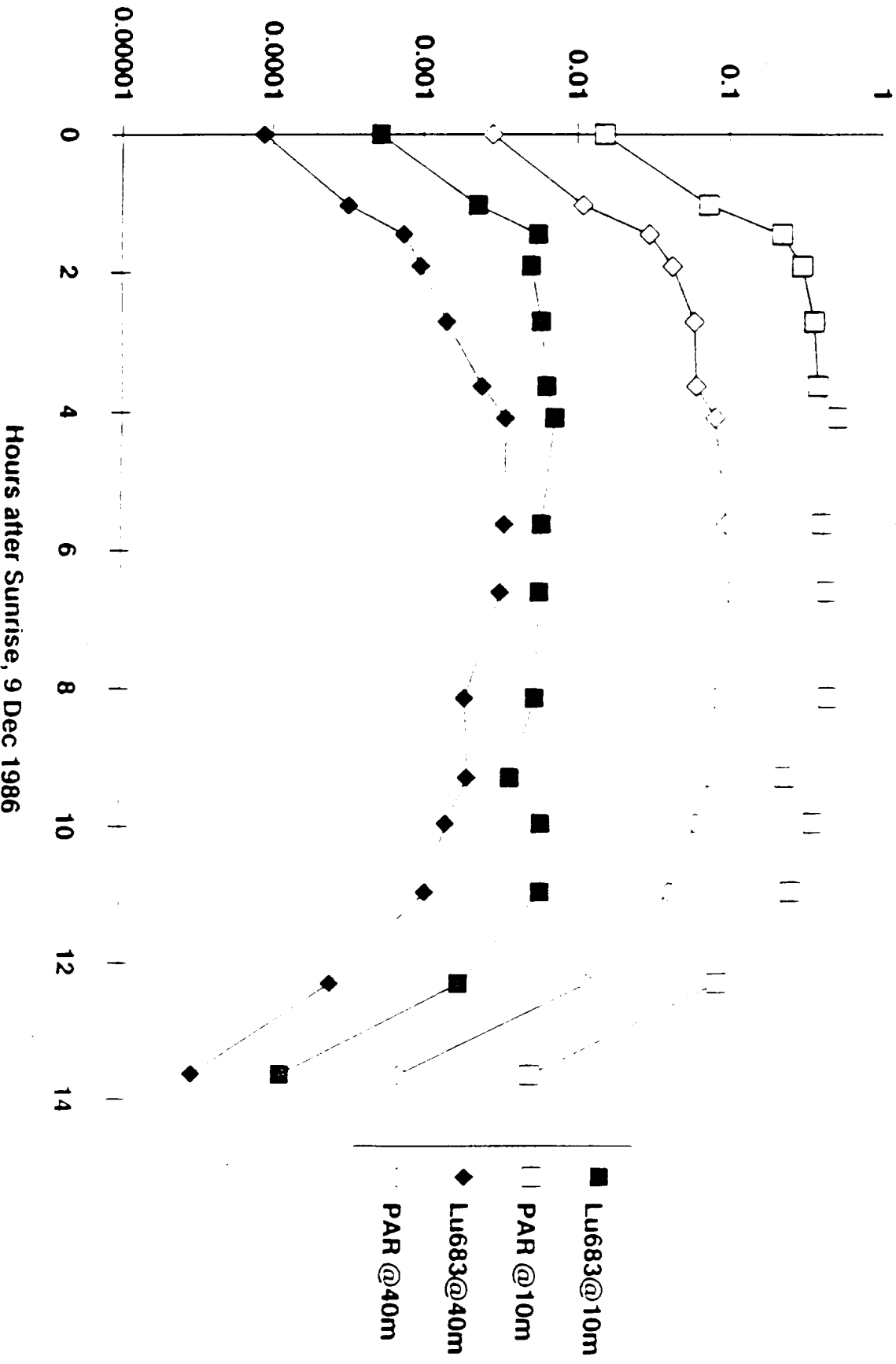


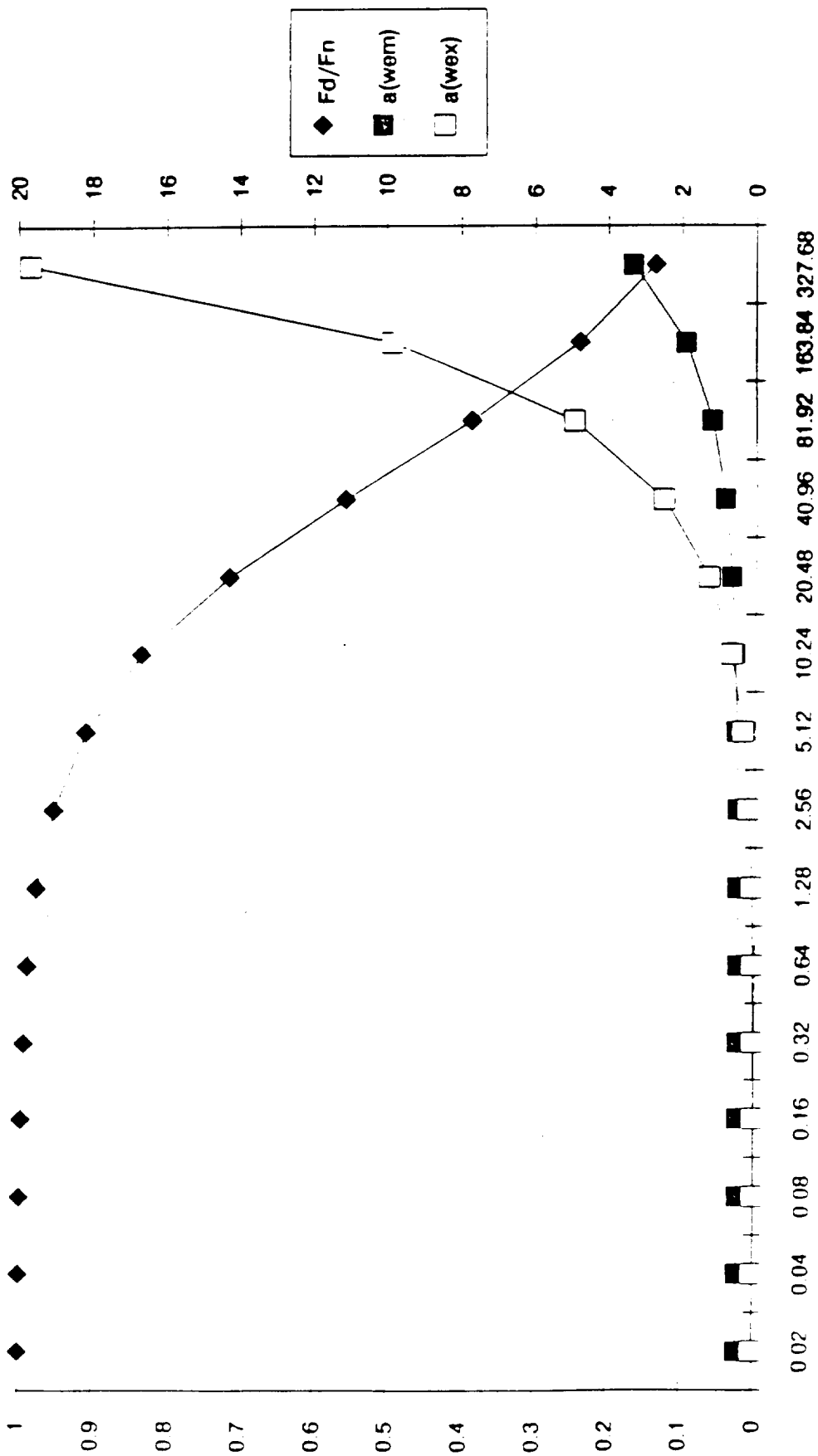




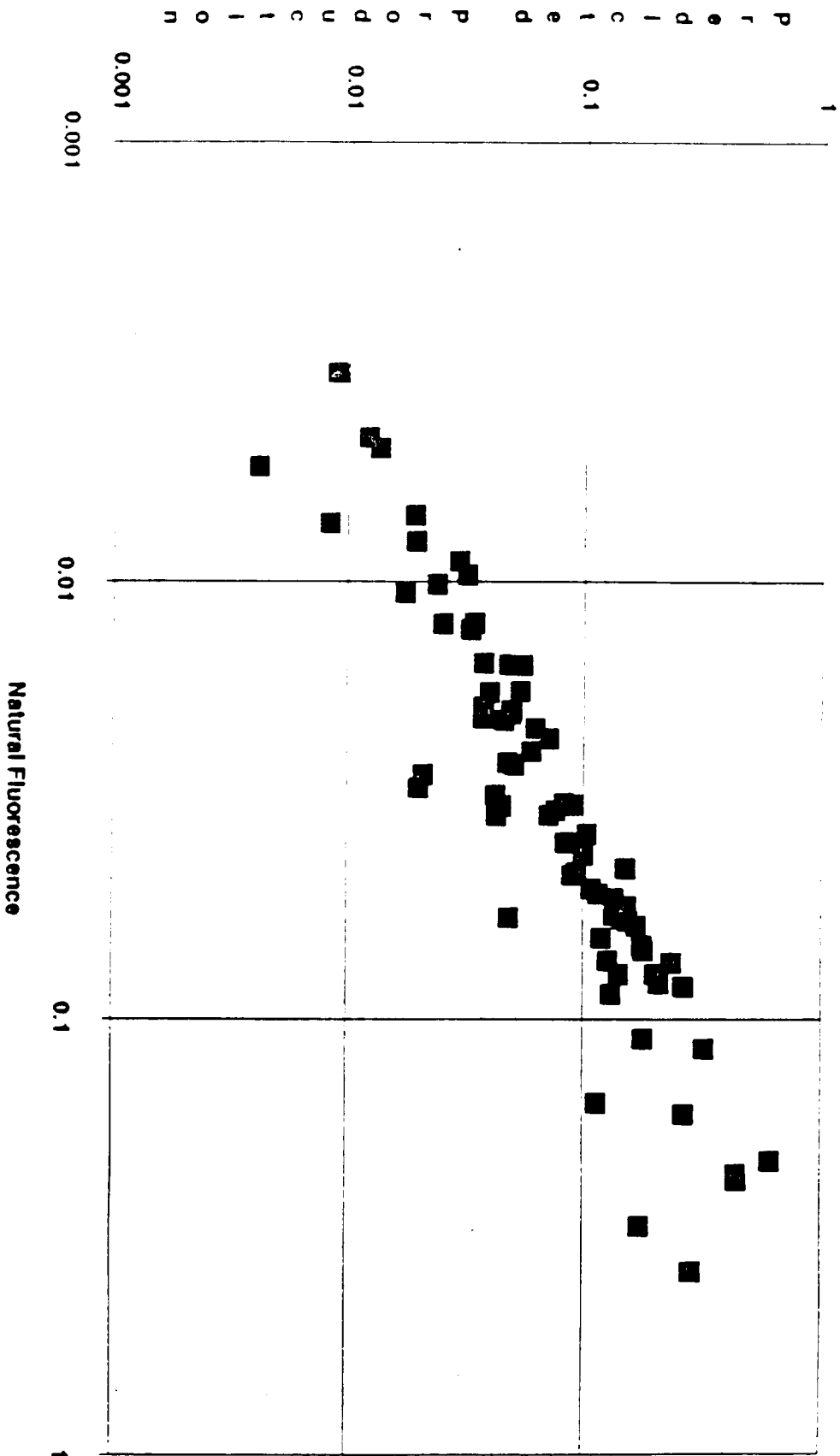




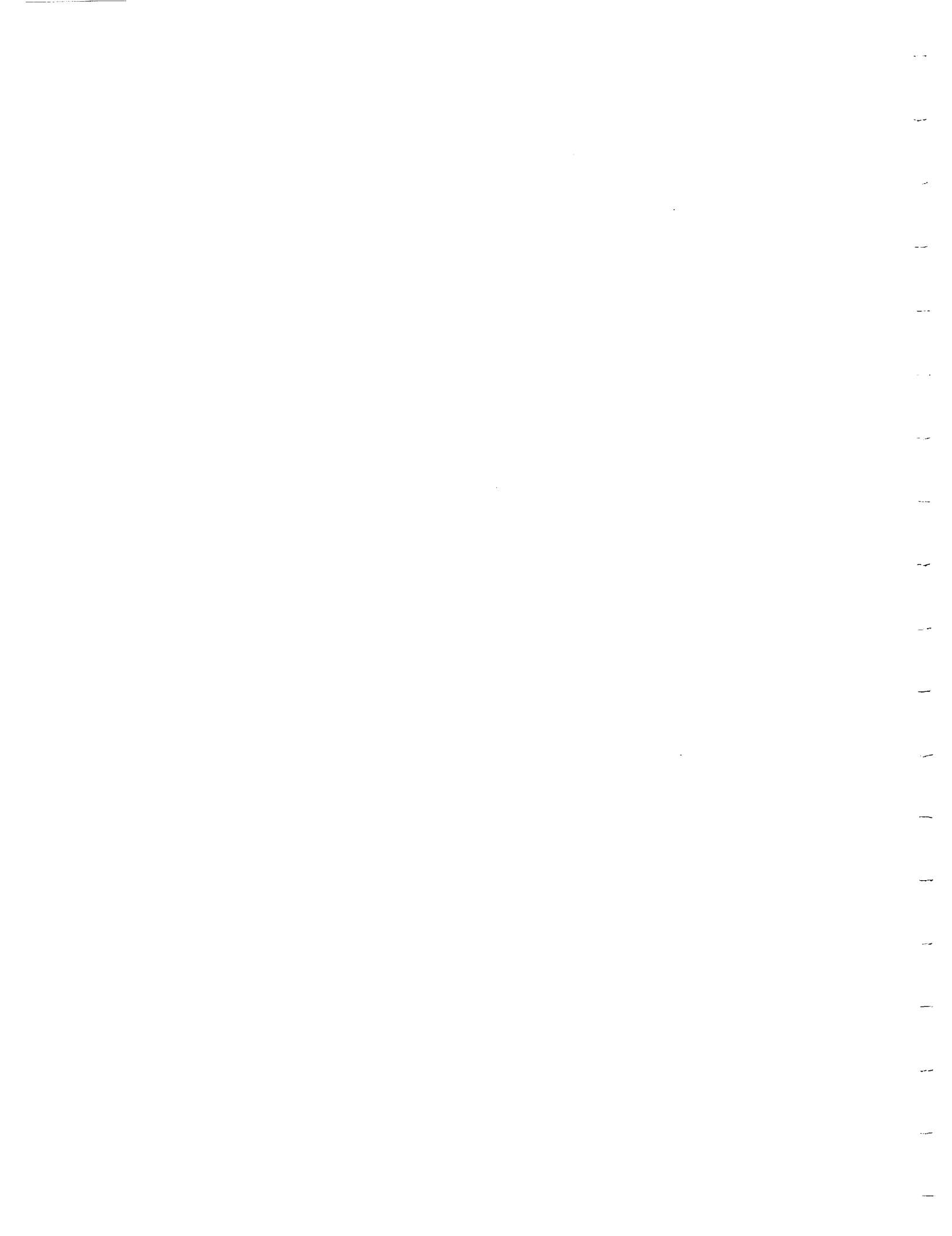




PRECEDING PAGE BLANK NOT FILMED



~~PRECEDING PAGE BLANK NOT FILMED~~



**Appendix 13**

Submitted manuscript: Evidence for a simple relationship between Natural Fluorescence, Photosynthesis, and Chlorophyll in the Sea". Submitted to Deep Sea Research, July 1989.

---

# Appendix D: Research Paper on Natural Fluorescence and Photosynthesis

Contained herein is the research paper: "Evidence for a Simple Relationship between Natural Fluorescence and Photosynthesis in the Sea." Chamberlin, W.S., C.R. Booth, D.A. Kiefer, J.H. Morrow, and R.C. Murphy. 1989. Submitted to Deep-Sea Research.

A layman's overview is presented in Chapter 4.

**Evidence for a Simple Relationship between Natural Fluorescence, Photosynthesis, and Chlorophyll  
in the Sea**

by

W. S. Chamberlin, C. R. Booth\*, D. A. Kiefer, J. H. Morrow, and R. C. Murphy

Submitted to:

John. D. McMilliman, Editor, Deep-Sea Research  
Dept. Geology and Geophysics  
Woods Hole Oceanographic Institute  
Woods Hole, MA 02543  
July 25, 1989

**Running Head: Natural fluorescence and photosynthesis**

\*To whom reprint requests should be sent.

1. Lamont-Doherty Geological Observatory of Columbia University, Palisades, NY 10964
2. Biospherical Instruments, Inc., 4901 Morena Blvd. #1003, San Diego, CA 92117
3. The Cousteau Society, 8440 Santa Monica Blvd., Los Angeles, CA 90069-4221
4. Department of Biological Sciences, University of Southern California, Los Angeles, CA 90089-0371

## Natural fluorescence and photosynthesis

### **Abstract**

We have recently proposed that the natural or solar induced fluorescence of chlorophyll a in the sea provides a purely optical measure of chlorophyll and the rate of photosynthesis in the sea. To test this proposal, we performed field studies of the relationship between natural fluorescence and photosynthesis in several environments including the central South Pacific, the western Sargasso Sea, and two sheltered bays. The results of 76 such measurements between 2 and 150 meters depth and covering a 1500 fold range in production indicate that photosynthesis is highly correlated ( $r > .9$ ) with natural fluorescence. Further, a substantial portion of the remaining variability can be explained by an examination of the relationships of the quantum yields of photosynthesis and fluorescence as a function of light level. Specifically, the quantum yield of photosynthesis decreases more rapidly with increasing irradiance than does the quantum yield of natural fluorescence. This paper develops these relationships and presents a formulation to predict rates of primary production from measures of natural fluorescence and PAR. These predictions fall within  $\pm 30\%$  for half of the samples, and within  $\pm 75\%$  for 90% of the cases (assuming that the carbon fixation measurements were without error). The prediction of chlorophyll from natural fluorescence and PAR exhibited similar correlations. This suggests that natural fluorescence measurements, either as a supplement to direct measurements or as independent optical measurements, provide a new and rapid means of estimating gross photosynthesis in the sea.

### **Introduction**

Natural fluorescence in the sea, which is the solar-stimulated emission of chlorophyll a in a narrow band centered at 683 nm, results from the absorption of light by the phytoplankton crop. Because red light is strongly absorbed by water, solar radiation at the wavelengths of chlorophyll a emission disappears within the upper few meters of the water column, and the remaining upwelling radiance in the red comes almost entirely from the phytoplankton crop. A number of studies indicate that this fluorescence signal is sufficiently strong to be detected through the euphotic zone. Since it was first identified as originating from the crop of phytoplankton (Morel and Prieur, 1977; Neville and Gower, 1977), natural fluorescence has been widely investigated as a means for rapidly assessing the distribution and biomass of oceanic phytoplankton. Numerous mathematical descriptions have been presented of the relationship between natural fluorescence, the concentration of chlorophyll a, and the ambient light which excites the fluorescence (Gordon, 1979; Kattawar and Vastano, 1979; Kishino et al., 1984 a,b; Topliss and Platt, 1986). Recently, it has also been proposed that rates of primary production may be estimated from measurements of natural fluorescence (Kiefer et al., 1989; Chamberlin, 1989).

Because measurements of natural fluorescence are rapid, and can be performed without perturbation of the phytoplankton crop, estimates of photosynthetic rate from natural fluorescence has certain advantages over in vitro measurements of photosynthesis. Since the measurement is instantaneous and can be performed without the necessity of incubating a water sample, natural fluorescence might prove useful in mapping photosynthetic rates during hydrocasts or in continuous monitoring from moorings and drifters. The rapidity and detailed temporal and spatial resolution of the fluorescence measurement makes it extremely useful in regions where hydrographic conditions are complex. Given the limited spatial and temporal coverage and the potential uncertainties of fixed-depth, long-term incubations of water samples (e.g. Williams et al., 1983; Marra, et al., 1988; ; Fahnenstiel et al. 1988; Falkowski, 1988), natural fluorescence may provide a suitable supplemental or alternative measurement of photosynthesis. We have examined the relationship between natural

## Natural fluorescence and photosynthesis

fluorescence and photosynthesis with the specific aim of evaluating its usefulness as a measure of primary production.

In a previous publication (Kiefer, et al., 1989), we demonstrated the feasibility of measuring natural fluorescence within the euphotic zone of the extremely clear waters of the southeastern Pacific and developed the theoretical framework for examining natural fluorescence and photosynthesis. In this paper, we present direct evidence that a strong correlation exists between natural fluorescence and primary production. This evidence is based on simultaneous measurements of natural fluorescence and carbon 14-labeled, inorganic carbon assimilation at stations off Tahiti and Moorea in the South Pacific Ocean, at the Biowatt II station in the northwestern Sargasso Sea, and in two protected bays: Cooks Bay, Moorea, and Friday Harbor, Washington. These studies consisted of both short and long term measurements of photosynthesis as well as both instantaneous and integrated measurements of natural fluorescence.

In the work described below, we attempted to answer several questions: What is the relationship between natural fluorescence and photosynthetic rate in natural phytoplankton populations? Does this relationship vary as a function of irradiance? How precisely can photosynthetic rate be estimated from natural fluorescence? What are the potential sources of error in making such an estimate?

### **Background:**

The formulations derived by Kiefer et al. (1989) provide the basis for the comparison of instantaneous rates of natural fluorescence and carbon assimilation. Natural fluorescence ( $F_f(t, z)$ ) of chlorophyll a at a given depth ( $z$ ) in the water column at time  $t$  is defined as the flux of light emitted by the chlorophyll a in a suspension of phytoplankton of unit volume (units Einsteins  $m^{-3} sec^{-1}$ ).

The relationship between natural fluorescence and photosynthesis will depend upon the probabilities that the light absorbed by a cell will be immediately transformed into either heat, fluorescence, or photochemical work. This simple relationship may be expressed phenomenologically:

$$F_f(t, z) = O_f(t, z) * F_a(t, z) \quad (1)$$

$$F_c(t, z) = O_c(t, z) * F_a(t, z) \quad (2)$$

$$F_c(t, z) = O_c(t, z) / O_f(t, z) * F_f(t, z) \quad (3)$$

where  $F_c(t, z)$ ,  $F_a(t, z)$ ,  $O_c(t, z)$ , and  $O_f(t, z)$  are, respectively, the rate of photosynthesis ( $g-at C m^{-3} sec^{-1}$ ), the rate of light absorption ( $Ein m^{-3} sec^{-1}$ ), the quantum yield of photosynthesis ( $g-at C fixed/Ein absorbed$ ), and the quantum yield of fluorescence ( $Ein emitted/Ein absorbed$ ). Since the instantaneous rate of light absorption,  $F_a$ , appears in both equations 1 and 2, its variability will cause proportional changes in both natural fluorescence and photosynthesis.

Estimates of the flux of light absorbed by the crop can be made by the approximation:

$$F_a = ac(PAR, t, z) * E_o(PAR, t, z) \quad (4)$$

## Natural fluorescence and photosynthesis

$ac(\text{PAR}, t, z)$  ( $\text{m}^{-1}$ ) is the mean value of the cellular absorption coefficient in the visible spectrum, and  $E_o(\text{PAR}, t, z)$  ( $\text{Ein m}^{-2} \text{sec}^{-1}$ ) is the integrated value of the flux of quanta over this spectrum (Morel, 1978).

By substitution, the flux of natural fluorescence can be described by:

$$F_f(t, z) = O_f(t, z) * ac(\text{PAR}, t, z) * E_o(\text{PAR}, t, z) \quad (5)$$

It is useful to define the product  $O_f(t, z) * ac(\text{PAR})$  found in equation 5, as the natural fluorescence coefficient,  $Y_f(t, z)$  (following Gordon, 1979). This coefficient, which has units of  $\text{m}^{-1}$ , can be applied to the calculation of both chlorophyll a concentration and daily rates of photosynthesis.  $Y_f(t, z)$  is simply calculated by dividing  $F_f(t, z)$  by  $E_o(\text{PAR}, t, z)$ . As demonstrated by Gordon (1979), Topliss (1985), and particularly Kishino and co-workers (1984a,b), the relationship between chlorophyll concentration and natural fluorescence is determined by the natural fluorescence coefficient, the quantum yield of natural fluorescence, and the mean chlorophyll a specific absorption coefficient for the phytoplankton crop:

$$\text{chl}(t, z) = Y_f(t, z) / (ac(\text{PAR}, t, z) * O_f(t, z)) \quad (6),$$

$$\text{chl}(t, z) = F_f(t, z) / (E_o(\text{PAR}, t, z) * O_f(t, z) * ac(\text{PAR}, t, z)) \quad (7).$$

Daily rates of gross photosynthesis,  $F_c(z, 24 \text{ hr})$  can be estimated at depth by calculating the product of the fluorescence coefficient,  $Y_f$ , the integrated daily flux of scalar irradiance,  $E_o(\text{PAR}, 24 \text{ hr}, z)$ , and the daily mean value for the ratio of the quantum yields,  $O_c(24 \text{ hr}, z)/O_f(24 \text{ hr}, z)$ :

$$F_c(z, 24 \text{ hr}) = O_c(24 \text{ hr}, z)/O_f(24 \text{ hr}, z) * Y_f(t, z) * E_o(\text{PAR}, 24 \text{ hr}, z) \quad (8).$$

### **Methods**

#### **Site description**

Natural fluorescence and photosynthesis were measured during two cruises in the western Sargasso Sea in March and May, 1987, at several stations in the South Pacific, in September, 1987, and at the dock of the Friday Harbor Research Laboratory (Friday Harbor, Washington) on July 27, 1987.

Measurements in the Sargasso Sea were conducted at the site of the Biowatt II mooring ( $34^\circ\text{N}:70^\circ\text{W}$ ) in conjunction with the Biowatt II program. The Calypso '87 cruise, which occurred in the waters near Papeete, Tahiti and Cook's Bay, Moorea ( $17.29^\circ\text{S}:149.49^\circ\text{W}$ ) in the South Pacific Ocean, was undertaken specifically to examine natural fluorescence and primary production.

#### **Optical measurements**

The natural fluorometer is an optical sensor measuring upwelling radiance with a known spectral responsivity,  $R(w)$  (volts Einsteins $^{-1}$  sec  $\text{m}^2$  str). The response of the sensor ( $V$ : volts) to a flux

## Natural fluorescence and photosynthesis

with the emission characteristics of chlorophyll,  $L_c(w)$  (Einsteins  $\text{sec}^{-1} \text{m}^{-2} \text{nm}^{-1} \text{str}^{-1}$ ) can be calculated in terms of a chlorophyll fluorescence signal as follows

$$L_u(\text{chl}) = \frac{V * \text{Integral } L_c(w) dw}{\text{Integral } R(w) * L_c(w) dw} \quad (9)$$

In the following discussions,  $L_u(\text{chl})$  will refer to the spectrally integrated radiance of a chlorophyll-like source in  $\text{Ein sec}^{-1} \text{m}^{-2} \text{str}^{-1}$ .

In normal use, the natural fluorescence sensor is combined with a PAR sensor (Booth, 1976), pressure and temperature sensors, and a surface irradiance sensor. In our studies this sensor package was a Profiling Natural Fluorometer (PNF-300, Biospherical Instruments Inc), or a subset of sensors within a larger system. The sensor assembly is lowered from shipboard during routine profiling of the euphotic zone.

The natural fluorescence  $F_f(t,z)$  at time  $t$  and depth  $z$  is calculated from the following relation:

$$F_f(t,z) = 4 * \pi * (k(\text{PAR},t,z) + a(\text{chl},t,z)) * L_u(\text{chl},t,z) \quad (10)$$

where  $k(\text{PAR},t,z)$  is the diffuse attenuation coefficient for scalar irradiance integrated over the spectral region of 400-700nm (Kiefer, et al, 1989).  $k(\text{PAR},t,z)$  accounts for the attenuation of exciting irradiance as a function of depth below the sensor. The term  $4 \pi$  is a geometrical constant with the units of (1/steradians) used in transforming the radiance to a volume emission. The term  $a(\text{chl},t,z)$  is the total absorption coefficient of the water plus constituents. This term accounts for the decay of the sensed signal as a function of distance from the sensor.  $a(\text{chl})$  is a composite quantity composed of the sum of the absorption coefficients weighted by the spectral distribution of the emission of chlorophyll:

$$a(\text{chl}) = a_w(\text{chl}) + a_d(\text{chl}) + a_c(\text{chl}) + a_y(\text{chl}) \quad (11)$$

where  $a_w(\text{chl})$ ,  $a_d(\text{chl})$ ,  $a_c(\text{chl})$ , and  $a_y(\text{chl})$  are the absorption coefficients for pure water, detritus, chlorophyll, and yellow substance, respectively. This weighting is calculated by

$$a(\text{chl}) = \frac{\text{Integral } (a_x(w) * L_c(w)) dw}{\text{Integral } L_c(w) dw} \quad (12)$$

where  $L_c(w)$  expresses the weighting factor describing the fluorescent emission of chlorophyll for each of the absorption components, and the term  $a_x(w)$  is for the various components of the absorption coefficient.

To evaluate the variability of the absorption coefficients in equation 10 we used particulate spectral absorption data  $a_p(w)$  recorded for the Biowatt II data set and for data from an earlier cruise transect from Tahiti to New Zealand (Kiefer et al. 1989) that we consider to be similar to the present

## Natural fluorescence and photosynthesis

data set. From particulate absorptions,  $a_p(\text{chl})$  is the sum of the detrital and plankton components, weighted as in (4) above. From these data we conclude that the  $a_p(683)$  is not significantly different ( $r = .9999, n = 44$ ) from  $a_p(\text{chl})$ . Furthermore, comparison of the values of  $a_p(\text{chl})$  (mean = 0.0155,  $\sigma = 0.00817$ ) are much less than the values of  $a_w(683)$  (0.46, see Smith and Baker, 1981). A review of the literature (e.g. Kishino, et al., 1984b) indicates that values of  $a_p(683)$  is much less than  $a_w(683)$ . For those reasons, in this analysis we use the value of 0.5 for  $a(\text{chl})$ .

The signal from the natural fluorescence sensor  $L_u(\text{chl}, t, z)$  is a combination of signals from sources in addition to the fluorescence of phytoplankton. These sources may include backscattered sunlight, raman scattering, and bioluminescence. Based on Sugihara, et. al (1984), we judge only backscattered sunlight to be significant at these wavelengths, and only within the top few meters of the water column. To account for this backscattered signal, a reflectance value for seawater at 683nm  $R(683)$  of 0.00026 associated with clear water is used in calculating the upwelling radiance from reflected sunlight from the following relation:

$$L_u(\text{chl}, z)_b = E_d(\text{chl}, 0) * R(683) * e^{-(k(683)*z)} \quad (13)$$

where  $E_d(\text{chl}, 0)$  is the downwelling irradiance just below the surface integrated over the response spectrum of chlorophyll fluorescence. The values of  $R(683)$  and  $k(683)$  are the reflectance and diffuse attenuation coefficients for 683nm, considered to be an approximation of the same quantities for light with the spectral distribution of chlorophyll. For depths greater than 5 meters,  $L_u(\text{chl}, z) \gg L_u(\text{chl}, z)_b$ , and thus the backscattered component can be neglected.

The optical instrument packages used included a Profiling Natural Fluorometer PNF-300, and either a MER-1048 Reflectance Spectroradiometer and a MER-2020 Spectroradiometer (Booth and Smith, 1988). The MER-1048 was configured as part of a Bio-Optical Profiling System (Smith et al., 1984). Data from the profiling system was recorded on a shipboard personal computer. Approximately 5 sets of readings from all sensors were digitized and averaged for each one meter depth increment. The system was lowered at a rate of one meter per second, and the ship was normally positioned to minimize the shadow cast by the ship. During Calypso '87, the MER-2020 was attached to a drifting buoy for continuous measurements, and during Biowatt II it was attached to a mooring (Smith, unpublished data). At Friday Harbor both a MER-2020 and a MER-1048 were deployed from the dock during the incubations.

### **Photosynthetic and biological measurements**

Photosynthetic rate measured using the  $^{14}\text{C}$ -technique, followed the protocols of Fitzwater et al. (1982). Water for analyses of photosynthetic rate and chlorophyll concentration was obtained using pre-cleaned 30 l Go-Flo Niskin samplers configured with a CTD rosette during Biowatt II; pre-cleaned 10 l Niskin bottles refitted with silicon tubing were used during Calypso '87. Additional precautions against contamination included the use during Biowatt II of a CTD frame painted with teflon and the use during Calypso '87 of a Kevlar hydrowire and silicon coated messengers. At Friday Harbor samples were obtained with a hand lowered Niskin bottle.

The photosynthetic rate of the phytoplankton crop was measured by inoculating water samples with  $^{14}\text{C}$ -labeled bicarbonate and incubating in situ near the optical packages. During Biowatt II, water

## Natural fluorescence and photosynthesis

samples were subdivided into 250 ml polycarbonate bottles and inoculated with an aqueous solution of labeled sodium bicarbonate. During Calypso '87, samples were incubated in 250 ml tissue culture flasks (Corning). All samples were kept dark during inoculation, deployment, and retrieval. At the end of the incubation period, the suspended particles were collected onto Millipore HA filters (Biowatt II) or GF/F filters (Calypso '87). During Biowatt II, samples were placed in scintillation vials containing 0.10 ml of 10% HCl. During Calypso '87, filters were fumed for >30 seconds over concentrated HCl. All samples were assayed in a liquid scintillation counter. Counts were converted to disintegrations with quench curves and internal standards during Biowatt II, and using the external standards ratio method during Calypso '87. Chlorophyll *a* was measured spectrophotometrically after separation by HPLC during Biowatt II, and fluorometrically after 90% acetone extraction of filtered (GF/F) particles during Calypso '87 (following Smith et al., 1981). Measurements of photosynthetic rate were made in duplicate during Biowatt II and in triplicate during Calypso '87. The Friday Harbor samples were incubated in scintillation vials suspended between docks below the moored MER-2020.

Incubations of  $^{14}\text{C}$  inoculated samples were classified into "short" and "long" incubations. Short incubations varied from 0.5 to 3.25 hours. Long incubations varied from 4.1 to 12 hours. During Calypso '87 24 long and 30 short incubations were conducted. During the Biowatt II cruises, all 18 incubations were 12 hours. At Friday Harbor all 5 incubations were incubated 0.5 hours. To emphasize the "instantaneous" nature of the natural fluorescence method we have chosen to report the production values in nanogram-atom Carbon  $\text{m}^{-2} \text{sec}^{-1}$ , regardless of the length of the incubations.

Additional complications in these tests arose from the desire to incubate at depths where continuously recording natural fluorescence sensors were not available. In these cases the vertical profiling natural fluorescence sensors were periodically deployed next to the fixed depth integrating sensor. The average vertical gradients in PAR and natural fluorescence were then computed and these gradients were used to scale the integrated readings taken where integrating instruments were deployed to the other incubation depths.

### **Results**

#### **Statistical Treatment:**

In this data set, both the natural fluorescence and production values cover a large range (see Table 1) and are highly skewed toward lower values. This departure from a normal distribution can be overcome by the use of a multiplicative model ( $Y = aX^b$ ), or log transformation (Sokal and Rohlf, 1969). In all cases the multiplicative model yields lower regression coefficients than the linear model, but due to the skewed distributions the transformed regressions are more useful. The original data set consisted of 78 observations, two points were removed in calculating the regressions. One point from 150 meters was eliminated since its value was below the useful range of the sensor at the time of incubation. Another point was eliminated since its value was grossly inconsistent with the other measurements at that time. The distribution of errors between the reported and predicted productivity were based on the actual distributions of the errors. All regressions and error analyses assumed that all of the error was in the predictions.

#### **General**

The general hydrographic conditions during the studies are summarized in Table 1. In the Sargasso Sea, chlorophyll concentration ranged from 0.03 to 0.6  $\text{mg m}^{-3}$ . The highest stock of chlorophyll was measured in March, when the mixed layer was deepest, about 80 m, and the surface water was coldest, about 19.2 °C. At this time the highest concentration of chlorophyll within the water

## Natural fluorescence and photosynthesis

column was within the surface mixed layer. A lower stock of chlorophyll occurred in May, when the surface water was warmest, about 22.2 °C. During May, the chlorophyll maximum was well below the mixed layer. Chlorophyll concentrations ranged 0.09 to 0.53 mg m<sup>-3</sup> in the South Pacific Ocean. The largest crop of phytoplankton was found in Friday Harbor and at Cook's Bay. Oceanic sites were oligotrophic, and the maximum concentration of chlorophyll was consistently below 45m depth.

### **Photosynthesis and Natural Fluorescence**

Measured production from all sites ranged from 0.37 to 546 ng-atom C m<sup>-3</sup> sec<sup>-1</sup>. Light (PAR) ranged from 2.5 to 1550 uE m<sup>-2</sup> sec<sup>-1</sup>. Depth ranged from 2 to 150 meters. Table I presents the variability of these parameters by date and location. Rates of natural fluorescence varied over 1500 fold, from .36 to 547 nEin m<sup>-2</sup> sec<sup>-1</sup>. In order to illustrate the characteristics of the natural fluorescence signal, we have chosen as an example data taken from 18 September 1987, recorded off Tahiti. Figure 1a shows the time course of irradiance at 488nm recorded both from the ship and from the moored natural fluorescence package at 30 meters depth. In this figure, rectangles at the bottom of the plot mark the times that the vertical profiling package was deployed. Changes in irradiance caused by clouds can be seen. For example, irradiances elevated from the "clear sky" values at around 7:00 is probably due to light reflected from towering cumulonimbus clouds over nearby Tahiti. Figure 1b shows the record of continuous beam transmission and active fluorescence recorded from the 30 meter drifter. It is interesting to note the almost 10 fold variability in the fluorometer signal during the day. This may be caused by variations in chlorophyll concentration, either as a result of biological processes such as growth, or mortality or physical processes such as mixing and advection of a crop that is patchy in its distribution. Figure 1c shows the signal from the natural fluorometer at the 30 meter drifter. Sample times and duration of the in-situ incubations conducted that day are shown as horizontal lines. Figure 1d shows the vertical profiles of production predicted from natural fluorescence recorded during the times indicated in figure 1a. Differences in the traces are attributed to different light levels and temporal variability of the crop.

To evaluate the relationship between natural fluorescence and primary production, we have plotted all of the data where simultaneous measurements are available. Figure 2 demonstrates that a strong correlation exists between rates of natural fluorescence (F<sub>f</sub>) and production (F<sub>c</sub>). The correlation coefficient for these data is .92 (n = 76) with a 1500 fold range in the original data. The slope of this regression, the ratio of quantum yields, O<sub>c</sub>/O<sub>p</sub> is 1.53 (standard error = .109) indicating that approximately 16 photons are fluoresced for 10 carbon atoms fixed. This regression suggests that 84% of the variability in photosynthesis is associated with variability in natural fluorescence. Referring to equations 3 to 5, we interpret this to mean that variations in the rate of light absorption by the crop (which can be caused by changes in light intensity, spectral composition of the light, and pigment composition of the phytoplankton) accounts for 84% of the variability in photosynthetic rate. The remaining 16% of the variability in photosynthetic rate is caused by variations in the ratio of quantum yields of photosynthesis and fluorescence  $\phi_{i_c}(t,z)/\phi_{i_f}(t,z)$  and in errors associated with the measurement of photosynthesis.

The natural fluorometer can also be used to predict chlorophyll concentration based solely on the optical measurements using equation 7 if we assume that the fluorescence efficiency (O<sub>f</sub>(t, z)) is constant. Using this same data, equation 7 yields a correlation coefficient of .927 (n = 76) and predicts chlorophyll concentration with a standard deviation of 47% (-115% to +35% for 90% of the points;

## Natural fluorescence and photosynthesis

+/-20% for half the points). A best fit solution for  $O_f(t, z)$  for the entire data set is .028. This compares with values of .045 for "open ocean" and .022 for Tokyo Bay reported by Kishino et al. (1984b). Many workers have noted the variability of the fluorescent efficiency with both light and nutrients (cf. Kolber, 1988).

Since it is known that the quantum yields of photosynthesis and fluorescence decrease at high light intensity, we have further examined this relationship. In figs. 3 and 4 we have plotted the estimated quantum yields for photosynthesis and fluorescence as a function of mean irradiance during the period of incubation. The calculation of quantum yields is based on eqs. 4 and 5, where  $F_a$  is calculated from measurements of chlorophyll a concentration and irradiance,  $E_o(\text{PAR}, t, z)$ , and from estimated values for the specific absorption coefficient of phytoplankton,  $^{\circ}\text{ac}(\text{PAR})$ , and the mean cosine of the light field,  $u(\text{PAR})$ :

$$F_a = ^{\circ}\text{ac}(\text{PAR}) * E_o(\text{PAR}, t, z) * \text{chl}(t, z) / u(\text{PAR}, t, z) \quad (13)$$

Based on measurements from the Sargasso Sea and the South Pacific Ocean (Chamberlin, 1989), the specific absorption coefficient was assigned a value of  $0.012 \text{ m}^{-1}$ , and the mean cosine of the light field was assumed to be a constant value of 0.8. In this plot the highest two values are the deepest where the resolution of the light sensor is minimal. The next two highest samples are from the chlorophyll maximum on Biowatt II, where the chlorophyll variability was the highest over time. Although the scatter in the data is large, quenching of fluorescence and saturation of photosynthesis appears to occur at high light intensities.

To explore how such processes affect the accuracy of our estimates of photosynthesis from measurements of natural fluorescence, we have also plotted the ratio of photosynthesis to fluorescence,  $F_c(t, z) / F_f(t, z)$ , as a function of  $E_o(\text{PAR}, t, z)$  (Figure 4). According to equations 2 and 3, this ratio is equal to  $O_c(t, z) / O_f(t, z)$ . A trend of decreases in the ratio with increases in light intensities is apparent. This indicates that at higher light levels, decreases in the quantum yield of photosynthesis exceed the decreases in the quantum yield of fluorescence.

In order to improve the predictive capability of natural fluorescence measurements, we propose a simple empirical formulation that relates the ratio of photosynthetic and fluorescence quantum yields to the irradiance of PAR:

$$F_c(t, z) / F_f(t, z) = O_c(t, z) / O_f(t, z) = (O_c / O_f)_{\text{max}} * \text{kcf} / (\text{kcf} + E_o(\text{PAR}, t, z)) \quad (14)$$

$(O_c / O_f)_{\text{max}}$ , an empirical constant, is the maximum value of the ratio of quantum yields, and  $\text{kcf}$ , another empirical constant, is the value of irradiance when the ratio is equal to half of its maximum value. The curve in figure 3 is this function when  $(O_c / O_f)_{\text{max}}$  and  $\text{kcf}$  are given "best-fit" values of 2.3 Carbon atoms/photon and  $133 \text{ mE in m}^{-2} \text{ sec}^{-1}$ , respectively. A regression analysis of such a proposed relationship between the ratio of quantum yield and irradiance indicates that about half of the variability in the ratio can be accounted for by variability in irradiance. This means that in our database about 6% of the variability in photosynthetic rate may be attributed to the changes in the ratio of quantum yields that was caused by variations in irradiance.

## Natural fluorescence and photosynthesis

When combined, equations 3 and 14 provide a formulation of the relationship between photosynthesis, fluorescence, and irradiance.

$$F_c(t,z) = (O_c/O_f)_{\max} * k_{cf} * F_f(t, z)/(k_{cf} + E_o(\text{PAR}, t, z)) \quad (15)$$

Figure 4 is a log-log graph of the measured photosynthetic rate and the rate predicted by introducing values for  $F_f(t, z)$  and  $E_o(\text{PAR}, t, z)$  into equation 10. The correlation coefficient for the multiplicative regression is 0.95, the slope is approximately 1, and the standard error of the estimate is 0.48. The difference between predicted and observed rates of photosynthesis indicate that 9 out of 10 predictions are within 65% of the measured rate.

Using equation 15 as the predictor of production, we can examine the residuals in the regression with the goal of further explaining the variability. Nine points were flagged with high leverage. Of these, the 4 points with the largest distance from the regression line were a point from 150 meters, at approximately the 0.1% light (PAR) level, a point 2 meters deep during the May Biowatt II cruise, and two points in the chlorophyll maximum layer also on the May Biowatt II cruise. The remaining points with high leverage or influence on the regression, but shorter distance from the regression line, were the data from Friday Harbor, and represented the highest production values. The error in the surface data point could be explained by a variety of factors including the inherent variability of the surface light field due to waves, the component of reflected sunlight, and the highly turbulent nature of surface ocean waters. The points from Biowatt II that were sampled in the chlorophyll maximum layer were subject to internal waves that, for example, displaced the chlorophyll maximum layer at times completely out of the region where it was located at the start of the incubation. From available data, it is impossible to estimate how much of the unexplained variability can be explained by such sampling errors.

We examined the residuals by experiment date and location. This showed that the spring (March 5 and 7, 1987) Biowatt II data clustered tightly with prediction about 40% high. May Biowatt II data averaged 20% low. Friday Harbor data clustering from 10 to 40% low. Data sampled from Cook's bay averaged 30% low. Figure 7 is a plot of the percent error of the predictions from these data and shows the relationship of site and prediction error.

An examination of the residuals in the prediction of chlorophyll shows that the Biowatt II data were less well correlated than other data. The standard deviation of the error in prediction of the data set less Biowatt II improved to 35% error ( $n=53$ ) from 47% ( $n=76$ ). This can partially be accounted for by the fact chlorophyll concentrations used were sampled at sunrise while the natural fluorescence measurements were the average of data obtained throughout the day in support of the production estimates.

When the residuals in the prediction of productivity were examined by length of time of incubation, no significant trends were noticed. However, a trend can be seen that indicates that incubation time was correlated somewhat ( $r=.41$ ,  $n=51$ ) with the error in the prediction for the Calypso data set alone. This trend indicated that predicted productivity from long incubations is high relative to short incubations.

## Natural fluorescence and photosynthesis

### **Discussion**

The data on photosynthesis and natural fluorescence covers a wide range of photosynthetic rates and chlorophyll concentrations. It includes measurements from several distinct geographical locations during several seasons. While more data from other regions and more diverse hydrographic conditions would be advantageous to evaluate more thoroughly the relationship between natural fluorescence and photosynthesis, we conclude from this study that a useful and predictable relationship exists between photosynthetic rate, natural fluorescence, and irradiance. Introduction of values of natural fluorescence and irradiance into equation 15 yields predictions of photosynthetic rate that accounts for 90% of the variability in the rate measured by incubating in situ water samples inoculated with radioactive bicarbonate and 9 of 10 predictions are within 65% of the measured value. As discussed below, some significant fraction of the variability between predicted and observed rates of photosynthesis may be caused by reproducibility of the  $^{14}\text{C}$  measurement as well as by problems inherent in comparing an instantaneous measurement of an unperturbed sample with an integrated measurement from an enclosed water sample. An example of the types of changes that occur in an unperturbed sample may be seen in figures 1b and 1d. The results reported in this paper are derived from a comparison of a trapped population suspended at the same location in the ocean as the natural fluorescence sensor.

In waters that range from euphotic to extremely oligotrophic, 84% of the variability in measured photosynthetic rate can be accounted for by changes in the natural fluorescence signal (Figure 2). By definition (Equation 3), the remaining 16% of the variability in measured photosynthetic rate is associated with variations in the ratio of quantum yields of photosynthesis to fluorescence. Accounting for the decrease in the quantum yield of photosynthesis relative to the yield of fluorescence with increasing ambient irradiance (Figure 4) allows us to increase the percent of variability explained to 90%. This relationship is interpreted to mean that the decrease in fluorescence yield caused by quenching at high light intensities are not as great as the decrease in photosynthetic yield associated with saturation and the inhibition of the rate of carbon fixation.

In our data set the ability to predict chlorophyll from equation 7 was about the same as the ability to predict production from equation 3 ( $r = .92$ ). However, predictions based on both natural fluorescence and irradiance (equation 14) were improved ( $r = .95$ ). Furthermore, the residuals of the regressions on equations 3 and 7 showed little correlation with each other. We would expect the measures of natural fluorescence to be more highly correlated with production than with concentrations of chlorophyll (or chlorophyll and irradiance) since the primary source of fluorescence is thought to be from photosystem II, with little emission from photosystem I. Furthermore, changes in the ratios of other photosynthetic pigments to chlorophyll a should influence predicted chlorophyll a concentrations while having little effect in the natural fluorescence based prediction of production. Another factor in the prediction of chlorophyll is the dependence of  $^{\circ}\text{ac}(\text{PAR})$  on the spectral distribution, and thus depth and chlorophyll concentration. For a discussion of this see Collins, et al. (1988). If this is true, then the improvement of production prediction over the observed chlorophyll prediction may indicate that a significant amount of the residual variability in the production correlations may be caused by production measurement by  $^{14}\text{C}$ .

There are several reasons why predictions from natural fluorescence of photosynthetic rate measured during short incubation should be better than predictions of photosynthetic rate during long incubations. First, the probability that the measured instantaneous fluorescence is representative of a cell suspension within an incubation bottle will decrease as the duration of the incubation increases.

## Natural fluorescence and photosynthesis

Also, if the distribution of the phytoplankton crop is patchy, horizontal and vertical motion at the sensor will cause changes in the fluorescence signal that are unrelated to the processes that are occurring with an incubation bottle. Second, the amount of carbon assimilated by the cell suspension within the sample is a function of the net rate of production; it is the integral of the difference between the photosynthetic rate and the rate of respiration of labeled cellular carbon over the time of incubation. Natural fluorescence is, on the other hand, a gross rate, since it is unaffected by the rate of respiration. Thus, the ratio of the average rate of carbon assimilation to the average natural fluorescence will tend to be lower for longer incubations. This tendency will be greater for incubations near the bottom of the euphotic zone where the time interval during which irradiances that exceed compensation intensities is short. Finally, because of the quenching of natural fluorescence and saturation and possibly inhibition of photosynthesis at high light intensities, neither photosynthesis nor fluorescence is a linear function of irradiance. Thus, a comparison based upon the time-averaged values of fluorescence and photosynthesis during long incubations near the sea surface may be biased.

Another type of fluorescence measurement of photosynthetic rate in the sea that has been proposed recently is based upon an analysis of the fluorescence of phytoplankton exposed to repetitive flashes of light (Kolber et al., 1988). The probe or measuring flashes are sufficiently short and infrequent that they do not perturb the steady state condition of cells in the sample. When the fluorescence induced by the probe flashes is measured under ambient conditions, variations in the signal depend both upon quenching and the fraction of reaction centers that are closed at that instant. When the fluorescence induced by the probe flash is measured shortly after an exciting or pump flash large enough to close all the reaction centers, variations in fluorescence induced by the probe flash are interpreted in terms of chemical quenching. Among other things, such information can be used to estimate the quantum yield of photosynthesis. The estimated yield is then multiplied by an estimate of the rate of light absorption by the cells to obtain a prediction of photosynthetic rate.

At present there are insufficient data to determine which of the two types of fluorescence measurements will be more useful and provide the more accurate estimates of photosynthetic rate. In a general sense, natural fluorescence provides a measure of the rate of light absorption by photosystem II, and predictions of photosynthesis are based upon the assumption that the ratio of photosynthetic to fluorescence yields is a predictable function of light intensity. On the other hand, flashed fluorescence provides detailed information related to the quantum yield of the photosystem II, and predictions of photosynthesis are based upon the assumption that the rate of light absorption by the cells is a predictable function of light intensity.

Unfortunately, the interpretation of either natural fluorescence or flash induced fluorescence in the sea may be complicated by at least four factors. First, detrital chlorophyll such as the phaeopigments may contribute to the signal at 683 nm. If this is the case, estimates of photosynthetic rate from natural fluorescence will tend to be too high. However, little is known about the fluorescence yield of the chlorophyll-like pigments in detritus. Second, we expect that the ratio of photosynthetic yield to fluorescence yield will be much higher for species of Synechococcus than for the eucaryotic species of photosynthetic plankton. In cyanobacteria, the fluorescence yield of chlorophyll is very low because the fluorescent photosystem II contains little chlorophyll a; most of the chlorophyll is found in the antenna of photosystem I and is not fluorescent. Therefore, a significant increase in the contribution to the total photosynthetic rate within the water column by cyanobacteria may not be reflected by corresponding increases in fluorescence. Because there is no data on the photosynthetic and fluorescence yields of natural populations of Synechococcus, it is difficult to assess the importance

## Natural fluorescence and photosynthesis

of this potential problem. We note, however, that our data likely includes samples with large differences in the concentration of cyanobacteria. Third, laboratory studies of limitations to the growth rate of phytoplankton cultures by nitrogenous nutrients have been shown to effect the efficiency of both photosynthesis (Cleveland and Perry, 1987) and fluorescence (Kiefer, 1973b; Falkowski and Kiefer, 1985). Severe nutrient limitation causes increases in fluorescence by chlorophyll a and decreases in photosynthetic quantum yields. The range in growth rates and nutrient status of natural phytoplankton crops has not been established. Finally, since the information obtained from both pump and probe and natural fluorescence signals pertains only to the photochemical energy conversion, these measurements can only provide estimates of gross photosynthetic rate. Losses of fixed carbon by respiration and photorespiration, which determine the difference between gross and net rates of carbon fixation, are unrelated to the fluorescence signal.

Despite these limitations, we suggest that the measurement of natural fluorescence will aid in routine mapping and monitoring of photosynthetic rate. Just as the introduction of the rapid measurements of chlorophyll a through strobe-induced fluorescence (Lorenzen, 1967) significantly improved our ability to sample and study phytoplankton biomass, the natural fluorescence signal, as an estimator for photosynthesis, can have a similar influence on ocean productivity studies. The measurement provides detailed spatial and temporal information on photosynthesis that can not be achieved by incubation of water samples that have been inoculated with  $^{14}\text{C}$ . Profiles of natural fluorescence can aid in choosing sampling depths and light intensities for incubations, extrapolating or interpolating information obtained by the  $^{14}\text{C}$  method, or independently estimating productivity when time and manpower is limited. Because the instrument package can be moored unattended or deployed from drifters, natural fluorescence measurements offer the greatest potential for providing estimates of primary productivity over large seasonal scales. Furthermore, hand-lowered instrument packages for vertical profiling can be deployed quickly (< 10 minutes for a 200 meter profile) by a single individual without special winches allowing productivity estimates in situations that would otherwise prohibit such measurements.

# Natural fluorescence and photosynthesis

Table Of Units:

$F_f(t,z)$	natural fluorescence	$\text{Ein m}^{-3} \text{sec}^{-1}$
$F_c(t, z)$	rate of photosynthesis	$\text{g-at C m}^{-3} \text{sec}^{-1}$
$F_a(t, z)$	rate of light absorption	$\text{Ein m}^{-3} \text{sec}^{-1}$
$O_c(t, z)$	quantum yield of photosynthesis	$\text{g-at C fixed/Ein absorbed}$
$O_f(t, z)$	quantum yield of photosynthesis	$\text{g-at C fixed/Ein absorbed}$
$F_a$	flux of light absorbed by crop	$\text{Ein m}^{-3} \text{sec}^{-1}$
$ac(\text{PAR}, t, z)$	mean cellular absorption coefficient	$\text{m}^{-1}$
$E_o(\text{PAR}, t, z)$	scalar irradiance 400-700nm	$\text{Ein m}^{-2} \text{sec}^{-1}$
$Y_f(t, z)$	natural fluorescence coefficient	$\text{m}^{-1}$
$chl(t, z)$	concentration of chlorophyll a	$\text{mg m}^{-3}$
$^{\circ}ac(\text{PAR}, t, z)$	specific absorption coefficient of phytoplankton	$\text{m}^{-2} \text{mg}^{-1}$
$L_c(w)$	radiance over chlorophyll emission	$\text{Ein sec}^{-1} \text{m}^{-2} \text{nm}^{-1} \text{str}^{-1}$
$R(w)$	sensor responsivity	$\text{volts Ein}^{-1} \text{sec m}^2 \text{str}$
$L_u(chl)$	radiance of a chlorophyll-like source	$\text{Ein sec}^{-1} \text{m}^{-2} \text{str}^{-1}$
$k(\text{PAR}, t, z)$	diffuse attenuation coefficient for $E_o(\text{PAR})$	$\text{m}^{-1}$
$a(chl, t, z)$	total absorption coef. of water + constituents	$\text{m}^{-1}$
$E_d(chl, 0)$	downwelling irradiance over chlorophyll emission	$\text{Ein sec}^{-1} \text{m}^{-2}$
$u(\text{PAR})$	mean cosine of the light field	
$(O_c/O_f)_{\text{max}}$	max value of the ratio of quantum yields	Carbon atoms/photon
$k_{cf}$	value of irradiance @ 1/2 $(O_c/O_f)_{\text{max}}$	$\text{Ein m}^{-2} \text{sec}^{-1}$

Note: inclusion of table of units is at the editor's preference.

## Figure Legends:

Figure 1a: Downwelling irradiance ( $\text{microwatts cm}^{-2} \text{nm}^{-1}$ ) at 488nm both above (upper trace) and at 30 meters (lower trace) on the incubation platform.

Figure 1b: Beam attenuation coefficient ( $\text{meters}^{-1}$ ) and strobe based fluorescence at 30 meters on the incubation platform. Fluorometer reading restated in chlorophyll concentrations ( $\text{mg m}^{-3}$ ) for that day.

Figure 1c: Upper trace is downwelling irradiance at 488nm from the incubation platform as seen in figure 1a. Lower trace is predicted production from natural fluorescence using equation 15. Units are nanogram-atom Carbon  $\text{m}^{-3} \text{sec}^{-1}$ . Horizontal lines show the time extent and value obtained from incubations conducted at the same depth. The symbols to the left mark the time the sample was collected, the middle symbols mark the start of the  $^{14}\text{C}$  incubation and the right symbol marks the end of the incubation. The vertical extent of the lines mark the total production divided by the incubation time.

Figure 1d: Shows vertical profiles of predicted production (equation 15) at various times on 18 September 87. Profiles occurred during the times indicated on the bottom of figure 1a. Units are meters depth and  $\text{nEinsteins m}^{-3} \text{sec}$  (LOG scale).

## Natural fluorescence and photosynthesis

Figure 2a: Natural Fluorescence (Ff) versus Production: units are nEinsteins  $m^{-3} \text{ sec}$  and ng-at C  $m^{-3} \text{ sec}$ .

Figure 2b: Predicted (from equation 7) versus Observed chlorophyll a concentration.

Figure 3: Semi-log plot of quantum yield of photosynthesis versus Irradiance  $E_o(\text{PAR},t,z)$  in ( $\mu\text{Einsteins } m^{-2} \text{ sec}^{-1}$ ).

Figure 4: Semi-log plot of the quantum yield of natural fluorescence versus Irradiance  $E_o(\text{PAR},t,z)$  in ( $\mu\text{Einsteins } m^{-2} \text{ sec}^{-1}$ ).

Figure 5: Ratio of photosynthetic rate to natural fluorescence,  $F_c(t,z)/F_f(t,z)$ , versus Irradiance  $E_o(\text{PAR},t,z)$  in ( $\mu\text{Einsteins } m^{-2} \text{ sec}^{-1}$ ).

Figure 6: Measured photosynthesis versus predicted photosynthesis from equation 16. Units are nanogram-atom C  $m^{-3} \text{ sec}^{-1}$ . Line represents ideal fit.

Figure 7a: Analysis of the prediction error of production from equation 16 as a function of site and day. See Table One for site codes. Figure 7b: prediction error of chlorophyll as a function of site and day.

### **Acknowledgements:**

We wish to thank Captain Albert Falco, Bertrand Sion and the crew of Calypso for their indefatigable esprit de corps during the Calypso '87 cruise. We also acknowledge Dale Robinson for his invaluable assistance during the cruise. We thank the Captain and crew of the Oceanus for their professional and enthusiastic support during the Biowatt II cruises. We thank Don Collins and Curt Davis (JPL) for lending hands and instrumentation at the Friday Harbor experiments, and for their very helpful comments and guidance. Special thanks to Dr. John Marra who provided  $^{14}\text{C}$  productivity data for the Biowatt II data set.

We express our gratitude to the Cousteau Society for their support of the Calypso '87 cruise during Jacques Cousteau's "Rediscovery of the World" expedition. This work was also supported by NASA grants to C. R. Booth (Contract NAS7-969), D.A.Kiefer (Contract NAGW-317), R. C. Smith (NAGW-290-10), and Office of Naval Research grants to D. A. Kiefer (Contract N300014-87-K-0287), to R. C. Smith (N300014-84-C-0382) and to J. Marra, (Contract N00014-84-C0132). This is Biowatt II contribution number \_\_\_\_.

### **References:**

Booth, C. R. (1974). The design and evaluation of a measurement system for photosynthetically active quantum scalar irradiance. *Limnology and Oceanography* 21: 326-336.

Chamberlin, W. S. (1989). Light absorption, natural fluorescence, and photosynthesis in the open ocean. Ph.D. dissertation. University of Southern California, Los Angeles, California.

Cleveland, J.S. and M.J. Perry (1987). Quantum yield, relative specific absorption, and fluorescence in nitrogen-limited *Chaetoceros gracilis*. *Marine Biology* 94: 489-497.

Fahnenstiel, G. L., D. Scavia, G. A. Lang, J. H. Saylor, G. S. Miller, and D. J. Schwab (1988). Impact of inertial period internal waves on fixed depth primary production estimates. *Journal of Plankton Research*, 10, 77-87.

## Natural fluorescence and photosynthesis

- Falkowski, P. G. (1988). Ocean productivity from space. *Nature*, 335, 205.
- Falkowski, P. and D.A. Kiefer (1985). Chlorophyll a fluorescence in phytoplankton: relationship to photosynthesis and biomass. *Journal of Plankton Research* 7: 715-731.
- Fitzwater, S.E., G.A. Knauer, and J.H. Martin (1982). Metal contamination and its effect on primary production. *Limnology and Oceanography*, 27: 544-551.
- Gordon, H. (1979). Diffuse reflectance of the ocean: the theory of its augmentation by chlorophyll a fluorescence at 685 nm. *Applied Optics*, 18, 1161-1166.
- Kattawar, G. W. and J. C. Vastano (1982). Exact 1-D solution to the problem of chlorophyll fluorescence from the ocean. *Applied Optics*, 21, 2489-2492.
- Kiefer, D.A. (1973b). Chlorophyll a fluorescence in marine centric diatoms: Responses of chloroplasts to light and nutrient stress. *Marine Biology* 23: 119-1208.
- Kiefer, D. A., W. S. Chamberlin, and C. R. Booth (1989). Natural fluorescence of chlorophyll a: Relationship to photosynthesis and chlorophyll concentration in the western South Pacific gyre. *Limnology and Oceanography*, in press.
- Kishino, M., S. Sugihara, and N. Okami (1984a). Influence of fluorescence of chlorophyll a on underwater upward irradiance spectrum. *La mer*, 22, 224-232.
- Kishino, M., S. Sugihara, and N. Okami (1984b). Estimation of quantum yield of chlorophyll a fluorescence from the upward irradiance spectrum in the sea. *La mer*, 22, 233-240.
- Kolber, Z., J. Zehr, and P. Falkowski (1988). Effects of growth irradiance and nitrogen limitation on photosynthetic energy conversion in photosystem II. *Plant Physiology* 88: 923-929.
- Lorenzen, C. J. (1967). A method for the continuous measurement of in vivo chlorophyll concentration. *Deep-Sea Research*, 13, 223-227.
- Marra, J., L. W. Haas, and K. R. Heinemann (1988). Time course of C assimilation and microbial food web. *Journal of Experimental Marine Biology and Ecology* 115, 263-280.
- Morel, A. (1978). Available, usable and stored radiant energy in relation to marine photosynthesis. *Deep-Sea Research*, 25, 673-688.
- Morel, A. and L. Prieur (1977). Analysis of variations in ocean color. *Limnology and Oceanography*, 22, 709-722.
- Neville, R. A. and J. F. R. Gower (1977). Passive remote sensing of phytoplankton via chlorophyll a fluorescence. *Journal of Geophysical Research*, 82, 3487-3493.
- Smith, R. C., and K. S. Baker (1981). Optical properties of the clearest natural waters. *Applied Optics*, 20: 177-184.
- Smith, R. C., K. S. Baker, and P. Dustan (1981). Fluorometric technique for the measurement of oceanic chlorophyll in support of remote sensing. *SIO Reference 81-17: 1-13*.
- Smith, R. C., C. R. Booth, and J. Starr (1984). An oceanographic bio-optical profiling system. *Applied Optics*, 23, 2791-2797.
- Sugihara, S., M. Kishino, and N. Okami (1984). Contribution of Raman scattering to upward irradiance in the sea. *Journal of the Oceanographical Society of Japan*, 40: 397-404.
- Topliss, B. J. (1985). Optical measurements in the Sargasso Sea: solar stimulated chlorophyll fluorescence. *Oceanologica Acta*, 8, 263-270.
- Topliss, B. J. and T. Platt (1986). Passive fluorescence and photosynthesis in the ocean: implications for remote sensing. *Deep-Sea Research*, 33, 849-864.

## Natural fluorescence and photosynthesis

Williams, P. J. le B., K. R. Heinemann, J. Marra, and D. A. Purdie (1983). Comparison of  $^{14}\text{C}$  and  $\text{O}_2$  measurements of phytoplankton production in oligotrophic waters. *Nature* 305, 49-50.

---

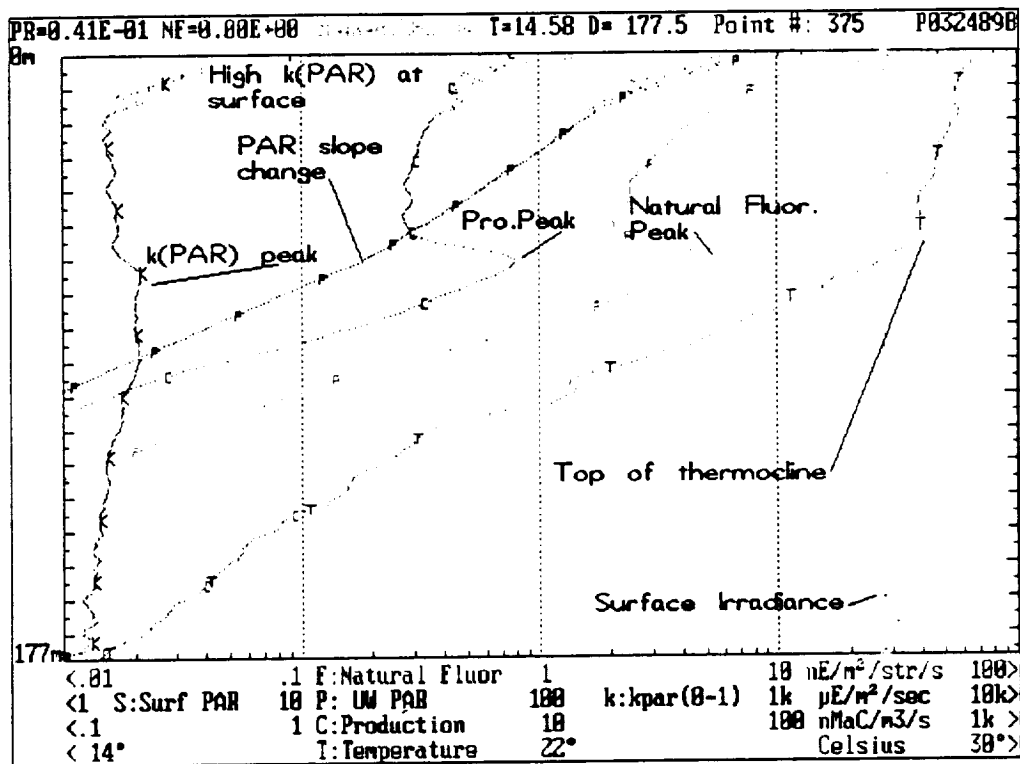
## Appendix E Interpreting the Data



As with any oceanographic data, the quality of the natural fluorescent data and methods of interpretation depend to some degree on the prevailing conditions. This section contains a number of sample profiles obtained under the kinds of conditions that the user is likely to encounter. They vary from ideal, easy-to-interpret profiles to ones slightly blurred by turbulent conditions, or worse, damaged by exposure of the instrument to the ship's underwater shadow. The profiles illustrated described below are:

- Strong data gradient--calm conditions
- Strong data gradient--turbulent conditions
- Smoothing of the Attenuation Coefficient  $k(\text{PAR})$
- Internal Waves or Platform Drift
- Clouds
- Ship's Shadow
- Uneven Lowering Rate

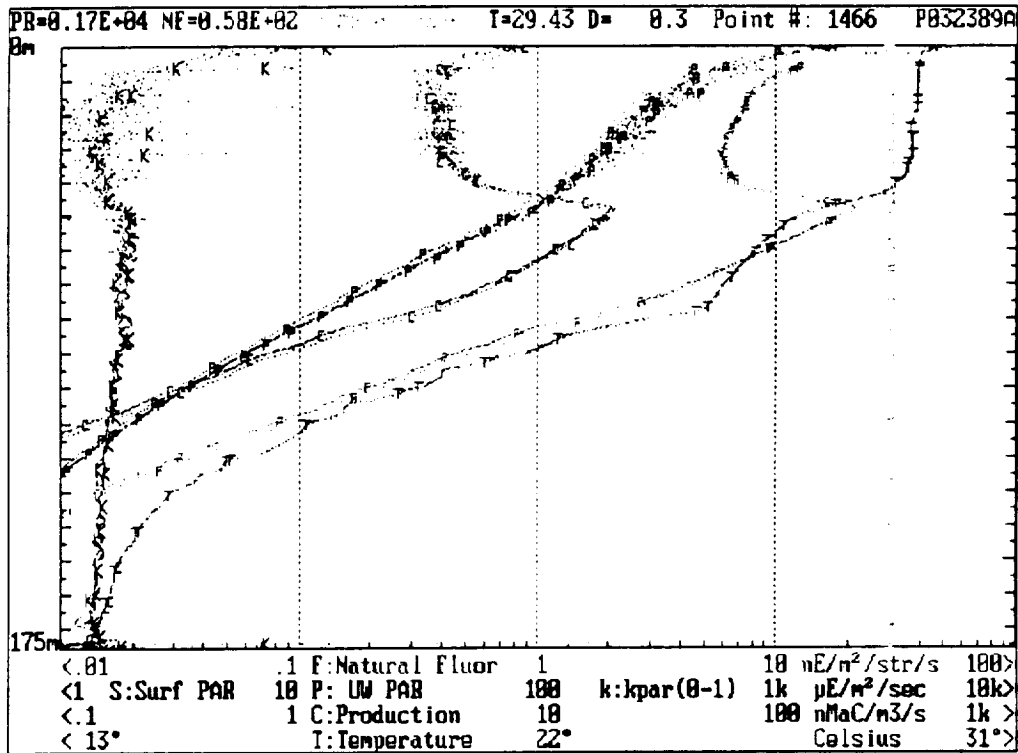
## Stratified Oceanic Calm Environment



The above profile, obtained in the Indian Ocean, is a good example of a strong subsurface production (line C) maxima starting at the top of the thermocline. This profile was obtained under clear skies and relatively calm conditions. As is typical in all profiles, PAR declines faster in the top few meters compared to the rest of the profile. This is due to the rapid absorption of the red part of the spectrum. In this profile 375 points were recorded during the downcast segment of the profile.

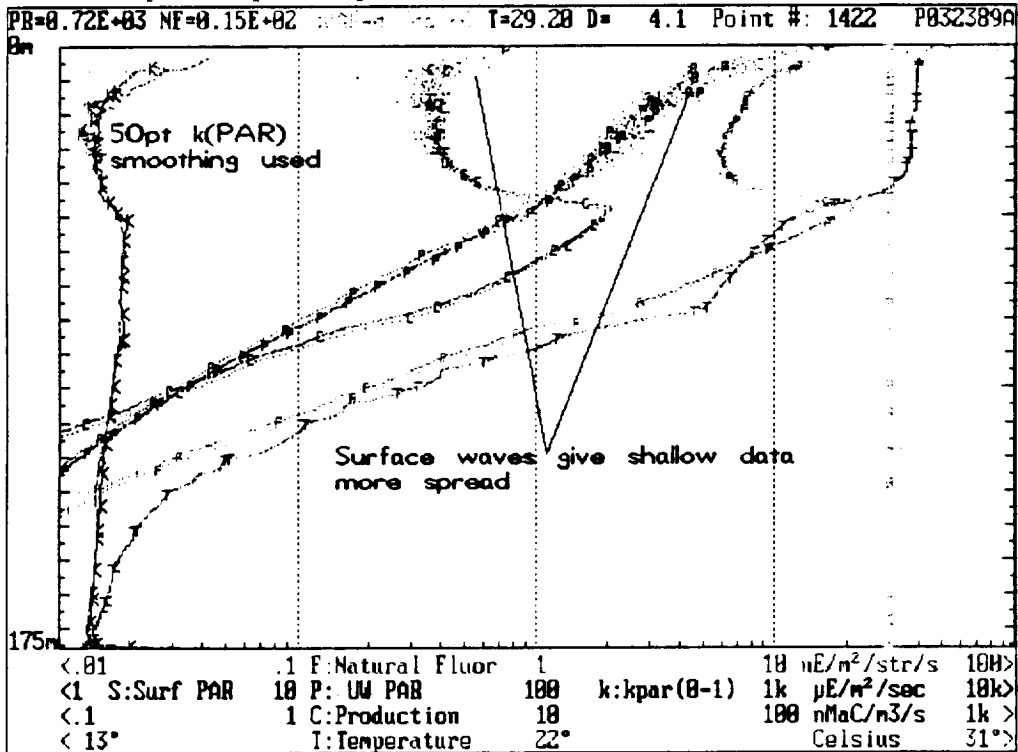
## Stratified Oceanic Environment - Rough Conditions

The following profile was also taken in the Indian Ocean. In this profile, the surface wave conditions were rougher causing more scatter in the PAR data. Since the natural fluorescence signal originates over a large volume relative to the size of the PAR collector, natural fluorescence shows less variability. Production incorporates PAR in its calculation, and consequently also shows some variability.



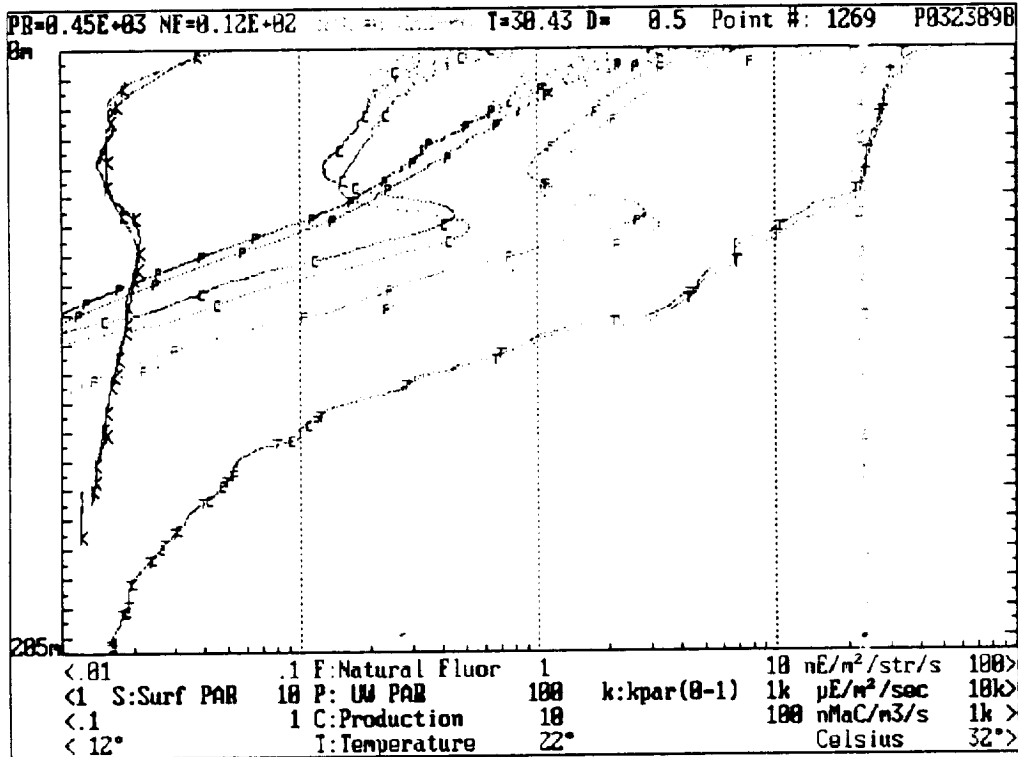
### Smoothing the Attenuation Coefficient for PAR

The following profile shows how increasing the interval over which the diffuse attenuation coefficient for PAR ( $k(\text{PAR})$ ) is calculated (see equation 9, Appendix D) can reduce the scatter in this parameter. The previous plot was plotted with the smoothing factor at 15 and the next plot at 50.



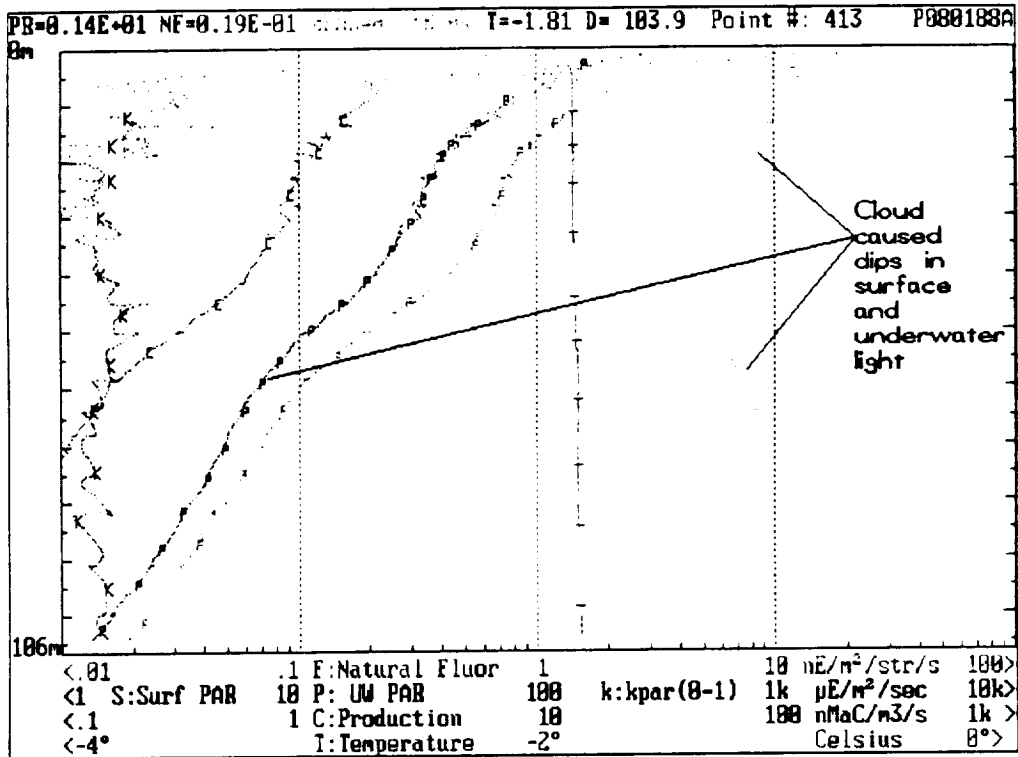
## Internal Waves or Ship Drift

The following case, also from the Indian Ocean, shows the effects of internal waves, (or platform drift) on a vertical profile. In the few minutes between the up and the down casts, the thermocline and the natural fluorescence maxima have moved vertically. This profile was also processed with 50-point k(PAR) smoothing.



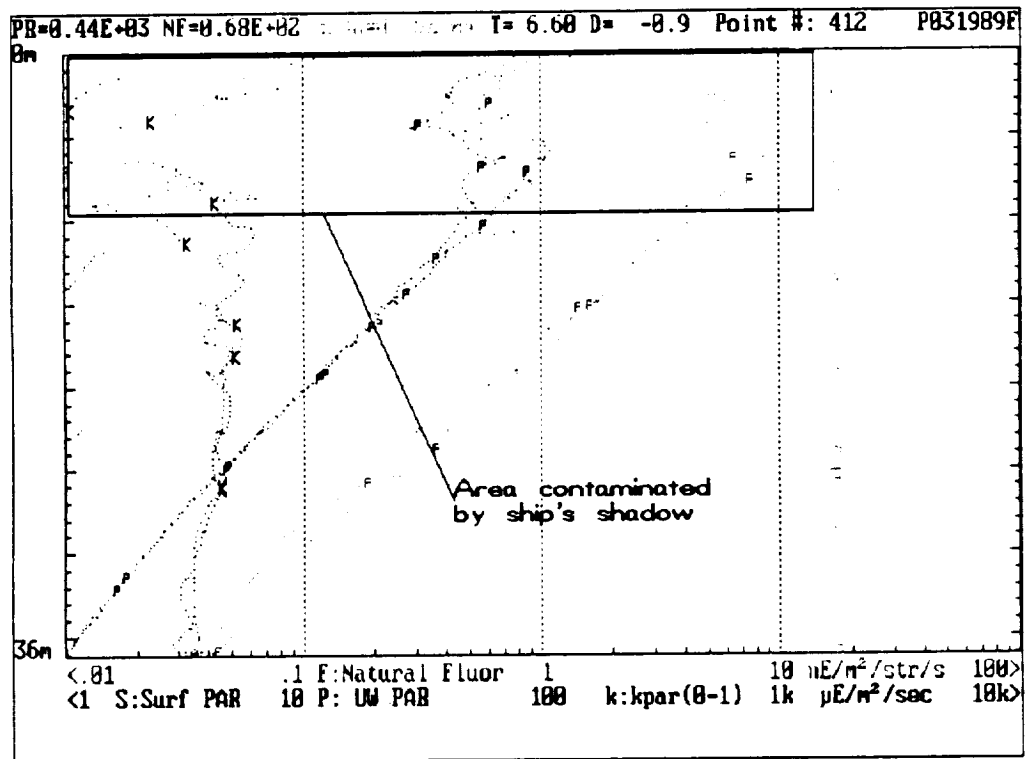
## Clouds

The next profile shows the effects of clouds. In this profile the surface light shows considerable variation. During cloudy conditions it is important to have surface light correction enabled. This will calculate the ratio of the underwater PAR to surface PAR before calculating k(PAR). The production values will **not** be adjusted however. It must be remembered that this instrument measures instantaneous production. When using the productivity measurements, the surface PAR levels must also be considered, as you are measuring production at that surface light condition. Presumably, and unless you are near the surface and there is light inhibition of production, variations in surface irradiance will show up in the production rates throughout the water column.



### Ship's Shadow

The following plot shows an example of the shadow cast by the ship contaminating the measurements. This contamination will effect not only the underwater PAR and the resultant calculation of  $k(\text{PAR})$ , but will also depress the calculated measurement of primary production.



## Uneven Lowering Rate

The PNF-300 should be lowered at a constant rate if the best results in the calculation of  $k(\text{PAR})$  are desired. The following profile illustrates what happens when the sensor is lowered, then held at a fixed depth, then lowered a few meters more, etc. This method will result in uneven spacing of the data as shown below. While this does not normally effect underwater PAR or Lu(Chl) (the radiance from chlorophyll) measurements, it will effect the calculation of  $k(\text{PAR})$ , thus effecting the Ff (natural fluorescence), and production estimates somewhat. To understand these effects, review the equations (also, see Appendix D for a definition of these terms) that are used in the data processing. A prolonged vertical profile will also suffer to a greater extent from changes in cloud cover, and even sun angle changes if the profile extends long enough. If it is necessary to conduct extended sampling from a series of discrete depths, then we recommend that you first conduct a downcast in a continuous mode, then close the data file and open a new file, pausing on the upcast as desired. The smooth downcast can then be compared with the upcast to detect any adverse effects of stopping mid-profile.

